

TASK ORIENTED TACTILE SENSING FOR A ROBOTIC GRIPPER

A Thesis

Submitted to the College of Graduate Studies and Research
in Partial Fulfillment of the Requirements
for the Degree of
Doctor of Philosophy
in the
Department of Electrical Engineering
University of Saskatchewan

G059
Apr. 19/91
10AR

by

CHELAKARA S. VAIDYANATHAN
Saskatoon, Saskatchewan
February 1991

Copyright (C) 1991 CHELAKARA S. VAIDYANATHAN

dedicated to
my beloved family

COPYRIGHT

The author has agreed that the Library, University of Saskatchewan, may make this thesis freely available for inspection. Moreover, the author has agreed that permission for extensive copying of this thesis for scholarly purposes may be granted by the Professor who supervised the thesis work recorded herein or, in his absence, by the Head of the Department or the Dean of the College in which the thesis work was done. It is understood that due recognition will be given to the author of this thesis and to the University of Saskatchewan in any use of the material in this thesis. Copying or publication or any other use of this thesis for financial gain without approval by the University of Saskatchewan and the author's written permission is prohibited.

Requests for permission to copy or to make any other use of the material in this thesis in whole or in part should be addressed to:

Head of the Department of Electrical Engineering

University of Saskatchewan

Saskatoon, Canada S7N 0W0.

ACKNOWLEDGEMENTS

The author would like to express his gratitude and appreciation to Dr. Hugh C. Wood for his guidance and consistent encouragement throughout the course of this work. His timely advice during execution of the project and assistance in the preparation of this thesis is thankfully acknowledged. The author would like to thank all the members of his advisory committee for their suggestions and encouragement.

The author takes this opportunity to acknowledge the encouragement and moral support provided by his parents and family members. The assistance provided by the staff of computing and printing service departments is gratefully acknowledged.

Financial assistance provided by the University of Saskatchewan in the form of Graduate Scholarship is thankfully acknowledged.

UNIVERSITY OF SASKATCHEWAN

Electrical Engineering Abstract 91A338

**TASK ORIENTED TACTILE SENSING FOR A
ROBOTIC GRIPPER**

Student: C. S. Vaidyanathan Supervisor: Dr. H. C. Wood

Ph. D. Thesis Presented to the

College of Graduate Studies and Research

February 1991

ABSTRACT

The sense of touch is a very useful property of the human hand that is important for grasping and manipulating a variety of objects. The adaptation of this ability in mechanical grippers would facilitate skillful performance of operations by robots in unstructured environments.

This thesis describes the design, development and implementation of a task oriented procedure to determine the status of a robotic gripper during grasping and releasing operations. The task status obtained using this procedure, provides a complete set of information about the task including the direction of object displacement relative to the gripper.

The computer aided procedure uses the dynamic forces measured during grasping and releasing operations. A prototype gripper system was designed and built to measure the real time dynamic forces during selected tasks. An integrated computer program performed tactile imaging and image interpretation to facilitate decision making based on the force data. The decisions obtained from each block of data were displayed in the form of a set of task status parameters describing grasping and releasing levels with associated confidence factors. Using the task status information, a method was designed and implemented to determine a set of control decisions to aid in the completion of a task.

The computer aided procedure is a useful contribution to the development of intelligent grippers. The suitability of the procedure has been demonstrated using a set of control decisions obtained from the expert system. Since the procedure was validated using experimental data obtained while performing real tasks on a set of selected laboratory samples, its applicability in practical industrial environments is promising.

Table of Contents

COPYRIGHT	i
ACKNOWLEDGEMENTS	ii
ABSTRACT	iii
TABLE OF CONTENTS	iv
LIST OF FIGURES	ix
LIST OF TABLES	xv
LIST OF ABBREVIATIONS	xix
1. INTRODUCTION	1
1.1. Problem Definition and Motivation	2
1.1.1. Human adaptive grasping theories	3
1.1.2. Mechanical grasping	5
1.2. Statement of Objectives	5
1.3. Overview of the Thesis	6
2. TACTILE SENSING, HUMAN GRASPING AND RECENT DEVELOPMENTS	8
2.1. Introduction	8
2.2. Tactile Sensing	8
2.3. History and Evolution of Tactile Sensing	9
2.4. Grasping and Object Handling by Humans	9
2.5. Survey of Selected Literature	13
2.6. Summary of the State-of-the-art	20
2.7. Concluding Remarks	20
3. HARDWARE SPECIFICATIONS AND DESIGN OF THE PROTOTYPE GRIPPER SYSTEM	21
3.1. Introduction	21
3.2. The Tactile Sensing System	21
3.2.1. Design specifications	21
3.2.1.1. Basic considerations	22
3.2.2. Sensor material	23
3.2.2.1. Force Sensing Resistor	24
3.2.3. Typical characteristics of an FSR element	26
3.2.4. Design of finger pad	27
3.2.5. Energizing circuit for sensors	28
3.2.5.1. Design criteria	28
3.2.5.2. Design of multiple output current source	30

3.2.6. Implementation of multiple output constant current sources	31
3.2.6.1. Tests for crosstalk and performance evaluation	32
3.3. Data Acquisition System	34
3.4. Tactile Data Acquisition System Using VAXlab Real Time Data Acquisition Facility	35
3.4.1. Implementation	36
3.4.1.1. Trigger mode and buffer size specifications for ADQ32	38
3.5. The Robotic Gripper and its Actuation	40
3.5.1. Fabrication of the tactile sensing gripper	41
3.6. Conclusion	41
4. SYSTEM MODELLING AND CALIBRATION: AN EXPERT SYSTEM-BASED APPROACH	45
4.1. Introduction	45
4.2. System Component Characteristics	46
4.2.1. Energized FSR elements	46
4.2.2. Compliant medium and mechanical overlays	47
4.2.3. The complete system hardware	50
4.3. Characterization of the System Behaviour	51
4.3.1. Mathematical modelling methods	53
4.3.2. Approximation using least-squares polynomial	54
4.3.3. Curve fitting using cubic splines	56
4.3.4. Non-linear curve-fitting using exponential functions	56
4.4. Modelling and Calibration Procedure	57
4.4.1. Data collection	58
4.4.2. Uncertainties	59
4.4.2.1. Collection of sample data	59
4.4.2.2. Statistical analysis	60
4.4.2.3. Analysis of variance	61
4.4.2.4. Evaluation of system uncertainty	62
4.4.3. Expert system for modelling and calibration	65
4.4.3.1. Expert System Development Tools	65
4.4.3.2. Embedding the expert system	66
4.4.4. Design considerations	66
4.4.4.1. Knowledge base development	67
4.4.4.2. HT Process	67
4.4.5. Development of Interface Program I	68
4.5. Implementation Results and Discussion	69
4.5.1. Operating procedure	69
4.5.2. Test results and discussion	72
4.6. Conclusion	74
5. TACTILE IMAGING AND INTERPRETATION OF DYNAMIC FORCE DATA	79
5.1. Introduction	79
5.2. Principles of Tactile Imaging	79
5.2.1. Forming a force image	81

5.2.1.1. Selection of ranges and force thresholding	82
5.2.1.2. Accuracy and related issues	83
5.2.2. Transitional uncertainties	84
5.2.3. Forming a tactile image	87
5.2.4. Interpretation of a tactile image	89
5.2.4.1. Criteria for interpretation	90
5.2.4.2. Interpretation of errors and selection of error margin	91
5.2.4.3. Prefiltering of force data	92
5.3. Implementation of the Imaging Technique and Results	94
5.3.1. The imaging procedure	94
5.3.2. The conventional approach	95
5.3.2.1. Timing considerations for real time implementation	97
5.3.3. Modified tactile imaging scheme	99
5.3.3.1. On-line imaging filter	100
5.3.4. Results and discussion	106
5.3.5. Limitations of the method	108
5.4. Conclusion	109
6. DECISION FILTER AND THE TASK STATUS INDICATOR	111
EXPERT SYSTEM	
6.1. Introduction	111
6.2. Formulating Decisions From a Tactile Image	111
6.2.1. Design considerations	113
6.2.1.1. Number of sensors	115
6.2.1.2. Time constraints and error tolerance	115
6.2.1.3. Implementation issues	116
6.2.2. Requirement specifications for the decision filter	116
6.2.3. Decision parameters	117
6.2.4. Design and implementation of the decision filter	118
6.2.5. Analysis of filter performance	122
6.3. Interpretation of the Decision Parameters	127
6.3.1. Design considerations for the expert system	131
6.3.1.1. Requirement specifications	132
6.3.1.2. Inferencing mechanisms and the knowledge representation technique	132
6.4. The Task Status Indicator Expert System	133
6.5. Design and Development of the TSI Knowledge Base	136
6.5.1. Implementation of the TSI expert system	138
6.5.1.1. Inferred attributes and the method of evaluation	138
6.5.1.2. Confidence level for the grasping and the releasing decisions	141
6.5.1.3. Object displacements	143
6.5.2. Performance evaluation of the TSI expert system	145
6.5.3. Interpretation of results	153
6.5.4. Limitations	154
6.6. Summary and Conclusions	154
7. SYSTEM INTEGRATION, RESULTS AND PERFORMANCE	157
EVALUATION	

7.1. Introduction	157
7.2. Software Integration	158
7.2.1. Software subsystems	158
7.2.1.1. User inputs section	159
7.2.1.2. Application program section	159
7.2.1.3. Embedded expert system section	160
7.2.1.4. Levels of embedding	162
7.2.2. Development of Interface Program II	163
7.2.3. Summary of software integration	165
7.3. Testing, Validation and Performance Evaluation	166
7.3.1. Performance of the VAXlab data acquisition system	166
7.3.2. Procedures to obtain real time task data	168
7.3.2.1. Apparatus for the Test Procedure 1	168
7.3.2.2. Selection and specifications of samples	171
7.3.2.3. Definition of task	171
7.3.2.4. Task time and sampling rate selection	172
7.3.3. Artificial slip and the Test procedure 2	172
7.3.4. Implementation of the two test procedures	173
7.3.4.1. Category 1: Independent grasping followed by releasing test	173
7.3.4.2. Results from test Category 1	175
7.3.4.3. Category 2: Combined grasping followed by releasing test	186
7.3.4.4. Results from test Category 2	186
7.3.4.5. Category 3: Repeatability test	187
7.3.4.6. Results from test Category 3	190
7.3.4.7. Category 4: Artificial slip test	193
7.3.4.8. Results from test Category 4	193
7.3.5. Performance of the task oriented procedure	195
7.4. Control Decisions From Task Status	204
7.4.1. Scope of the work	204
7.4.1.1. Hierarchy of the control decision parameters	204
7.4.1.2. Heuristic reasoning	206
7.4.2. Assignment of confidence levels	207
7.4.3. Preliminary design of a Control decision indicator expert system	208
7.4.4. Control decisions from sample test data	210
7.4.4.1. A preliminary analysis of the control decisions	212
7.4.5. Limitations and recommendations	219
7.4.5.1. Timing analysis	220
7.5. Conclusion	223
8. SUMMARY, CONCLUSIONS AND FUTURE DIRECTIONS	225
8.1. Summary	225
8.2. Conclusions	230
8.3. Major Contributions	231
8.4. Future Directions	232
REFERENCES	234

Appendix A. Specifications of the Prototype Gripper System	242
Hardware	
A.1. Implementation Results of ARIEL DSP-16 DAS for Force Data Acquisition	244
A.2. Design of the gripper motor controller	247
Appendix B. Results of Model Development for the Prototype Gripper System	251
B.1. Listing of the Modelling and Calibration Expert System Knowledge Base	251
B.2. A Typical User Session with the Interface Program I	260
Appendix C. Performance Evaluation of Decision Filter Output	264
C.1. Effect of dead band size on filter output	264
C.2. Effect of block size on filter output	267
Appendix D. Performance Evaluation of Interface Program II Using Data from Test Category 1: Independent Grasping and Releasing Tasks	270
D.1. Validation results from Sample 5 and Sample 7 test data	270
D.2. Performance tables using Sample 5 and Sample 7 test data	277
Appendix E. Performance Evaluation of Interface Program II Using Data from Test Category 2: Combined Grasping and Releasing Tasks	282
E.1. Validation results from Sample 5 and Sample 7 test data	282
E.2. Performance tables using Sample 5 and Sample 7 test data	289
Appendix F. Performance Evaluation of Interface Program II Using Data from Test Category 3: Repeatability Tests	292
F.1. Validation package obtained using sample 1 test data	292
F.2. Performance tables obtained using Sample 1 repeatability test data	301
Appendix G. Performance Evaluation of Interface Program II Using Data from Test Category 4: Simulated Slip Tests	310
G.1. Validation package obtained using data from artificial slip tests 2, 3 and 4	310
G.2. Performance tables obtained using artificial slip test data	317
Appendix H. Performance Evaluation of the Control Decision Indicator Expert System	321
H.1. Control decisions obtained from sample 1 test data	321
H.2. Control decisions obtained from sample 5 test data	325
H.3. Control decisions obtained from sample 7 test data	329
Appendix I. A Typical User Session with the Task Status Indicator Expert	333

List of Figures

Figure 1.1: Structure of a typical hairy skin [from Matlin [6], page 202, Fig. 9-2]	4
Figure 1.2: Gripper states during grasping and releasing	6
Figure 2.1: Forces during a human lifting operation and various afferent responses [from Westling [18], 1986, Fig. 8]	10
Figure 2.2: Tactile units in a typical human hand and some of their features [from Westling [18], 1986, Fig. 1]	12
Figure 3.1: A shunt-mode style FSR [from FSR User's Manual [93], Fig.1]	24
Figure 3.2: A through-conduction style FSR [from FSR User's Manual [93], Fig.2]	25
Figure 3.3: Resistance versus force for an FSR [from FSR User's Manual [93], Fig.3]	26
Figure 3.4: Force versus resistance on a log-log plot [from FSR User's Manual [93], Fig.4]	27
Figure 3.5: Prototype sensor array pattern	29
Figure 3.6: Voltage drop versus force for various currents [from FSR User's Manual [93], Fig.6]	30
Figure 3.7: Circuit diagram of an eight-output constant current source for energizing the tactile sensing elements	31
Figure 3.8: Block diagram of data acquisition system used for acquiring tactile data	36
Figure 3.9: Flow chart of the Data acquisition program	37
Figure 3.10: Burst point clock sweep mode of sampling data [from ADQ-32 Converter Module User's Guide [96], Fig.A-11, page A-22]	39
Figure 3.11: Grasping forces measured by sensor #1 using VAXlab data acquisition system	40
Figure 3.12: Home position setting of RM-101 Micro-robot [from RM-101 Movemaster Instruction Manual [97], Fig.3.4]	42
Figure 3.13: Typical gripper arrangement of the RM-101 robot [from RM-101 Movemaster Instruction Manual [97], Fig.8.2]	43
Figure 3.14: Exploded view of the tactile sensors which were mounted on the gripper surface	44

Figure 4.1:	Maxwell-Kelvin model of viscoelasticity [from Fearing [33], Fig. 5, page 964]	48
Figure 4.2:	[a] Step response of a typical Maxwell medium, and [b] Step response of a typical Kelvin medium [from Fearing [33], Fig.6, page 964]	49
Figure 4.3:	Variables of a real system [from Ziegler [101], Fig.1, page 28]	52
Figure 4.4:	A typical experiment to determine system specifications [from Ziegler [101], Fig. 2, page 203]	53
Figure 4.5:	Flow chart of the system modelling scheme	70
Figure 4.6:	Flow chart of the system calibration scheme	71
Figure 4.7:	A third degree polynomial fit to the sensor 1 input-output data	73
Figure 4.8:	A fourth degree polynomial fit to the sensor 1 input-output data	74
Figure 4.9:	A fifth degree polynomial fit to the sensor 1 input-output data	75
Figure 4.10:	A cubic spline interpolation function fit to the sensor 1 input-output data	76
Figure 4.11:	A non-linear [sum of four exponentials] function fit to the sensor 1 input-output data	77
Figure 5.1:	Characterizing a dynamic force	81
Figure 5.2:	Equal range thresholding of dynamic force	83
Figure 5.3:	Raw and filtered data from sensor #1 during grasping	86
Figure 5.4:	Force image obtained from sensor # 1, using raw data	87
Figure 5.5:	Details of the transitional uncertainties - image from raw data	88
Figure 5.6:	Transitional uncertainties in the force image obtained from sensor #1 filtered data - 5 point moving average filter	89
Figure 5.7:	Transitional uncertainties in the force image obtained from sensor #1 filtered data - 10 point moving average filter	90
Figure 5.8:	Flow chart of a conventional approach to obtain a tactile image	96
Figure 5.9:	Off-line modelling and thresholding filter	101
Figure 5.10:	Process diagram of the on-line tactile imaging filter	102
Figure 5.11:	Flow chart of the task oriented procedure to obtain a tactile image from dynamic force	105
Figure 6.1:	Transitions during the grasping operation	113
Figure 6.2:	Transitions during the releasing operation	114
Figure 6.3:	Process diagram of the decision filter	119
Figure 6.4:	Spatial distribution of sensors on the gripper fingers	121
Figure 6.5:	Cumulated grasped levels and released levels obtained from the decision filter using grasping data and releasing data	123

Figure 6.6:	Total gripper force during grasping and releasing	124
Figure 6.7:	Cumulated grasped levels obtained using a 10 point dead band in the decision filter	126
Figure 6.8:	A typical attribute hierarchy	134
Figure 6.9:	Decision hierarchy for a four transition case	140
Figure 6.10:	Hierarchy to determine task categorization	141
Figure 6.11:	Attribute hierarchy for force decisions in the TSI knowledge base	142
Figure 6.12:	Attribute hierarchy for displacement decisions in the TSI knowledge base	144
Figure 6.13:	Raw force data measured by the 8 sensors of the prototype system during grasping and releasing of the sample	147
Figure 6.14:	Task status parameters obtained from TSI expert system - Test 1	151
Figure 6.15:	Object displacement parameters obtained from TSI expert system - Test 1	152
Figure 6.16:	A typical flow diagram of the task oriented procedure used to determine the task status parameters from dynamic force data	156
Figure 7.1:	Flow chart of the Application program section of Interface Program II	160
Figure 7.2:	Integrating a C program with a Knowledge base [from KES Knowledge Base Author's Manual [107], Fig.12-14, page 12-7]	162
Figure 7.3:	The outputs from channels 1 to 8 to test for switching delays in the DAS	168
Figure 7.4:	The outputs from channels 1 to 8 to test for channel cross-talk in the DAS	169
Figure 7.5:	The measured output from channels 1 to 8 of the DAS	170
Figure 7.6:	A typical sample built for the artificial slip tests	173
Figure 7.7:	Test set up used to perform artificial slip tests	174
Figure 7.8:	Raw force data measured by the tactile sensors during independent grasping and releasing operations performed on sample 2	176
Figure 7.9:	Cumulated grasped levels and primitive force variations from grasping and releasing data of sample 2	178
Figure 7.10:	The force decision parameters of the task status obtained from the TSI expert system using sample 2 grasping data	181
Figure 7.11:	The object displacement parameters of the task status obtained from the TSI expert system using sample 2 grasping data	182
Figure 7.12:	The force decision parameters of the task status obtained from the TSI expert system using sample 2 releasing data	184

Figure 7.13:	The object displacement parameters of the task status obtained from the TSI expert system using sample 2 releasing data	185
Figure 7.14:	Raw force data measured by the tactile sensors during the combined grasping and releasing operation performed on sample 2	188
Figure 7.15:	Cumulated grasped levels and primitive force variations from the combined grasping and releasing data of sample 2	189
Figure 7.16:	The force decision parameters of the task status obtained from the TSI expert system using the combined grasping and releasing data of sample 2	190
Figure 7.17:	The object displacement parameters of the task status obtained from the TSI expert system using the combined grasping and releasing data of sample 2	191
Figure 7.18:	Raw force data measured by the tactile sensors during the artificial slip test 1	196
Figure 7.19:	Cumulated grasped levels and primitive force variations obtained from the artificial slip test 1 data	197
Figure 7.20:	The force decision parameters of the task status obtained from the TSI expert system using the data from the artificial slip test 1	198
Figure 7.21:	Hierarchy diagram for the parameter "Conaction"	205
Figure 7.22:	Hierarchy diagram for the parameter "Movcond"	206
Figure 7.23:	Complete flow chart of the task oriented procedure	214
Figure A.1:	Block diagram of data acquisition system using DSP-16 system	244
Figure A.2:	Grasping forces measured by sensor #1 using DSP-16 system	245
Figure A.3:	Analog output from the multiplexer, typical clock waveform and timing partition diagram of DSP-16 DAS	246
Figure A.4:	Block diagram of logic and drive circuitry for a stepper motor [from Martin [115], Fig. K.1, page 443]	247
Figure A.5:	Current pulse sequence for a two-phase, four winding stepper motor [from Martin [115], Fig. K.2, page 444]	248
Figure A.6:	A driver amplifier for stepper motor control	249
Figure A.7:	The complete diagram of the stepper motor control for actuating the grippers of the RM-101 robot	250
Figure C.1:	Cumulated grasped levels using a 5-point dead band filter	264
Figure C.2:	Cumulated grasped levels using a 15-point dead band filter	265
Figure C.3:	Cumulated grasped levels using a 20-point dead band filter	266

Figure C.4:	Cumulated grasped levels using 30-point data blocks	267
Figure C.5:	Cumulated grasped levels using 50-point data blocks	268
Figure C.6:	Cumulated grasped levels using a 200-point data blocks	269
Figure D.1:	Raw force data measured by the tactile sensors during independent grasping and releasing operations performed on sample 5	271
Figure D.2:	Cumulated grasped levels and primitive force variations from grasping and releasing data of sample 5	272
Figure D.3:	The force decision parameters of the task status obtained from the TSI expert system using sample 5 grasping and releasing data	273
Figure D.4:	Raw force data measured by the tactile sensors during independent grasping and releasing operations performed on sample 7	274
Figure D.5:	Cumulated grasped levels and primitive force variations from grasping and releasing data of sample 7	275
Figure D.6:	The force decision parameters of the task status obtained from the TSI expert system using sample 7 grasping and releasing data	276
Figure E.1:	Raw force data measured by the tactile sensors during the combined grasping and releasing operations performed on sample 5	283
Figure E.2:	Cumulated grasped levels and primitive force variations from sample 5 test data	284
Figure E.3:	The force decision and the object displacement parameters of the task status obtained from the TSI expert system using sample 5 test data	285
Figure E.4:	Raw force data measured by the tactile sensors during the combined grasping and releasing operations performed on sample 7	286
Figure E.5:	Cumulated grasped levels and primitive force variations from sample 7 test data	287
Figure E.6:	The force decision and object displacement parameters of the task status obtained from the TSI expert system using sample 7 test data	288
Figure F.1:	Raw force data measured by the tactile sensors during the independent grasping and releasing operations performed on sample 1, trial 1	293
Figure F.2:	The force decision parameters of the task status obtained from the TSI expert system using sample 1, trial 1 grasping and releasing data	294
Figure F.3:	Raw force data measured by the tactile sensors during the independent grasping and releasing operations performed on sample 1, trial 2	295

Figure F.4:	The force decision parameters of the task status obtained from the TSI expert system using sample 1, trial 2 grasping and releasing data	296
Figure F.5:	Raw force data measured by the tactile sensors during the independent grasping and releasing operations performed on sample 1, trial 3	297
Figure F.6:	The force decision parameters of the task status obtained from the TSI expert system using sample 1, trial 3 grasping and releasing data	298
Figure F.7:	Raw force data measured by the tactile sensors during the independent grasping and releasing operations performed on sample 1, trial 4	299
Figure F.8:	The force decision parameters of the task status obtained from the TSI expert system using sample 1, trial 4 grasping and releasing data	300
Figure G.1:	Raw force data measured by the tactile sensors during the artificial slip test 2	311
Figure G.2:	The force decision and object displacement parameters of the task status obtained from the TSI expert system using artificial slip test 2 data	312
Figure G.3:	Raw force data measured by the tactile sensors during the artificial slip test 3	313
Figure G.4:	The force decision and object displacement parameters of the task status obtained from the TSI expert system using artificial slip test 3 data	314
Figure G.5:	Raw force data measured by the tactile sensors during the artificial slip test 4	315
Figure G.6:	The force decision and object displacement parameters of the task status obtained from the TSI expert system using artificial slip test 4 data	316

List of Tables

Table 3.1: No load sensor outputs when all the eight sensors are simultaneously energized	33
Table 3.2: Summary of voltage readings for cross-talk test	33
Table 3.3: Constant current values from each source and errors	34
Table 4.1: Hierarchy of system specifications [from Ziegler [101], Table 2, page 255].	52
Table 4.2: ANOVA table for the data in set A, set B, and set C	63
Table 4.3: Coefficient of Variation of the four uncertainty factors	64
Table 4.4: Modelling errors obtained by using the five functions for characterizing sensor 1 grasping behaviour	78
Table 4.5: A summary of modelling errors obtained for the eight sensors of the prototype gripper system	78
Table 5.1: Structure of a typical tactile image	91
Table 5.2: Delay introduced by the moving average pre-filter of various data windows	94
Table 5.3: A tactile image obtained using the conventional approach using grasping data	98
Table 5.4: The processing time for data blocks of different lengths using the conventional approach	99
Table 5.5: A tactile image obtained using the modified approach - grasping data	103
Table 5.6: A tactile image obtained using the modified approach - releasing data	104
Table 5.7: The processing times for five groups of data using the modified approach	106
Table 5.8: Differences in the tactile images obtained from raw and filtered force data	107
Table 5.9: Processing times to obtain tactile images from filtered data using the modified approach	108
Table 6.1: Assignment of direction of displacement under different conditions	121
Table 6.2: Processing time taken by the decision filters which used various sizes of dead bands	125
Table 6.3: Processing time taken by the decision filter for different block sizes of data	127

Table 6.4:	Decision parameters from the grasping data	128
Table 6.5:	Decision parameters from the releasing data	129
Table 6.6:	Summary of the task status determined by the TSI expert system from the grasping data	149
Table 6.7:	Summary of the task status determined by the TSI expert system from the releasing data	150
Table 7.1:	Mechanical specifications of the samples used in grasping and releasing tests	171
Table 7.2:	A summary of the task status parameters obtained from the TSI expert system using sample 2 grasping data	179
Table 7.3:	A summary of the task status parameters obtained from the TSI expert system using sample 2 releasing data	183
Table 7.4:	A summary of the task status parameters obtained from the TSI expert system using sample 2 combined grasping and releasing data	192
Table 7.5:	Summary of parameters used in test category 4	194
Table 7.6:	A summary of the task status parameters obtained from the TSI expert system using the data from the artificial slip test 1	199
Table 7.7:	Performance index of the task oriented procedure using results from independent grasping and releasing [Category 1] tests	201
Table 7.8:	Performance index of the task oriented procedure using results from Combined grasping and releasing [Category 2] tests	202
Table 7.9:	Performance index of the task oriented procedure using results from Repeatability [Category 3] tests	202
Table 7.10:	Performance index of the task oriented procedure using results from artificial slip [Category 4] tests	203
Table 7.11:	Assigned confidence values for symbolic values of the parameter "Forcinc"	210
Table 7.12:	Assigned confidence values for symbolic values of the parameter "Relcond"	211
Table 7.13:	Assigned confidence values for symbolic values of the parameter "Conaction"	212
Table 7.14:	Confidence level assignment for the parameter "Movcond" and its associated decisions	213
Table 7.15:	Relationship between the "Indicated direction" and the "Opposite direction" used in CDI knowledge base	213
Table 7.16:	Summary of the results displayed by the CDI expert system - Test Category 1: sample 2 grasping	215
Table 7.17:	Summary of the results displayed by the CDI expert system - Test Category 1: sample 2 releasing	216
Table 7.18:	Summary of the results displayed by the CDI expert system - Test Category 2: sample 2 combined grasping and releasing	217

Table 7.19:	Summary of the results displayed by the CDI expert system - Test Category 4: artificial slip test 1	218
Table 7.20:	Average time to execute Interface Program II to process two blocks of data	221
Table A.1:	Specifications of RM-101 MICROBOT robot	243
Table D.1:	A summary of the task status parameters obtained from the TSI expert system using sample 5 grasping data	278
Table D.2:	A summary of the task status parameters obtained from the TSI expert system using sample 5 releasing data	279
Table D.3:	A summary of the task status parameters obtained from the TSI expert system using sample 7 grasping data	280
Table D.4:	A summary of the task status parameters obtained from the TSI expert system using sample 7 releasing data	281
Table E.1:	A summary of the task status parameters obtained from the TSI expert system using sample 5 test data	290
Table E.2:	A summary of the task status parameters obtained from the TSI expert system using sample 7 test data	291
Table F.1:	A summary of the task status parameters obtained from the TSI expert system using sample 1, trial 1 grasping data	302
Table F.2:	A summary of the task status parameters obtained from the TSI expert system using sample 1, trial 1 releasing data	303
Table F.3:	A summary of the task status parameters obtained from the TSI expert system using sample 1, trial 2 grasping data	304
Table F.4:	A summary of the task status parameters obtained from the TSI expert system using sample 1, trial 2 releasing data	305
Table F.5:	A summary of the task status parameters obtained from the TSI expert system using sample 1, trial 3 grasping data	306
Table F.6:	A summary of the task status parameters obtained from the TSI expert system using sample 1, trial 3 releasing data	307
Table F.7:	A summary of the task status parameters obtained from the TSI expert system using sample 1, trial 4 grasping data	308
Table F.8:	A summary of the task status parameters obtained from the TSI expert system using sample 1, trial 4 releasing data	309
Table G.1:	A summary of the task status parameters obtained from the TSI expert system using artificial slip test 2 data	318

Table G.2:	A summary of the task status parameters obtained from the TSI expert system using artificial slip test 3 data	319
Table G.3:	A summary of the task status parameters obtained from the TSI expert system using artificial slip test 4 data	320
Table H.1:	Summary of the results displayed by the CDI expert system - Test Category 1: sample 1 grasping	322
Table H.2:	Summary of the results displayed by the CDI expert system - Test Category 1: sample 1 releasing	323
Table H.3:	Summary of the results displayed by the CDI expert system - Test Category 2: sample 1 combined grasping and releasing	324
Table H.4:	Summary of the results displayed by the CDI expert system - Test Category 1: sample 5 grasping	326
Table H.5:	Summary of the results displayed by the CDI expert system - Test Category 1: sample 5 releasing	327
Table H.6:	Summary of the results displayed by the CDI expert system - Test Category 2: sample 5 combined grasping and releasing	328
Table H.7:	Summary of the results displayed by the CDI expert system - Test Category 1: sample 7 grasping	330
Table H.8:	Summary of the results displayed by the CDI expert system - Test Category 1: sample 7 releasing	331
Table H.9:	Summary of the results displayed by the CDI expert system - Test Category 2: sample 7 combined grasping and releasing	332

LIST OF ABBREVIATIONS

A/D	Analog to digital
CDI	Control decision indicator
CI	Confidence interval
DAS	Data acquisition system
DF	Degrees of freedom
FA	Fast adapting
FSR	Force sensing resistor
HT	Hypothesize and Test
I/O	Input output
JFET	Junction field-effect transistor
KES	Knowledge Engineering System
LIO	Laboratory input output
MS	Mean square
PCT	Percent
RMS	Root mean square
SA	Slowly adapting
SS	Sum of squares
STDEV	Standard deviation
TSI	Task status indicator

1. INTRODUCTION

Dextrous manipulation is an important human skill that is yet to be duplicated by robotic hands. Humans can grasp objects having a variety of shapes and sizes, perform complicated operations, and switch grasps according to changing task requirements. Sophisticated control capabilities and the physical structure of human hands contribute to these skills. To design an anthropomorphic hand, it is necessary to consider at least 20 degrees of freedom exhibited by a human hand with efficient sensor information and actuation to control each of them. The control capabilities are facilitated by tactile and force sensors which sense conditions at the finger-object contacts. It has been shown [1] that people become very clumsy when deprived of reliable tactile information.

Intelligent robotic grippers will be useful in the areas of tele-operation in space and other hazardous environments, and in factory automation. In space, for example, the cost of having a robot repair or service a module is a small fraction of the cost of using a human, and much safer. With tele-operation, humans can be included in the control loop to make complex decisions. The inspection and repair of ageing nuclear reactors and site cleanup of radioactive and other hazardous waste materials are future important application areas for dextrous robotic hands. Though assembly robots are not yet common in the factory, there is interest in a vertically integrated manufacturing system that could use CAD/CAM models and sensor based robots in the design, assembly and inspection of manufactured components.

Research into robotic sensing has been directed towards two main areas, namely, machine vision and tactile sensing. Vision sensors have many advantages for remote sensing, however they have some practical limitations when the hand occludes regions of the workspace. Low light conditions and varying reflectance also present difficulties for the use of vision systems. It is recognized that tactile sensing is essential for a robotic hand which attempts dextrous manipulation tasks. However, being an active sensing modality, tactile sensing has to be incorporated directly into the gripper control loop as opposed to vision sensing where a passive look at a scene is sufficient to obtain an image. In the ideal case, for robotic manipulation with an artificial hand, a vision sensor could be used to obtain a global image of an object's location and orientation, and tactile sensors could be used to obtain more detailed information from grasping contacts and to control the grasp during the task.

Research into tactile sensor-based robot hands to perform dextrous gripping operations is currently directed toward the investigation of real time gripping mechanisms. A variety of systems have been investigated and a widespread optimism exists regarding the potential application of tactile systems in robotic end-effectors. Presently, most systems which are in actual use are limited to static sensing for simple contact imaging rather than for active manipulation. Though many tactile sensor designs exist, much work remains to be done at various levels before automated gripping and manipulation is clearly understood and used in dynamic manipulation processes. It is believed that future assembly tasks will require manipulation capabilities possible only with low-mass, compliant and mobile fingers that can participate in intelligent gripping of objects in unstructured environments.

1.1. Problem Definition and Motivation

Grasping and holding an object with a hand is a complex mechanical process which involves many sensors, control systems and actuators. The physiology of touch, grip and gait in humans has been studied [2], [116],[117],[118] and the details of the processes involved in human taction have been investigated to provide the direction for developing grasping techniques for robotic hands. In humans, the thumb plays a vital role in grasping and provides the stability and strength to oppose the force applied by one or all of the four fingers [2]. In holding an object, a momentary force as high as 72.4 N has been detected between the thumb and the index fingers [3]. By studying the biomechanics of the static forces in the thumb during normal hand functions, Cooney and Chao [4] have found that during sustained actions, pinch forces can rise to 300 N and grasp forces can reach 500 N. The pressure exerted on finger surfaces during normal activities is between 0 and 245 kPa [5].

In a general sense, intelligent grasping consists of two main functions; spatial positioning of the end-effector relative to an object, and orientation of the movable elements of the end-effector so that they contact, grip without slippage, move, and release an object in a desired way. Robotic vision performs the first task in a relatively efficient way with reasonable accuracy in an industrial environment. The second task may be accomplished by a tactile sensing gripper. For handling different kinds of objects, a tactile sensing system should possess the following general characteristics. The sensors should be conformable to the shape of the fingers on which they will be mounted. The fingers should be compliant so that they can grasp an object of unknown shape by conforming the fingers to the object. The system should provide a reliable, spatially localized and high bandwidth signal to locate contact points. The system should also be able to obtain accurate force measurements to enable estimation of finger forces from tactile information. The approaches used by researchers to build prototype tactile sensing robots suffer from some disadvantages. They suggest complex procedures for performing

simple tasks because the procedures do not exploit the full potential of modern high speed signal processing techniques. In most of the cases, object oriented approaches for handling objects have been proposed rather than task oriented procedures. It has been suggested by some researchers that the performance of mechanical gripping systems could be enhanced by incorporating principles from the human grasping process which is quite efficient and is highly adaptive.

In order to develop a task oriented robot gripper, which can perform common object handling tasks like humans, it is necessary to address a number of problems related to tactile sensing, tactile signal processing and interpretation. A logical starting point in such a development is an investigation of the human tactile sensing system in order to understand the methods of tactile data acquisition, signal processing and interpretation used by humans.

1.1.1. Human adaptive grasping theories

Many basic ideas for tactile sensing in machines can be obtained from a knowledge of sensing in human finger tips. A brief review of the known physiology of human tactile sensing is given here in order to provide a basis for presenting the direction of the work that is described in this thesis. Further details of the human grasping process have been included in Chapter 2 which presents a review of literature in all areas of grasping and dextrous manipulation.

There are three basic theories [6] about human skin senses : the Specificity theory, the Pattern theory, and the Combined approach. These theories have been explained by Matlin [6], and some details have been explained using Figure 1.1. Human skin can be divided into three layers. The **epidermis**, on the outside, is composed primarily of dead skin cells. The **dermis** is the lower layer where new cells are formed. These new cells move to the surface and replace the epidermis cells as they are rubbed off. Underneath the dermis is the **subcutaneous tissue**, which contains connective tissue and fat globules. The skin also has an array of veins, arteries, sweat glands, and receptors. Of these, the primary interest for this work is the role and behaviour of receptors.

All skin receptors are the endings of neurons that carry information from the skin to higher processing systems. Some skin receptors have free nerve endings, while others have encapsulated endings on the end nearest to the epidermis. These endings differ in their shape, size and degree of organisation.

The Specificity theory states that each of the different kinds of receptors responds exclusively to only one kind of physical stimulus, and each kind of receptor is therefore responsible for only one kind of sensation. The Pattern theory suggests it is the pattern of

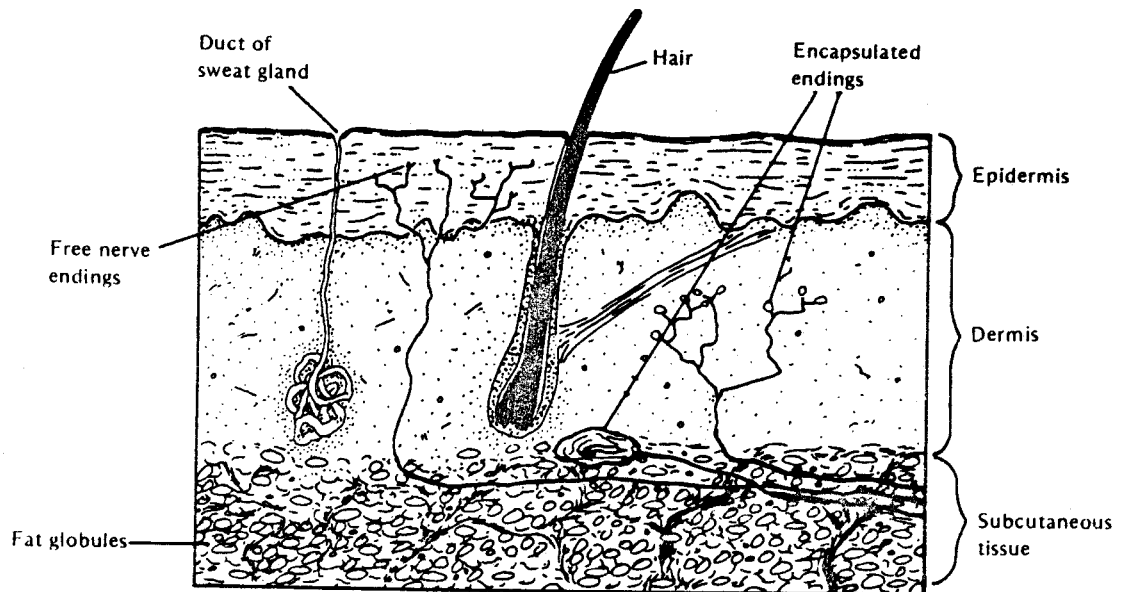


Figure 1.1: Structure of a typical hairy skin [from Matlin [6], page 202, Fig. 9-2].

nerve impulses that determines the sensation. According to this theory, each kind of receptor responds to many different kinds of stimulations, but it responds more to some than to others. For example, a particular receptor might respond vigorously to a cold stimulus, less vigorously to a tactile stimulus, and even less to a pain stimulus. The brain can eventually interpret a code in terms of the relative strengths of the receptor responses. Melzack and Wall [7] have proposed a theory which combines both of the above theories. According to this Combined theory, receptors are different from one another, and each kind of receptor is specialised so that it can convert a particular kind of stimulus into a specific pattern of impulses. This theory was developed with regard to pain perception and is popularly known as the **Gate control theory** [8], [9], [10].

There are two separate systems by which information travels from the skin receptors to the brain; the Lemniscal system and the Spinothalamic system [6]. Several factors distinguish the two systems. For example, the Lemniscal system has large fibres which convey information very quickly. In contrast, the Spinothalamic system has small nerve fibres which carry information more slowly. The acuity of the Lemniscal system is much

greater, and it can transmit very precise information about the physical location of the stimulus. Both Lemniscal and Spinothalamic systems pass their information to the somatosensory cortex of the brain.

The tactile sensors in the grasping surfaces of a human hand are classified into four predominant types; Type I, which are surficial, Type II which are deeply embedded, FA which are fast adapting, and SA which are slow adapting [11]. By measuring the nerve signals from these tactile sensors it has been shown [1], [12] and [13] that manipulation in humans is event driven, and the tactile sensors provide information about the progress of the task.

1.1.2. Mechanical grasping

When the gripper of a robot contacts an object to perform a grasping or releasing operation, the forces acting on each tactile sensing element (tactel) will vary with time. When the object is firmly grasped, the force variation will become small, and if the object is fully released, the value of the force as well as the force variation will become zero. While handling an object, the gripper status can therefore be either grasping the object, releasing the object, or neither grasping nor releasing. In each of these three states of the gripper, the object can experience slip. These states, and the relationships between them are illustrated in Figure 1.2.

1.2. Statement of Objectives

The objective of the project has been to design and develop a task oriented procedure using concepts of human tactile sensing theories. The goal is to use ideas from the Pattern theory of interpretation of stimulating impulses for skin sensing as a basis for analysis of instantaneous forces acting on each tactile sensing element while a gripper contacts an object. The word "task" as used here will refer to a grasping or a releasing operation performed by a gripper system. A laboratory prototype tactile sensing system will be used to measure the instantaneous normal forces acting on each tactile element.

A procedure will be developed to process and interpret force signals from gripper fingers in order to determine quantified decision parameters. The decision parameters will be interpreted to identify the status of the gripper during the performance of a task. The task oriented procedure will be implemented in the form of an integrated computer program which will be executed on a dedicated work station. The performance testing and validation of the procedure will be carried out using stored real time task data obtained while performing a selected set of grasping and releasing operations.

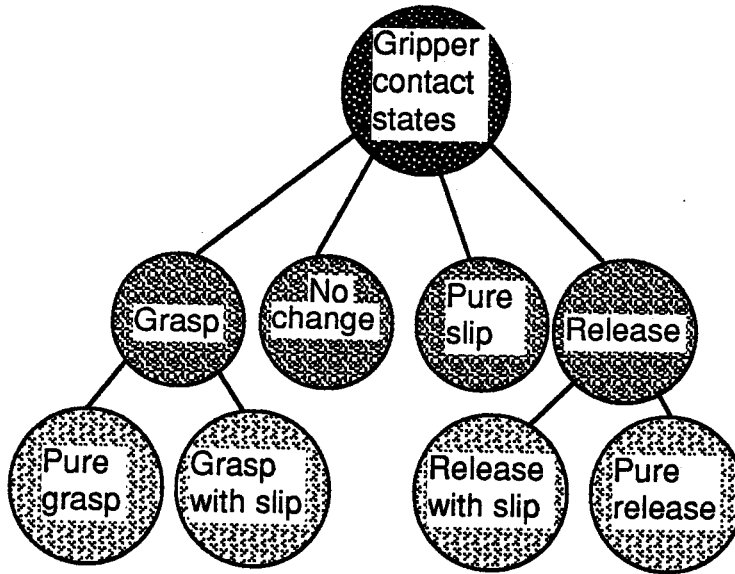


Figure 1.2: Gripper states during grasping and releasing.

1.3. Overview of the Thesis

In order to achieve the stated objectives, a number of activities were carried out in the project. A comprehensive survey of the available literature in the areas of tactile sensing, dextrous manipulation and robot gripper mechanisms was done in order to gain knowledge about the current state of the art in robotic grasping and object manipulation using tactile sensors. An overview of this survey is presented in Chapter 2.

The design and development of a prototype tactile sensing and data acquisition system was carried out in order to obtain a laboratory model of a prototype gripper system. This system consisted of tactile sensors, the driving electronics, a data acquisition system and a commercial robot equipped with a parallel-jaw gripper. The design details and the implementation of this prototype system have been covered in Chapter 3.

The prototype gripper system was a nonlinear system and hence it had to be carefully modelled and calibrated. An expert system-based modelling and calibration technique was developed to facilitate this task so that changes to the system system con-

figuration could be accommodated. The implementation of the modelling technique was tested using the prototype system and the details of the development and subsequent testing are described in Chapter 4.

The next segment of the project consisted of the development of a procedure to characterize the dynamic force data acquired during real time tasks. This procedure was implemented in the form of a program as described in Chapter 5. This program considered the uncertainties and the errors present in the formulation of tactile images from raw force data. By analyzing the results of the characterization, a method to interpret the tactile images in order to obtain useful information was developed.

Formulation of the task status decisions was done in two stages. In the first stage, a decision filter was designed and implemented to obtain a set of decision parameters by processing the tactile image, as discussed in Chapter 6. In the subsequent stage, which is also described in Chapter 6, these decision parameters were interpreted by an expert system.

The programs designed to process the raw force data to obtain tactile images, determine the decision parameters using these images, and the expert system which was developed to interpret the decision parameters were integrated into a single computer program. The details of this software integration, its testing and performance evaluation are described in Chapter 7. To validate the task oriented procedure, a number of tests belonging to different categories of tasks were conducted. The performance evaluation of the complete procedure was done using the real time task data. Chapter 7 also describes the design and implementation of a control decision indicator expert system which was used for validating the task status decisions obtained from the integrated procedure.

The major contributions and the significant conclusions drawn from the investigation have been summarized in Chapter 8. Potential areas for further investigations have also been identified.

Technical specifications of the RM-101 Microbot robot were used in order to develop an external gripper motor controller circuit. This circuit was designed using discrete electronic components as discussed in Appendix A. A typical user session with the modelling and calibration expert system and the listing of the knowledge base used by this expert system have been documented in Appendix C. The listing of a typical user session with the task status indicator expert system has been given in Appendix I. The performance validation results of the task oriented procedure are presented in Appendices D to H.

2. TACTILE SENSING, HUMAN GRASPING AND RECENT DEVELOPMENTS

2.1. Introduction

Much research in tactile sensor-based robot hands to perform dextrous gripping operations is currently directed toward the investigation of autonomous gripping mechanisms using a variety of techniques. The potential application of tactile systems in robotic end-effectors have been established. Contact imaging is being performed using the tactile systems which sense static forces and displacements. However, it is believed that more research is needed in the area of gripping and dextrous manipulation to cater to future assembly tasks which will require intelligent gripping in an unstructured environment.

In this chapter, the definition and main principles of tactile sensing are given and the evolution of the topic since 1970 is traced. The grasping process in humans has been described using the nature of forces recorded during a typical lifting operation. A review of literature on tactile sensing, grasping, and manipulation, highlights the diversity of techniques tried out at various research laboratories. The principles tried out by various investigators will be briefly outlined. A summary of the areas to be investigated further, in order to develop a truly intelligent robotic gripper, has been given at the end of this chapter.

2.2. Tactile Sensing

Tactile sensing is defined [119] as a continuous sensing of variable contact forces, commonly by an array of sensors. Ideally, it should be possible to perform continuous sensing in an arbitrary three dimensional space. According to this, touch sensing may be defined as a binary sensing process which is a simple contact detection at one or a few points [14]. Tactile sensing generally refers to devices having skin-like properties, where areas of force sensitive or displacement sensitive surfaces are capable of detecting many levels of force and patterns of touch.

ing may be considered as a two stage process including both transduc-
processing. Transduction occurs when features of an object being ex-

14v1

WL =

WH =

amed are converted into signals of some form, as in the case of the conversion of forces into electrical impulses. Data processing then interprets these signals to obtain useful information about the features of interest.

2.3. History and Evolution of Tactile Sensing

Interest in touch sensing for a flexible robot dates back to that period when researchers recognised the need for contact feedback, especially in remote manipulation in radiation contaminated areas or in other dangerous or remote places. A major problem however was and still is the lack of adequate commercial tactile sensors. Among the first to report pattern classification of a grasped object by an artificial hand, were Kinoshita, Aida and Mori in 1973 [15]. The artificial hand had an array of 20 pressure sensitive elements (5 rows by 4 columns) and the shape of a surface was identified during a single grasp. Similar tactile array arrangements placed on a tong shaped hand were reported by Hill and Sword in 1973 [16]. Until 1979, touch sensing technology for robotics was still in its infancy [14]. Industrial and other commercially available manipulators having touch capability were crude devices using simple limit switches, potentiometers, and photo electric sensors. Some other primitive (but useful) force sensing systems monitored air pressure or electric currents. Most provided binary signalling only.

Laboratory developments reported in the last decade [14] demonstrated many new approaches. Multi-jointed fingers and hands employed pressure sensitive conductive material. Simple point sensing arrays (3×3 , 4×4) showed early success in discriminating generic geometric shapes by touch (e.g. cube, cylinder, pyramid). Other laboratory developments indicated that the same simple tactile arrays could detect object surface characteristics such as ridges, edges, pits and cracks. Strain gauge technology, semiconductor arrays and conductive polymers were being used for force, torque, slip and simple pattern sensing. A number of ingenious proximity sensing systems (e.g. optical, ultrasonic) were being considered as possible alternatives to touch and vision. By 1985, a number of approaches for tactile sensing were reported. The principles of operation, characteristics, and the relative merits and demerits of the important tactile and slip sensors are reported by Vaidyanathan [17].

2.4. Grasping and Object Handling by Humans

Grasping and holding an object with a hand is a complex mechanical process which involves many sensors, control systems, and actuators. Figure 2.1 shows some of the forces occurring during a lifting operation [18].

The sequence of operations performed were lifting an object from the table, holding

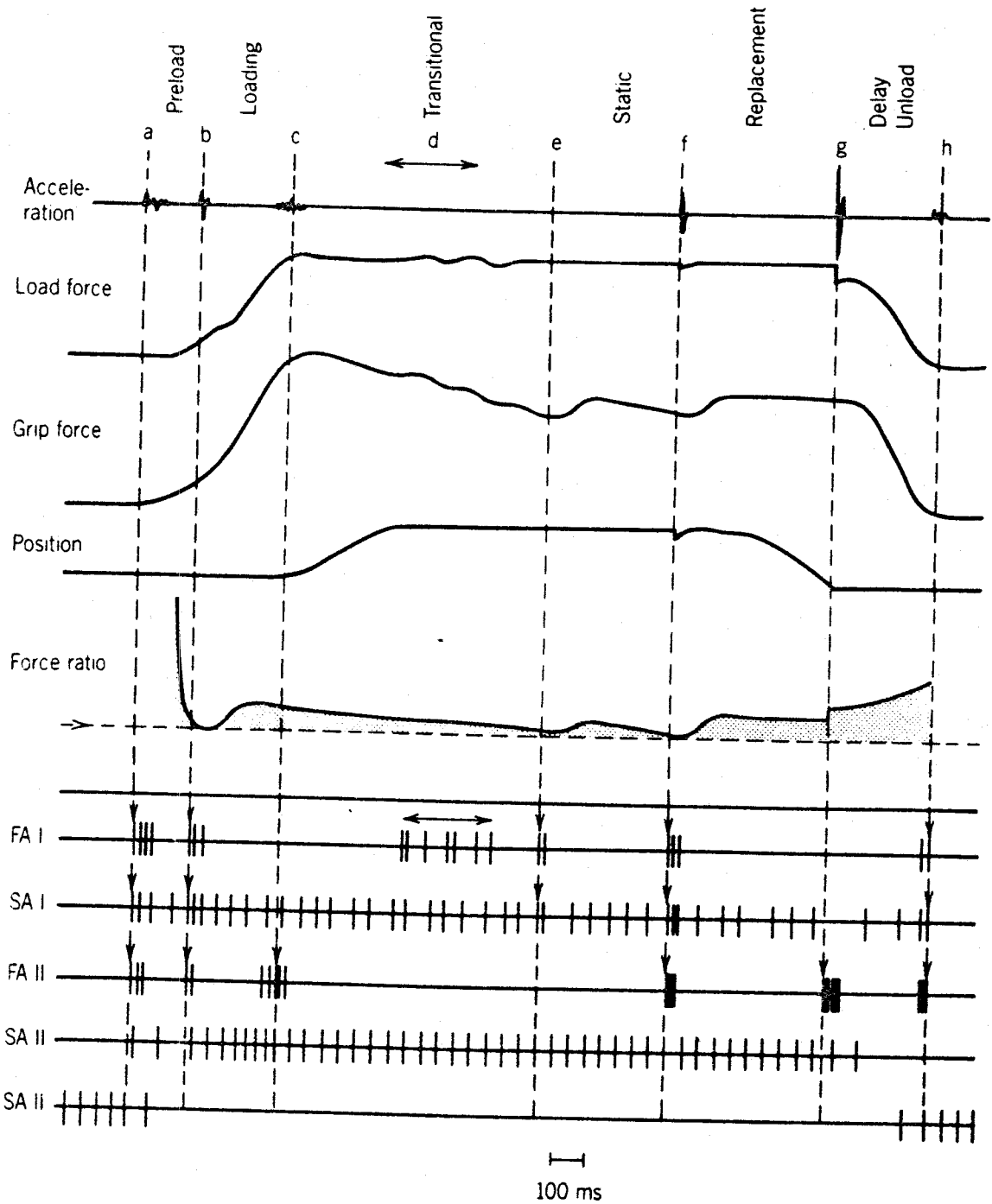


Figure 2.1: Forces during a human lifting operation and various afferent responses [from Westling [18], 1986, Fig. 8].

it in mid-air and placing it back on the table. These have been divided into seven distinct phases: preload, loading, transitional, static, replacement, delay and unload. The load force was the force exerted by the weight of the object, the grip force was measured perpendicular to the load force, and the position was measured from the table. When a grip was established, (preload phase), the load and grip force increased in parallel until the load force overcame gravity and load movement started. The transitional phase is the

phase during which the load was raised to a pre-determined height. In the following static phase, no work was done and the ratio of the two forces remained constant as the height of the load remained steady. After replacement, there was a delay before unloading. During the unloading phase, the load and grip forces decreased in parallel. The ratio of grip to load force during the loading and unloading phase was approximately constant. The minimal grip/load ratio which prevented the object from slipping is called the "slip ratio". The slip ratio depends on the frictional coefficient between the object and the skin.

By experimenting with different surface materials, Johansson and Westling [1] have determined a relationship between the slip ratio and the coefficient of friction. It was also observed that the profiles of the motion and the load force were not affected by the surface conditions. However, there was a significant change in the profile of grip forces. Both the rate of change of grip force and the final value of grip force increased with the degree of smoothness. The slip ratios showed that force coordination was adjusted to the frictional condition of the surface and provided a lower slip ratio for rougher surfaces. The weight of the object did not affect the slip ratio but influenced the duration of the force change. By anesthetizing the fingertips, Westling and Johansson [19] have found that the profile of the grip force and load force does not change indicating that there is no automatic adaptation to frictional conditions. By localizing the tactile afferents, it was found that tactile signals guide the force coordination to the frictional limiting conditions. Figure 2.1 shows the various kinds of afferent responses observed in the four types of tactile units.

The tactile units, FAI, FAII, SAI and SAII, are defined in Figure 2.2. The mechanoreceptors, which belong to a "slowly adapting" class, are designated as SA receptors while those belonging to the "rapidly adapting" class are called FA receptors. Each adaptation class is further divided into two types, namely, type I and type II, based on their number densities and areas of receptive fields. Type I receptors are better at supplying information on velocity or movement, and type II are better for static stimulation. The graphs in the middle portion of Figure 2.2 show the schematic of an impulse discharge (lower traces) due to perpendicular ramp indentations of the skin (upper traces) for each unit type. The dark patches and the dashed areas of the drawings of the hand on the left show the extent of typical receptive fields for type-I and type-II units, while the drawings on the right show the average densities of the two units.

Referring to Figure 2.1, Event (a) is the initial touch which results in responses in all the four tactile units, FAI, FAII, SAI and SAII. Event (b) indicates slip during the loading phase, which elicits tactile slip responses in FAI, SAI and FAII units. Subsequently, the force ratio was upgraded [18] and the beginning of the vertical movement is identified by FAII units. FAI movements were detected during periods of pronounced physiological muscle tremor as shown in (d), and at the instant (e) the activities in FAI and SAI units

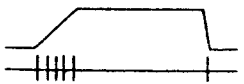
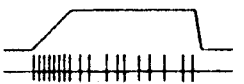
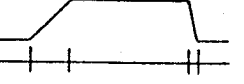
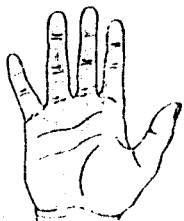
		ADAPTATION			
		Fast, no static response	Slow, static response present		
RECEPTIVE FIELDS	Small, sharp borders 	 FAI (43%) Meissner	 Irregular Edge sensitive SAI (25%) Merkel		INNERVATION DENSITY
	Large, obscure borders 	 FAII (13%) Pacini Golgi-Mazzoni	 Regular Sensitive to lateral skin stretch SAII (19%) Ruffini		

Figure 2.2: Tactile units in a typical human hand and some of their features [from Westling [18], 1986, Fig. 1].

due to localized slip were observed. At the event (f), slip-triggered responses in FAI, SAI and FAII units cause an upgrading of the force ratio during the static phase. There is a burst at the moment of support contact as shown at (g) and the final release responses in FAI, SAI and FAII units occur at (g).

These human grasping principles may be summarized [2] as follows: adaptation of force coordination to frictional changes occurs for a variety of tasks during precision grip. The adaptation process depends only on the coefficient of friction and not on the texture properties of the surface. The force to load ratio is automatically maintained at a level adequate for the current frictional demands. However, the final steady state force depends on the surface friction.

Those features of human grasping which have been clearly identified and which could be readily implemented using artificial tactile sensors were considered in the development of this project. The concepts used were based on the Pattern theory of tactile sensing, which states that tactile sensing in humans is performed by a number of similar type of sensors which are responsive to the intensity of force rather than the type of force.

Subsequent processing of the tactile signals is performed by the Central Nervous System which considers both the spatial and time varying nature of these signals in order to interpret them. Similar type of sensing, processing and interpretation were considered appropriate for a task oriented procedure designed and developed in this project.

2.5. Survey of Selected Literature

Recent work on dextrous manipulation in machines covers a wide range of areas which include tactile sensing, stability and optimization of grasp, dynamic control, and specific issues directly related to perception, such as geometric modelling, active touch, and uncertainties. Only a brief overview of some of these techniques is presented in the following section to provide a perspective of the current technology in tactile sensing for analysis and control of mechanical grasping.

The design of tactile sensing arrays has been attempted by many researchers throughout the world. This work has resulted in the investigation of practically every conceivable means of force and displacement transduction. A variety of tactile sensing arrays have been reported, some of which rival the spatial densities of sensors on the human hand [20]. The phenomena that have been investigated include elastomeric piezoresistance, piezoelectricity, optical reflection and absorption, capacitance, inductance, magnetostriction and a score of others. Surveys of tactile sensing research [14] reflect a greater emphasis on transduction techniques rather than on tactile data interpretation [21].

A comprehensive bibliography of earlier work on tactile sensing has been compiled by Harmon [22]. Jacobsen et al. [23] have discussed the general issues and trade-offs governing the design of extended tactile sensing systems with special emphasis on practical necessities such as simplicity, reliability, and economy. Recently, a high resolution tactile sensor consisting of a 64 by 64 element array has been discussed by Clark [24] based on the idea of compliance matching. Here, the high compliance of the contacting element is matched to the low compliance of the sensing element using a magnetic field as the matching medium.

Analysis and synthesis of stability in static grasps have been extensively studied for different types of finger configurations, contact types, and object types. The idea of point contact with friction dominates most of the characterizations. Stability of grasps with soft fingers leading to the development of analytic techniques for automated grasp has been studied by Jameson [25]. In his thesis, he deals with statically indeterminate grasps with distributed contacts. Using a model-based optimization technique, both first order stability (perturbation due to sliding motion), and second order stability (perturbation due to the compliance of the load) were analyzed, and criteria for the maintenance of a secure

dynamic grasp during manipulation were suggested. Jameson and Leifer [26] have proposed a method for the synthesis of stable grasps. Given geometric models of the object and the gripper, a stable grasp is found by optimizing a grasp goal function, which represents how far away the grasp is from stability. Physical constraints like torque and motion are included. Using point contacts without friction, stable force closure grasps have been synthesised in 2 dimensions [27] and 3 dimensions [28] by determining appropriate relations between the stiffness of the grasp and the spatial configurations of virtual springs at the contact. An algorithm [29] for constructing force closure grasps based on the shape of the grasped object has also been proposed. This method finds independent regions of contact for the fingertips such that the motion of the grasped object is totally constrained. By constraining objects to belong to a particular class, Berkemeier and Fearing [30] have suggested a technique to determine the axis of the surface of revolution using three tactile curvature measurements.

In contrast to the above methods which deal with static grasping, Fearing [31] has proposed a method for stable grasping of polygonal objects when object models are not available. Assuming point contact with friction (with no moments), local tactile information is used to determine finger motion in the presence of disturbances and uncertainty in contact locations. A stable force strategy for regrasping and part re-orientation has also been proposed by Fearing [32]. To estimate the dynamic forces on tactile sensors containing viscoelastic materials, he has advocated the use of a Maxwell-Kelvin model instead of an elastic model [33]. Once a dynamic modelling technique is developed, this could be used to advantage. Further details of this model are presented in Section 4.4.5.

Three basic problems of grasp optimization have been defined by Kerr and Roth [34]. They are the following: how hard to squeeze for a secure grasp, what finger motions are required to produce the desired motion, and, what is the useful work area of the hand. By using constraints imposed by the object (based on its CAD geometry), task (at every stage of the gripping process), and gripper characteristics, the problem of grasp optimization has been unified by Feddema and Ahmed [35]. Kerr and Roth have also analyzed over-constrained, under-constrained and degenerate grasping configurations [36]. For known geometries of objects, Yoshikawa [37] has proposed a method of determining gripping positions automatically. He has used resilience to slippage and twisting of the gripper due to external forces as criteria for determining stability.

Yoshikawa and Zheng [38] have proposed a co-operative dynamic hybrid force control method for simultaneous control of object motion and internal forces exerted by the arms or the fingers on the object. Both the manipulator dynamics and object dynamics have been considered for their formulations. Using dynamic models for two coordinated robots, Dudar and Eltimsahy [39] have proposed a near-minimum time controller for object manipulation. The dynamic models are updated at every control interval and bang-

bang control theory, in conjunction with synchronization of execution times, is used to derive the control laws. A process-based model of robot task plan representation has been described by Lyons [40]. Using techniques of process algebra, the author has introduced a way to analyze plans for efficiency and has indicated a method for plan generation.

An algorithm for finding the distribution of force among fingers based on superposition of finger-interaction forces and equilibrating forces is proposed by Kumar and Waldron [41]. Cutkosky and Wright [42] have suggested that the use of compliant materials on gripping surfaces of a robotic hand leads to the development of models for pointed, curved, flat, soft and soft-curved fingertips. By comparing these models in terms of their contribution to stiffness and stability of a simple grasp, a grip taxonomy has been established in order to codify knowledge for manipulation in small batch manufacturing. Fabrication of electrorheological (ER) fluid-based robotic fingers with tactile sensing capability has been described by Kenaley and Cutkosky [43]. Compatibility between skin materials and ER fluids and the causes and prevention of fluid stratification and electrical arcing have also been discussed by the authors. The visco-plastic nature of soft fingertips affects the dynamics of manipulation by dissipating energy. Prasad et al. [44] have discussed this effect in the context of simulating manipulator dynamics.

Based on the singular values of a grasp matrix, three measures for grasp evaluation in the force domain have been proposed by Li and Shastry [45]. One of these measures, which is task oriented, models tasks as ellipsoids in wrench space. A complete and parametrically continuous kinematic model for robot calibration has been described by Zhuang et al. [46]. The parametric continuity of such a model has been achieved by a singularity-free line representation.

Tomovic, Bekey and Karplus [47] have proposed a comprehensive framework for high level grasp control which consists of the following : (i) a target approach phase, which includes target identification, hand preshaping and orientation (ii) a grasp execution phase, which includes shape and force adaptation, and (iii) a reflex control phase, which uses a knowledge base for the design of human operator interface, trajectory generation, a hand structure generation, and manipulator control.

A high level control mechanism in a distributed computing environment has been proposed by Lyons [48] wherein, the characteristics of the object to be grasped as well as the actions to be performed are considered. The grasp is characterised by the preshaped finger configuration and the degrees of freedom of the hand once the object has been grasped. However, the author does not take into account the slippage of the object in the grip phase of the motion control where forces applied by the fingers to any object are considered [49]. The force, dynamics, and local obstacle avoidance issues are also ig-

nored during the manipulation phase. Using stiffness control and tension management, Biggers, Jacobsen and Gerpheide [50] have discussed the low level control of the Utah/MIT hand. The paper ignores the dynamic modelling effects, and adaptation to time varying conditions when different objects are grasped.

Shape recovery is an important task for self teaching robots and for exploratory operations in unknown environments. The concept of virtual fingers is used as the organizing principle for the theory of prehension in general, and a grasp taxonomy in particular by Iberall [51]. Potential theory [52] has been used to specify preshaping configurations of the hand in which tagged potentials allow limbs to react differentially to fields. An algorithm which directs a position controlled robot around an unknown planar contour using the steady state contact force information has been described by Ahmad and Lee [53].

It has been suggested that vision can be used to guide active tactile systems [54]. Constraints and some strategies for active touch exploration have been proposed by Roberts [55]. Jacobsen [23] et al. have discussed the general issues and trade-offs governing the design of extended tactile sensing systems with special emphasis on practical necessities such as simplicity, reliability and economy. Tactile perception with an active exploratory finger has been discussed by Dario et al [56] [57]. Based on an hierarchical control architecture, a high level planner supervises the execution of tactile primitives based on the shape, texture, and temperature. The dynamic selection of sensors for interrogation, and subsequent information retrieval and integration are described by Jacobsen et al [58]. Some of the key issues discussed are selection of sensor density, location, resolution and their utility during grasping and manipulation.

Using principles from human haptics, Allen [59] has built an intelligent robotic system that can perform shape recognition from touch sensing. He has found a number of mappings between exploratory procedures and shape modelling primitives and presents results from experiments with the Utah-MIT dextrous hand system. A vision algorithm to complement active touch sensing is also described. Paul, Durrant-Whyte and Mintz [60] have proposed a distributed network of intelligent agents for sensing, action and reasoning as part of a robust robot control system. These agents are linked by a blackboard architecture and are used to integrate uncertain and partial observations from vision, range, touch, force and motion sensors. A fully decentralized architecture for multi-sensor data fusion has been developed and implemented by Durrant-Whyte et al. [61]. A current survey of the state of the art in multi-sensor fusion has been presented by Hackett and Shah [62].

A quantitative approach to the integration and propagation of disparate sensor observations is discussed by Durrant-Whyte [63]. Using partial and uncertain geometric

sensor observations, robust and consistent estimates of the state of the environment are derived. A Bayes procedure compares the disparate observations of the geometric features, rejects spurious measurements, and provides updated information about object location to a world model. Smith and Cheeseman [64] also describe a Bayesian representation of spatial uncertainty. By modelling tasks as geometric goals in configuration space, Brost [65] discusses motion planning in the presence of uncertainty. Uncertainties in sensing, control and geometric model of the robot are also discussed by Donald [66] who has derived a method for error detection and recovery.

Development of a mathematical model for a photoelastic touch sensor based on continuum mechanics and stress analysis techniques is reported by Cameron et al [67]. A light weight end-effector for a commercial robot manipulator based on impedance control has been designed and built by Kazerooni [68]. The device, which is a planar five-bar linkage driven by two direct-drive brushless DC motors, consists of a two-dimensional piezo-electric force cell on the endpoint of the device. Two 12-bit encoders and two tachometers on the motors form the measurement system which has a 15 Hz bandwidth impedance control. The bandwidth is determined by the high structural stiffness and light weight of the material used in the system. Recently, Kazerooni (op cit.) has analyzed the dynamics and control of robotic systems worn by humans. These "Extenders", which are a class of robotic manipulators worn by humans to increase mechanical strength, act as a robotic system controlled by the wearer.

Based on the kinematics of contact, Montana [69] has derived a set of equations called contact equations to determine the curvature form of an unknown object at a point of contact. He employs these equations to follow the surface of an unknown object using an end-effector with tactile sensing capability. The paper also explores two specific applications, namely, rolling a sphere between two arbitrarily shaped fingers, and, fine grip adjustment, having two fingers that grasp an unknown object locally optimize their grip for maximum stability. A computationally efficient method of calculating the finger forces in the case of point contacts with friction without using Jacobians has been derived by Hollerbach, Narasimhan and Wood [70]. A tactile array sensor for object identification using complex moments has been proposed by Luo and Loh [71]. Some complex moment invariants have been derived and implemented to eliminate the effects of lateral displacement and rotation from tactile images.

Intelligent control of multi-fingered robot hands implemented by integrating perception and action has been attempted by Stephanou and Erkmen [49]. In their work, a classification algorithm based on Fuzzy Set theory determines the most appropriate grasp, given an incompletely specified descriptions of an object and a manipulation task. This algorithm generates a "grasp" situation by recognizing two components: the graspable points of 3-D objects in the manipulation environment, and the grasp characteristics of the given task. The algorithm has been illustrated with an example.

Sensing of small accelerations of the outer skin covering of the fingers of a manipulator has been proposed by Howe and Cutkosky [72]. Using test results, the ability of the scheme to detect the onset of slip has been verified. The use of tactile sensors to enhance the flexibility and robustness of robotic manipulation has been described by Howe et al. [73]. They have obtained information about the changing contact conditions of a two-fingered gripper using dynamic tactile sensors.

A system for extracting feature information in different application contexts has been described by Falcidieno and Giannini [74]. This procedure consists of two steps; the first step starts from the boundary of an object and identifies pre-defined generic shape features by considering only geometric and topological aspects. These features are classified in the second step according to their functional meaning in the application context. Other interesting results reported include model-based recognition of planar polygons [75] and polyhedra [76] from sparse data, and determination of contact geometry from force measurements [77]. An algorithm for the recognition and localization of 3 dimensional polyhedral objects based on an optical proximity sensor system capable of measuring the depth and local area of an object surface has been proposed by Lee and Hahn [78].

Erdmann [79] has proposed that randomization can be used as a useful primitive in the solution of robot tasks. According to the author, randomization can increase the class of solvable tasks, can reduce a strategy's knowledge requirements and simplify the planning and execution process. Planning of multi-fingered dextrous grasps to meet physical constraints of some anticipated actions has been proposed by Nguyen and Stephanou [80] using an hierarchy of topological and geometrical spaces. The algorithm has been illustrated by a pinch grasp example using a stick model of a four fingered hand.

For implementing real time robotic systems, a programming environment called "CHIMERA II" has been developed at Carnegie Mellon University [81]. This supports flexible hardware configurations which are based on one or more VME-backplanes. This provides a real time kernel which supports deadline and highest-priority-first scheduling. Grasping of a moving target to adaptively control a robot manipulator has been proposed by Houshangi [82]. An auto-regressive discrete-time model has been used to predict the future position of an end-effector; its relation to the current end-effector position is used to determine the desired trajectory. On-line changes to the target are also accommodated by the planner.

The use of kinematic redundancy in reducing impact and contact effects in manipulators has been studied by Walker [83]. He has shown how manipulator redundancy may be used to configure mechanisms so as to reduce resulting impulsive contact forces at the instant of contact. The investigation of the stability and control of robotic

manipulators during the execution of tasks that require a manipulator to make a transition from non-contact motion to contact motion, or vice versa, has been reported by Mills [84]. Experiments in automatic collision avoidance for robots using acceleration-based reflex control for industrial manipulators have been conducted by Newman and Branicky [85] and the results have been used for designing higher levels of hierarchical controls.

A Bayesian framework has been applied to a grasping task by Goldberg and Mason [86] to obtain a method of autonomous manipulation in the presence of state uncertainties. In situations where the manipulation tasks are relatively simple, a knowledge-based robotic grasping technique, which uses computer vision and a limited amount of heuristics, has been proposed by Stansfield [87]. In this article, the implementation of a two-stage grasping process, in which the first stage orients the hand and the wrist and reaches the object while the second stage performs hand preshaping and adjustments, using an expert system, has been described by the author.

A learning system implemented in a real-world robot for sensing objects and selecting appropriate grasping procedures in a cost effective way has been proposed by Tan [88]. A scheme for searching for a contact point between a multi-fingered hand and an unknown object has been described by Kaneko and Tanie [89]. The scheme consists of two phases, the approach phase and the detection phase. In the approach phase, each finger is widely opened and approaches an object until a part of a finger link contacts the object. In the detection phase, each finger posture is changed even allowing slip, while maintaining contact between the object and the finger. Using two selected postures during the detection phase, an intersection point is obtained as the approximate contact point. Automatic grasping using a combination of partial geometric models and vision data has been proposed by Laugier and Troccaz [90]. In their work, the robot motions and sensing operations are combined to acquire information to guide grasping movements.

A grasp quality has been defined by Park and Starr [91] using two indices - uncertainty grasp index and task compatibility grasp index. The uncertainty grasp index represents the effect of grasp position error on stable grasp while the task compatibility grasp index represents how well the identified grasp can perform the task. Formulation of an optimization problem to compute the grasp index and its solution procedure has also been described by Park and Starr (op cit.).

2.6. Summary of the State-of-the-art

In spite of the progress in various areas of dextrous manipulation, little has been reported on substantially universal methods which show how machine manipulation can productively utilize tactile information in an industrial environment. Development of enhanced grasping skills for robots needs further research into all the topics in dextrous manipulation currently being investigated. The development of a sensory gripper which uses optical tactile sensors for three-dimensional object recognition, orientation control and manipulation has been recently reported by Mehdian and Rahnejat [120]. The absence of a single rigorous tactile sensing theory to explicitly specify important system parameters such as sensor density, resolution, location, and bandwidth is perhaps the reason why robotic touch has been implemented in its most rudimentary forms and only a few substantial tactile systems are commercially available. The main obstacle in this area seems to be that of understanding the relationship between mechanical, sensing, and control aspects of the manipulator. The real time operation of the manipulator essentially depends on how the above aspects interact with the environment.

2.7. Concluding Remarks

This chapter has outlined the basic principles of tactile sensing and reviewed its history and evolution over the last two decades. A framework for understanding the human grasping mechanism, based on Johansson and Westling's experiments with human subjects, was provided and important aspects of these techniques applicable for robotic grasping were indicated. A comprehensive survey of research work carried out in the areas of dextrous manipulation, grasping and tactile sensing has been conducted to determine possible future directions for investigation. The research problems which are yet to be solved have also been briefly stated.

The next chapter will describe the design and specifications of the major hardware components used to build a laboratory prototype gripper system.

3. HARDWARE SPECIFICATIONS AND DESIGN OF THE PROTOTYPE GRIPPER SYSTEM

3.1. Introduction

Commercially available tactile sensing devices have not been advanced past the rudimentary sensing options provided by manipulator manufacturers. In order to build a prototype gripper system to facilitate acquisition of dynamic forces during a task, a tactile sensing system was first designed and built. This was interfaced to a high speed data acquisition system which provided digitized values of dynamic forces. The tactile sensors were mounted onto the gripper fingers of a robot which performed various tasks. This chapter will discuss the hardware design and characteristics of the tactile sensing system, the data acquisition unit and important specifications of the robot and its gripping mechanism used in the prototype. Selection of test samples for the study will be discussed in Chapter 7.

3.2. The Tactile Sensing System

The hardware design and fabrication of the tactile sensing system consisted of a study of criteria for the design of subsystems, the selection of components, the design of subsystems, and the integration of the subsystems to form the complete system.

The detailed design and construction of three subsystems, namely, the tactile sensor array, the energizing unit and the data acquisition system are discussed in the following sections.

3.2.1. Design specifications

The main design specifications for the tactile sensing system of the prototype gripping mechanism were based on the type of force data to be acquired. Some features of a five-fingered tactile sensing system, which was developed earlier [17], and summarized below, were used to formulate some of these specifications. Salient features of the five-fingered system were:

1. Each finger was equipped with a tactile array of 8×2 sensing sites, with each site measuring $5 \text{ mm} \times 5 \text{ mm}$.

2. Each of the five fingers had the same size and the same number of sensors, making a total of 80 sensors distributed equally among the five fingers.
3. The sensors were mounted on a finger pad made of a custom made printed circuit board having interlinking conducting patterns.
4. Each finger pad was mounted on the surface of a mechanical finger.
5. The sensing elements were held in position with tape preventing any sliding motion due to applied forces.
6. The system could interface easily with standard peripherals such as a keyboard and video terminal for performance monitoring and control.

This basic system had to be modified substantially in order to use it with a robot equipped with a two-fingered parallel-jaw gripping mechanism. The modified design and construction methods have been described in the following sections.

3.2.1.1. Basic considerations

An important consideration in the design of a tactile sensor is the mode of operation. Tactile sensors can obtain information by measuring either force or displacement. Force sensors can be used to monitor forces at a location on the finger which occur due to gripping pressures exerted by the grippers as they grasp an object while displacement sensors can be used to study surface relief properties, such as texture. The desired application often dictates the type of tactile sensor to be employed. It is also possible to use the same sensor system to measure force as well as displacement by mounting the sensor on a spring or other compliant material.

The second consideration is the data handling and output systems. High resolution tactile sensors can require a large number of connecting leads to attach the active tactile elements to processing electronics. This causes problems in the geometric layout of the sensor, due to the physical difficulty in connecting leads to the closely spaced sensors. In addition, for remote operation, the entire bundle of leads must be routed through the end-effector, taking up considerable space. For this reason, on-site data multiplexing and limited processing is desirable; a small data acquisition system consisting of multiplexers, amplifiers and analog to digital converters could considerably reduce the number of connecting leads back to the controller.

The third important aspect is the mechanical flexibility of the sensor. In some applications, it will be desirable to mount tactile sensors on an irregular surface such as an anthropomorphic end-effector. The use of a compact, lightweight, and flexible sensor for these applications would be ideal. Other important design considerations for a tactile sensor are its sensitivity, hysteresis, crosstalk, resolution and repeatability. Testing procedures must be designed to evaluate a tactile sensor's performance in each of these areas.

3.2.2. Sensor material

The material from which the sensor is constructed is of paramount importance. This is the interface between the real world and the robot gripper, and must be mechanically tough, yet compliant and flexible. The material must also convert forces and deformations into monotonically varying electrical signals for processing and analysis. The fundamental properties of electrical resistance, capacitance, inductance, or light propagation are generally considered with material properties such as piezoelectricity sometimes being employed. Capacitive techniques are quite sensitive to electrical noise and stray capacitance effects and inductive techniques use bulky hardware which are difficult to implement. A resistive technique offers several advantages, and is the method chosen for this project.

Piezoresistivity is the phenomenon in which minute displacement or strain of a sensor induces changes in the condition of conducting particles suspended in a compliant medium and gives rise to changes in the electrical contact resistance. Rubber is commonly chosen as the compliant medium, and it naturally provides a restoring force after deformation. The category of piezoresistive tactile sensors is quite broad and includes a multitude of different device types and approaches. These range from simple strain gauges and solid state silicon devices to conductive elastomers and foams. These devices are all included in this category because they rely on materials whose electrical conductivity varies with applied pressure.

The use of conductive elastomers [121] as the basis for a tactile sensor has been studied for some time. A conductive elastomer is an elastic rubber-like material that has variable electrical conductivity properties. Many different conductive elastomer and foam materials have been examined, and most of the sensor designs based on these materials use an approach similar to that used by John Purbick of MIT [92]. Most of the piezoresistive tactile sensors developed so far suffer from one or more of the problems of hysteresis, nonlinearity, sensitivity and fragility as discussed in Reference [17].

One of the few commercially available sensor materials, and the one chosen for the sensors in this project was a thick polymer film component marketed by M/S Interlink Electronics, U.S.A. Sold under the trade name of **Force Sensing Resistor**, abbreviated as FSR, it is a patented, newly developed type of thick polymer film component which has the property that the resistivity of the film decreases as increasing force is applied to it. Being a proprietary component, detailed information about its chemical composition and method of manufacture are not available. However, a brief summary of its operating modes, principal characteristics, and method of application are described here.

3.2.2.1. Force Sensing Resistor

The Force Sensing Resistor consists of a "sandwich" formed with electrically conductive polymer layers. The sensitivity and resistivity of the component depend upon the polymer formulation. The component is formed by silk screening polymer material onto Mylar sheets. The components may be formed into almost any shape and size.

There are two possible arrangements in which an FSR may be used, namely, the shunt mode and the through-conduction mode. The choice of mode for a particular application depends primarily upon economics and convenience. In the shunt mode, the sandwich is formed from a Mylar sheet, with a printed area of FSR polymer as shown in Figure 3.1. The FSR surface is laid in contact with a second surface containing a pair of interlinking conductive "fingers". When a force is directed perpendicular to the FSR area, a conducting circuit is formed between the fingers. The circuit resistance decreases as the force increases due to the greater contact area between the compressible polymer and the conducting fingers.

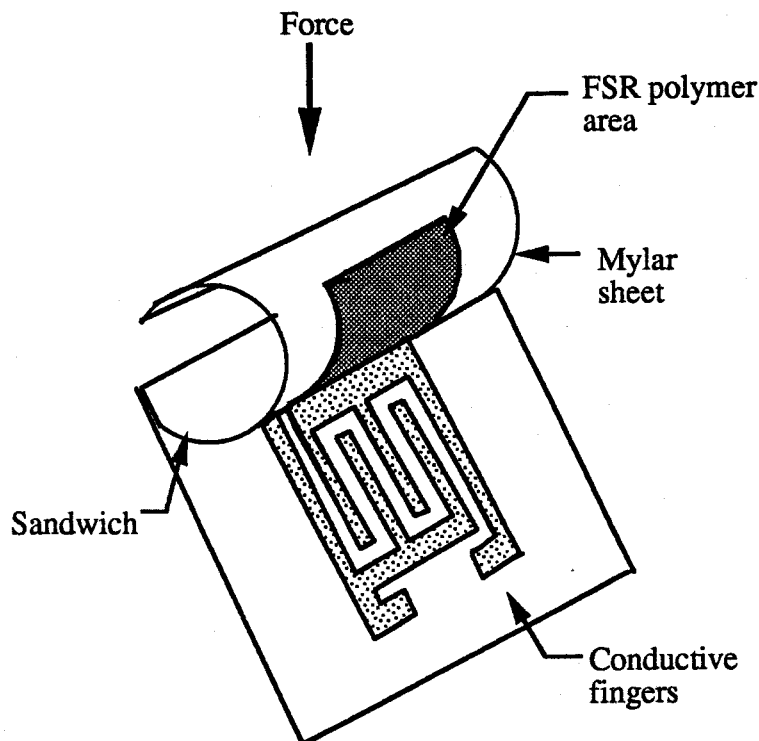


Figure 3.1: A shunt-mode style FSR [from FSR User's Manual [93], Fig.1] .

In the through-conduction mode, two similar Mylar sheets are prepared. Each sheet consists of an area of FSR polymer printed over a conductive pad. The two sheets are

sandwiched together, with the two FSR polymer areas in contact as shown in Figure 3.2. A force perpendicular to the polymer areas lowers the resistance value between the two conductive pads.

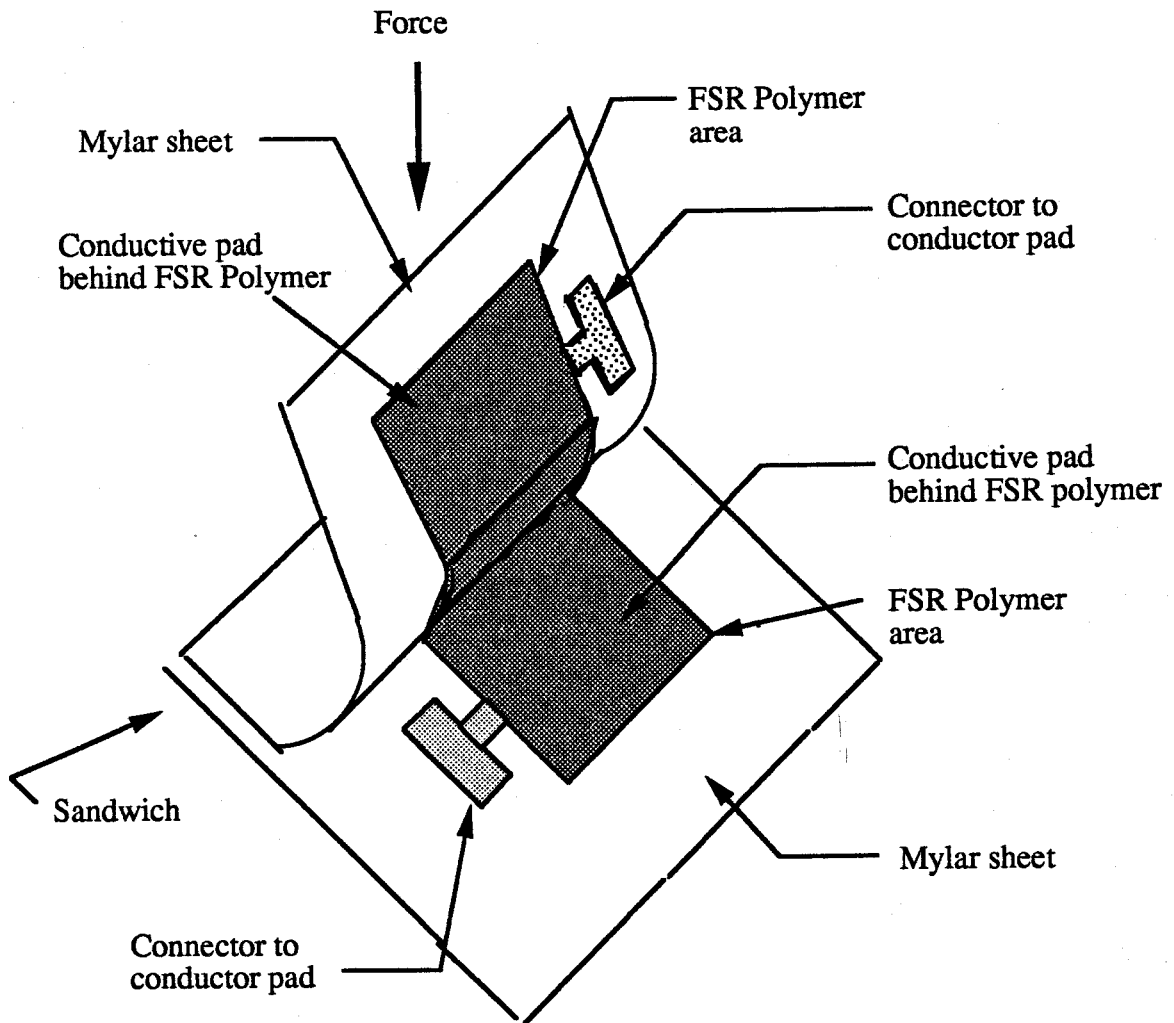


Figure 3.2: A through-conduction style FSR [from FSR User's Manual [93], Fig.2] .

For tactile sensing applications, it has been found [17] that the shunt mode is better than the through-mode. This conclusion has been confirmed by researchers at Sandia Laboratories [94].

3.2.3. Typical characteristics of an FSR element

Depending upon formulation, the operating resistance of FSRs can range from about 10 Megohms to a few hundred ohms. There are three useful working ranges as shown in Figure 3.3. They are the switch range, the linear Log/Log range, and the linear range.

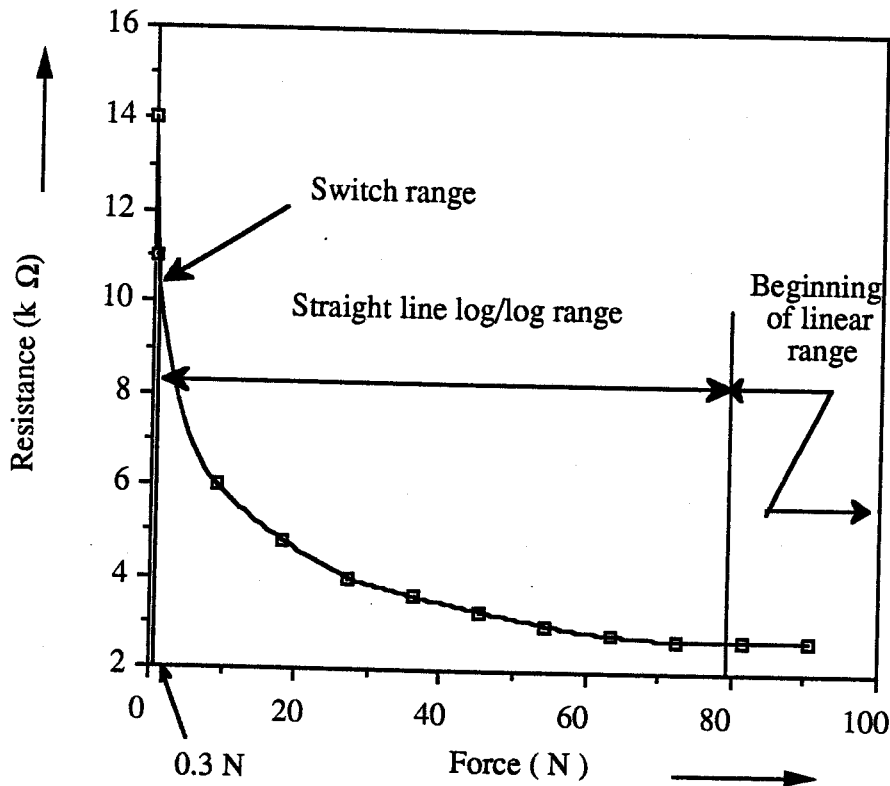


Figure 3.3: Resistance versus force for an FSR [from FSR User's Manual [93], Fig.3]

Considering a unit area of the sensor, if the applied force is between 0 to 0.3 N then the FSR will operate in its switch range. In this range the FSR exhibits very large changes in resistance and can be readily used for switching applications. In an unloaded condition, the resistance value is very high (between 10 to 100 Megohm), and a slight amount of loading (less than 0.3 N) will cause an abrupt resistance change of about a factor of one hundred.

If the FSR is loaded with a force value exceeding 0.3 N, but less than 80 N, the component responds in the linear Log/Log range. In this region, the FSR characteristics

are more stable and predictable. Therefore, this is the region chosen for most applications. If this region is re-plotted with a log/log axis, then the variation of resistance with load is approximately a straight line as shown in Figure 3.4. At still higher loads, the

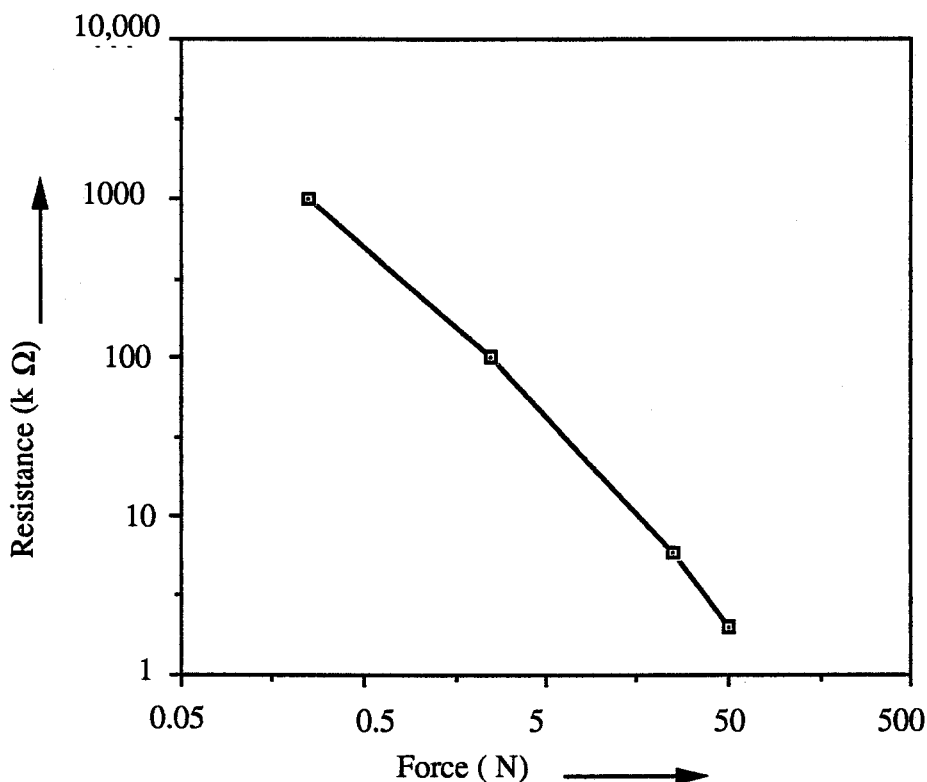


Figure 3.4: Force versus resistance on a log-log plot [from FSR User's Manual [93], Fig.4]

change of resistivity with applied load becomes small and approximately linear. For a typical FSR, this range starts above a load value of 80 N. The maximum useful load that can be measured with FSR is about 4550 N [93].

3.2.4. Design of finger pad

An FSR sample kit consisting of four sheets of silk screened FSR components in different shapes and sizes was procured from Interlink Inc. To effectively sense the variable contact forces as accurately as possible, experiments were done with various conducting patterns. Finally, an interleaved conducting pattern with approximately equal conducting areas for the sensor signal line and the ground line as shown in Figure 3.5 was designed and used for the sensor.

The main hardware features of the finger pad are listed below:

1. The overall dimensions of the sensor array of each finger pad is 50 mm × 15 mm.
2. Each sensing site consists of an interleaved pattern of a 5 mm × 5 mm square area with the pattern providing nearly equal area of conducting path for the sensor signal and ground lines.
3. Four of the sensing sites are grouped together in a 2 by 2 array and any two such adjacent areas are separated by 1 mm.
4. Adequate space is provided at the corners of the pad to enable mounting of a compliant pad over each sensing site. The signal and ground lines are brought out via the back side of the board using standard double sided PCB technology.
5. The FSR elements are cut to dimensions of 5 mm × 5 mm, and positioned accurately over the conductor patterns to minimise interference from adjacent channels.
6. The FSR sensor elements are laid in position over the conducting pattern and a compliant rubber cut in a square shape fitting exactly on top of each sensor element is laid over the sensors. The gripping forces are transmitted to the sensors through this rubber material.

3.2.5. Energizing circuit for sensors

3.2.5.1. Design criteria

In order to ascertain the range in which the FSR is to be operated for this application, some preliminary laboratory tests were conducted. A constant current source was connected across an FSR element and the voltage variations across the element were measured. The voltage across the FSR was found to vary significantly and was predictable and stable with low hysteresis. When the value of the constant current was changed, the location of the voltage versus load curve changed as predicted by the manufacturer [93]. Figure 3.6 depicts the data representing the voltage drop across the FSR plotted against the load applied to the component, with the constant current as the parameter. The principal effect of varying the constant current was to expand and contract the scales in the working area as is evident from Figure 3.6. The geometry of the printed area, and the FSR polymer chemical composition also contributed to the determination of working ranges.

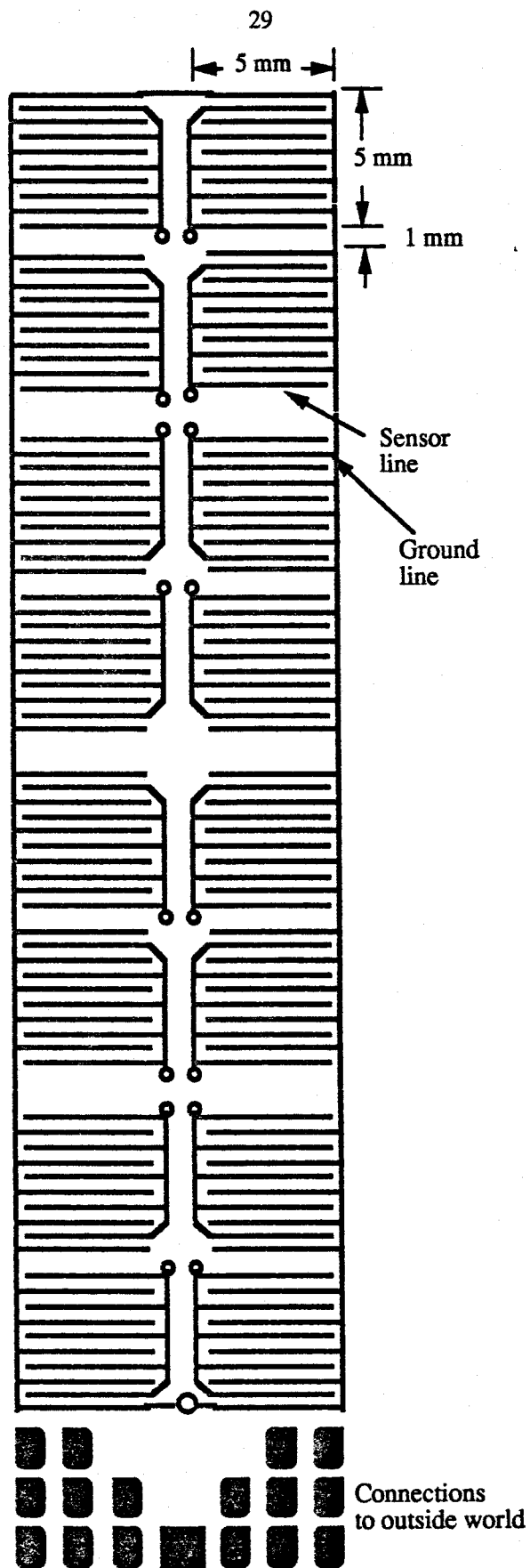


Figure 3.5: Prototype sensor array pattern .

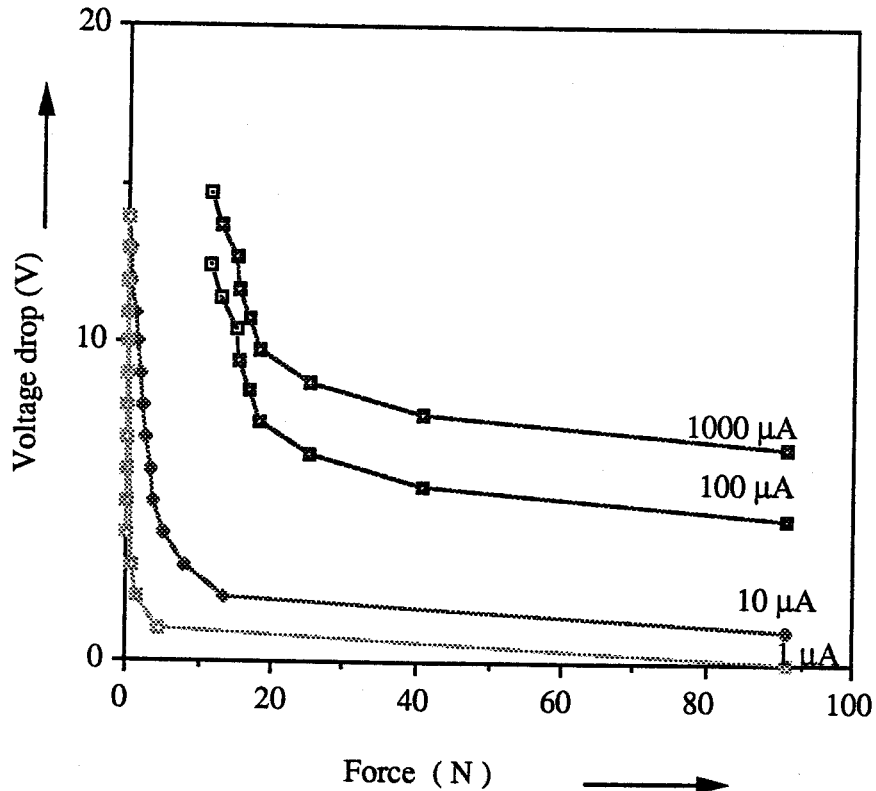


Figure 3.6: Voltage drop versus force for various currents [from FSR User's Manual [93], Fig.6]

3.2.5.2. Design of multiple output current source

The FSR component was activated by a stable, low noise constant current source in order to obtain monotonic responses. A low-noise JFET input operational amplifier (National Semiconductor current-differencing Quad amplifier, LM 3900) device was chosen. In this device, instead of using a standard differential amplifier at the input, the non-inverting input function has been achieved by making use of a "current mirror" to "mirror" the non-inverting input current about ground and then to extract this current from that which is entering the inverting input terminal. Since this amplifier differences input currents rather than voltages, it is referred to as a "Norton Amplifier" configuration.

The amplifiers of the LM3900 device were used in a feedback loop to regulate current in external PNP transistors to provide current sources. A single amplifier from the quad device was used to design a circuit to energize eight FSR elements of the tactile sensing system.

3.2.6. Implementation of multiple output constant current sources

The circuit diagram of an eight output constant current source is shown in Figure 3.7. The resistive divider network of R3 and R4 was used to establish a reference voltage

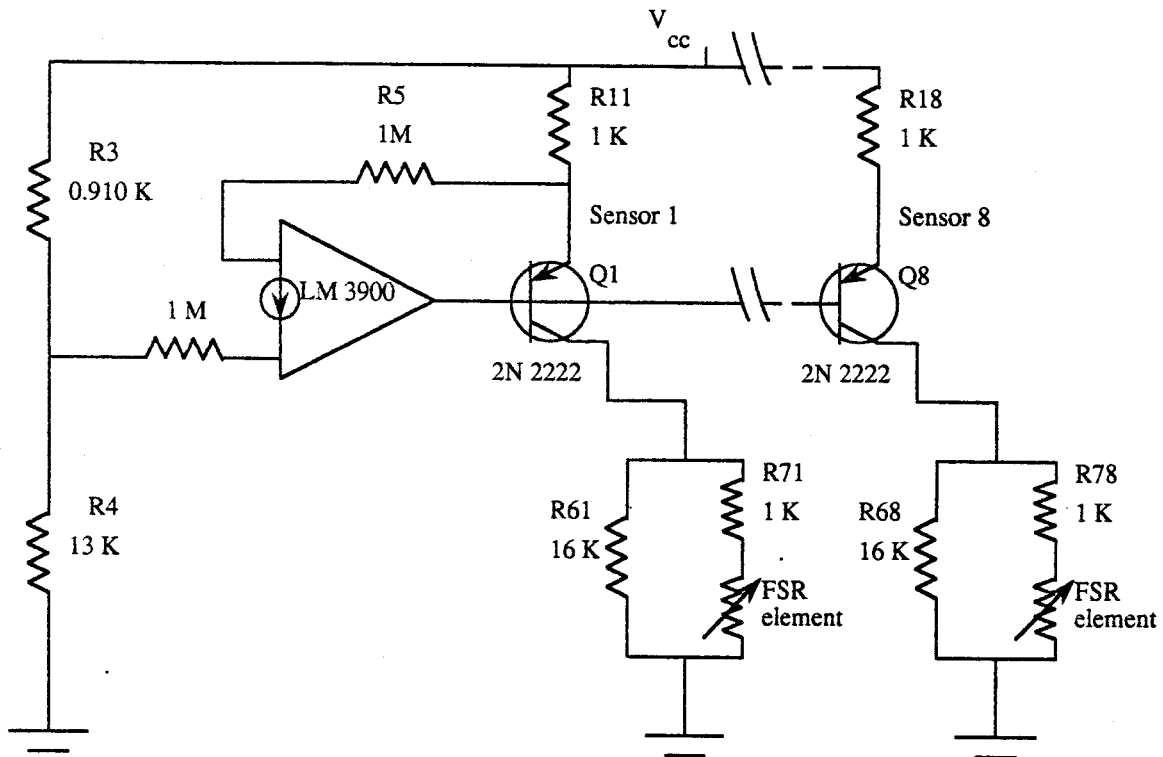


Figure 3.7: Circuit diagram of an eight-output constant current source for energizing the tactile sensing elements .

across R3. When negative feedback was employed as shown in Figure 3.7, the same reference voltage appeared as the voltage drop across R11. This was used to control the emitter current of transistor Q1. The current diverted into the (-) terminal of the amplifier via the resistor R5 and the base currents of the transistors were made negligible to ensure that the collector currents from the transistors were nearly equal to the respective emitter currents. Typically, if a 1 M resistor was used for R5, the current into the (-) terminal was

about 13.52 μA , and for transistors with typical β of 100, the base currents drawn were about 1 % of the collector current.

The currents in the other eight sections are governed by the resistance ratios given below:

$$I_1 = \frac{V_{\text{REF}}}{R_{11}}, \quad (3.1)$$

and

$$I_i = \frac{R_{11}}{R_{1i}} \times I_1 \quad \text{for } 2 \leq i \leq 8 \quad (3.2)$$

The design of the multiple output source consisted of determining the value of the resistors to satisfy the stated design criteria. The circuit was designed to deliver a constant current of 600 μA to each of the eight sensing sites. The circuit diagram shown in Figure 3.7 depicts the component values for the design. The series resistors, R71 to R78, were connected to prevent shorting of the respective collectors due to faulty FSR elements.

3.2.6.1. Tests for crosstalk and performance evaluation

The multiple output current source circuit was connected to the eight sensing sites of the finger pad and tested to determine crosstalk and any variations in the constant current outputs when forces were applied to the sensors.

A no load test was first performed in which the output voltages from all of the eight sensor output terminals were measured without any load on the sensors. The readings are shown in Table 3.1. Subsequently, a second test was conducted to ascertain the amount of crosstalk. In this test, various values of force were applied to each of the sensors, successively from sensor #1 to sensor #8, and the voltage readings at the remaining seven unloaded sensors were recorded for each set of forces. Table 3.2 presents a summary of these readings giving average measured values for all non-loaded sensors. By comparing the two tables, 3.1 and 3.2, it is evident that there is no significant cross talk between channels due to the sensor construction. The error in the value of constant current was evaluated by measuring the voltage across the 1 K resistor under no load conditions and using the relation

$$\text{error} = \frac{\text{theoretical value} - \text{measured value}}{\text{theoretical value}} \times 100 \%. \quad (3.3)$$

The error was determined for each of the eight sources and tabulated in Table 3.3. The maximum value of error, observed in the source supplying sensor #8, was 1.667%.

Table 3.1: No load sensor outputs when all the eight sensors are simultaneously energized .

Sensor number	Output voltage, V
1	9.27
2	9.23
3	9.25
4	9.22
5	9.26
6	9.23
7	9.29
8	9.24

Table 3.2: Summary of voltage readings for cross-talk test .

Loaded sensor	Sensor 1 output, V	Sensor 2 output, V	Sensor 3 output, V	Sensor 4 output, V	Sensor 5 output, V	Sensor 6 output, V	Sensor 7 output, V	Sensor 8 output, V
1	--	9.28	9.29	9.27	9.30	9.28	9.32	9.28
2	9.27	--	9.25	9.22	9.26	9.23	9.29	9.24
3	9.27	9.23	--	9.22	9.26	9.23	9.29	9.24
4	9.27	9.23	9.25	--	9.26	9.23	9.29	9.24
5	9.27	9.22	9.25	9.22	--	9.23	9.29	9.24
6	9.27	9.22	9.25	9.22	9.26	--	9.29	9.24
7	9.27	9.22	9.25	9.22	9.26	9.23	--	9.24
8	9.26	9.20	9.23	9.20	9.26	9.22	9.29	--

Table 3.3: Constant current values from each source and errors

Sensor source	Volt. across resistor, V	Constant current, μA	Error in %
1	0.602	602	0.333
2	0.599	599	0.167
3	0.599	599	0.167
4	0.602	602	0.333
5	0.603	603	0.500
6	0.606	606	1.000
7	0.605	605	0.833
8	0.610	610	1.667

3.3. Data Acquisition System [DAS]

It was decided to analyze digital representation of the data, so analog data had to be acquired and converted to digital form for the purposes of storage, transmission, processing and display. The primary device for achieving this task is the analog to digital converter (A to D). To accommodate the FSR output voltage which appears as the input to the DAS so that it would be compatible to a specified conversion relationship, signal conditioning consisting of scaling and offsetting was performed.

The properties of a data acquisition system to be chosen to acquire dynamic force data depends on the form in which the measured sensor data is available, and on the processing to which the data will be subjected. Some of the presently available data acquisition systems include devices to perform functions such as multiplexing, signal conditioning, sampling, analog to digital conversion, and data storage. However, the choice of DAS hardware was made by considering the task and the environment in which the prototype system was to operate. For robotic systems to be operated in hostile environments it will be necessary to select the DAS which have electronic devices capable of operation over a wide temperature range. The DAS should be well shielded, and carefully designed for eliminating common-mode errors while preserving resolution, conversion, and suitable for digital data transmission. In the case of the laboratory prototype DAS, with narrower temperature variations and fewer sources of ambient electrical interference, it was possible to consider readily available data acquisition systems. These could provide a low cost circuit configuration with the desired overall performance for the system.

In order to investigate the possibility of building a tactile sensing system in which a dedicated micro computer may be used to acquire and store dynamic forces, a commercial data acquisition system, ARIEL DSP-16¹, was installed in an IBM-XT personal computer and the real time forces were acquired. It was found that data synchronization problems introduced excessive noise, as is evident from the raw data plot shown in Figure A.2, Appendix A. This plot was obtained from one of the eight sensors which measured the forces during a grasping task performed on a sample object. To reduce noise, it was necessary to modify the DAS hardware to ensure accurate clock synchronization. The results of this case study is summarized in Section A.1, Appendix A. An alternative data acquisition facility, the VAXlab-based real time data acquisition system installed in a MicroVAX 3600² mini computer, was used in the project.

3.4. Tactile Data Acquisition System Using VAXlab Real Time Data Acquisition Facility

The real time data acquisition facility consisted of a hardware device, the "ADQ32" [95], and a set of library routines, the "VAXlab Laboratory I/O Software" running on the VMS operating system, which was used to initiate and control the acquisition of data. The VAXlab Laboratory I/O (LIO) routines were used as program modules and linked to application programs, coded in the Fortran-77 programming language.

The "ADQ32" device had a high-speed A/D converter with an onboard clock, 32 single-ended channels, double buffered DMA, random channel-select, programmable gain, differential capability, and high speed sampling (up to 200 KHz) capability. The device contained five on-board counters. The LIO used combinations of the five counters to merge them into two clocks, a primary clock and a sweep clock, for actual use. The device supported a mixture of single-ended and differential channels, and could be set up with different gains on each channel.

The two basic triggering modes provided for ADQ32 were: all points triggered by the same source, and channel sweeps triggered by one source and points within each channel sweep triggered by a second source. Using these modes, flexible triggering scheme could be designed to allow the A/D channels to be scanned in any order.

Using ADQ32 device, the data input could be performed either synchronously or asynchronously using the LIO routines. Synchronous I/O enabled a user program to transfer data to or from a device with one routine call. The routine call stopped program

¹DSP-16 is a registered product of ARIEL Data Systems Inc.

²VAXlab and MicroVAX 3600 are registered products of Digital Equipment Corporation Inc.

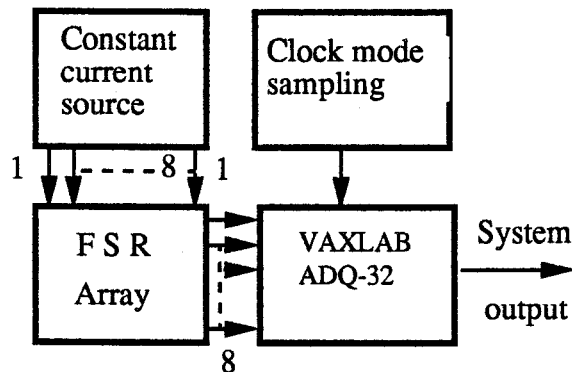
execution until I/O operation was complete. The device does not continue to transfer data while the program is preparing for the next I/O operation. An asynchronous I/O enables a user program to queue several values or arrays of data to be transferred while continuing execution of the program.

There were eight LIO routines used to develop the application program for data acquisition. They were grouped into four pairs:

1. ATTACH/DETACH, which logically connected or disconnected a device,
2. SET/SHOW, which set or returned the status of various device characteristics such as channel lists, triggering modes, clock rate, gains, and synchronous or asynchronous transfers,
3. READ/WRITE, which transferred data to or from a device, using synchronous I/O, and
4. ENQUEUE/DEQUEUE, which put data buffers on a queue and removed them from the queue when data transfer was complete.

3.4.1. Implementation

The apparatus, which was used to acquire data from the tactile sensors is shown in the form of a block diagram in Figure 3.8.



FSR: Force sensing resistor

Figure 3.8: Block diagram of data acquisition system used for acquiring tactile data.

Outputs from the eight sensors were hardwired to eight input channels of the ADQ32 device. An application program was written in Fortran-77 language to set up and control the ADQ32 device. A flow chart of this program is shown in Figure 3.9.

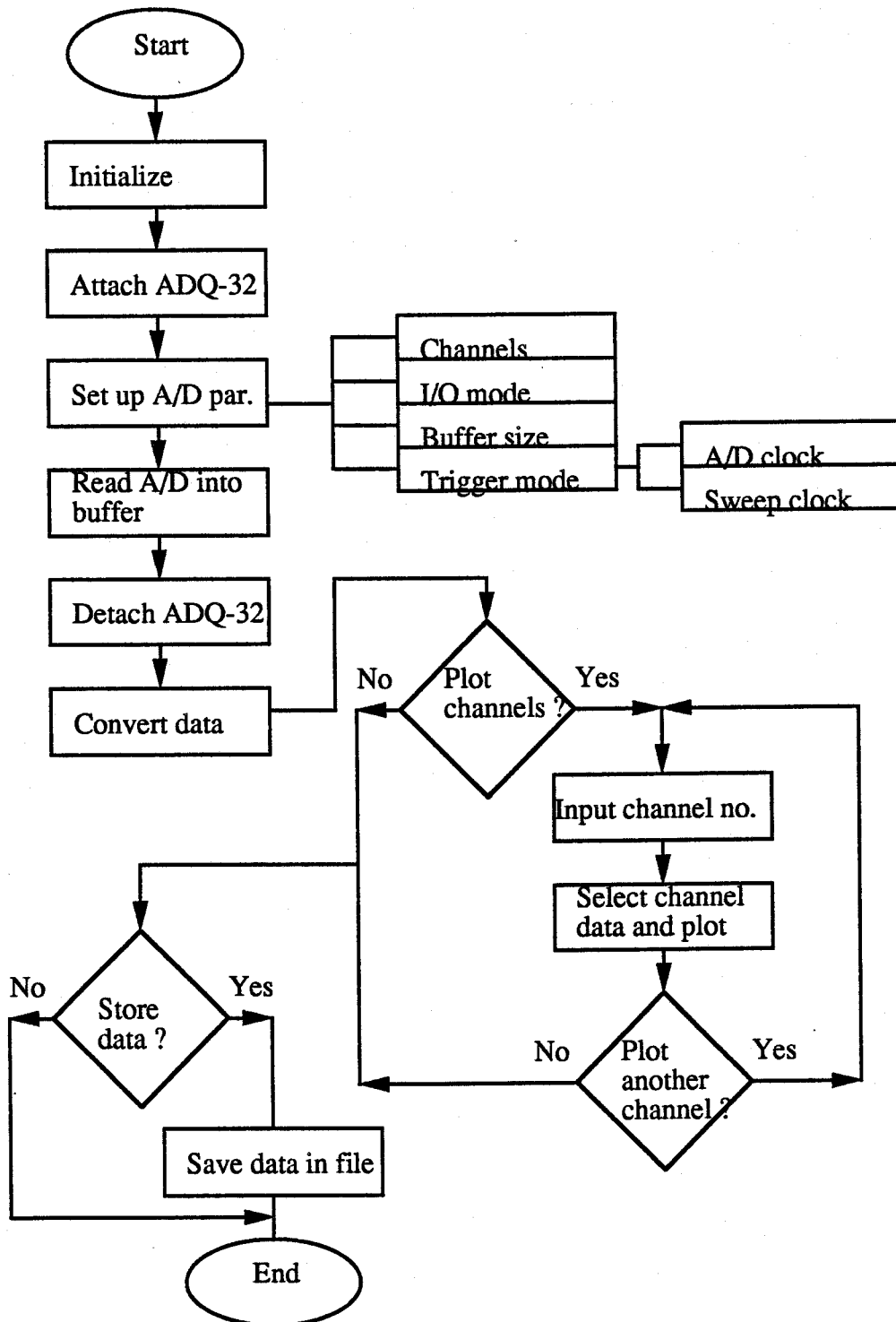


Figure 3.9: Flow chart of the Data acquisition program.

The program was initialized by including the symbolic definition files required by the VAXlab software, and by declaring the data types and variables. The ADQ32 device was attached by assigning a VMS I/O channel to the device. The LIO data structures for, and pointers to, the device were then initialized. A synchronous I/O interface was selected for the ADQ32 device and a unity channel gain for each of the specified eight channels was selected. The buffer size and the triggering mode were decided based on the considerations presented in the following sections.

3.4.1.1. Trigger mode and buffer size specifications for ADQ32

A number of preliminary grasping and releasing tests were conducted to determine the average time needed for completing the grasping or the releasing of the selected samples. A total time of 4 s was found to be sufficient to complete the tasks in a majority of cases. The capacity of the buffer in the Microvax 3600 computer for storing the acquired data using the VAXlab DAS was 64 K-bytes or 32,768 words. Therefore, to obtain the actual data from eight channels, the maximum number of samples which could be obtained using the system was limited to 4000. In order to obtain the 4000 samples from each channel within a time period of 4 s, a sampling rate of 1 KHz was chosen.

An ideal method of triggering would be one which samples all the eight channels simultaneously. However, for practical purposes, small errors in time can be tolerated, if it results savings in additional hardware, and is sufficient for demonstrating the technique. Therefore, the trigger mode selection was restricted to those choices which were readily available on the VAXlab data acquisition system without attaching any additional hardware. The triggering method selected was "Burst point clock sweep", which is illustrated in Figure 3.10.

In this method, the ADQ32 makes each pass through the eight channels at the "burst rate". The burst clock rate provided data acquisition at a rate controlled by the "ADQ" state machine. This rate, which was 166 KHz, was the fastest possible rate that could be used to guarantee precision of the acquired data to be within $\pm 1/2$ LSB [96]. Each pass through the specified channel was controlled at a clock rate, t_2 . The clock rate selected was greater than the product of the burst rate times the number of conversions per pass in order to ensure that a clock overrun error did not occur [96]. The selected value of the sampling rate which defined the clock rate (i.e. 1 KHz) was found to be appropriate for the prototype gripper system. This selection of triggering mode resulted in a sampling delay of 6 μ s between two successive channels which was small compared to the 1 ms sampling period.

The data acquisition program was designed such that acquisition commenced after receipt of a signal from the keyboard and, on completion, (after 4 s) the sensor data were stored in the buffer. The ADQ32 device was then detached from the system. The last two

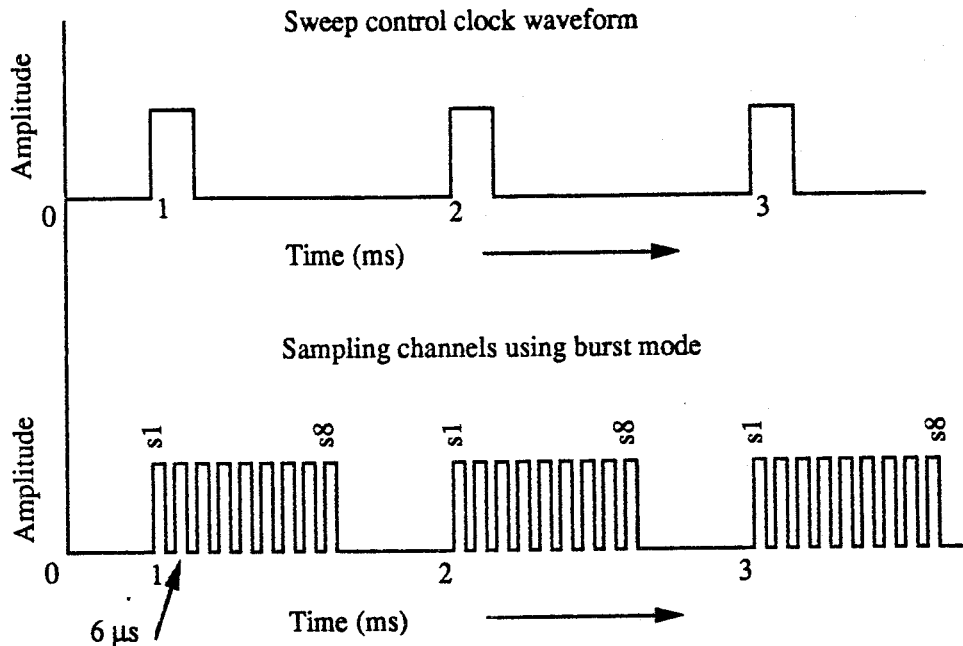


Figure 3.10: Burst point clock sweep mode of sampling data [from ADQ-32 Converter Module User's Guide [96], Fig.A-11, page A-22].

sections of the program performed data conversion for interactive display of acquired data in graphical form and storage of the data in designated files. To design these two parts of the program, a performance evaluation of the data acquisition process was done to determine the errors and nonlinearities of the VAXlab data acquisition facility. The details of this study are described in Section 7.3.1. It was found that a linear relationship could be used to convert the 12-bit digitized data values to their corresponding analog voltages. Therefore, the VAXlab library routines (LSP\$FORMAT_TRANSLATE_ADC) could be directly used for format conversions. After conversion, the plotting section of the data acquisition program called the graphic plotting routines (LGP\$PLOT) to plot the raw data measured by the sensors. After acquiring data, the interactive section of the program prompted the user to choose the desired channel or channels for plotting and/or obtaining a hard copy. After this, the user could direct the program to store the data in designated files.

Results from an experiment, which consisted of acquisition of force data using the data acquisition program while grasping a sample object using the prototype system, are shown in Figure 3.11. The plot shows the raw forces measured by sensor #1, in terms of the variation of digitized sensor output as a function of task time.

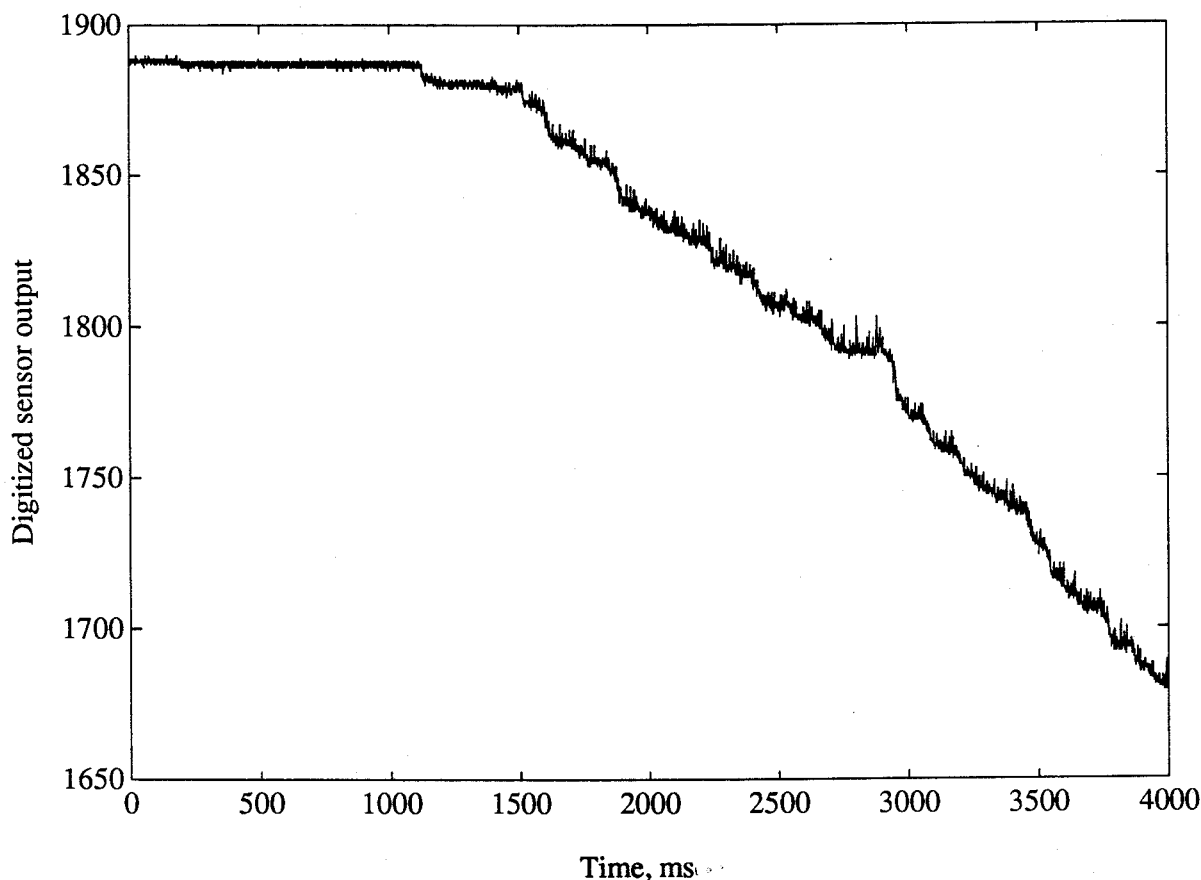


Figure 3.11: Grasping forces measured by sensor #1 using VAXlab data acquisition system

3.5. The Robotic Gripper and its Actuation

To develop a task oriented procedure based on actual grasping and releasing data, dynamic force data had to be acquired during the performance of a task. In order to perform grasping and releasing tasks, a small commercial robot equipped with parallel jaw grippers was selected. Manufactured by Mitsubishi Corporation, the RM101 MOVE-MASTER Micro-robot [97] has five degrees of freedom and is constructed of jointed metal plates. The surface areas of the parallel jaws are 15 mm by 15 mm, and the opening grasp of the hand is 80 mm with no tactile sensors mounted on the gripper surface. The maximum gripping force of the hand is 8 N and the maximum lifting capacity is 500 g. The maximum operating speed of the grippers is 7 cm/s and the grippers are actuated by a stepper motor whose speed is controllable using trapezoidal voltage waveforms.

waveforms. Other relevant specifications of the robot are given in Appendix A. Figure 3.12 shows the home position setting of the robot and Figure 3.13 shows the gripper arrangement.

3.5.1. Fabrication of the tactile sensing gripper

Four tactile sensors were mounted on each of the two gripping surfaces. The exploded view of the sensors is shown in Figure 3.14.

The compliant material and its thickness was chosen after a study of a variety of materials, in which their behaviour for modifying the FSR sensor signals, was investigated. The overall sensor hysteresis, repeatability and the response time were the three main factors evaluated to compare the different materials. The details have been reported by Vaidyanathan [17]. To prevent cross talk, the dimensions of the compliant material were made equal to those of the underlying FSR element [i.e. 5 mm by 5 mm]. In construction, the FSR material was cut into 5 mm by 5 mm squares that were laid on the printed circuit board and secured using an adhesive tape. The squares of compliant rubber material were laid individually over the FSR elements and were also secured using a layer of tape. This arrangement was checked for its suitability by observing the no load outputs from each of the eight sensing sites. In all cases, the corresponding value of the analog output voltage was measured and found to be the same value as that obtained prior to the final mounting of the sensors on the respective sites.

The last part of the hardware development for the prototype system consisted of designing a motor control circuit for actuating the grippers of the robot. To obtain raw data which could be used to test the proposed task oriented strategies, it was necessary to independently control the beginning and the completion of a task (i.e. grasping or releasing objects) using a push-button switch. The stepper motor provided in the robot was therefore controlled by an external controller circuit, designed for the experiment. The design details are given in Section A.2, in Appendix A.

3.6. Conclusion

The hardware designed for the prototype tactile sensing system was integrated into a robotic gripper in order to conduct the experiments. This chapter has discussed the basis of design and selection of the various system components, and described the relevant design steps followed to build the prototype gripper system. The first section considered the design of the tactile sensing system consisting of the selection of the transducer and its features, design of the tactile array, the design of energizing circuit, and construction of the eight-element tactile system for mounting on a commercial parallel-jaw robotic

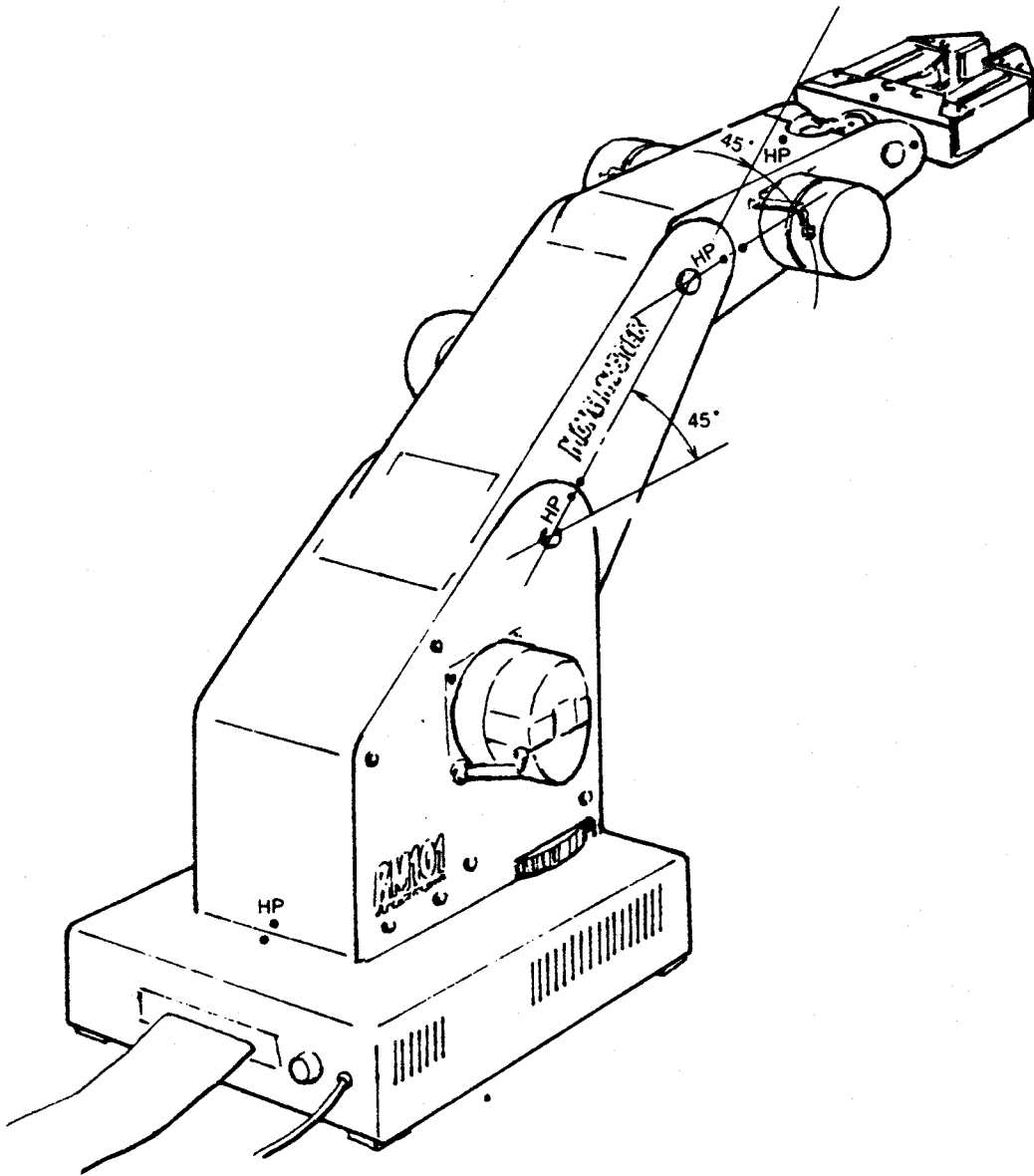


Figure 3.12: Home position setting of RM-101 Micro-robot [from RM-101 Movemaster Instruction Manual [97], Fig.3.4] •

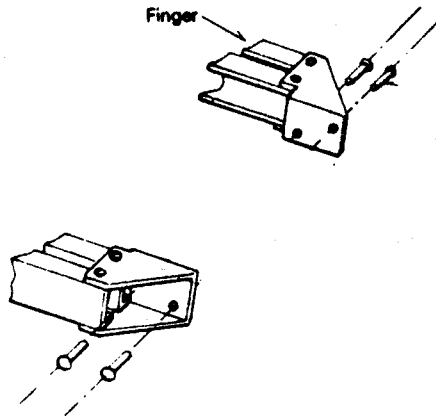


Figure 3.13: Typical gripper arrangement of the RM-101 robot [from RM-101 Movemaster Instruction Manual [97], Fig.8.2].

gripper. The following section discussed the criteria for selecting the data acquisition system. The VAXlab real time data acquisition system was explained and a procedure to use it for obtaining task data was described with the help of detailed flow diagrams. The last part dealt with the design and selection of a gripper actuator mechanism for handling objects in order to acquire real time data.

The prototype tactile sensing and data acquisition system is a complex system with nonlinearities. The entire system has to be modelled and periodically calibrated in order to obtain consistent results during real time tasks. An expert system-based combined modelling and calibration procedure was developed for this purpose and will be described in the next chapter.

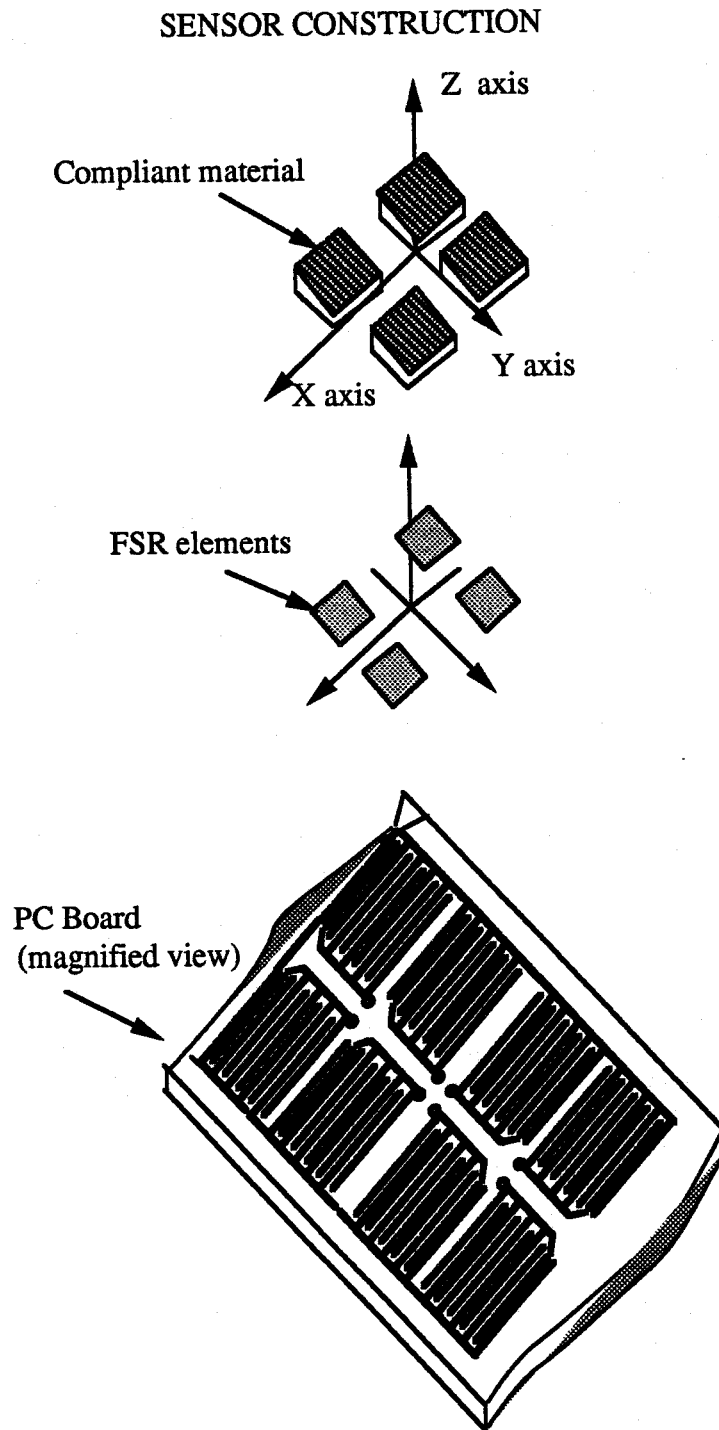


Figure 3.14: Exploded view of the tactile sensors which were mounted on the gripper surface •

4. SYSTEM MODELLING AND CALIBRATION: AN EXPERT SYSTEM-BASED APPROACH

4.1. Introduction

In the process of grasping or releasing an object, the gripper imparts time varying forces on the object being handled, and vice versa. The viscoelastic nature of the fingers of the gripper system causes the contact forces to vary in such a way that classical modelling procedures become very complex and often impossible to apply. Static models are inappropriate to use because of the time varying nature of the forces, permanent deformations from past stresses, creep, and relaxation dynamics associated with the tactile sensor data [98]. Modelling a system to characterize its dynamic behaviour using standard techniques results in complex mathematical formulations and solutions which are difficult to implement in a real time environment. In order to further understand the tactile sensing system and its behaviour, a model was developed which would permit various components to be studied and which could facilitate a detailed examination of the effects of nonlinearities and other features of the system.

The purpose of modelling a system is to expose its internal structure and to represent it in a form useful to engineering interpretations. Models are used extensively to understand the behaviour of a system. A model can be formulated based on the application of the system; the level of abstraction depends on how it is used. Examples include physical models which describe the physical properties of the system components, mathematical models which describe the input-output relationships, economic models which predict economic trends and developments, and data models which partially capture the meaning of the data as related to the complete meaning of the task. The model selected for a particular system should be such that it provides the desired information about the system to facilitate proper interpretations. Within the broad field of modelling there are certain specialities whose aim is to highlight or isolate certain specifics of a given system. However, such a concentration on a specific area of a system has the risk of overlooking hidden coupled effects.

A robotic gripper system may be considered as a coupled system consisting of a collection of interconnected subsystems. To model such a system with an emphasis on its dynamic response, a composite modelling and calibration scheme was developed and im-

plemented. The characteristics of the constituent subsystems were first evaluated. In order to select a suitable computer model for the complete system, three types of mathematical formulations of the system transfer function were studied. Performance was compared using modelling error as the criterion. The computer model finally selected for the system was able to estimate the magnitude of a point contact force on each tactile sensor located on the gripper surface.

This chapter outlines the characteristics of the subsystems and describes the mathematical formulations which can be used to model them individually. The criteria used for the selection of a computer model for the system are stated, and its design and method of implementation are given. An expert system designed to assist in the modelling and calibration of the prototype gripper system is outlined. Results of the expert system implementation, and the structure of the computer model developed for the eight sensors of the prototype system are also given. A discussion of the sources of modelling and calibration errors concludes the chapter.

4.2. System Component Characteristics

In an effort to develop individual models on a functional basis, the prototype gripper system was divided into three blocks:

1. the energized FSR elements,
2. the elastic medium and the mechanical overlays, and
3. the data acquisition system.

The characteristics of these three subsystem were evaluated to explore the possibility of developing a classical model for the system.

4.2.1. Energized FSR elements

The energized FSR elements convert a force excitation into corresponding analog voltage responses. When used with a non-elastic backing, the FSR material can be modelled [94] using the mathematical relationship

$$R = KF^{-c}, \quad (4.1)$$

where,

R = resistance of FSR in its through conduction mode,

F = applied force in N,

c = 1.0, a constant, and

K = $19.756 \times 10^3 \Omega\text{-N}$ for typical FSR materials.

This relationship does not hold when FSR is used in its shunt mode. When the material is energized using a constant current source, the behaviour is further modified and precludes definition by a simple mathematical relationship. As the piezoresistive material is screen printed onto the Mylar sheets, variations in the thickness of the material deposited also result in changes in its behaviour.

4.2.2. Compliant medium and mechanical overlays

Forces are applied to the energized FSR elements through a viscoelastic medium (i.e. the rubber pads). Therefore, the behaviour of the viscoelastic material was characterized. This behaviour is somewhat similar to human skin, which has been investigated by Dinnar [99]. The strain of human tissue increases under constant stress and does not return quickly to its original shape and dimension. This was characterized by Dinnar using a four parameter Maxwell-Kelvin model. The applicability of this model for a tactile sensor which used a soft skin-like compliant medium has been investigated by Sladek and Fearing [98] in which the model was fit to data obtained from several experiments. The data were obtained by measuring the force applied to the finger and recording the strain response of a tactile element directly below the force probe. The Maxwell-Kelvin model predicted the finger response better than a simple elastic model. A general second order transfer function was also fit to the data, and its inverse was used to predict the force at the surface of the finger.

The transfer function for the Maxwell-Kelvin model and its step response have been derived by Mase [100], a summary of which is given here. The model is shown in Figure 4.1 and has two spring elements and two dashpot elements. The springs are considered ideal with a linear stress-strain relationship. The dashpot represents the viscous response. The time rate of change of the strain of a dashpot is proportional to the stress applied. The first spring in series with the dashpot represents the Maxwell type response for a viscoelastic medium. The spring element reacts immediately to stress and the dashpot accounts for the drifting effect. The relationship between strain, ϵ , and stress, σ , for the spring element is given by

$$\epsilon = \frac{\sigma}{G_1}, \quad (4.2)$$

and for the dashpot element it is given by

$$\frac{d\epsilon}{dt} = \frac{\sigma}{N_1}, \quad (4.3)$$

where,

G_1 = spring or elastic constant, and
 N_1 = dashpot or viscous constant.

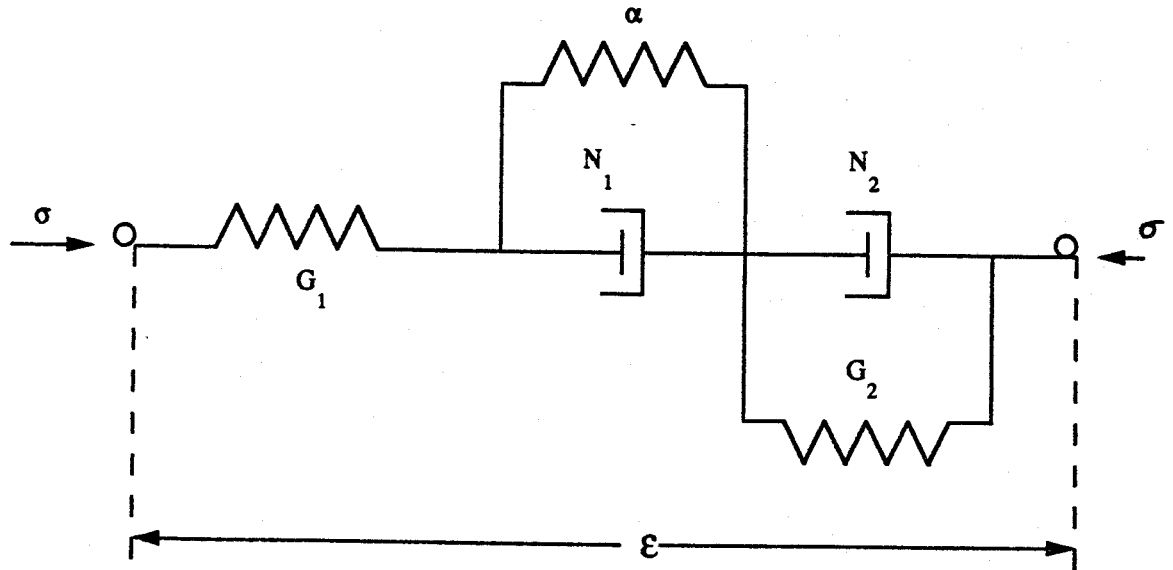


Figure 4.1: Maxwell-Kelvin model of viscoelasticity [from Fearing [33], Fig.5, page 964] .

Figure 4.2(a) shows the step response of a Maxwell medium. The strain response with respect to time for a step stress of σ_0 is:

$$\epsilon(t) = \frac{\sigma_0}{G_1} + \frac{\sigma_0}{N_1} t + \epsilon_0, \quad (4.4)$$

where ϵ_0 = initial strain.

The Kelvin model in series with the Maxwell model behaves as a delay device. Its step response exhibits an exponential increase until it reaches a maximum strain level as shown in Figure 4.2(b). The response $\epsilon(t)$ is given by

$$\epsilon(t) = \frac{\sigma_0}{G_2} (1 - \exp[-G_2 t / N_2]). \quad (4.5)$$

The total strain for the two models in series is the sum of the individual strains. The stress on each section in series is the same. The state space equations for the single-input single-output, two state system are given by:

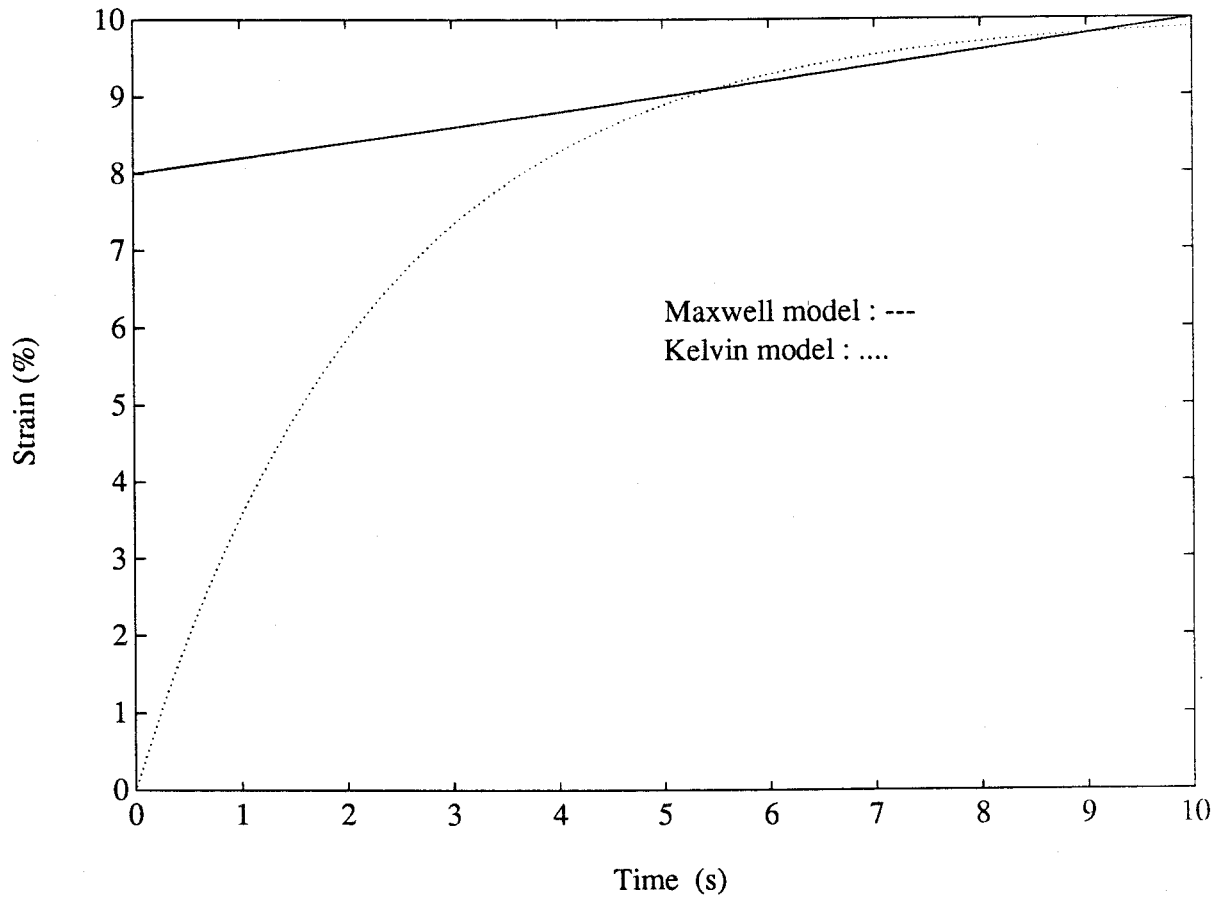


Figure 4.2: Step response of a typical Maxwell medium, and Step response of a typical Kelvin medium [from Fearing [33], Fig.6, page 964].

$$\begin{bmatrix} \dot{\epsilon}_m \\ \dot{\epsilon}_k \end{bmatrix} = \begin{bmatrix} 0 & 0 \\ 0 & G_2/N_2 \end{bmatrix} \begin{bmatrix} \epsilon_m \\ \epsilon_k \end{bmatrix} + \begin{bmatrix} 1/N_1 \\ 1/N_2 \end{bmatrix} \sigma \quad (4.6)$$

$$\epsilon = \begin{bmatrix} 1 & 1 \end{bmatrix} \begin{bmatrix} \epsilon_m \\ \epsilon_k \end{bmatrix} + 1/G_1 \sigma \quad (4.7)$$

where the dot denotes differentiation with respect to time and

ϵ_m = strain for the dashpot of the Maxwell part of the model,

ϵ_k = strain for the Kelvin section of the model,

ϵ = total strain, and

σ = input stress.

Using the Laplace operator 's' to designate differentiation, the transfer function relating strain to stress is given by:

$$\frac{\epsilon(s)}{\sigma(s)} = \frac{1}{G_1} + \frac{1}{sN_1} + \frac{1}{sN_2 + G_2} \quad (4.8)$$

The third block of the prototype gripper system had the data acquisition system (DAS) perform the digitization of the analog sensor outputs using the real time data acquisition facility of VAXlab. A model for this system consists of a linear input output relationship for the allowable range of inputs, namely, 0 to 10 V, equally divided into 2^{12} levels. It has been assumed for this model that the quantization error introduced by the A/D converter is negligible.

4.2.3. The complete system hardware

The simplest model for the complete gripper system could be obtained by cascading the transfer functions of the three subsystems. A transfer function for the FSR behaviour in its shunt mode of operation was not available. Therefore the first block was treated as a black box and it was characterized mathematically by fitting cubic spline interpolants to the experimental input-output data obtained for this block. The Maxwell-Kelvin model could not be used for the rubber pads since the same model was not applicable at all

stress values [33]. Another problem with the Maxwell-Kelvin model was the presence of a pole at the origin. This made the model simulated response unstable. The instability was due to the fact that the model predicted that the strain will increase indefinitely as a constant stress is applied. This was not acceptable since the material was of finite dimensions. Because of these considerations, the second block was also modelled using a cubic spline interpolation function fitted to the block input-output data. The third block was modelled with a linear function. When these three functions were cascaded, and tested with the actual system input-output data, large errors, as high as 100 % were found to occur between the modelled outputs and the actual measured outputs. Such a model was, therefore, clearly inadequate. The nonlinear nature of the of the FSR material, the mechanical overlays and the flexible rubber pad, and the effect of combining them were considered as the likely causes for the discrepancies.

In order to develop a better model, a modelling scheme was formulated in which the prototype system was characterized in terms of eight sensor models. Each sensor model defined the relationship between the force applied at the sensor location on the gripper and the resulting digitized sensor output as recorded and stored by the computer. Such models were developed using the input-output behaviour measured at each sensing site. This modelling technique is based on the system modelling principles suggested by Ziegler [101].

4.3. Characterization of the System Behaviour

Following the method of Ziegler [101], a real system may be considered as a source of observable data. A real system can be visualised, as in Figure 4.3, as consisting of observable and non-observable variables.

The system input and the output are observable variables. Input variables are considered to be those which perturb, influence or affect the system from the outside. Output variables are those considered to take on values as a result of the values assumed by the input variables. The output variables are directly observable by measurement. The hierarchy of levels at which a system may be specified is given in Table 4.1.

Consider the following experiment. In a system, if an input segment from (X,T) is applied which results in an output segment from (Y,T) , a diagram such as that shown in Figure 4.4 may be obtained.

In this figure, a segment $\omega \in (X,T)$ is an *input* segment and $\rho \in (Y,T)$ is an *output* segment. If the output segment observed in response to an input segment is recorded over the same observation intervals, then ω and ρ can be associated at the domain level. That is, the domain of ω equals the domain of ρ . Such a pair (ω, ρ) is called the *input-output*

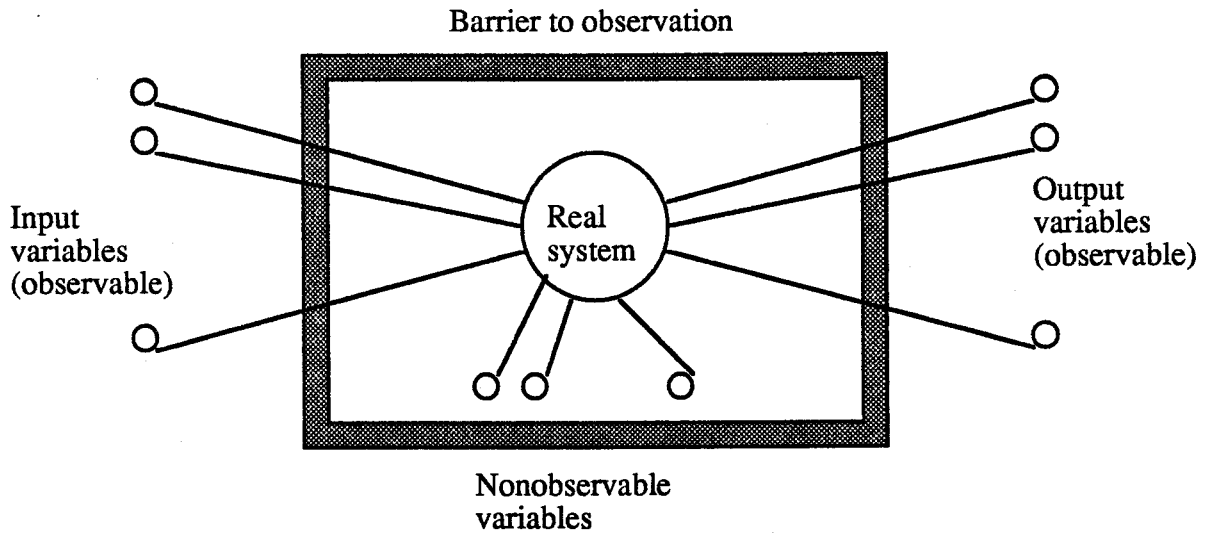


Figure 4.3: Variables of a real system [from Ziegler [101], Fig.1, page 28].

Table 4.1: Hierarchy of system specifications [from Ziegler [101], Table 2, page 255].

Level	Specification
0	I/O relation observation
1	I/O function observation
2	I/O system
3	Iterative specification
4	Structured system specification
5	Network of specifications

(or I/O) pair. A collection of such I/O pairs is called an I/O relation. An experiment performed in a finite duration will yield a finite number of I/O pairs. This will consist of a subset of all possible input segments, denoted by Ω . Thus an I/O relation observation (IORO) can be expressed in the form of a structure (T, X, Ω, Y, R)

where,

T = time base,

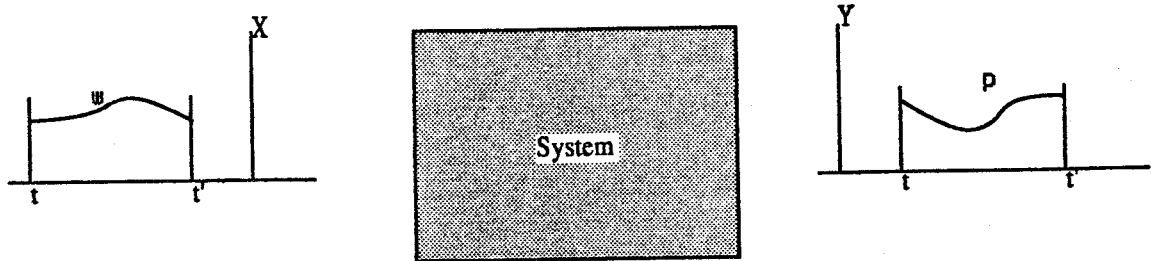


Figure 4.4: A typical experiment to determine system specifications [from Ziegler [101], Fig. 2, page 203].

X = input value set,
 Y = output value set,
 Ω = input segment set, and
 R = the I/O relation,

with the constraints that

- (a) $\Omega \subseteq \{(X, T)\}$, and
- (b) $R \subseteq \Omega \times (Y, T)$,

where,

$(\omega, \rho) \in R$ which implies
 domain of (ω) = domain of (ρ) .

Thus an IORO summarizes what can be known about the system as a black box.

4.3.1. Mathematical modelling methods

Modelling of the gripper system consisted of determination of the parameters characterizing the input-output relationship for each of the eight sensing sites. This non-linear relationship could be represented using a variety of mathematical approximations. To approximate a function $f(x)$ by another function $g(x)$ which is a simple function such as a polynomial or a rational function, interpolation and curve fitting techniques were considered.

Suppose the values of $f(x)$ is known for each x in the set

$$I = \{x_0, x_1, \dots, x_n\}, \quad (4.9)$$

where

$$x_k < x_{k+1} \text{ for } k = 0, 1, \dots, n-1. \quad (4.10)$$

If

$$g(x_i) = f(x_i) \text{ for } i = 0, 1, \dots, n \quad (4.11)$$

then $g(x)$ is an *exact approximation* to $f(x)$ and $g(x)$ is said to *interpolate* $f(x)$. If $g(x_i)$ is not equal to $f(x_i)$ for one or more of the data points in I , then $g(x)$ is an *inexact approximation* or *curve fitted function*. Curve fitted functions are useful to approximate the trends rather than exactly mimic data points [102]. The common approximating functions $g(x)$ which were considered for modelling were those involving linear combinations of simple functions drawn from a class of functions $\{g_i(x)\}$ of the form

$$g(x) = a_0g_0(x) + a_1g_1(x) + \dots + a_n g_n(x). \quad (4.12)$$

The classes of functions most often encountered are the monomials $\{x^i\}$, $i = 0, 1, \dots, n$, the Fourier functions $\{\sin kx, \cos kx\}$, $k = 0, 1, \dots, n$, and the exponentials $\{e^{bx}\}$, $i = 0, 1, \dots, n$. Linear combinations of monomials lead to polynomials of degree n , $P_n(x)$.

For modelling the complex non-linear prototype gripper system, three curve fitting techniques which could be implemented using the library routines of a readily available laboratory software package, MATLAB⁵ were selected. These techniques were: curve fitting using a least error square polynomial, curve fitting using a set of cubic splines, and curve fitting using a sum of exponential functions. Each technique had its advantages and disadvantages. The selection of a particular method for characterizing a system had to consider factors such as the accuracy of modelling, the complexity of the procedure and the computation time required for modelling, and ready availability of the model parameters in a form suitable for on-line computation. The principles of the three chosen techniques and their relative merits and demerits are described in the following sections.

4.3.2. Approximation using least-squares polynomial

The algebraic polynomials $P_n(x)$ are by far the most popular approximating functions because the underlying theory is well developed and simple. Polynomials are easy to evaluate and their sums, products, and differences are also polynomials. They can be differentiated and integrated easily. If the origin of the coordinate system is shifted, or if

⁵MATLAB is a registered product of The Mathworks Inc.

the scale of the independent variable is changed, the transformed functions remain polynomials. Most of the other functions considered as candidates for the approximating functions must themselves be evaluated by using approximations; almost invariably, these approximations are given in terms of polynomials or ratios of polynomials. Also, any continuous function $f(x)$ can be approximated to *any* desired degree of accuracy on a specified closed interval by some polynomial $P_n(x)$. This follows from *Wiestrass approximation theorem* [103].

In the polynomial approximation, first an n th-degree polynomial was chosen as the approximating function and then a criterion for fitting the data was applied to compute the coefficients. Given the paired values $x_i, f(x_i)$, a reasonable criterion for determining the coefficients of $p_n(x)$ was to require that

$$p_n(x_i) = f(x_i), \quad i = 0, 1, 2, \dots, n. \quad (4.13)$$

Since the paired values were from experimental data, it was possible to represent the trend of the behaviour using a polynomial of a degree m where $n > m$. Instead of requiring that the approximated polynomial reproduce the given function values exactly, the degree of the polynomial was chosen such that it satisfied a *least-squares* criterion. According to this criterion, the given $n+1$ functional values were fitted with a polynomial $p_m(x)$, such that the sum of the squares of the discrepancies between the $f(x_i)$ and $p_m(x_i)$ was a minimum. The discrepancy at the i th base point is given by

$$\delta_i = p_m(x_i) - f(x_i), \quad (4.14)$$

The least squares criterion required that the $a_j, j=0, 1, \dots, m$, be chosen so that the aggregate squared error

$$E = \sum_{i=0}^n \delta_i^2 = \sum_{i=0}^n [p_m(x_i) - f(x_i)]^2. \quad (4.15)$$

$$= \sum_{i=0}^n \left[\sum_{j=0}^m a_j (x_i^j) - f(x_i) \right]^2. \quad (4.16)$$

was as small as possible. If $m = n$, then the error E was 0 and the least squares polynomial was identical to the interpolating polynomial.

However, there is no way of ascertaining whether the approximate polynomial generated using the above technique was the one which the Wiestrass theorem shows must exist. This was especially so in cases where the function $f(x)$ was known only at a few sampled values. Therefore, two other approximating functions were considered for characterizing the tactile sensor behaviour. These functions were chosen after a preliminary observation of the trend of the sensor input-output characteristics.

4.3.3. Curve fitting using cubic splines

In this technique, instead of interpolating a function $f(x)$ by the same polynomial over the whole domain of interpolation points, different interpolating polynomials were used over different subsets of points $\{x_i\}$ such that the polynomials agreed at the interpolation points, or *knots*. Such a piecewise interpolating polynomial function offered the advantage of using several lower degree polynomials instead of a single higher order polynomial. This resulted in smaller errors because of reduced oscillations occurring between the knots.

In order to fit a different polynomial on each data interval $[x_i, x_{i+1}]$, where $x_i < x_{i+1}$, $i = 0, 1, \dots, n-1$, the polynomials were so chosen that they were of the same degree. Cubic polynomials were chosen such that they agreed at the knots and these cubic splines, denoted by S_x were represented by

$$S(x)_i = y_i \text{ for } i = 1, 2, \dots, n. \quad (4.17)$$

The function $S(x)$ was written in the form

$$S(x) = y_i + a_i(x - x_i) + a_i(x - x_i)^2 + a_i(x - x_i)^3, x_i \leq x \leq x_{i+1}, i = 1, 2, \dots, n-1. \quad (4.18)$$

In addition,

$$S(x_n) = y_n. \quad (4.19)$$

The $3(n-1)$ unknowns in Equation (4.17), $\{a_i, b_i, c_i\}$, for $i = 1, 2, \dots, n-1$, were determined as follows: at each of the interior knots, $\{x_1, x_2, \dots, x_{n-1}\}$, the two cubics on either side were made to agree and, to enforce continuity and smoothness of splines at the interior knots, the first and second derivatives of the two splines were also made to agree. The detailed mathematical formulation of this condition, which is known as the "not-a-Knot" condition, has been discussed by Deboor [104]. A primary requirement to use this curve fitting technique is that all x_i s have to be distinct. This method was also very sensitive to the range of the data set from which the interpolants were extracted.

4.3.4. Non-linear curve-fitting using exponential functions

The third type of curve fitting function considered for characterizing the prototype gripper system was a function consisting of n linear and n nonlinear (exponential) parameters. The function was defined as:

$$y = c(1)\exp(-\text{lam}(1)t) + c(2)\exp(-\text{lam}(2)t) + \dots + c(n)\exp(-\text{lam}(n)t) \quad (4.20)$$

in which $c(i)$, $i=1, 2, \dots, n$, represented the linear parameters and $\text{lam}(i)$, $i=1, 2, \dots, n$, represented the coefficients of the non-linear parameter.

This function was selected because the nonlinear parameters could be determined by minimizing the nonlinear function corresponding to a pre-defined tolerance. The function could be iteratively fitted to a data set using two subprograms provided in the MATLAB

software library. The first subprogram, called "Nelder" uses the Nelder-Mead simplex algorithm [105] for minimizing a non-linear function of several variables, and was invoked using the recursive relation:

$$[x, cnt] = \text{nelder}(F, x, \text{tol}) \quad (4.21)$$

where,

x = output vector,

x = starting value of the output vector,

F = the function to be minimised,

tol = tolerance value to be reached before stopping recursion, and

cnt = the step count for convergence.

The value for tol was specified as 0.001 and the chosen function, which is given by Equation (4.20), with $n=4$, was used in place of F . This resulted in 4 non-linear parameters, which were represented by the vector lam . The initial guess for the vector lam was selected to be equal to [1 0 0 0] and the four nonlinear parameters were determined using the recursive relation given in Equation (4.22).

$$[lam, cnt] = \text{nelder}('fitfun', lam, \text{tol}). \quad (4.22)$$

The second subprogram, called "fitfun", was used to display the values of the 4 linear and 4 non-linear parameters, as well as the fitted curve, after every step of iteration. When the mean value of absolute error was less than the specified tolerance, then the iteration stopped and the number of iterations was indicated by the value of the parameter cnt .

This method of curve fitting was the slowest of the three methods but could reduce the modelling error to very low values. However, the definition of 4 linear and 4 non-linear parameters for every tactile sensor resulted in a complex system model which was computationally intensive compared to the other two methods.

4.4. Modelling and Calibration Procedure

For a complex system such as the prototype gripper system, the choice of a particular method of curve fitting to be used at all times was found to be a difficult task. Since the system was built using non-linear components, such as different sensors, pads and mechanical overlays, it was necessary to develop a modelling scheme which would provide a user with a facility to try all the three methods of curve fitting in order to obtain the best model for a system. Such a modelling scheme could use the expertise of an experienced person stored in a computer program. In addition, a facility to calibrate a model to account for component ageing and other factors should be provided, if an accurate representation of the dynamic force data has to be obtained during the performance of a task.

Therefore, an expert system-based modelling scheme was designed and implemented in order to model the prototype gripper system. This scheme, which was implemented in the form of an integrated computer program, guides a user in an appropriate selection of a model for the system. Facility to calibrate this model was also provided to make it a single composite package. This package offers the user a facility to select the best system model after viewing the result of fitting a selected set of pre-defined functions to the system input-output data set, and their associated modelling errors. Calibration and remodelling facilities were also provided. After experimenting with a number of functions of varying degrees in each of the three methods of curve fitting, a set of five functions was selected for the modelling and calibration procedure. They were: third, fourth, and fifth degree polynomial curve fitting, curve fitting using the cubic spline interpolants, and the fourth degree non-linear function with 4 linear and 4 non-linear parameters.

The modelling and calibration procedure consisted of the following stages:

1. collection of the system input-output data for modelling/calibration,
2. estimation of system uncertainty due to main contributors,
3. formulation of a set of five pre-selected mathematical models using the collected data,
4. development of a user friendly expert system for model selection, and
5. development of an integrated program, called Interface Program I, which embeds the expert system into the modelling/calibration program.

The design and implementation details of the various sections of the modelling and calibration scheme are discussed in the following sections.

4.4.1. Data collection

To obtain the input-output data for modelling the tactile sensors, an experimental apparatus was designed in the laboratory.

The apparatus consisted of a tactile sensing finger mounted horizontally on an X-Y translation table, and a force fixture to apply normal forces to the sensing site. The finger was rigidly held with set screws. Each sensor consisted of an FSR transducer cut into a 5 mm by 5 mm square and placed over a metallic pattern etched on a printed circuit board. Each finger had 16 such patterns corresponding to 16 sensing sites. A compliant rubber pad cut to the same size as that of the FSR element, was placed on top of the transducer. The forces could be applied on the rubber pads via a threaded lead screw attached to a load cell. The load cell was connected to one of the four arms of a balanced Wheatstone bridge. The sensors were energized with the multiple-output constant current source and normal forces were applied using the force fixture. The applied forces were

measured using a digital force indicator⁴, and the sensor outputs were recorded with a digital voltmeter. For every value of the applied force, the resistance at the sensor output terminals was also recorded. The range of forces used for the tests were from 0 to 15 N which was the allowable range of applicable forces to the gripper system.

4.4.2. Uncertainties

The model developed for the sensors should be able to account for their behaviour while ensuring that the modelling errors are within an acceptable limit. The error limit is generally governed by uncertainties contributed by the system components. Three main contributors to the uncertain behaviour of the tactile sensor were identified. To determine the uncertainties caused by these variants, a suitable uncertainty factor for each was defined and estimated using the data from simple statistical experiments.

In order to develop a practical quantitative estimate for the system uncertainty, the three major contributing factors considered were:

1. the uncertainty due to the varying position of the object relative to the gripper fingers,
2. the uncertainty due to the variation of properties of the rubber pads, and
3. the uncertainty due to the variation of the characteristics of the FSR elements.

A definition for uncertainty was formulated consistent with the major requirements of the sensing system, which were to differentiate between varying forces acting on the sensors and to decide the current gripping status. The variation in the sensor output due to each of the three factors contributing independently was treated as the corresponding uncertainty. These uncertainties served to estimate the robustness of the sensor output during the performance of a task. The following sections describe the estimation procedures.

4.4.2.1. Collection of sample data

Three sets of laboratory tests were performed to obtain sample data pertaining to the position, rubber pad, and FSR uncertainties. The test apparatus used was similar to the one described in Section 4.4.1. The data for position uncertainty were obtained by recording the DAS output for a constant applied force of 5 N acting on a sensing site, and by repositioning the force fixture to contact the sensor pad at 100 different locations selected arbitrarily on the sensor surface. The data for rubber pad uncertainty and the FSR uncertainty were obtained in the following way. The force fixture was mounted so that a constant force of 5 N was applied to the same location on the sensing site via a threaded

⁴Model P-3500, manufactured by Intertechnology Inc.

screw. The force was measured using a calibrated digital force indicator. One hundred different samples of rubber pads and FSR elements were selected. Using the same FSR element, the different rubber pads were inserted separately and each time the force was applied on the sensing element at the same point. The corresponding DAS output constituted the sample data for rubber pad uncertainty. Finally, using one rubber pad and different FSR elements, the above test was repeated to obtain the sample data for FSR uncertainty. These three sets of sample data are referred to as set I data.

During each of the above three experiments, the reading of the digital force indicator was recorded. These three sets of data, each pertaining to the force indicator reading, were used to characterize the uncertainty associated with the applied force. This set of sample data is referred to as set II data.

4.4.2.2. Statistical analysis

Comparisons between the three sets of data were made using the coefficients of variation. This statistical measure expresses the standard deviation of a data set as a percent of the mean of the same data set [106]. This method was used for comparison because it was simple and the differences in units of measurement or gross differences in scale did not dominate the results of comparisons.

To determine the coefficient of variation for the sensing system considering the three identified uncertainties, the following criteria were used:

- If the hypothesis of equal population means of the three sample sets of data contained in set I could be validated, then, the ratio of the pooled standard deviation and the average of the three sample mean values were used to determine the composite coefficient of variation.
- If the population means could not be treated as equal in a statistical sense, then the coefficient of variation was determined for each of the three individual populations corresponding to the three sets of sample data of set I, and the mean of these values was considered as the coefficient of variation.

To check the validity of the assumption, that the same value of applied force (5 N) was used during all the three sample tests discussed in Section 4.4.2.1, it was necessary to apply relevant hypothesis test procedures to test the equality of the means of the three sets of sample data pertaining to set II. The following sections describe the analysis procedure carried out to estimate the various statistical quantities using a general purpose statistical computer package, MINITAB⁵, on a VAX⁶ 8650 main frame computer.

⁵MINITAB is registered trademark of Minitab, Inc.

⁶VAX is a registered trademark of Digital Equipment Corporation, Inc.

- set A - sample data for determining the position and the rubber pad uncertainties,
- set B - sample data for the two different batches of FSR elements encountered, and
- set C - sample data for force indicator uncertainty.

The validation of the ANOVA assumptions were carried out for these sets of data. The ANOVA table with all the relevant test parameters were generated using the MINITAB software package and the results were interpreted as described in the following section.

4.4.2.4. Evaluation of system uncertainty

A partial MINITAB output for the one-way ANOVA model of the data in set A, set B and set C is shown in Table 4.2. In order to determine whether the means of the various groups are all equal, two different variances were examined, one based on differences between groups and the other based on differences within groups. The test statistic based upon the ratio of the two variances, determined the F values in the ANOVA tests. The F values, obtained from the ANOVA test results pertaining to the data in set A, set B and set C were tested against the corresponding critical values obtained from the F-Distribution tables [106]. In each of the three cases, the null hypothesis of equality of the population means, had to be rejected. In the case of the data in set C, the pooled standard deviation was found to be 2.47 and the two sample means were 500.76 and 502.74. Therefore, the error in assuming that the applied force was 5 N, is 0.49 %.

Table 4.2: ANOVA table for the data in set A, set B, and set C**Set A data**

'out1' = Sample data for position uncertainty

'out2' = sample data for rubber pad uncertainty

ANALYSIS OF VARIANCE

SOURCE	DF	SS	MS	F	p
FACTOR	1	5592245	5592245	39.81	0.000
ERROR	200	28093260	140466		
TOTAL	201	33685504			

INDIVIDUAL 95 PCT CI'S FOR MEAN

BASED ON POOLED STDEV

LEVEL	N	MEAN	STDEV	-----+-----+-----+-----+			
out1	101	5404.4	288.7	(---*---)			
out2	101	5737.1	444.5		(---*---)		
POOLED STDEV =			374.8	5400	5550	5700	5850

Set B Data

'c9' = Sample data for FSR uncertainty from Batch 1

'c10' = Sample data for FSR uncertainty from Batch 2

ANALYSIS OF VARIANCE

SOURCE	DF	SS	MS	F	p
FACTOR	1	417660672	417660672	1455.75	0.000
ERROR	99	28403418	286903		
TOTAL	100	446064096			

INDIVIDUAL 95 PCT CI'S FOR MEAN

BASED ON POOLED STDEV

LEVEL	N	MEAN	STDEV	-----+-----+-----+-----+			
C9	50	4316.5	572.7	(*)			
C10	51	8383.8	496.7		(*)		
POOLED STDEV =			535.6	4800	6000	7200	8400

Set C data

'sg2' = sample data for force indicator readings set 1

'sg3' = sample data for force indicator readings set 2

ANALYSIS OF VARIANCE

SOURCE	DF	SS	MS	F	p
FACTOR	1	109.90	109.90	18.01	0.000
ERROR	200	1220.59	6.10		
TOTAL	201	1330.50			

INDIVIDUAL 95 PCT CI'S FOR MEAN BASED ON POOLED STDEV

LEVEL	N	MEAN	STDEV	-----+-----+-----+-----+--
sg2	101	500.76	2.22	(-----*-----)
sg3	101	502.24	2.69	(-----*-----)
-----+-----+-----+-----+--				
POOLED STDEV =		2.47	500.50	501.20 501.90 502.60

The coefficient of variation, calculated for each of the four different uncertainty factors (from data set A and set B) are shown in Table 4.3. The coefficient of variation for

Table 4.3: Coefficient of Variation of the four uncertainty factors.

Sl. No.	Uncertainty	Coefficient of variation (%)
1	position uncertainty	5.34
2	rubber pad uncertainty	7.74
3	FSR Batch A uncertainty	13.26
4	FSR Batch B uncertainty	5.91
5	Mean system uncertainty	8.06

the system uncertainty, which is taken to be the average value of the four factors, was found to be 8.06 %. Expressed as a percentage, this value of coefficient of variation represented the deviation which can be expected in the sensor output because of the uncertainties. Other types uncertainties which could be encountered in a practical situation might modify the deviations, but the averaging method used was considered as the best approximation. Other alternatives were investigated to develop a procedure which would account for the variations in the measured force values due to other unpredictable uncertainties.

Considering that the system uncertainty as well as the modelling errors were both variable quantities, a method which could determine the system modelling errors and compare it with the estimated value of uncertainty was required for modelling and calibrating the prototype system. The method could use inputs from a user and guide him through the different steps of modelling using the five selected functions in order to arrive at a best model. The best model could be characterized as that which yields the lowest value of modelling error, with the additional requirement that the modelling error should be less than the estimated system uncertainty. These tasks were achieved by

designing an expert system-based modelling and calibration scheme in which a basic model could be updated using a knowledge base. The expert system was used to aid the user in selecting an appropriate model based on the input output data set furnished by the user.

4.4.3. Expert system for modelling and calibration

An expert system was designed to assist the user to model and calibrate the tactile sensors. The results of the studies on system uncertainties were used to determine whether a selected model was appropriate. The expert system was embedded in the application software to achieve fast operation and flexibility in processing the expert system decisions.

4.4.3.1. Expert System Development Tools

An expert system is a computer program that uses knowledge, and reasoning techniques, to make decisions. An expert development tool is a program which has been pre-defined in the methods by which the knowledge will be represented in the expert system; the knowledge itself will have to be incorporated. An inference engine provides the decision making ability based on a pre-defined control and search procedure.

There are vast differences in the quality and sophistication of the available development tools. For the proposed application, the KES⁹ development tool was selected. This program had several attractive features for this project, including the ease with which it could be embedded in application software. Out of the three types of inference engines supported by the KES tool, the Hypothesize and Test (HT) method of inferencing was selected because it could arrive at a decision from incomplete knowledge. The HT inference engine used backward chaining to make inferences. This method, also called the goal oriented approach, is a technique in which the value for a goal attribute is determined using a typical hierarchical structure. In this technique, the primary subgoals are determined from knowledge about the facts obtained from an end-user, or from other knowledge sources such as external communication files, or from other related event-driven inferences. Further description of the technique is given in Section 6.3.1.2, Chapter 6. The pursuit of a goal generally drives an interactive session with the end-user. Event-driven inferencing could be incorporated into the KES knowledge base using "demons", which are a set of special constructs based on if..then rules. The HT inference engine reasons through an iterative procedure which consisted of hypothesis formulation and subsequent verification through abductive reasoning until a value can be determined

⁹Knowledge Engineering System, KES, is a registered trademark of Software Architecture & Engineering Inc.

for the goal attribute. It determines the smallest number of causes, represented by descriptions in the knowledge base, that explains all known manifestations of the problem of interest. The concept is described as minimal set covering [107].

4.4.3.2. Embedding the expert system

Embedding is the term used to describe the process of tightly integrating an expert system with another application program. When embedded, a KES expert system becomes a part of a single executable program which contains KES runtime functions, and possibly other applications. These runtime functions provide a method of controlling the expert system and of sending, receiving and manipulating information in a parsed knowledge base. Parsing a knowledge base consists of checking the structure and syntax of the knowledge base to satisfy the pre-defined logical rules of the development tool.

Embedding an expert system provides two key advantages over stand-alone systems. It provides an efficient and cost-effective method of incorporating expert system technology into conventional programs. Through embedding, a pre-written, tested and documented decision making component can be added to any application. Embedding facilitates many flexible ways to supply and retrieve information from the expert system. The inputs may be provided through a customized user interface, and outputs may be directed to execute other processing software.

4.4.4. Design considerations

To design the expert system, a requirements analysis was carried out to determine the tasks to be performed by the embedded expert. The tasks that were identified to be performed by the expert system, are stated as follows:

1. to read the values of modelling/calibration errors calculated for the five selected models of the prototype gripper system,
2. to seek a value for the system uncertainty from the user,
3. to determine the lowest value of modelling/calibration error,
4. to identify the best model based on the error criteria, and
5. to provide an English language display of the best model along with comments on the suitability and complexity of the model.

To perform the above tasks, the design of the embedded expert was divided into two parts: building and testing a knowledge base that could run as a stand alone system, and integrating the knowledge base with the application software developed and tested separately.

4.4.4.1. Knowledge base development

This section gives a brief summary of the knowledge base development carried out for the modelling and calibration expert system. Details of the procedures are given in the KES Knowledge base author's manual [107]. The HT knowledge base had six sections, each of which contained or manipulated domain knowledge. The sections and the sequential order in which they were included were: constants, text, patterns, attributes, externals, demons and actions.

The *constants* section was used to store long or frequently used phrases as string constants or numbers in numeric expressions. The *attributes* represented the knowledge about a domain. The *externals* were used for communicating and executing programs outside the expert system. For actions based on events (forward chaining) *demons* were used. Finally, the *actions* section was used to issue the instructions that controlled the expert system execution and conducted dialogue between the user and the expert system.

Domain knowledge consisted of facts about the domain and the relationships among these facts. In the KES tool, an attribute represents some piece of knowledge (such as a fact or a characteristic) about a domain. Therefore, the domain knowledge was incorporated in the form of attributes. An attribute was assigned with a value which was either input by the end-user or inferred by the **Hypothesize and Test (HT)** procedure. Occasionally, the attribute values were also asserted in the actions section or obtained from an embedded interface. The values of some attributes depended on the values of other attributes. The range of valid values for an attribute varied with the type, and some attributes had multiple values.

The HT inference engine used an attribute knowledge source to determine the attribute value. When the inference engine was activated by a KES command, the program sets the goal of finding values for the attribute named in the command. If the sought attribute had no knowledge sources, then the inference engine requested the end-user to input a value. If the goal attribute depended on other undetermined attributes, the inference engine tried to determine the values for the sub-goal attributes using the backward chaining process. The HT process to find a value to a goal attribute is described in the following section.

4.4.4.2. HT Process

Given an initial set of manifestations, HT creates an hypothesis that explains the first manifestation. Other manifestations are then considered in turn and the hypothesis is adjusted to explain each additional manifestation. After HT comes up with an hypothesis that explains the initial manifestation, it looks for manifestations that can be used to confirm or reject its hypothesis. When all of the manifestations have been explained, HT

evaluates the likelihood of each hypothesis and returns a solution that contains the hypotheses ranked according to their likelihood.

The knowledge base developed for the modelling and calibration expert system was written in KES syntax [107] to perform the listed tasks. The complete listing of the knowledge base is given in Section B.1, Appendix B.

4.4.5. Development of Interface Program I

Interface Program I was designed to integrate the data processing program and the modelling/calibration expert system into a single executable program. The data processing program was designed to offer a set of five mathematical functions which could be used to approximate the system input-output behaviour. Four of these five functions were incorporated in such a way that the user could select the degree of the functions by specifying numerical values for the arguments. The five functions defined in the data processing program were: three least error square polynomial functions of degrees n_1 , n_1+1 and n_1+2 , a cubic spline interpolation function, and a nonlinear function consisting of n_2 linear and n_2 nonlinear (exponential) terms. The values for n_1 and n_2 were made user selectable. If the user is not sure of selecting a value, then a default value is taken by the program for developing the model or calibrating the system. The default for n_1 is 3 and for n_2 it is 4. The data processing program was written using the built-in functions of the MATLAB library.

Each function which was fitted to the system input-output data set, was displayed to the user. The user had an option to store it in designated files for re-plotting at a later time. In case of the nonlinear curve fit, a tolerance value was chosen by the program and the curve fitting proceeded in a number of steps until the mean squared value of error between the fitted curve and the data was below the tolerance. The model parameters in each case were stored in designated files. The percentage mean squared error was calculated using the relation

$$\text{error} = 100 \times \frac{\text{norm}(y - yy)}{\text{mean}(y)}, \quad (4.23)$$

where,

y = actual output data vector,

yy = modelled/calibrated output data vector,

error = percentage error, and

norm = built-in function which determines the root mean square error at every point using the relation

$$\text{norm}(x-y) = \sum_{i=1}^{i=n} \frac{(x_i - y_i)^2}{(n+1)^{1/2}} \quad (4.24)$$

The error in modelling was calculated in each case and stored separately. For calibrating the model, the user could either select a specific model (i.e. function) to fit the input-output data set and obtain the calibration errors, or let the program try out all of the five models and display the results from which a selection could be made. The actual data and the modelled data were plotted in each case and displayed to the user. The calibration errors were calculated using Equation (4.24) and stored in designated files.

The modelling/calibration expert system embedded in Interface Program I read the values of errors and interpreted them based on the action type, input by the user (i.e. modelling or calibration). The user was asked to provide the system uncertainty value for which a default could be chosen if so desired. The best model for a set of system input-output data was chosen by the modelling/calibration expert system based on a minimum error criterion which was displayed to the user. The flow charts shown in Figures 4.5 and 4.6 indicate the sequence of program flow in Interface Program I used to perform system modelling and calibration for the prototype system.

4.5. Implementation Results and Discussion

4.5.1. Operating procedure

The prototype tactile sensing system was modelled using Interface Program I which obtained the transformation parameters to be used for each of the eight sensing sites. Each model provided the relationship between the applied force and the analog sensor output voltage. The models were developed using a set of experimental input-output data and calibrated using a second set of data. The grasping and releasing type of data were separately processed to obtain two models for each sensor, and a set of 16 input-output functions were obtained for the eight sensors.

The sequence of operations of the interfacing software consisted of first displaying a welcome message and the purpose of the Program. Then the user was prompted to enter the name of the file which contained the input-output data in the form of paired row entries for each observation. The total number of data pairs and the type of action desired, namely, modelling or calibration, was also entered by the user on the keyboard. Explanations of the different values to be entered were provided by the program as a guideline.

If the user selected the modelling option, he was prompted to enter the two values, n_1 and n_2 , to determine the degree of the three polynomials and the number of exponen-

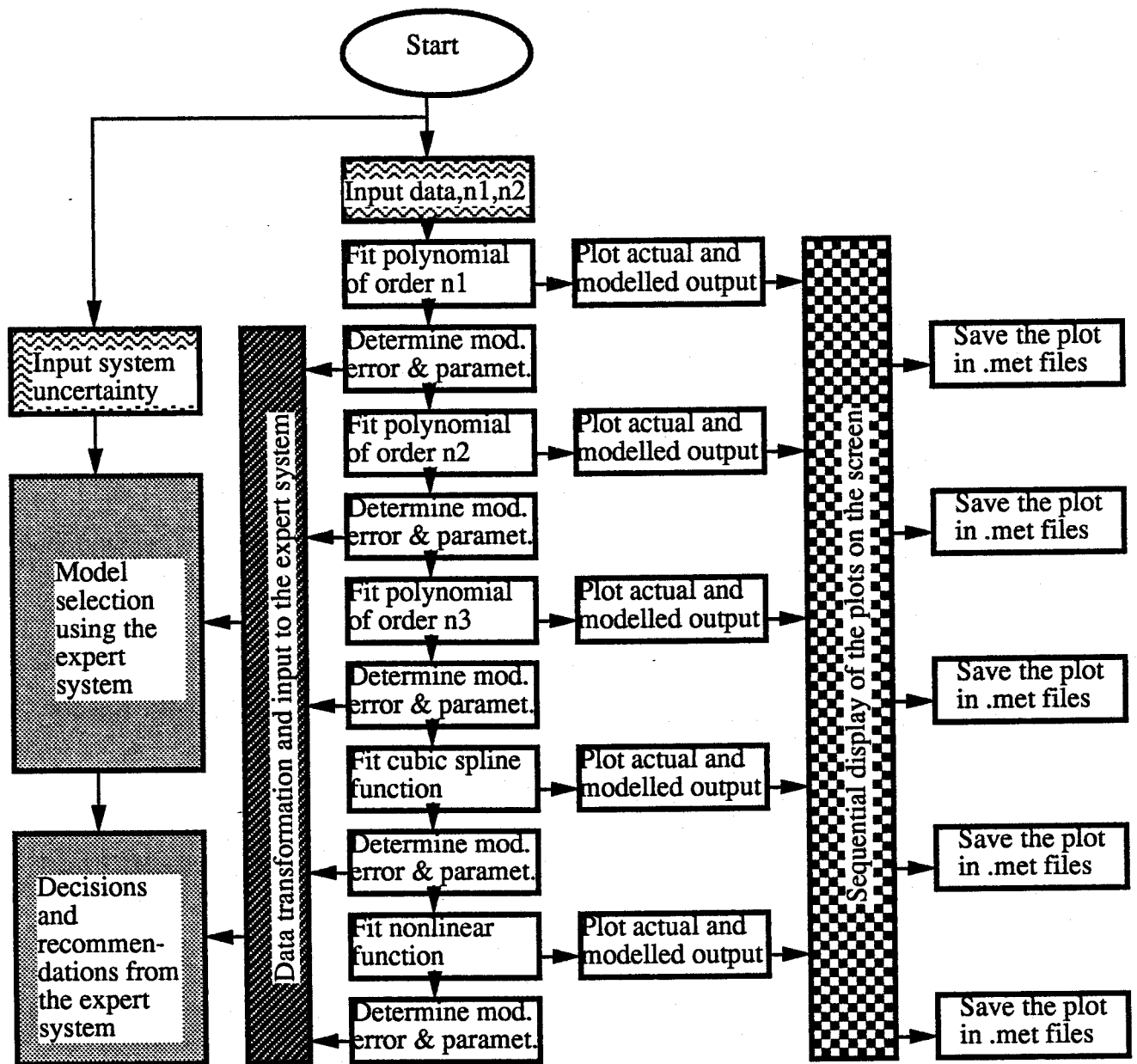


Figure 4.5: Flow chart of the system modelling scheme .

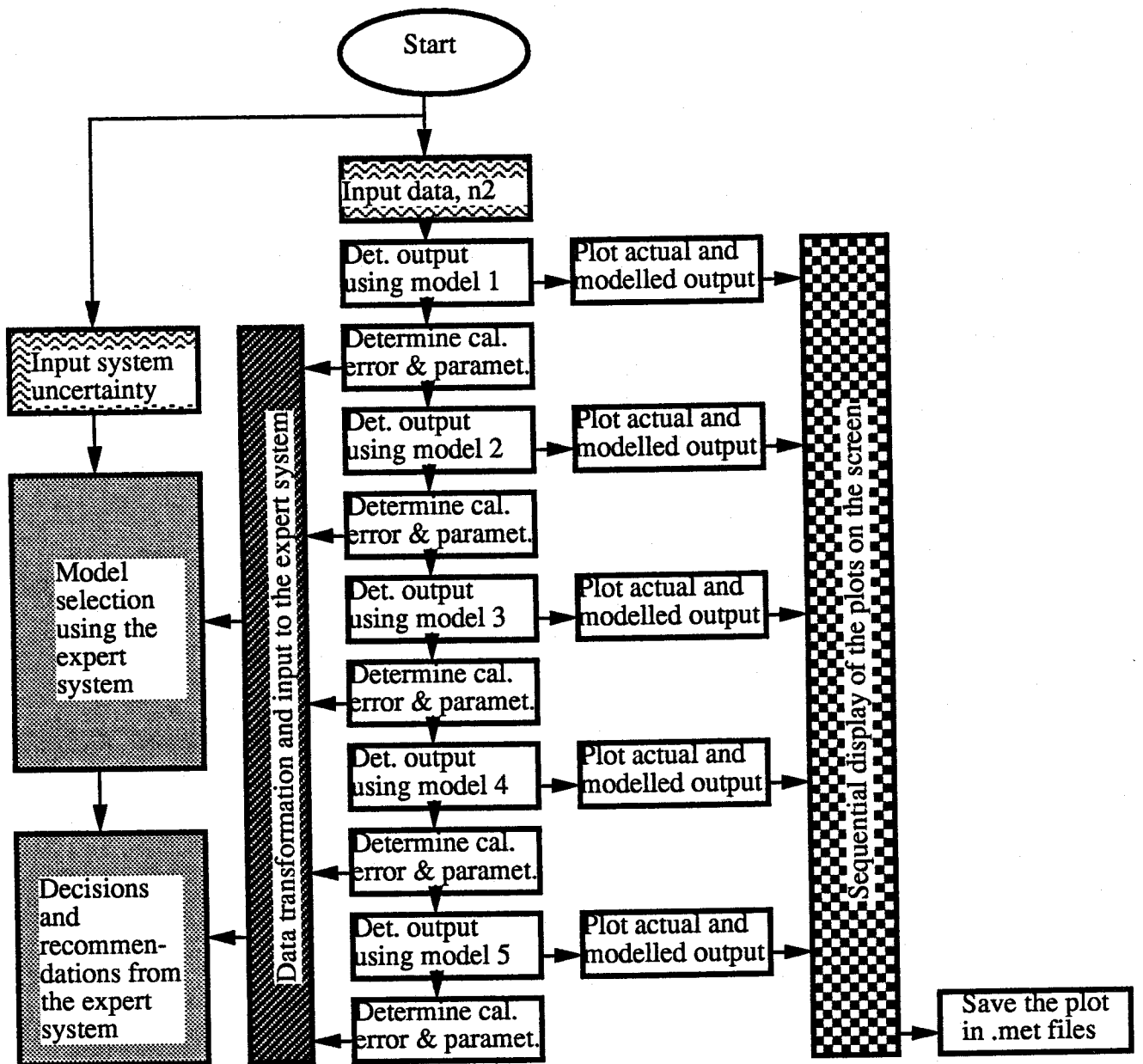


Figure 4.6: Flow chart of the system calibration scheme .

tial terms to be used for the nonlinear function. If the user selected the calibration option, then he was given a choice to select one of the five models. In both cases, default values were selected by the program if the user did not enter values. The information was then transferred to the appropriate processing modules which fit the five functions, one after the other. The fitted curve and the actual output were plotted on the same set of axes and displayed to the user. The root mean square (RMS) percentage errors between the fitted function and the actual data output were calculated in the five cases and stored separately.

Control was then passed to the embedded expert system. The expert system obtained the error values and requested the user to enter a value for the system uncertainty. After a decision was reached regarding the best model to be used, it was displayed to the user along with necessary comments. The expert system also displayed the location of the file where the model parameters were stored as well as the percentage modelling error for the selected model. At this stage, the user had a choice to remodel or re-calibrate the system if necessary. The listing of a typical user session carried out with the modelling and calibration program is given in Section B.2, Appendix B.

4.5.2. Test results and discussion

The plots of the five functions and the data to which they were fitted and displayed by Interface Program I were used to determine the best selection. The plots showing the actual and modelled system outputs pertaining to sensor 1 are shown in Figures 4.7 to 4.11.

These diagrams show the five selected functions fitted to the sensor 1 input-output data for a grasping operation (increasing forces). The percentage modelling error obtained in each case of modelling is shown in Table 4.4.

The expert system displayed a recommendation which is shown in the form of a listing of a typical user session with Interface Program I in Appendix B.2. The expert system recommended the model 4, which is the function consisting of piecewise cubic interpolation functions, as the best choice. However, due to the nature of this function, the user was advised by the expert system to try other models before arriving at a final selection. This was because cubic splines are known to behave unpredictably outside the range of data. In such a case, therefore, the user had two options: either to re-calibrate the model using a second set of data or to select another model. The latter is the second best choice based on the error criterion.

Re-calibration of the sensor using a second set of data yielded calibration errors well in excess of the system uncertainty value. The suggested alternative, namely model 2, which was the second best choice, yielded RMS percentage errors of 2.93 % using the

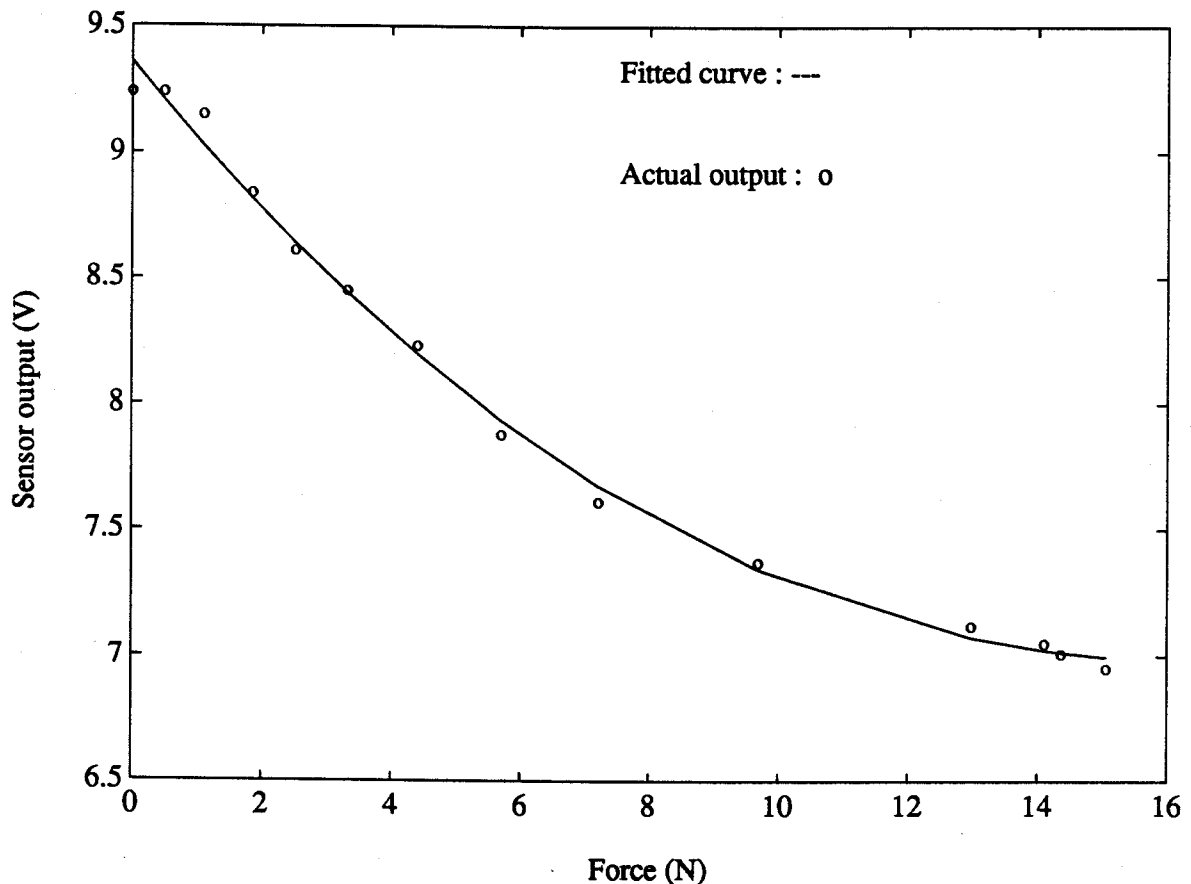


Figure 4.7: A third degree polynomial fit to the sensor 1 input-output data

first set of modelling data and 2.98% using the second set of (calibration) data. Thus, it was concluded that model 2 (fourth degree polynomial function) was appropriate for sensor I grasping data.

In a similar manner, the modelling functions and the modelling errors for all other sensors were determined. Table 4.5 gives the summary of the modelling errors obtained for the case of two models, namely, the one which yielded the lowest RMS error and the one which was the second best choice in each case. It is evident that for sensors 1, 6, 7, and 8, model 2 is the best selection whereas for sensors 2, 3, 4, and 5, the nonlinear model 5 gives the lowest error. Using a nonlinear model involves applying four linear and four nonlinear parameters to every data value and hence is computationally more complex than the fourth order polynomial function. Besides, application of the nonlinear model was considered necessary only for precision jobs in which finer variations of dynamic forces have to be interpreted. In view of these considerations, and in order to

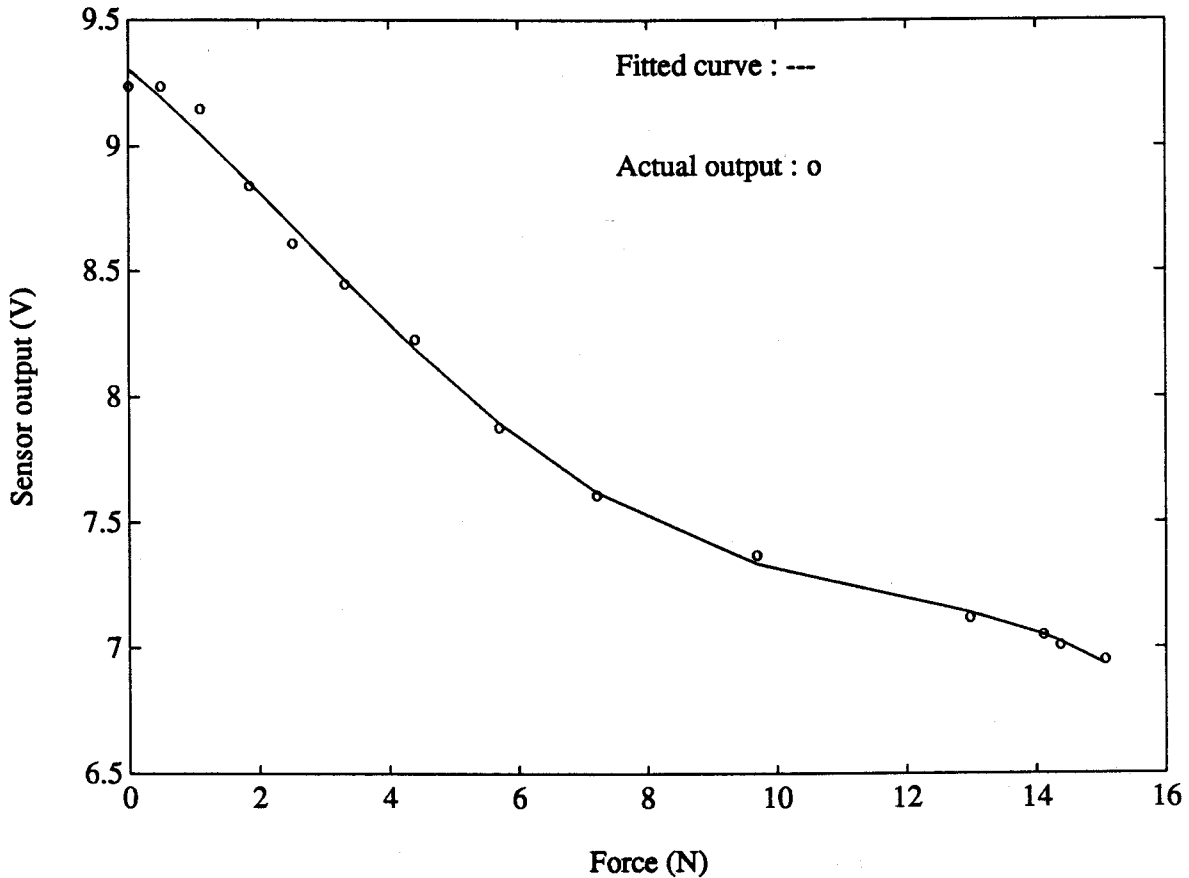


Figure 4.8: A fourth degree polynomial fit to the sensor 1 input-output data

use a relatively simple and uniform model, it was decided to use model 2, (a fourth order polynomial function) to characterize each of the eight sensors. The model parameters for all the eight sensors were obtained and stored in the form of ASCII files.

4.6. Conclusion

An expert system-based modelling and calibration scheme designed and implemented to obtain the model parameters of the prototype gripper system has been described. An expert system, embedded in the application software, guides the user to select the most appropriate mathematical model for the sensing system. The development of such a scheme was undertaken because of the inability of lumped parameter models to adequately characterize the input-output behaviour of the tactile sensors for a dynamic task. The mathematical formulations for characterizing the three major blocks of

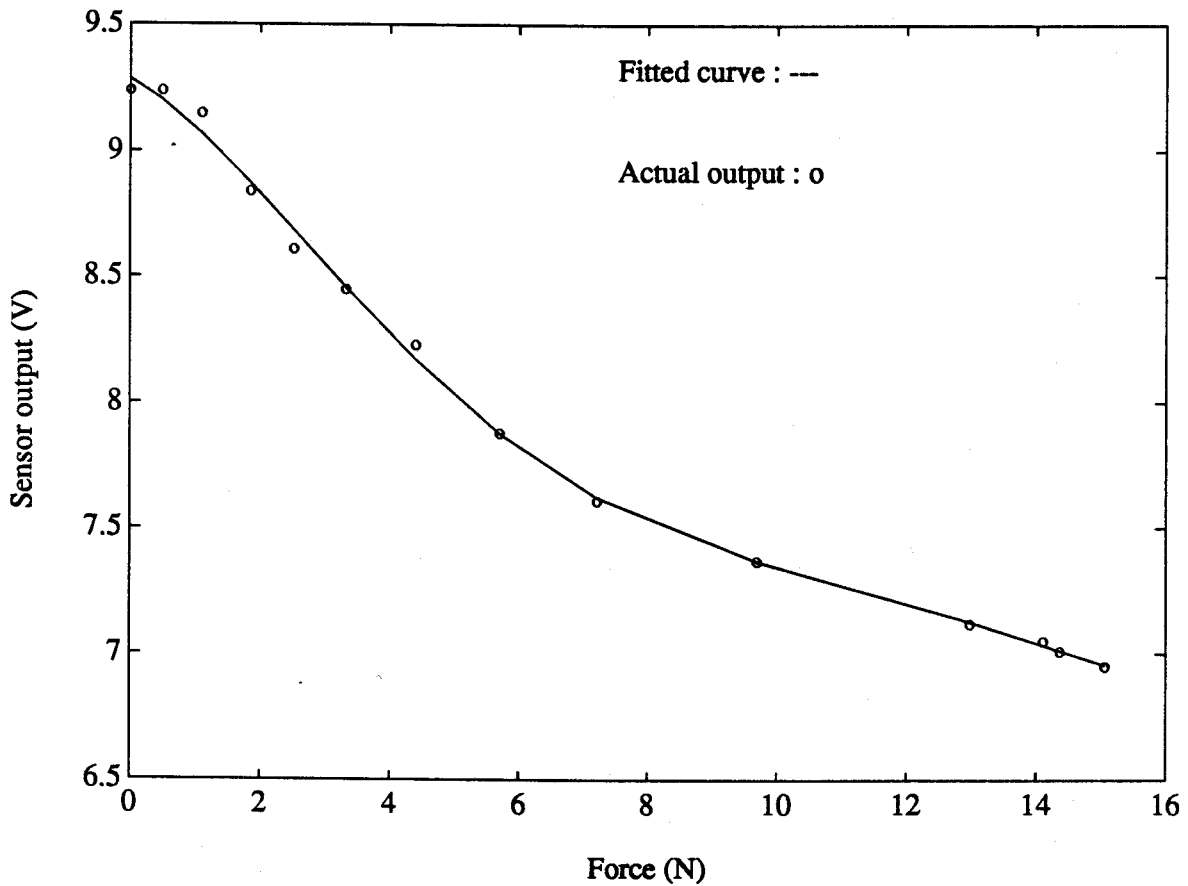


Figure 4.9: A fifth degree polynomial fit to the sensor 1 input-output data

the sensing system, namely, the FSR transducer, the mechanical overlays, and the data acquisition system were discussed using relevant equations. The requirement for the sensor model was that it should enable the dynamic force data measured at the sensor outputs to be transformed into the true values of applied forces at the sensing sites. This was necessary to form on-line tactile images from dynamic forces as described in the next chapter. An integrated program which embedded the expert system into a program containing the processing software modules was developed and implemented.

Using this scheme, models for the eight sensors of the prototype gripper system have been obtained. The validity of such a model is restricted to the particular configuration of the prototype system. If there is a change in the configuration, then the procedure suggested in this chapter could be used to remodel the system. Since the model can be updated, the variations in system components and their nonlinear behaviour can be accounted for. Besides, it is possible to ensure that the modelling error is less than a pre-estimated system uncertainty value.

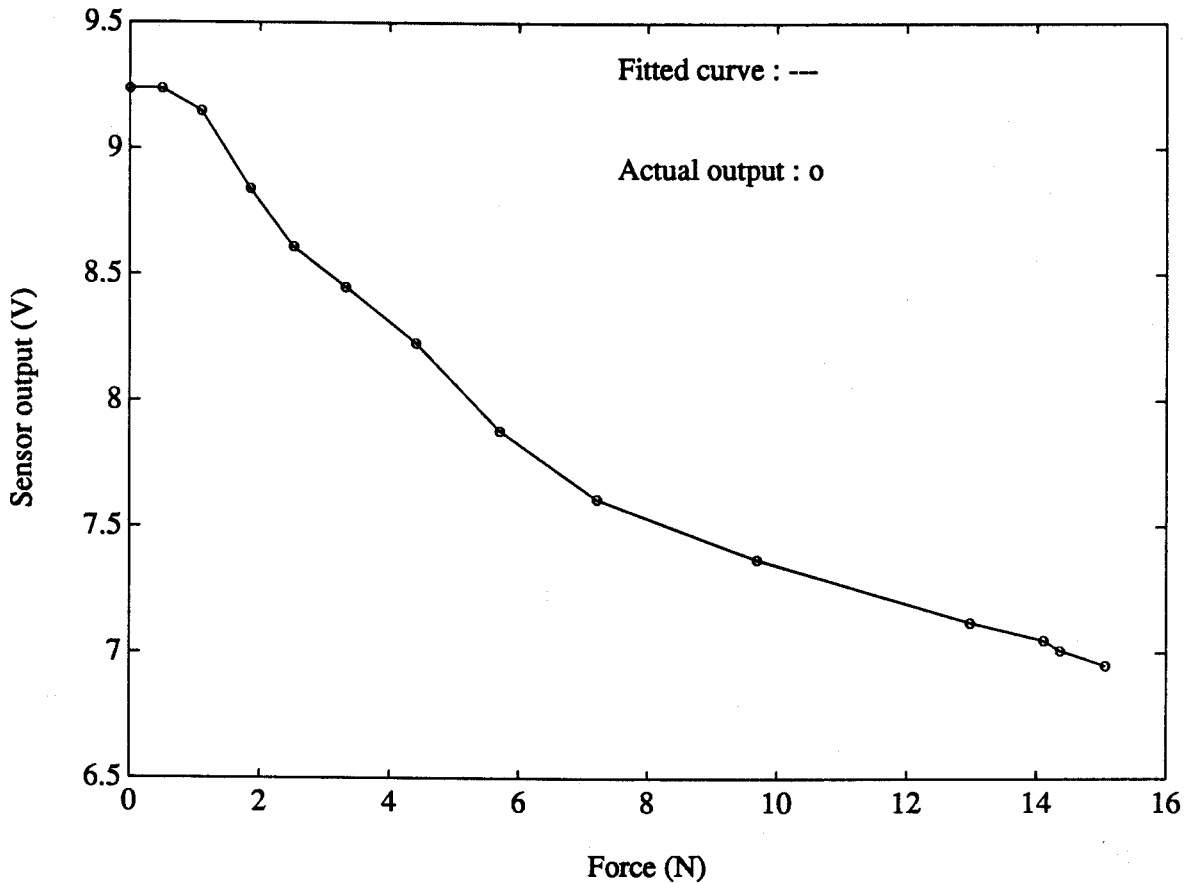


Figure 4.10: A cubic spline interpolation function fit to the sensor 1 input-output data

The maximum allowable modelling error in a particular system is dictated by the mean value of an uncertainty factor. For the prototype gripper system, this uncertainty factor included the contributions from the major variants involved in the sensing process. The uncertainty in the force measurement process was investigated and four major contributors to the uncertainty were identified. These were estimated using standard statistical analysis procedures applied to laboratory test data. Using these procedures, a mean value of system uncertainty was obtained for the prototype system. The embedded expert system used this uncertainty value to determine the suitability of the various models and to select one of them as the best choice. The unpredictable behaviour of some of the mathematical formulations was also considered before deciding on a specific model for the sensors. The next chapter will discuss the technique of tactile imaging and will outline the design and implementation steps necessary to obtain an on-line tactile image from the prototype system.

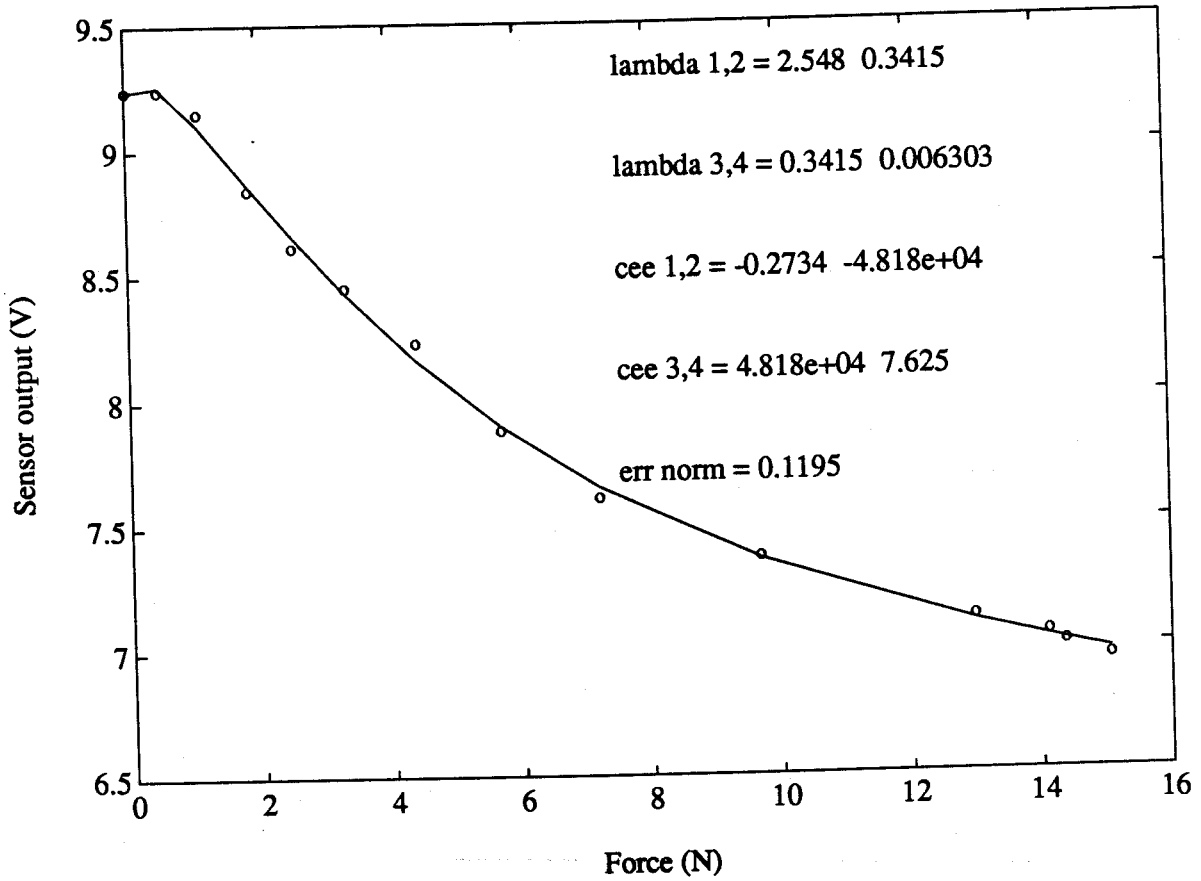


Figure 4.11: A non-linear [sum of four exponentials] function fit to the sensor 1 input-output data

Table 4.4: Modelling errors obtained by using the five functions for characterizing sensor 1 grasping behaviour

Model number	Function description	RMS modelling error (%)
1	3rd degree polynomial	3.34
2	4th degree polynomial	2.94
3	5th degree polynomial	134.59
4	piecewise cubic splines	0
5	nonlinear (sum of 4 exp.) function	5.12

Table 4.5: A summary of modelling errors obtained for the eight sensors of the prototype gripper system

Sensor no.	Type of data	Best model (out of 1, 2, 3, & 5)	Lowest error, %	Selected model number	Error in the selected model, %
1	grasping	2	2.94	2	2.94
1	releasing	2	2.99	2	2.99
2	grasping	5	10.46	2	11.29
2	releasing	5	8.69	2	8.81
3	grasping	5	4.76	2	7.97
3	releasing	5	7.23	2	7.89
4	grasping	5	4.57	2	6.43
4	releasing	5	5.69	2	7.72
5	grasping	5	3.39	2	7.57
5	releasing	5	2.52	2	6.76
6	grasping	2	0.90	2	0.90
6	releasing	2	1.00	2	1.00
7	grasping	2	1.10	2	1.10
7	releasing	2	1.21	2	1.21
8	grasping	2	1.24	2	1.24
8	releasing	2	1.99	2	1.99

5. TACTILE IMAGING AND INTERPRETATION OF DYNAMIC FORCE DATA

5.1. Introduction

The dynamic contact forces between a gripper and an object obtained during the performance of a task contain the information about the status of the task. The status of a task in this context refers to the state of the gripper which could be either grasping, releasing or neither grasping nor releasing an object. In order to extract the status information, the forces need to be analyzed. Earlier schemes suggested in the literature for this purpose were based on binary tactile imaging, in which only the presence or absence of a signal at a sensing site was determined. These approaches have not yielded all the necessary information about the on-line status of a task. Besides, binary imaging assumes that all the sensors in the system possess similar characteristics.

In order to determine the on-line status of a task, a technique to obtain a tactile image which portrays the dynamic forces in terms of graded intensities was necessary. In this chapter, the technique which was used to obtain the tactile image from the dynamic forces measured by the prototype gripper system while handling objects will be described. The technique will be introduced by first defining the basic characteristics of dynamic forces. Then the basic principles of thresholding will be established and a method to obtain a force image will be described. The formation of a tactile image and the criteria for its interpretation will be explained. The trade offs involved in the selection of threshold ranges and the design of a pre-filter will also be discussed. The modifications in the technique in order to make it suitable for on-line implementation will be described using results obtained from real data.

5.2. Principles of Tactile Imaging

A tactile image is a means of representing the values of instantaneous forces measured at the sensing sites. Three main characteristics of a dynamic force, namely, the force gradient, the force impulse and the relative force variation, may be represented mathematically as follows:

force gradient = rate of change of force with time, in N/s,

$$F_g = \frac{df}{dt}, \quad (5.1)$$

force impulse at time t, in N-s,

$$F_i = \int_{t_1}^{t_2} F(t) dt, \quad (5.2)$$

which could be approximated as,

$$F_i \approx \sum_1^n F_{av} dt, \quad (5.3)$$

and relative force variation, in %,

$$F_v = \frac{df}{F_{av}} \times 100 \%, \quad (5.4)$$

where,

dt = duration between successive sampling instants, t_1 and t_2
 $= t_2 - t_1$,

df = change in the force between two successive instants,
 $= f_2 - f_1$, and

$$F_{av} = \frac{F_1 + F_2}{2}. \quad (5.5)$$

A primary requirement to determine the above quantities from the dynamic forces is to measure the instantaneous values of contact forces unambiguously in real time. Specifically, one must select appropriate noise margins to account for the random errors arising in the tactile sensor hardware, and in the data acquisition and processing systems. The results of the statistical analysis carried out by Vaidyanathan [108] to determine the accuracy with which dynamic forces may be measured in a practical system indicated that the forces on gripper fingers of the prototype system may be estimated with a 95 % confidence level. This was interpreted to mean that the maximum accuracy with which the three dynamic force quantities can be estimated is 95 %. Application of a simple technique to estimate the force gradient, F_g , and the relative force variation, F_v , could be used if the force variations are relatively noise free.

In a practical system, the dynamic forces are generally corrupted with noise. For such a system, a method was formulated to determine the instantaneous forces on the

gripper fingers while performing a task. This method, known as the tactile imaging scheme, was used to determine primitive values of forces from the values of forces measured by the tactile sensors of the prototype gripper system. The design of the tactile imaging system which considered a number of factors that affect the accuracy of the image, is described in the next section.

5.2.1. Forming a force image

The first step in the formation of a tactile image was to obtain force images from the measured values of forces at each sensing site. An arbitrary force variation, plotted as a function of time, is shown in Figure 5.1. For the case of a discrete force distribution, the

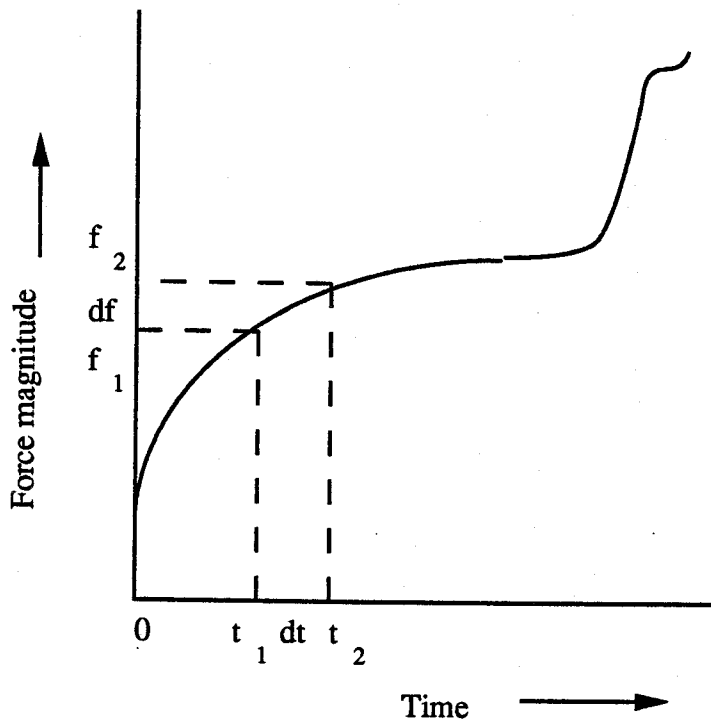


Figure 5.1: Characterizing a dynamic force .

force gradient was approximated using the simple relation for a derivative,

$$F_g = \frac{f_2 - f_1}{t_2 - t_1}. \quad (5.6)$$

By dividing the time axis into n equal discrete time periods, the force gradients at successive instants of time were determined by taking simple differences between the values of successive forces.

Knowing the total range of forces applicable for a task, it was possible to divide the total range into a number of thresholds. The force values between two successive thresholds were assigned a primitive value, which identified the threshold level to which the force belonged. An array was formed consisting of the time of the task and the corresponding primitive value of force experienced at a sensing site. This array was referred to as the force image of the sensor at that site. Such force images were formed for all the sensors of the tactile sensing system (i.e. eight in case of the prototype gripper system).

The main considerations in forming a force image in the manner described above were the selection of the range between two threshold points, known as the inter-threshold range, the resolution, and the accuracy of the force images.

5.2.1.1. Selection of ranges and force thresholding

Selecting a range between two threshold points (i.e. the inter-threshold range) was governed by an engineering trade-off between the resolution of the detected force and the filtering of the noise in the force image. The range also affected the computational complexity of processing the force images. A low value of range offered higher resolution suitable for precision jobs, but more expensive filtering procedures were necessary. Besides, a low value of inter-threshold range was not suitable when the dynamic forces were acquired using a system hardware which exhibited larger uncertainties. This was because the selected inter-threshold range always had to be higher than the system uncertainty value.

A large value of inter-threshold range resulted in missed detection of some small force variations which subsequently affected the task status of the gripper. These aspects indicated that the inter-threshold range was a critical value which had to be chosen carefully to obtain meaningful force images. For a specific gripper system, it was possible to provide a variable inter-threshold range, which could be selected based on the type of task to be performed. Therefore, a provision to select the inter-threshold range was incorporated into the processing software.

Force thresholding consisted of assigning either equal or unequal partitions to the total range of forces likely to be encountered in a task. The number of partitions assigned depended on the range between thresholds and the total range of forces to be measured. For extracting information from an on-line operation, the task of assigning the primitive values to the forces will also have to be performed on-line. This imposed restrictions on the method of applying the thresholding technique employed in a particular tactile sensing system and will be discussed in detail in a later section (Section 5.2.4.1).

5.2.1.2. Accuracy and related issues

The accuracy of a tactile image is a measure of the ability of the primitive values to exhibit the true characteristics of the forces from which they have been derived. Error in a force image can arise due to thresholding, imaging, and other operations performed on the dynamic force data. The error due to the thresholding operation could be defined mathematically, whereas the error due to imaging and other operations were analyzed qualitatively.

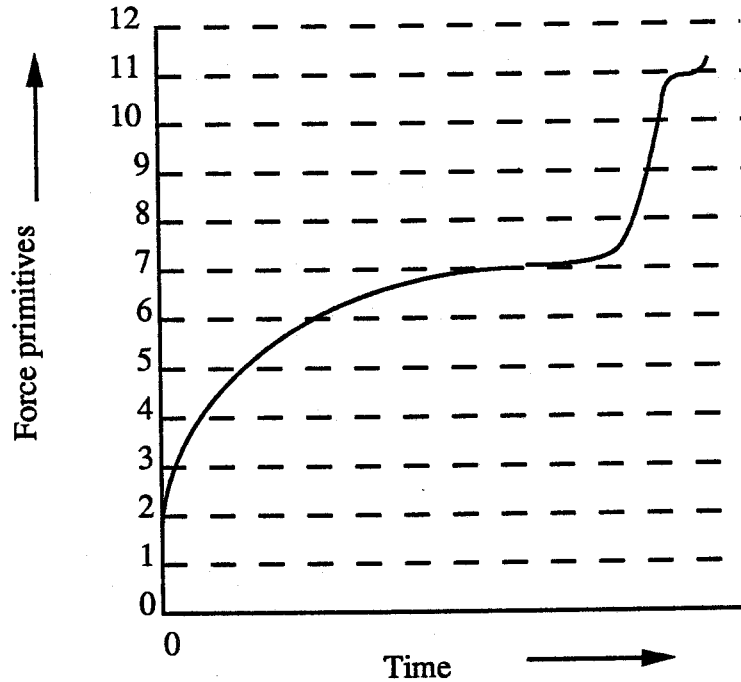


Figure 5.2: Equal range thresholding of dynamic force .

Figure 5.2 shows equal thresholds applied to a typical dynamic force variation as a function of time. With reference to this figure, the maximum percentage error at the m -th threshold level in a force image was defined as :

$$FI_{err,m} = \frac{|F_{Avm} - F_m|}{F_{Avm}} \times 100. \quad (5.7)$$

$$F_{Avm} = \frac{F_{m-1} + F_m}{2}. \quad (5.8)$$

where,

$FI_{err,m}$ = Maximum force imaging error at m-th level,

F_{Avm} = Mean force value at m-th level,

F_{m-1} = Force value at the (m-1)th level, and

F_m = Force value at the m-th level.

The value of the maximum imaging error decreased with increasing threshold levels in the case of equal range thresholding. The value was maximum when $m = 1$ and was minimum when $m = n$. If unequal thresholding was used, then it was possible to assign threshold levels such that the maximum error due to imaging was kept uniform throughout the range. This error is similar to the quantizing error in A to D converters.

Generally, the accuracy desired from a force image was largely task dependent. The accuracy indicated whether the primitive values were able to reflect the changing gripper status quickly enough to prevent an object slippage. For a precision grasping task which might require frequent regripping, the force images obtained have to be very accurate.

In the case of a general purpose grasping operation, the speed of grasping influenced the noise in the dynamic force data. This was especially true when a viscoelastic medium, such as a soft rubber pad, was used to transfer the forces onto the sensing sites. It was found that the higher the speed of gripping, higher was the noise in the raw force (dynamic force) data. The effect of the noise on the raw force data was separately investigated in a case study and its results were used to form the design criteria for a pre-filter. Specifically, noise in the raw data was found to significantly influence the transitional uncertainties in the force images.

5.2.2. Transitional uncertainties

Transitional uncertainty in a force image can be defined as the uncertainty in the primitive force value which causes ambiguity in its correct interpretation when a task is in progress. Due to the presence of noise in the measured force data, transitional uncertainties always exist in a force image. In order to clarify the definition of the transitional uncertainties, the results from a case study which was conducted using actual data obtained while grasping a sample object using the prototype system were used.

In this study, the raw and filtered force data were used for determining the force image from one of the sensors, sensor # 1. The variation of raw forces and filtered forces, as measured by sensor #1 is shown in Figure 5.3. The two curves for filtered

forces were obtained by using 5-point and 10-point moving average low pass filters, which were selected based on a separate study to be discussed later in this section. The curves in Figure 5.3 show sampled values of the forces plotted as a function of time. The noise present in the raw force data is clearly evident. The filtered data show a selective noise reduction obtained without significantly disturbing the trend of the data.

The raw data were processed to obtain a force image using a 0.5 N inter-threshold range. The force image was formed from the data measured by sensor #1 and a plot of the resulting primitive values as a function of time is shown in Figure 5.4. The time axis refers to the time of the task. From the force image, it can be seen that there is an uncertainty associated with some of the transitions when the primitive values change at various points on the time axis. These uncertainties are the transitional uncertainties introduced earlier.

The plot in Figure 5.5 shows the details of the transitional uncertainties obtained from the raw data using the grasping and the releasing data measured by sensor #1. In this plot, the portion of the force image from a task time, $t = 1400$ ms to $t = 1700$ ms, is shown. It can be seen that at $t = 1545$ ms, and for values of t between 1560 and 1590 ms, there is uncertainty in the image obtained during grasping while at $t = 1540$, 1550, 1560, 1570, and for values of t between 1580 to 1640 ms, there is uncertainty in the image obtained during releasing.

To study the effect of prefiltering of the raw data on the transition uncertainties, different types of low pass filters were tried. In each case, the force image from sensor #1 was formed and the occurrences of the transitional uncertainties were studied. When the raw data were filtered using a moving average filter of two different window sizes, consisting of 5 and 10 data points respectively, the number of uncertainties was found to decrease. This result can be seen by referring to the plots of Figure 5.5, 5.6, and 5.7 which show the transitional uncertainties in the images obtained from the raw and filtered data measured by sensor #1 obtained during the same task. Successively decreasing numbers of transitions are evident from the three plots for both the grasping and releasing data images as the width of the filter (in terms of the number of data points used for averaging) is increased.

The data for these plots were obtained by extracting the force image pertaining to sensor #1 during the same (i.e. 1400 to 1700) 300 ms period. The selection of the period was based on the presence of a maximum number of observed transitions. The duration of transitional uncertainty during grasping of the object is seen to progressively reduce from 50 ms to 25 ms to 15 ms by using the 5 point and 10 point wide moving average filters. A similar effect is seen in the releasing data where the transitional uncertainty reduces from 120 ms to 60 ms when using a 5 point wide moving average filter. Further, the frequency of transitions was also reduced by pre-filtering the raw data.

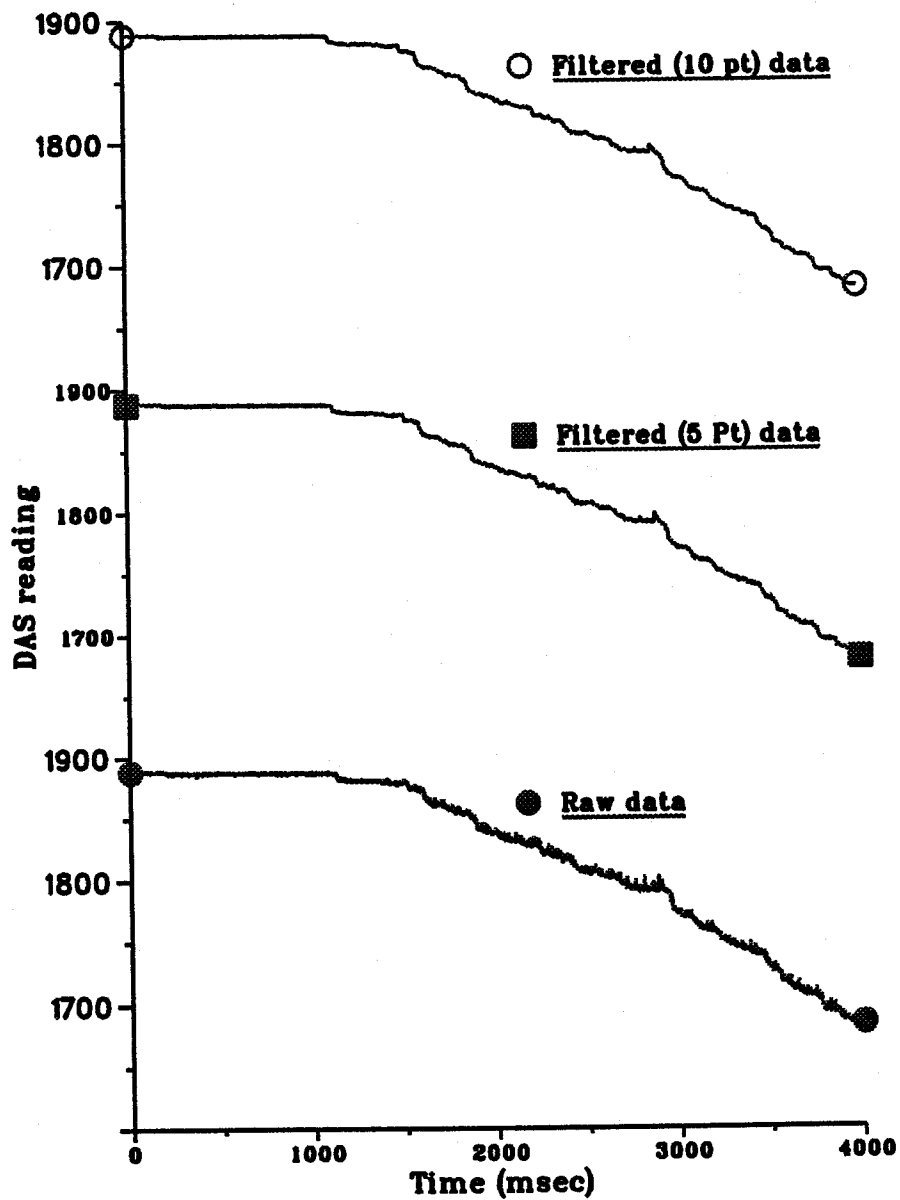


Figure 5.3: Raw and filtered data from sensor #1 during grasping.

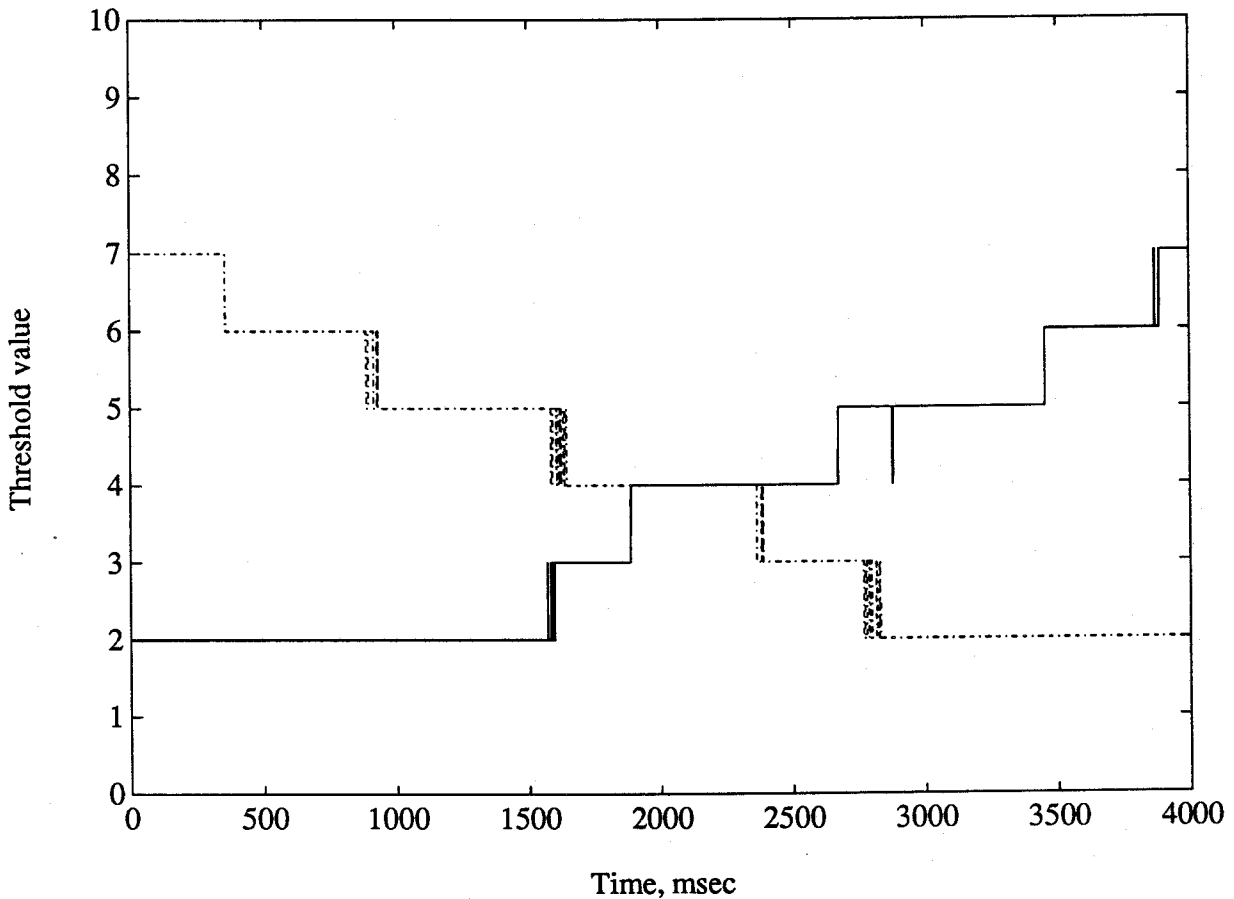


Figure 5.4: Force image obtained from sensor # 1, using raw data .

In addition to the transitional uncertainties, the design of the pre-filter also considered other factors such as the resolution desired for a particular task, the characteristics of the sensing system, and the time allowed for processing on-line data. In addition, the trade-off between the amount of prefiltering required for raw data and the total time allowable for tactile imaging was also studied. These aspects of prefiltering are separately discussed in a later section.

5.2.3. Forming a tactile image

In order to identify the changes in the measured forces during the performance of a task, it was decided to obtain an image which showed the simultaneous force images from all the tactile sensors of the prototype system. This was achieved by combining the force images from all the eight sensors of the prototype system in the form of a two

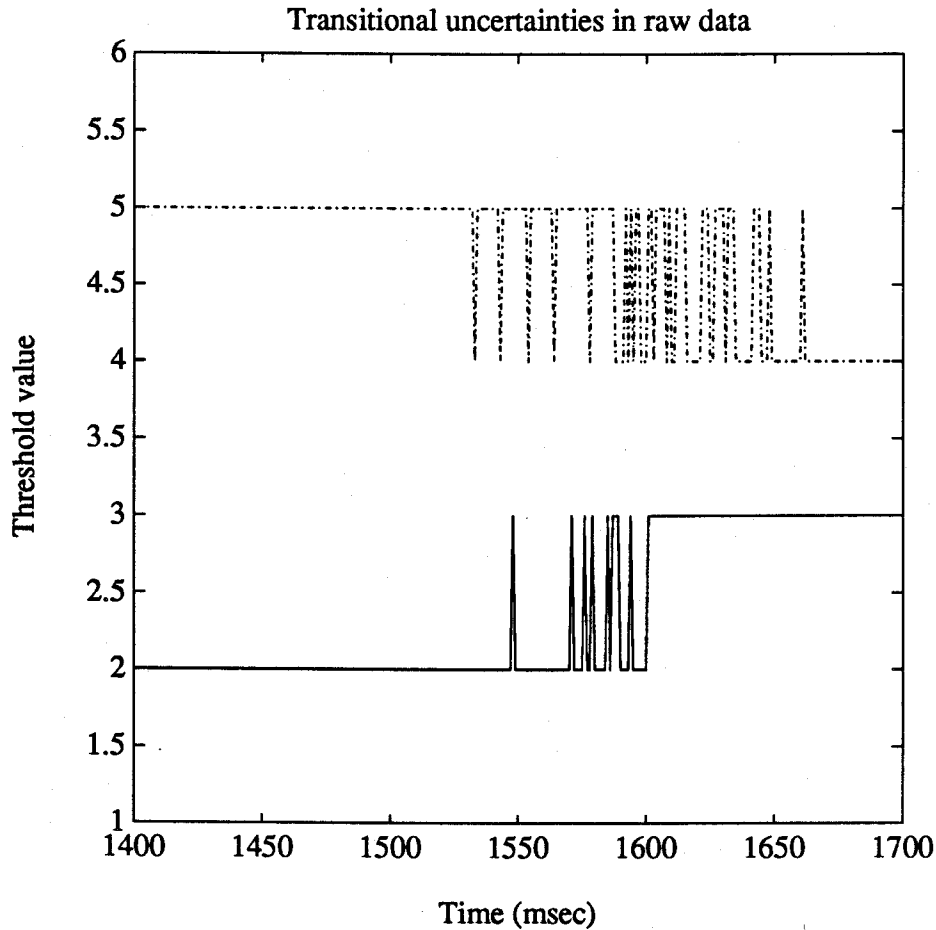


Figure 5.5: Details of the transitional uncertainties - image from raw data .

dimensional array. Such an array was referred to as a tactile image and it portrayed an instantaneous record of the forces on all sensing sites involved in the gripper system. The structure of a typical tactile image is shown in Table 5.1. The entries in the first column correspond to the time at which the force measurements were made. The subsequent columns denote the sensing site locations of the tactile sensing system. The row entries in these columns designate the primitive value of the force obtained using the imaging technique.

The purpose of forming a tactile image was to determine the changes in the measured forces between successive instants. By looking at two successive rows, a decision regarding the trend of the task could be formulated, and using the information from subsequent rows, the decision could be strengthened or weakened. A tactile image was also used to determine the instantaneous total force on the system by cumulating the force primitive values row-wise (by adding elements in a row together).

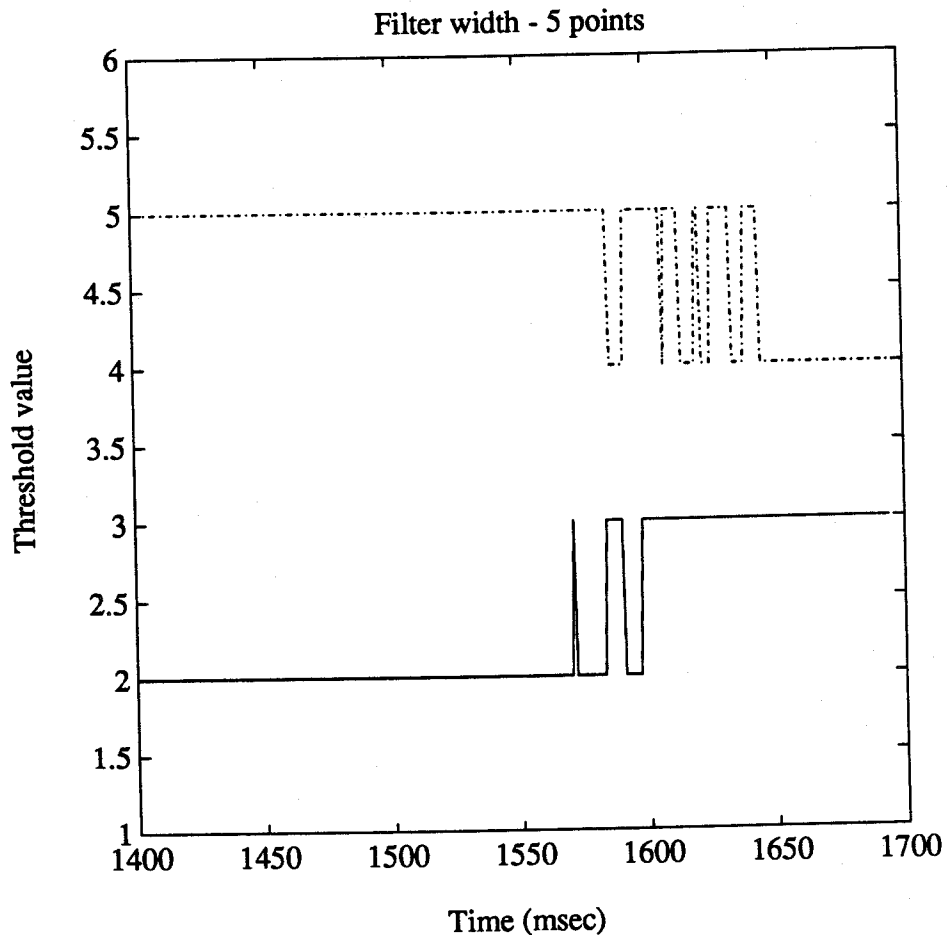


Figure 5.6: Transitional uncertainties in the force image obtained from sensor #1 filtered data - 5 point moving average filter .

5.2.4. Interpretation of a tactile image

The dynamic force variation in both space and time, depicted in a tactile image, contains information to determine the relative behaviour of the system at different times. These dynamic characteristics were used to obtain decision parameters which could be interpreted based on the immediate past history of the system. In a gripper system, the tactile image was formed from the forces measured at the sensing sites. Due to the viscoelastic nature of the finger surface, it was difficult to isolate the applied force component using conventional techniques. Tactile imaging technique provided a realistic solution if the associated errors could be estimated and tolerated in the task. Therefore, a set of conditions was formulated to interpret the tactile image.

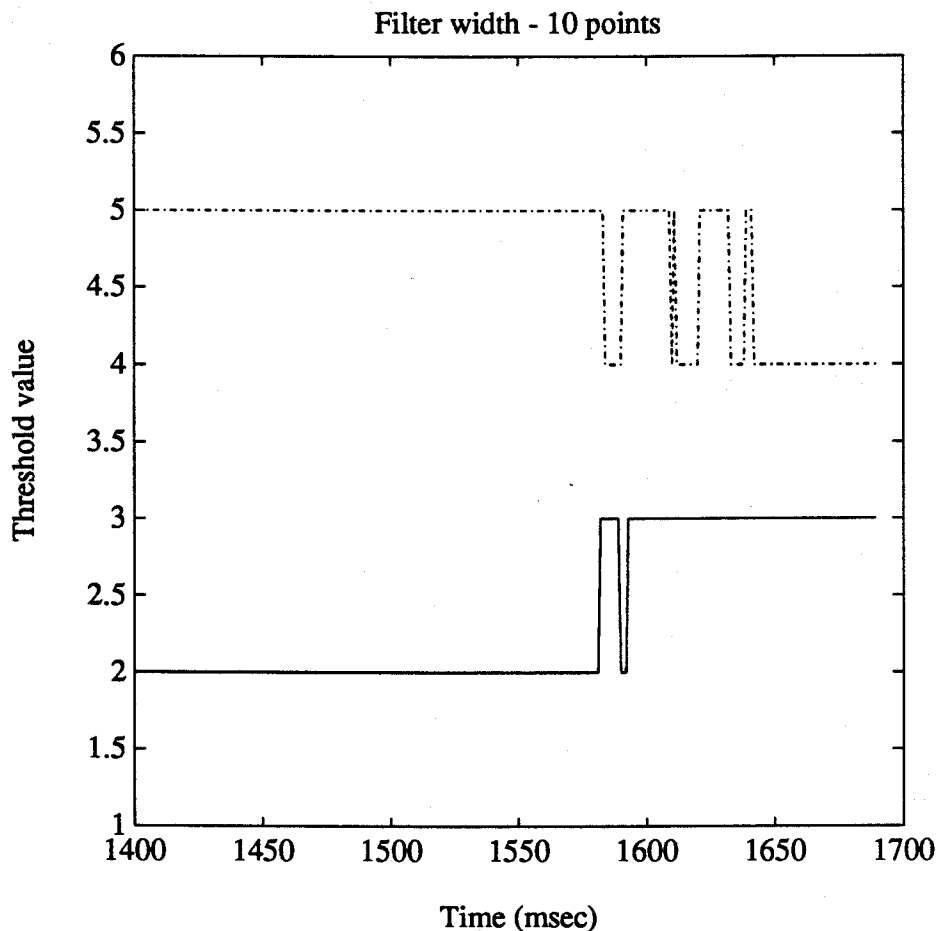


Figure 5.7: Transitional uncertainties in the force image obtained from sensor #1 filtered data - 10 point moving average filter .

5.2.4.1. Criteria for interpretation

If the tactile image could be formed for a selected block of data, then it was assumed possible to analyse the characteristics of the image within that block. It was also possible to determine the changes in the characteristics of the image between successive blocks.

A typical block consisted of a pre-defined number (for example, n) of sampled values of forces at each sensing site. Let the time interval elapsed during the acquisition of these n values be designated as t_b . An image formed from the block of data was used to obtain information about the force gradients and the cumulative forces within the time interval t_b . Considering the force image from one of the sensing sites, if the values of the force primitives at two successive time instants showed an increasing trend, then this was

Table 5.1: Structure of a typical tactile image .

Time of	Primitive force values at the sensing sites represented by the sensor number							
sampling	S #1	S #2	S #3	S #4	S #5	S #6	S #7	S #8
t_0	f_{10}	f_{20}	f_{30}	f_{40}	f_{50}	f_{60}	f_{70}	f_{80}
t_1	f_{11}	f_{21}
t_2	f_{12}
...
...
...
...
t_{n-1}
t_n	f_{1n}	f_{2n}	f_{3n}	f_{4n}	f_{5n}	f_{6n}	f_{7n}	f_{8n}

considered as a positive force gradient and was used to characterize the task as likely to be a grasping type. On the other hand, if the successive force primitives showed a decreasing trend, then it was considered likely to be a releasing type of operation. If there was no change between successive values, then the gripper status had not undergone any change in the interval of time corresponding to that block of data, and the task status was characterized as unchanged. Thus, by processing a tactile image from a block of data, it was possible to obtain the above information from all the sensing sites simultaneously. For a time duration t_p , all of the grasps and releases were cumulated. To increase the confidence in decision making, the number of sensing sites showing similar behaviour (i.e. increasing or decreasing forces) were counted and used to determine a sensor confidence factor. To determine relative displacement of the object with respect to the gripper fingers, the time instants at which the increase or decrease of the force primitive values had occurred at every sensing site were noted.

5.2.4.2. Interpretation of errors and selection of error margin

The accuracy of a tactile image depends on the range of forces between successive thresholds. While this range should be greater than the average noise and uncertainty levels, it should be small enough to enable detection of primitive level changes within a reasonable time. The different nonlinearities of the transducers further modify the ranges unequally.

The criteria formulated to interpret the tactile image assumed that the tactile image

obtained was error free. However, in a real task, the presence of noise in the force signal always resulted in imaging errors. The two main factors which contributed to the error in the tactile image were the error due to noise, which caused the transitional uncertainties in the force images, and the errors introduced due to the method of interpretation of the tactile image. The first type of error was reduced using prefiltering of the force data. The error due to the method of interpretation of the image was reduced by using a "dead band filter". This filter identified the positive and negative transitions in a tactile image and introduced suitable dead bands around the transition points. A transition validation procedure was designed to check every transition and identify true transitions. The details of implementation of this filter will be described in Section 6.2 in the next chapter which deals with the topic of decision-making using tactile images.

Another factor causing ambiguity in the tactile image interpretation was the uncertainty factor associated with the gripper system. As described in Chapter 4, the prototype gripper system exhibited a variation of about 8 % in the sensor reading for the same applied force due to the major variants, namely, the FSR material, the compliant backing, or the point of application of the force. These errors also contributed to the transitional uncertainties discussed in Section 5.2.2.

For an on-line task status determination, the time taken to obtain a tactile image was a critical factor. This depended on factors such as the number of sensors in the system, the real time taken to acquire and pre-filter raw force data, the cpu (Central processing unit) time taken by the computer to model the sensors and to apply the model to measured force data in order to linearize the sensor data, and the cpu time taken to form force images. The various cpu times used by the computer varied with the choice of the pre-filter and its characteristics, and with the imaging technique used. The design and implementation of the pre-filter is described in the next section while the implementation of the imaging technique is described in Section 5.3.

5.2.4.3. Prefiltering of force data

A simple moving window filtering technique was found to be sufficient for the application, to reduce the high frequency noise components. Using the features of the MATLAB package, it was possible to design a moving average type filter whose characteristics could be varied in order to determine the best filter. The number of points to be selected for averaging could be made variable and this number could be passed on to the filter in the form of an argument to a function. Moving average filters of different window sizes were tried in order to make a selection.

There were many conflicting factors involved in the selection of the the size of the moving average filter width. For example, the transitional uncertainties could be reduced to an arbitrarily small value by using a sufficiently large sized window (consisting of a

large number of averaging points). However, this caused large time delays to be introduced by the filter. A small sized data window left the filtered data with larger noise components. This resulted in ambiguity in the tactile image obtained from the raw data, which was not desirable since this in turn, resulted in longer times to process the data to obtain the tactile image. Further, the small window also resulted in additional delays in subsequent interpretation of the images to determine the decision parameters and removed the process farther from real time. The determination of decision parameters from a tactile image will be described in Section 6.5.1.1.

The selection of the window size of the low pass filter also influenced the selection of the inter-threshold range. Using a large window for averaging resulted in the loss of some information from the dynamic forces; this necessitated smaller inter-threshold ranges to be chosen to ensure that a correct tactile image was obtainable from the force data. A quantitative evaluation of the effects of these and other factors to determine the most optimum window size was not successful because of the conflicts and inter-dependencies among the variables.

Therefore, in the proposed imaging scheme, to arrive at the most suitable window size for pre-filtering force data, two main aspects were considered. The first aspect was to determine the delay introduced by the various data windows to obtain a tactile image from a 100-point force data from 8 sensors. The delay introduced was determined for the moving average filters of data window lengths 5, 7, 10, 15 and 20 points by using the built-in "elapsed time" routine of the MATLAB software package in a Sun 4/110 workstation. The delays are recorded in Table 5.7. The force data used for this test consisted of arrays of forces of various sizes consisting of "20 by 8" to "400 by 8" points. The filter delay was observed to vary almost linearly with the size of the data window. The program used to calculate the user time (i.e. cpu time taken to perform filtering operation), also calculated an average value for the number of floating point operations performed in each case. For a typical tactile image obtained from an array of 100 by 8 values of forces, the delay due to the pre-filter was found to be 1.11 s and it performed an average of 4364 floating point operations. The time displayed in Table 5.4 is the mean value of user times obtained from ten trials carried out for each experiment. Both grasping and releasing types of data were used and the averaging was necessary because of the time shared usage of the computing resources used in these tests. From the table it is evident that the shortest delay was caused by a 5-point filter.

The second aspect which was considered to select the size of the window was to determine the smallest data window which permitted filtering of the raw data to satisfy a pre-defined system uncertainty criterion. The system uncertainty criterion for this case was defined such that the random variation observed at any point on the dynamic force characteristics would always be less than or equal to the estimated system uncertainty

Table 5.2: Delay introduced by the moving average pre-filter of various data windows .

Force data, no.of points	5-point mvg.avg.	7-point mvg.avg.	10-point mvg.avg.	15-point mvg.avg.	20-point mvg.avg.
20 x 8	0.25 s	0.24 s	0.23 s	0.27 s	0.28 s
40 x 8	0.46 s	0.46 s	0.47 s	0.47 s	0.50 s
60 x 8	0.66 s	0.67 s	0.69 s	0.74 s	0.75 s
100 x 8	1.11 s	1.13 s	1.16 s	1.19 s	1.23 s
200 x 8	2.37 s	2.36 s	2.41 s	2.53 s	2.58 s
400 x 8	5.42 s	5.45 s	5.73 s	5.70 s	5.91 s

value, i.e. 8 %. This fact was validated by first obtaining the tactile image from the raw and filtered data and then making a comparison between the two images. This will be discussed further in the next section which describes the implementation steps to obtain a tactile image from real test data.

5.3. Implementation of the imaging technique and results

5.3.1. The imaging procedure

Using the prototype gripper system, test data were obtained during grasping and releasing operations performed on a sample object. The object was first mounted between the gripper fingers of the robot gripper which was equipped with an array of four tactile sensors on each gripping surface. The gripper motor was actuated at a constant jaw speed of 7 cm/s and the forces on all the eight sensors were recorded using a high speed data acquisition system.

The data were obtained using an aluminum disc of diameter 24 mm, thickness 17 mm and weight 21.5 g. The uncertainty in the measured value of forces due to the prototype system components was estimated to be 8.1 %, as stated in Section 4.4.2.4. The prototype system was modelled by fitting a fourth order polynomial characteristic curve in accordance with the recommendations of the modelling and calibration expert system described in Section 4.4.3.

In order to interpret the dynamic forces measured by the tactile sensors, the measured sensor data was filtered using a low pass filter and then linearized. This was done to facilitate interpretation of the tactile images obtained from this data. The next

step was the assignment of force primitive values using the force imaging procedure described in Section 5.2.1. Finally, the force images from all the eight sensors had to be combined to form the tactile image.

To implement the various steps described above, two methods were investigated. The first method was called the conventional approach and the second was called the modified approach since it retained a part of the procedure used by the conventional method. In the conventional approach, the steps described above were carried out in exactly the same sequential order. Significantly, the force primitive values for the measured sensor forces were assigned after the data were transformed to the force domain. In the modified approach, which was developed to reduce the processing time of the imaging operation, some of the listed steps were performed off-line and the results were loaded from files, and used to obtain the image.

5.3.2. The conventional approach

In this approach, the raw data were acquired by the data acquisition system (DAS), were then transformed to time varying forces on the sensing sites using an appropriate sensor model. This model accounted for the sensor nonlinearities which include the transducer, the compliant backing, and the associated driving electronics. A typical process diagram showing the steps involved in this conventional procedure is shown in Figure 5.8.

The range of applicable forces for the selected task was 0 to 16 N and it was divided equally into 32 threshold levels with a uniform inter-threshold range of 0.5 N. The selection of the inter-threshold range (of 0.5 N) was based on the various accuracy considerations discussed earlier. To compensate for the system uncertainty errors, a dead band of 0.04 N (which is 8 % of 0.5) around each threshold point was set and a rule was formulated. According to this rule, forces measured by the sensors were divided into two categories: the definite case in which the forces lie well within an inter-threshold range, and the marginal case, in which the forces lie in the "vicinity" of the threshold points. If the force lies in the vicinity, then the primitive value assigned to it is based on the past force gradient value, if the gradient exists; if the gradient does not exist, then the force gets a primitive value obtainable by treating it as a definite case. For example, suppose 1 N and 1.5 N are the two threshold points which define a primitive value of 3, then the vicinity for the lower threshold point is the region 0.98 N to 1.02 N and that for the higher threshold point is 1.48 N to 1.52 N. If a measured force has a value of 1.2 N, then it represents a definite case and hence gets a primitive value of 3 assigned to it. If two measured forces at successive instants read 0.75 N and 1.02 N, then the corresponding primitive value assigned would be 2 and 2, whereas if the two forces measured read 1.30 N and 1.02 N then it would be 3 and 3. It can be observed that the second value of

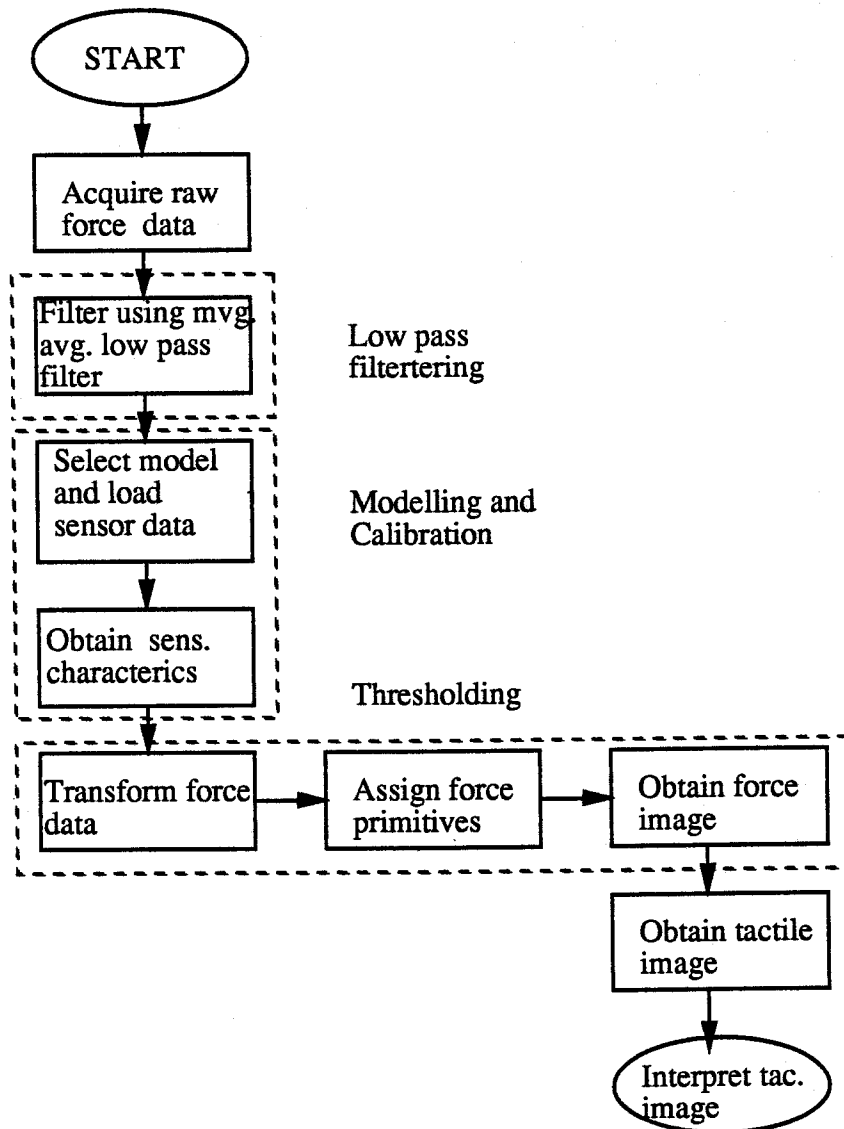


Figure 5.8: Flow chart of a conventional approach to obtain a tactile image measured force, i.e. 1.02 N was assigned a primitive value of 2 in first case because the previous value of the measured force was less than 1 N, whereas, the second value of the same force in the next case was assigned a primitive value of 3. In case the first value is 1.02 N then it is assigned a primitive value of 3.

Using these rules, a thresholding filter was applied to the transformed data and the force image for each of the eight sensors was obtained. The tactile image, which consists

of the force image for all the sensors involved in the task (eight in the case of the prototype) was then obtained.

A tactile imaging software was designed to carry out all the functions, except the data acquisition, listed in the flow chart shown in Figure 5.8. As the real time data acquisition facility was hard wired to the MicroVAX 3600 computer, the data acquisition and storage were done using the existing facility and the stored data were transferred in the form of ASCII files to the Sun 4/110 workstation. The tactile imaging program was coded in interpreted "C" language and was implemented using standard library routines of the MATLAB software package. The operation of the program consisted of first loading the files containing the force data, the threshold ranges and the sensor model parameters. This was followed by force transformation which determined the linearized value of the measured sensor force at every sensing site. This was necessary in order to form an equal basis for force thresholding (in terms of the applied force in N or g). Assignment of thresholds was done at this stage and the force images from all the sensing sites were combined to obtain the tactile image.

A typical tactile image obtained using the conventional approach is shown in Table 5.3. The time specified in the first column relates to the sampling instants when the data were measured by all the eight sensors. The total time of the task was 4 seconds. The image shown in Figure 5.3 pertains to the duration between 2000 ms to 2019 ms while the object was being grasped. Such images were obtained for the complete duration of the grasping and the releasing tasks, each lasting for 4 s. The resulting tactile images clearly displayed consistent primitive values indicating the type of tasks.

5.3.2.1. Timing considerations for real time implementation

For on-line extraction of such an image, the time taken to obtain the image by processing the raw data is a critical factor. This time depends on a number of inter-dependent factors, such as the amount of data, the type of low pass filter used to pre-filter the raw data, the type of model used for the sensors, and the criteria and the algorithm used for assigning forces primitives. To determine the processing time for the complete imaging operation, five groups of data, consisting of 30, 60, 100, 200 and 400 data points for each of the eight sensors, at a time $t = 2.0$ s during the grasping operation, were identified. Tactile images were formed from these groups of data using the conventional technique. The total cpu time taken to form the tactile image using the raw force data was calculated for each case. The time was calculated using the elapsed time as measured by the "clock" routine of the MATLAB library which was incorporated into the imaging program. The processing times were calculated for imaging the raw data as well as the filtered data in which a 5-point moving average pre-filter was employed. In each case the processing times taken in the thresholding section of the imaging program were separately identified. These results are shown in Table 5.4.

Table 5.3: A tactile image obtained using the conventional approach using grasping data .

Time of operation (ms)	Primitive force values at the sensing sites represented by the sensor no.							
	S #1	S #2	S #3	S #4	S #5	S #6	S #7	S #8
2000	3	1	1	1	1	3	6	2
2001	3	1	1	1	1	3	6	2
2002	3	1	1	1	1	3	6	2
2003	3	1	1	1	1	3	6	2
2004	3	1	1	1	1	3	6	2
2005	3	1	1	1	1	3	6	2
2006	3	1	1	1	1	3	6	2
2007	3	1	1	1	1	3	6	2
2008	3	1	1	1	1	3	6	2
2009	3	1	1	1	1	3	6	2
2010	3	1	1	1	1	3	6	2
2011	3	1	1	1	1	3	6	2
2012	3	1	1	1	1	3	6	2
2013	3	1	1	1	1	3	6	2
2014	3	1	1	1	1	3	7	2
2015	3	1	1	1	1	3	6	2
2016	3	1	1	1	1	3	7	2
2017	3	1	1	1	1	3	7	2
2018	3	1	1	1	1	3	7	2
2019	3	1	1	1	1	3	7	2

The tabulated results show that the total elapsed time to process the raw data for all the eight sensors ranged from 10.08 s for the 30 point case (consisting of 30 X 8 force values) to 80.25 s for the 400 point case of the grasping data. The time taken by the thresholding section of the program for the 30-point case was 1.14 s and for the 400-point case it was 11.82 s. Similar behaviour can be identified from the processing times for filtered data which are also shown in Table 5.4. These times were considered too high for a relatively simple task of imaging and methods to reduce the imaging time were explored.

A detailed study was undertaken to identify the sections of the imaging program which could be performed off-line. From Table 5.4, it can be seen that 10 to 15 % of the total time is spent by the program in characterizing the behaviour of the eight sensors.

Table 5.4: The processing time for data blocks of different lengths using the conventional approach .

Force data, no.of points	Times using raw data		Times using filtered data		
	Modelling	Imaging	filtering	modelling	imaging
30 x 8	1.14 s	10.08 s	0.32 s	1.73 s	10.27 s
60 x 8	2.15 s	18.92 s	0.61 s	3.32 s	20.06 s
100 x 8	4.12 s	32.32 s	1.03 s	6.01 s	31.41 s
200 x 8	9.27 s	64.15 s	3.10 s	12.93 s	62.47 s
400 x 8	11.82 s	80.25 s	5.37 s	16.86 s	86.37 s

The rest of the time was used in the thresholding operation. Therefore, it was concluded that by delegating the task of modelling of the sensors and a part of thresholding operation to an off-line filter, it would be possible to develop a faster imaging technique. The development of such a "modified" tactile imaging scheme is described in the next section.

5.3.3. Modified tactile imaging scheme

In this scheme, the two time consuming operations of modelling and thresholding were performed by an off-line filter. This filter was used to determine the threshold levels for a particular system configuration in terms of the digitized sensor outputs. The filter first performed individual sensor modelling for each of the eight sensors, using the function recommended by the modelling and calibration expert system. Since the mathematical formulations of the functions (fourth degree polynomial) used for describing the sensor behaviour were independent of the choice of the input and output variables (this was confirmed using experimental data), the filter used a simple data inversion technique to obtain the inverse relationship between the applied forces on the sensors and the digitized sensor output values. The inter-threshold range in the force domain was used to define the threshold levels. These levels were transformed to the corresponding threshold levels in terms of the digitized sensor outputs from each of the eight sensors. This resulted in the sensor nonlinearities being automatically incorporated in an indirect way into the different setting of threshold values. Therefore, different threshold levels were defined for each sensor.

A major time saving feature of this technique was that the threshold values could be

obtained off-line and stored as binary files for fast retrieval by the on-line imaging program. The flow chart for the off-line thresholding filter which performs the operations discussed above is shown in Figure 5.9.

The input parameters to this filter consisted of a two-element array, $n1$, in which $n1(1)$ defined the range between thresholds, in grams, and $n1(2)$, the degree of polynomial curve to be fitted to characterize the various sensors. These two parameters were dependent on the system configuration and the type of function chosen to characterize the tactile sensing sites. If different functions, such as nonlinear functions or piecewise cubic spline functions are used, then this filter program can be easily modified to accommodate such cases. In the case of the prototype gripper system, since it was decided to use a fourth degree polynomial curve for all the eight sensors, the value of $n1(2)$ was assigned as 4. To use a threshold range of 0.5 N, $n1(1)$ was assigned with a value 50. This filter calculated the threshold values for all the sensors of the tactile system in terms of digitized values of respective sensor outputs and stored them in designated binary files. The threshold levels for grasping and releasing data were separately calculated and stored. These files could be readily accessed by the on-line imaging filter with a small delay.

5.3.3.1. On-line imaging filter

The on-line process necessary to obtain the tactile image using the modified scheme consisted of a filter which loaded the threshold settings (i.e. levels) for all the sensors from designated binary files. The stored values of force data were also loaded and assigned with the primitive values using a simple comparison algorithm. These steps are as shown in Figure 5.10.

The program designed to perform on-line imaging accepted two arguments; the pre-filter type to be used for filtering raw force data and the type of the task, to identify and load the correct set of threshold settings for the eight sensors.

Both the off-line thresholding filter and the on-line imaging filter were designed and implemented using the library routines of the MATLAB [109] software package. The tactile images obtained using the modified approach were identical to the ones obtained using the conventional approach. These images were in the form of arrays in which the column 1 entries represented the time of the task and the entries in columns 2 to 9 represented the primitive values of force measured at the sensing site locations 1 to 8. Typical images from the grasping and releasing data were tabulated in a summarized form in Tables 5.5 and 5.6 respectively.

In these tables, the primitive values of force measured at the respective sites are entered in the form of cross-hatched circles. Different shadings are used to denote the

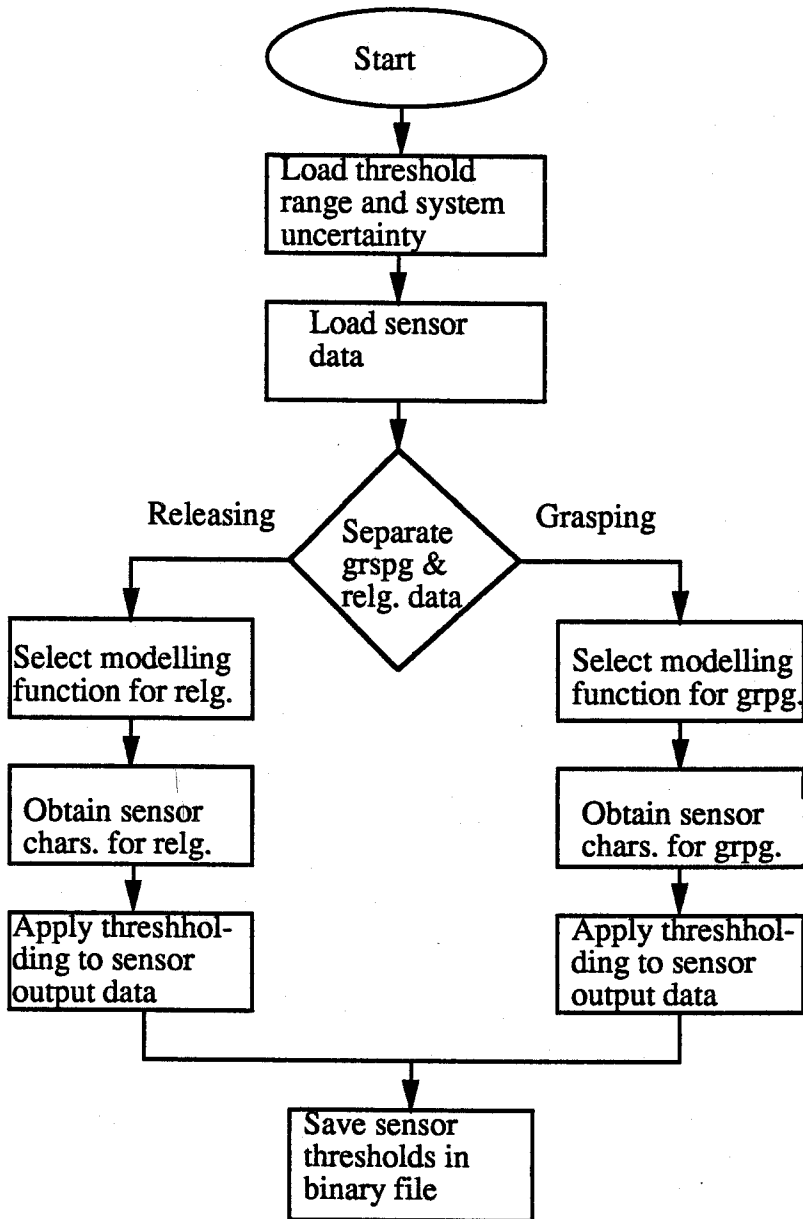


Figure 5.9: Off-line modelling and thresholding filter.

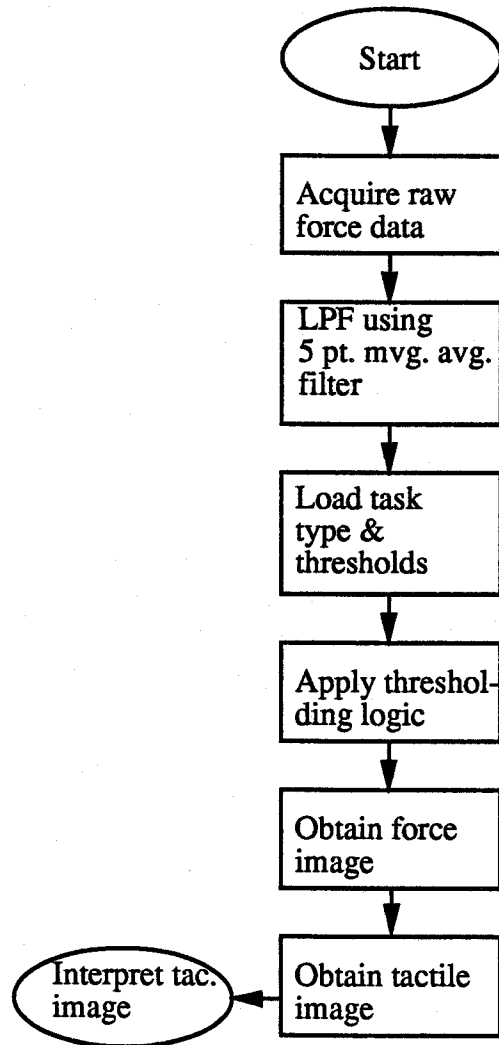


Figure 5.10: Process diagram of the on-line tactile imaging filter .

Table 5.5: A tactile image obtained using the modified approach - grasping data

Time, ms	s1	s2	s3	s4	s5	s6	s7	s8
201								
401								
601								
801								
1001								
1201								
1401								
2001								
2201								
2401								
2601								
2801								
3001								
3201								
3401								
3601								
3801								

Legend

- Th.level 0
- Th.level 1
- Th.level 2
- Th.level 3
- Th.level 4
- Th.level 5
- Th.level 6
- Th.level 7
- Th.level 8
- s# sensor no.

Table 5.6: A tactile image obtained using the modified approach - releasing data

Time, ms	s1	s2	s3	s4	s5	s6	s7	s8
201								
401								
601								
801								
1001								
1201								
1401								
2001								
2201								
2401								
2601								
2801								
3001								
3201								
3401								
3601								
3801								

Legend

- Th.level 0
- Th.level 1
- Th.level 2
- Th.level 3
- Th.level 4
- Th.level 5
- Th.level 6
- Th.level 7
- Th.level 8

s# sensor no.

various primitive values (or Threshold levels). By examining such an image, the status of a grasping or releasing operation in progress can be inferred. If successive rows indicate an increasing trend in the primitive values, then this implies a gripping process. A decreasing trend while grasping indicates the presence of slip. If successive row values are unchanged, then it signifies neither gripping nor slipping.

Figure 5.11 shows the steps involved in the task oriented procedure to obtain a tactile image from dynamic force data. To obtain decisions from such an image, a suitable decision strategy consistent with the speed and accuracy of the task at hand, was formulated as described in the next chapter.

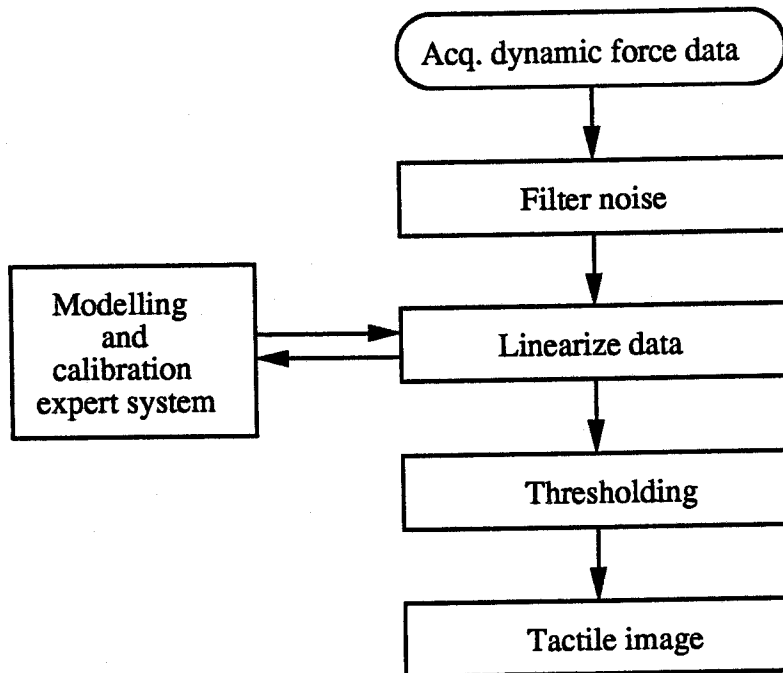


Figure 5.11: Flow chart of the task oriented procedure to obtain a tactile image from dynamic force .

5.3.4. Results and discussion

To evaluate the performance of the modified approach, the processing times to obtain tactile images from the same five groups of data were determined. To confirm the suitability of the modified tactile image extraction scheme, the tactile images were obtained from the same five groups (used earlier to estimate time to obtain a tactile image using the conventional approach) of force data using the programs developed for the thresholding and imaging filters. The processing time in these cases was the elapsed time measured by the on-line imaging filter. The time taken for thresholding and modelling was not considered since it was an off-line operation. The measured processing times are shown in Table 5.7.

Table 5.7: The processing times for five groups of data using the modified approach .

Force data, no.of points	Imaging time using modified scheme	Imging time using conven. scheme	Savings in time	Percentage savings in time
30 x 8	1.00 s	10.08 s	9.08 s	90.08 %
60 x 8	1.94 s	18.92 s	16.98 s	89.74 %
100 x 8	3.23 s	32.32 s	29.09 s	90.01%
200 x 8	6.20 s	64.15 s	57.95 s	90.03 %
400 x 8	13.17 s	80.25 s	67.08 s	83.59 %

In comparison with the total processing times shown in Table 5.4 for the conventional approach, the processing times for the corresponding blocks ranged from 1.0 s for a 30-point block to 13.17 s for a 400-point block. The corresponding time reduction is also calculated as a percentage and shown in Table 5.7. For a typical case of a 100 point force data, the time saving was of the order of 90 %.

The effect of prefiltering data to obtain the tactile image using the modified scheme was investigated to validate the selection of the pre-filter. Two moving average low pass filters of different window sizes were used to filter the raw data before forming the tactile image. To determine the changes in the tactile image due to filtering, three representative tactile images were obtained from the grasping test data obtained during a time $t = 2.0$ s to $t = 2.1$ s. The three images corresponded to the case of raw data image, 5-point filtered data image, and 10-point filtered data image. Each image consisted of the force primitive values arranged in a 100 by 8 array. To determine the variability in the images, the differences in the primitive values were calculated at every sampling point.

The differences in the primitive values between the raw force image and filtered force image were used to determine the effect of prefiltering. The sampling times (during the task time of 2 s to 2.1 s) at which the raw image differed from the filtered image were identified and are shown in Table 5.8. The table shows the difference in the images obtained in the two cases.

Table 5.8: Differences in the tactile images obtained from raw and filtered force data

Time at which difference occurred	Image from raw data		Image from filt. (5 pt.) data		Image from filt.(10 pt.) data	
	Sensor no.	Primitive value	Sensor no.	Primitive value	Sensor no.	Primitive value
2004 ms	7	7	7	6	7	6
2005 ms	7	7	7	6	7	6
2009 ms	7	7	7	6	7	6
2014 ms	7	7	7	6	7	6
2018 ms	7	7	7	6	7	6
2022 ms	7	6	7	7	7	6
2026 ms	7	7	7	6	7	6
2032 ms	7	7	7	6	7	6
2036 ms	7	7	7	6	7	6
2039 ms	7	7	7	6	7	6
2041 ms	7	7	7	6	7	6
2046 ms	7	7	7	6	7	6
2055 ms	7	7	7	6	7	6
2059 ms	7	7	7	6	7	6
2060 ms	7	7	7	6	7	6
2069 ms	7	7	7	6	7	6
2072 ms	6	4	6	3	6	3
2073 ms	7	7	7	6	7	6
2078 ms	7	7	7	6	7	6
2087 ms	7	7	7	6	7	6
2092 ms	7	7	7	6	7	6

From this table, it is evident that prefiltering the data modifies the raw image. But both the filters (of window size of 5 point or 10 points) may be used to obtain a tactile image which is less noisy compared with the raw data case. The pre-filter was added as a front end to the tactile imaging program developed for the modified scheme. The processing times for the same five groups of data were calculated as before and the results obtained are shown in Table 5.9.

Table 5.9: Processing times to obtain tactile images from filtered data using the modified approach .

Force data, no.of points	5-point moving average filter		10-point moving average filter	
	filtering time	tot.imging time	filtering time	tot.imging time
30 x 8	0.24 s	1.16 s	0.34 s	1.01 s
60 x 8	0.63 s	2.31 s	0.66 s	2.26 s
100 x 8	1.09 s	4.05 s	1.13 s	4.18 s
200 x 8	2.38 s	8.29 s	2.37 s	8.22 s
400 x 8	5.51 s	17.71 s	5.87 s	17.76 s

By comparing the processing times to obtain a tactile image from the raw and filtered data, it can be seen that inclusion of the filter increases the time in all the five cases. The increase is approximately equal to the time taken to filter the raw data. The time taken by the 10-point moving average pre-filter is marginally higher than the time taken by the 5-point filter. It is also clear from Table 5.9 that the increase in processing time is lowest for a 100 point data block. The total user time taken to process the 100 point force data was 4.05 s. The total number of floating point operations performed in the filtering and imaging process was also estimated using the MATLAB library routines. Using the modified scheme, for imaging a 100 point raw force data the average number of operations required was 2767, and for the filtered data it was 2633 and 2476 for the 5-point and 10-point moving average low pass filters respectively.

From the above results, a five point moving average filter was considered appropriate for the prototype sensing system. Any uncertainty prevailing in the image was accounted for in the decision logic which considered the contribution from the uncertain sensor image only if the decision reached was marginal.

5.3.5. Limitations of the method

The modified approach needs to perform off-line modelling and thresholding every time the system configuration is altered. Though this will not affect the on-line processing, still this may cause temporary delays in practical implementations. The selection of threshold ranges and the parameters for the pre-filter are largely governed by inferences

from analysis of the real data. Analytical or mathematical formulations may be desirable to develop and establish procedures to guide the design of tactile imaging schemes for other types of applications. The system uncertainty criteria may not be satisfied in some cases of object handling conditions and these have to be separately evaluated.

5.4. Conclusion

This chapter has described the development of a tactile imaging scheme. The relationship between the dynamic force parameters and a tactile image was established and the steps for the formation of a force image from tactile sensor data were described. To develop a technique suitable for on-line implementation, a conventional approach was first discussed. The program developed to implement this approach was used to identify the processing times required for various operations. These were studied to determine the operations which were time consuming and those which could be performed off-line. From this investigation, it was determined that off-line modelling and thresholding could yield considerable savings in time. A filter was designed for this purpose and was implemented off-line. The resultant thresholds were used in the on-line imaging software.

The trade offs involved in the design of the modified scheme were analyzed to determine the basis for selection of threshold range, error margin and the type of pre-filter. It was found that the problem of transitional uncertainty could be partially solved by prefiltering the raw sensor data. However, the prefiltering of data was seen to be a critical operation which played a vital role in deciding other trade off criteria.

The modified tactile imaging scheme was implemented using the prototype gripper system. In this scheme, the sensor nonlinearities were automatically accounted for in the calculations by applying a suitable model for each of the sensors involved in the task. By assigning equal ranges of forces between thresholds, the tactile image interpretation was made straightforward. The processing time required to form a tactile image was evaluated and the results showed that the modified scheme was considerably faster than the conventional technique. Results obtained from test data were used to estimate an error margin which could be used for interpreting the tactile image.

The applicability of the modified scheme for an on-line tactile imaging task was substantiated using on-line data collected during grasping and releasing of a sample aluminum disc. In the tactile image obtained, the onset of grasping at a sensing site was indicated by the first positive jump in the threshold value. Subsequent increases in the thresholds could be interpreted as an increasing grasping force. The information could be used to identify the status of the gripper during a task. In the case of a slip occurring during a task, the tactile image displayed a lower trend of primitive values. The decision software could use this information along with the spatial information describing the rela-

tive position of the object with respect to the gripper, to determine slip. Using the above ideas, a decision strategy was formulated to obtain and interpret decisions during a task. To implement this strategy, a decision filter was designed to obtain a set of decision parameters from a tactile image, and an expert system was developed to interpret these decision parameters. The details will be described in the next chapter.

6. DECISION FILTER AND THE TASK STATUS INDICATOR EXPERT SYSTEM

6.1. Introduction

In order to develop a method to automatically determine the task status of the gripper using a tactile image, the image formed from on-line data needs to be processed to determine a set of quantifiable decision parameters. Subsequently, these parameters should be interpreted using reasoning techniques developed from a knowledge of human reasoning procedures. The reasoning mechanism for the prototype gripper system could then be implemented using an expert system in which a part of human expertise has been incorporated in its knowledge base. The basic inverse problem of tactile perception and its real time solution using neural network techniques has been proposed by Pati et al.[122].

A set of seven decision parameters selected for determining the task status will be defined, and a decision filter designed and implemented to obtain these parameters from a tactile image will be described. An analysis of the behaviour of the selected decision parameters will be used to examine the design requirements for the filter. Using performance evaluation results, the applicability of the technique for on-line implementation will be discussed.

6.2. Formulating Decisions From a Tactile Image

When a human subject attempts to grasp a small object, compliant tissue in the fingers conforms to the object. When the object begins to move relative to the fingers, forces acting on the fingers result in a reaction which creates the necessary damping or velocity feedback to stabilize the grasp. In a similar manner, a set of decisions was formulated from a tactile image to guide an on-line task.

The tactile image was in the form of an array with the columns representing the sensor number and the rows corresponding to the time axis of the process, as defined in Section 5.2.3. In a case study, typical tactile images obtained during the grasping and releasing of a selected sample were used to analyze the images and formulate methods to obtain decisions from the images. The data for the case study were acquired during inde-

pendent grasping and releasing of a sample object, with each operation lasting for 4 s. The tactile image consisted of a 4000 by 8 array of force primitive values for each type of task. The image was divided into 40 consecutive blocks, each containing an array of 100 by 8 primitive values.

After forming the tactile images, the force primitive values corresponding to each of the eight sensors were identified and plotted as shown in Figures 6.1 and 6.2 respectively. Figure 6.1 was obtained using the grasping data and Figure 6.2 was obtained using the releasing data. These figures clearly show the force transitions measured during grasping and releasing. The tactile images in these two cases were obtained after filtering the raw data using a 5 point moving average low pass filter. For each sensor, the primitive value of force is indicated by the thickness of the bar. From these two figures, it is evident that sensors #3 and #5 have not indicated any change of status during the grasping. Sensors #3, #5 and #6 have behaved in a similar manner during the releasing operation. The single positive transition from sensor #6 during grasping could be due to two causes; either the presence of noise during grasping, or an escaped detection of threshold during releasing. To account for these and other ambiguities, it was found necessary to identify a confidence factor which could reflect the number of sensors showing positive (i.e. grasping) and negative (i.e. releasing) of transitions, and thereby eliminate false transient indications.

Based on the results of the case study, reasoning rules were formulated to make decisions from a tactile image. These rules were defined as follows: if successive rows of the tactile image indicated a decreasing trend, then the object was considered to be released from the gripper, whereas if the successive rows indicated an increasing trend then it was considered to indicate that gripping was under way. If successive row values were unchanged, then it signified neither gripping nor slipping. The number of sensors displaying similar characteristics of the measured forces was used to assign a sensor confidence factor for the grasping and releasing decisions determined as described above.

Another aspect of the tactile image which was used to make the decision was to identify the displacement of the object being handled relative to the gripper fingers. If a rapid movement of the object (occurring within a time duration of 10 ms) was identified, it was considered a dynamic object displacement, while slower object movements (occurring over a time period between 10 ms to 100 ms) were considered to be static object displacements. Based on these criteria, a set of seven decision parameters, namely, the grasped level, the released level, the sensor confidence factor for the grasping decision, the sensor confidence factor for the releasing decision, the static object displacement, the dynamic object displacement, and the points on the time axis (of the task) when the various transitions had occurred, were identified from a tactile image.

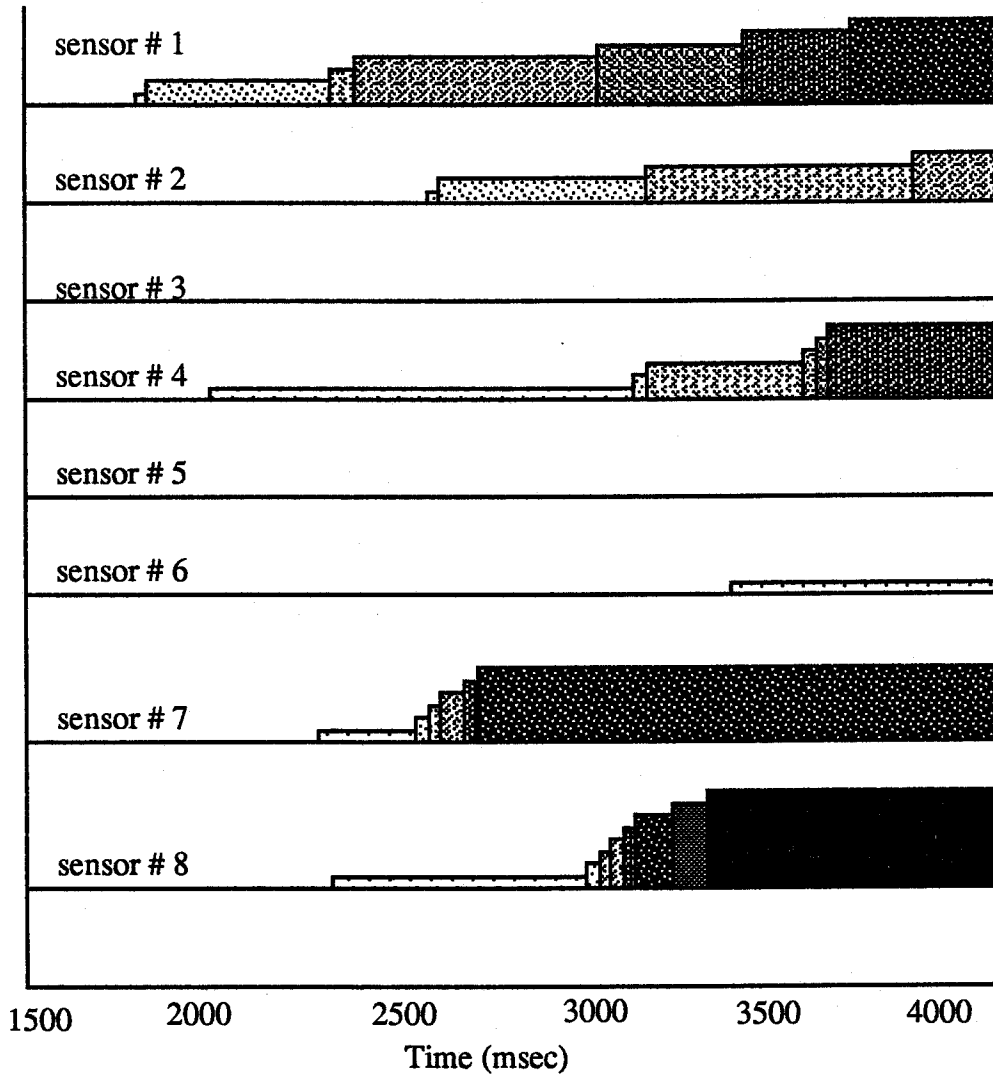


Figure 6.1: Transitions during the grasping operation .

6.2.1. Design considerations

In a situation where an array of sensors was involved, formulation of a decision based on the above reasoning depended on the speed and accuracy of the task to be performed using the gripper system. The following factors were found to affect the identified decision parameters:

1. the noise and uncertainty in the signal,
2. the number of sensors involved in the task,

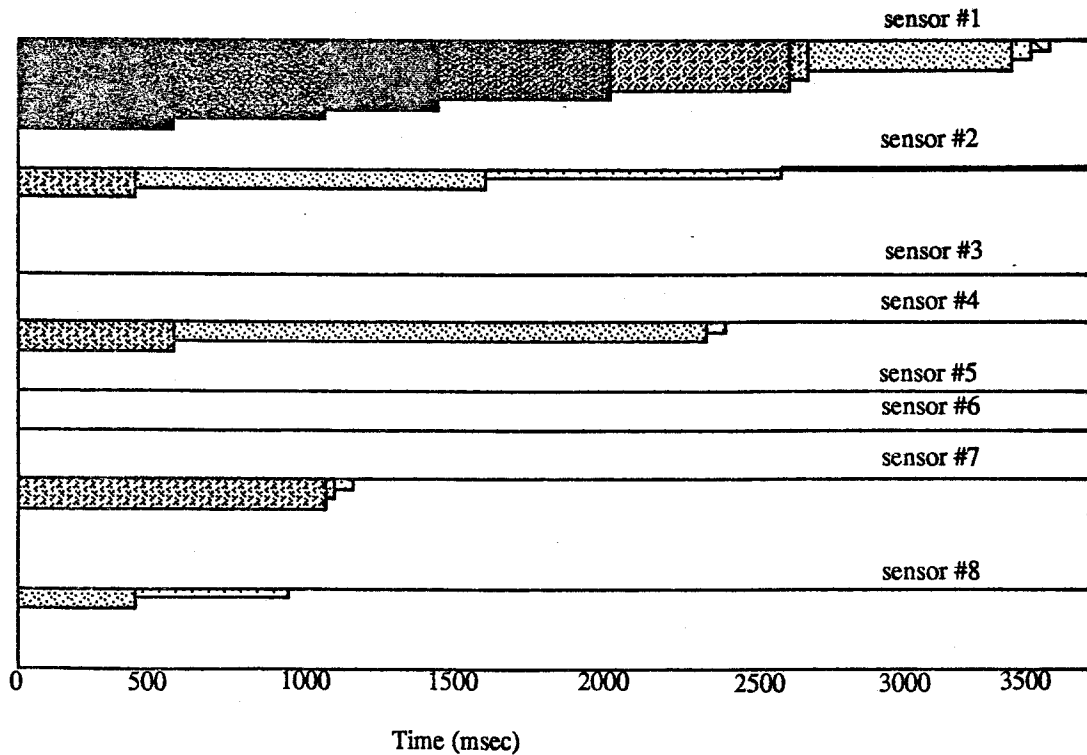


Figure 6.2: Transitions during the releasing operation

3. the time available for decision making,
4. the desired accuracy and margin of tolerance, and
5. the ease of implementation and on-line operation.

The impacts of the above factors on a decision formed from a tactile image, were investigated.

Noise in the acquired dynamic forces was a major contributor of uncertainties. The effects of noise and uncertainty in the force signals manifested themselves in the form of transitional uncertainties in the force image. The technique to reduce the uncertainties and the various criteria which were considered for determining an optimum pre-filter were outlined in the last chapter. The influence of other factors is discussed in the following sections.

6.2.1.1. Number of sensors

In the prototype gripper system, eight tactile sensors were mounted on the surface of the parallel jaws of the gripper. The location of the sensors with respect to the jaws remained fixed. The tactile image formed using a tactile sensing system with n sensors, consisted of an array of $(n+1)$ columns in which the first column indicated the time at which the dynamic forces on the eight sensors were acquired, and the other n columns contained the primitive values of forces at the sensing sites. The time needed to evaluate the chosen set of decision parameters from a tactile image was proportional to the size of the image, and hence proportional to the number of sensors measuring dynamic forces. For the prototype system, the total number of sensors was small and fixed. Therefore, all the sensor data were used to determine the decision parameters. In a gripper having a large number of sensors, it would be possible to select those sensors which are actively involved in measuring forces at any time.

6.2.1.2. Time constraints and error tolerance

These two factors were the most complex to determine for a practical system. To determine the time constraints, the primary time consuming operations involved in decision making were considered and analyzed. For an on-line operation, the size of the moving average pre-filter determined the time required before initiating a decision process. For example, if a window size of 5 points was used for the pre-filter, then it was necessary to wait until at least 10 samples of force data had been acquired. Larger window sizes required more sampled data before a tactile image could be formed and interpreted. To perform tasks using the prototype system, the sampling rate used was 1 KHz; therefore, a 5-point pre-filter caused a minimum of 10 ms waiting period before the decision parameters could be evaluated. However, for the purposes of establishing the general applicability of the task oriented procedure, stored force data were used. The data obtained from a 4 s task were partitioned into 40 blocks, each containing 100 measured force values per sensing site. A data block consisting of 100 samples of data per sensing site was used to form tactile images. Therefore, the size of the window used for the moving average filter was not of much significance as far as time constraints for decision making was concerned.

The accuracy of a decision also depended on the inter-threshold range. Since the decision parameters were obtained from a tactile image, the effects of inter-threshold range on the accuracy of a decision were similar to the effects of this range on a tactile image. While this range should be greater than the average noise and uncertainty levels, it should be small enough to enable detection of status changes within a reasonable time. The different nonlinearities of the tactile sensors further modified the ranges unequally; however, the value selected for the inter-threshold range based on accuracy considerations of a tactile image, namely, 0.5 N, was found to be reasonable for the purposes of this investigation.

A factor which affected both the time to form the decision parameters, and their accuracy, was the occurrence of uncertain transitions in combination with certain transitions. In general, when eight sensors were involved in a task, if more than one sensor experienced changes in forces resulting in transitions in the corresponding primitive values, none of them measured transitions at exactly the same instant. As well, the type of transitions (i.e. positive or negative) measured by the different sensors were also generally different. This may occur due to several reasons: the elastic nature of the compliant backing used in the fingers could have resulted in a reaction force at one or more sensors, or small movements of the object relative to the gripper might have caused delayed transitions at one or more sensing sites. Also, the object may not be truly perpendicular to the jaws of the gripper, or the object may be irregular in shape. The noise and transitional uncertainties also contribute to this behaviour. Therefore, to reduce the effects of these types of image noise, it was necessary to devise a method to identify "real" transitions resulting from a true increase or a true decrease in the sensed force from those caused by the image noise and other effects. For this purpose, a known amount of hysteresis was added at every observed transition point. The hysteresis was incorporated in the form of a "dead band", which was a predefined time duration at the transition point on the task time axis. Two values of the total gripper force, one measured at the identified transition point and the other measured at a point immediately after the dead band time period, were used to identify the real transitions. The time separation for a dead band was specified in terms of the number of sampled data points (for example, 10 ms corresponded to 10 points at 1 KHz sampling). The filter designed to incorporate hysteresis using the above technique was called the "dead band" filter.

6.2.1.3. Implementation issues

The decision filter was designed to determine the set of decision parameters from a tactile image. Since it was also required to be implemented on-line, the number and the complexity of computations involved in the filtering were kept to a minimum. From the point of view of software compatibility for the purposes of integration, the filter was implemented using the same software package used for the tactile imaging. The library routines available in the MATLAB package were found to be suitable for the various steps involved in the decision making. Some of the readily available functions in MATLAB were modified and used in the decision filter. The detailed design and implementation of the decision filter are described in the following section.

6.2.2. Requirement specifications for the decision filter

The main requirement specifications for the decision filter were formulated. Given a tactile image, the decision filter had to determine the following parameters:

1. the positive and negative transition points (in the time axis),

2. the number of sensors reporting positive and negative transitions, and
3. the cumulated sum of primitive values in each row.

After identifying the transitions, the decision filter had to separate the true positive and negative transitions by using a dead band filter with pre-defined hysteresis. Thereafter, it had to obtain the seven decision parameters, and store them in appropriate files.

6.2.3. Decision parameters

The parameters to be determined by the decision filter were selected so that the task status could be evaluated from the dynamic force data acquired during an on-line task. Out of the seven parameters, four decision parameters were used to form decisions about grasping forces. They were the grasped level, the released level, and the two sensor confidence factors associated with the grasped level and the released level respectively. The three parameters which were used to form decisions about relative object displacements were the transition times, the dynamic object displacement, and the static object displacement.

Both the grasped level (GL) and the released level (RL) counters were initialized to zero at the beginning of a block of data (i.e. at time $t = 0$), which consisted of 100 points of measured data from each of the eight sensing sites. Every time a real positive transition was identified, the force decision parameter, the grasped level (GL), was incremented. Similarly, every time a real negative transition was identified, the parameter released level (RL) was incremented. By continuing this operation for every identified real transition, by the end of the 100-point block, the values of GL and RL represented the total number of graspings and releasings identified within the interval corresponding to the block of data (i.e. 100 ms for a block containing 100 data points). For every data block, the sensors which measured positive and negative transitions were identified and used to calculate a sensor confidence factor using the relation

$$\text{Confidence factor} = 100 \times \frac{\text{no. of sensors showing transition}}{\text{total no. of sensors}} \quad (6.1)$$

In Equation (6.1), the sum of those sensors which measured positive transitions was used to calculate a sensor confidence factor for grasping and the sum of those which measured negative transitions was used to obtain a sensor confidence factor for releasing within the block.

In order to determine the object displacement parameters of the task status decision, the real transition points were first identified. For every real transition point, the corresponding location of the sensor which measured that transition was noted. Since the

sensor locations were fixed, it was possible to determine the direction in which the object had moved relative to the gripper, by observing the nature and location of successive transitions. In addition, those sets of transitions which occurred within the established dead band time interval were used to obtain the dynamic displacement of the object relative to the gripper fingers. The set of transitions which were outside the dead band interval were used to determine the static object displacement relative to the gripper.

6.2.4. Design and implementation of the decision filter

The design of a decision filter to satisfy the above requirements was carried out using a set of software modules. Since the filter had to process actual data using an intuitive logic, the design and implementation steps were carried out side by side. That is, each functional module was designed, implemented, and tested using real data acquired during grasping and releasing of a sample object, before combining with the next module. At the end, the filter was tested again to evaluate its performance.

The decision filter which determined the seven decision parameters consisted of two sections: the first section determined the transition points and the sensors which measured the transitions in terms of the primitive forces. The following section processed this information to assign values to the seven decision parameters. The process diagram of the decision filter, which is shown in Figure 6.3, lists the various modules, and the sequence in which they were accessed.

The filter loaded a typical tactile image consisting of a 100 by 8 array of force primitive values, and scanned the array to identify the instants at which the primitive values changed. These transition times from the image were stored. The positive and negative transitions were separated and the total number of sensors measuring positive and negative transitions was calculated.

The dead band filter was applied to every identified transition. This filter first determined the value of cumulated force primitives in the image, obtained by adding all the primitive values in each row of the image data array. This cumulated primitive value represented the total instantaneous gripper force. This instantaneous gripper force was used to identify a real transition, as explained in the following example. Suppose the first transition that occurred in a tactile image was a positive transition at a time, $t = 20$ ms. The value of the cumulated force would have been incremented at $t = 20$ ms. If a dead band equivalent to 10 sample periods, i.e. 10 ms was selected, then the dead band filter determined the value of the cumulated force at a time $t = 30$ ms. If the value of the cumulated force at 30 ms was higher than the corresponding value at $t = 19$ ms, then the transition at $t = 20$ ms was identified to be a real positive transition. Otherwise, it was considered to be an unconfirmed transition. Similar logic was used to determine a real nega-

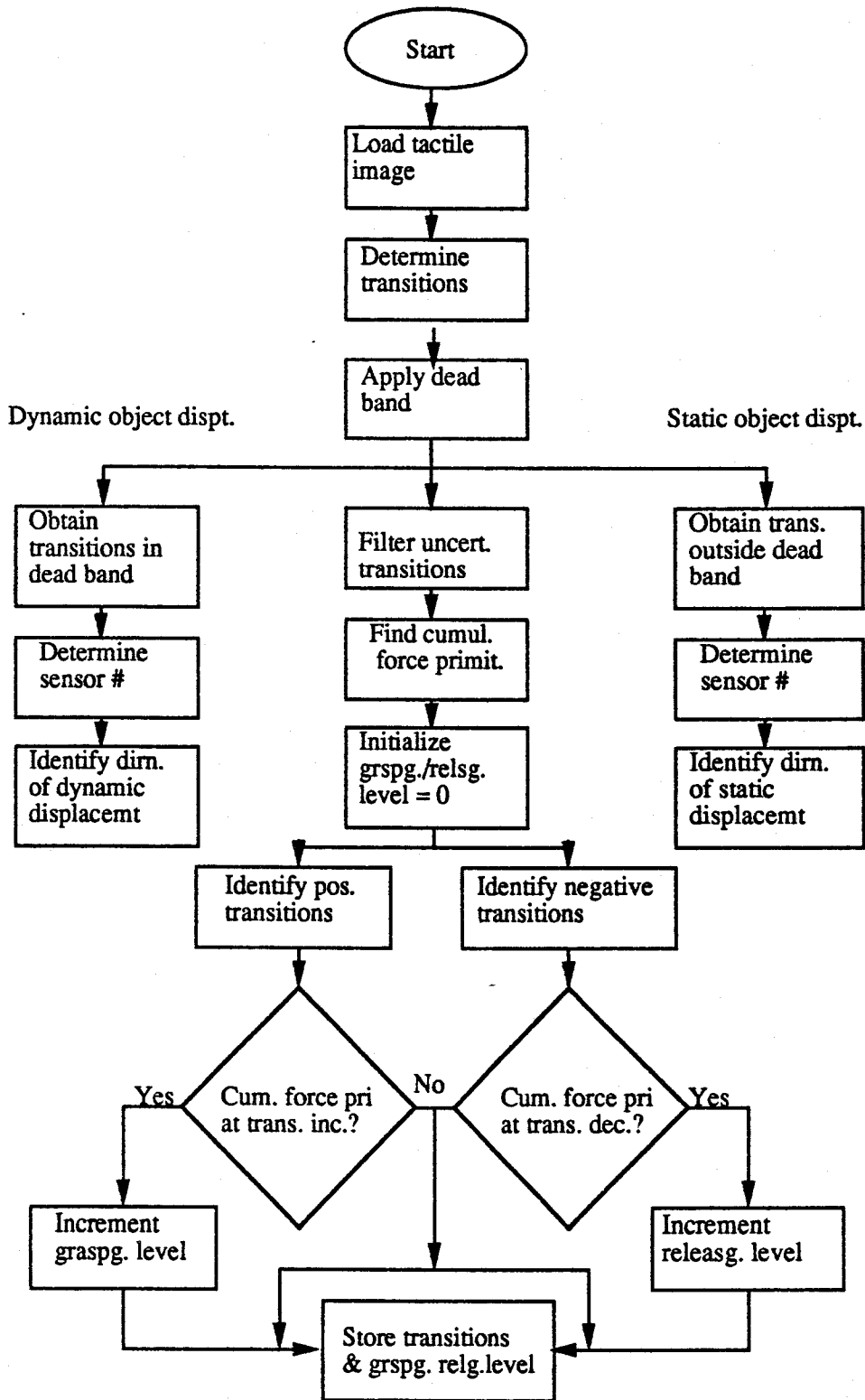


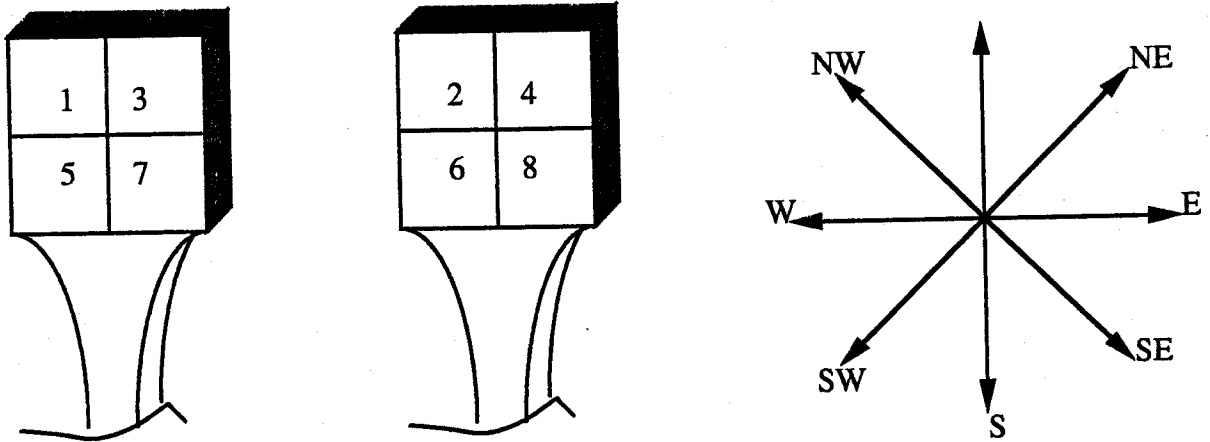
Figure 6.3: Process diagram of the decision filter .

tive transition. In this manner all the real or confirmed transitions were determined from a tactile image.

At every confirmed positive transition, the value of the force decision parameter "grasped level" (GL) was incremented and at every confirmed negative transition the value of the parameter "released level" (RL) was incremented. In a single tactile image, the sensors which measured one or more positive transitions were identified and their sum, expressed as a percentage of the total number of sensors taking part in the task, was evaluated to give the sensor confidence factor for grasping. In a similar manner, the number of sensors which measured one or more negative transitions was determined and expressed as a fraction of the total number of sensors, to obtain a value for the sensor confidence factor for releasing.

The two object displacement parameters, static and dynamic object displacements, were determined in the following way. The transitions which occurred in all of the eight sensors were identified before applying a "displacement classification" rule. In this rule, a set of displacement transitions were first identified. A displacement transition set was defined as a set consisting of two transitions of opposite types. According to the displacement classification rule, if a displacement transition set occurred within the dead band time period (expressed in terms of the number of sampled data points), then the object was considered to have moved "dynamically" from the sensor location which indicated the first transition to the sensor location which indicated the second transition. If the displacement transition set occurred over a period greater than the dead band time, then the object was considered to have moved "statically". An identified dynamic displacement was denoted by "dod" and an identified static displacement was denoted by "sod". For example, suppose a tactile image showed transitions at time $t = 24$ ms and at $t = 30$ ms measured by two sensors, sensor # 2 and sensor # 6 respectively, If the first transition at $t = 24$ ms was a confirmed negative transition and the other transition at $t = 30$ ms was a positive transition, then the two transitions at $t = 24$ and 30, constituted a displacement transition set. The object displacement in this case was classified as dynamic displacement (dod) if the selected dead band was 10 ms (or 10 samples, at a sampling rate of 1 KHz) but it was classified as static displacement (sod) if the selected dead band was 5 ms. The direction of displacement in either case was determined from the spatial distribution of the sensors. Table 6.1 shows the displacement directions for the spatial distribution of sensors depicted in Figure 6.4 defined with respect to the gripper jaw frame. This was the spatial arrangement of sensors that was used in the prototype gripper system.

The decision filter was implemented using the MATLAB [109] software library routines and a set of independently obtained grasping and releasing data were used to analyze the filter performance.



Left jaw of the gripper

Right jaw of the gripper

Figure 6.4: Spatial distribution of sensors on the gripper fingers .**Table 6.1:** Assignment of direction of displacement under different conditions .

Sensor # showing negative transition	Sensor # showing positive transition	Direction of displacement
1 or 2	3 or 4	East
1 or 2	5 or 6	South
1 or 2	7 or 8	South east
3 or 4	1 or 2	West
3 or 4	5 or 6	South west
3 or 4	7 or 8	South
5 or 6	1 or 2	North
5 or 6	3 or 4	North east
5 or 6	7 or 8	East
7 or 8	1 or 2	North west
7 or 8	3 or 4	North
7 or 8	5 or 6	West

6.2.5. Analysis of filter performance

The actual force data obtained from the case study described in Section 6.2 was used to determine and evaluate the performance of the decision filter. To recapitulate, the data for the case study were acquired during independent grasping and releasing tasks of a sample object, with each operation lasting for 4 s. The tactile image obtained consisted of a 4000 by 8 array of force primitive values for each type of task. The image was divided into 40 consecutive blocks, each containing an array of 100 by 8 primitive values.

The data from the grasping operation and the releasing operation were separately used to determine the effectiveness of the decision filter. The force data were filtered with the 5-point moving average filter, and the tactile images obtained were processed by the decision filter using a 10-sample dead band. In each case, the grasped levels, GL, and released levels, RL, determined by the decision filter from each block of data, were successively cumulated. In the test which used the grasping data, the cumulated grasped level was plotted as a function of task time, and in the test which used the releasing data, the cumulated released level was plotted. The resulting curves are shown in Figure 6.5. The cumulated grasped level is seen to increase monotonically in the curve which used grasping force data. In a similar manner, the cumulated released level decreases monotonically with a few exceptions, using releasing data. These results substantially validate the procedure used to determine the grasped and released level parameters from actual force data. These results also show that the decision parameters, grasped level and released levels, are useful parameters to determine the task status during grasping or releasing operations.

In order to validate the decision filter parameters, the corresponding variations of total gripper force, determined from the cumulated force primitives of the tactile image, were obtained from the grasping and releasing data. These variations were plotted as a function of task time in Figure 6.6. If it is assumed that a grasping task should always indicate progressively increasing grasped levels and a releasing task should indicate progressively decreasing grasped levels, the following inferences may be drawn from the decision filter parameters.

By comparing Figures 6.5 and 6.6, it can be clearly seen that in the case of a grasping operation, the decision parameter, GL, indicates the status of the gripper correctly in 13 out of 15 occasions and incorrectly in only 2 occasions. From the releasing data, the correct status was inferred in 10 out of 12 instances. It is clear that the decision filter helps to remove a majority of the ambiguities present in the cumulated force data by eliminating most of the incorrect transitions that can be seen, for example, in Figure 6.6.

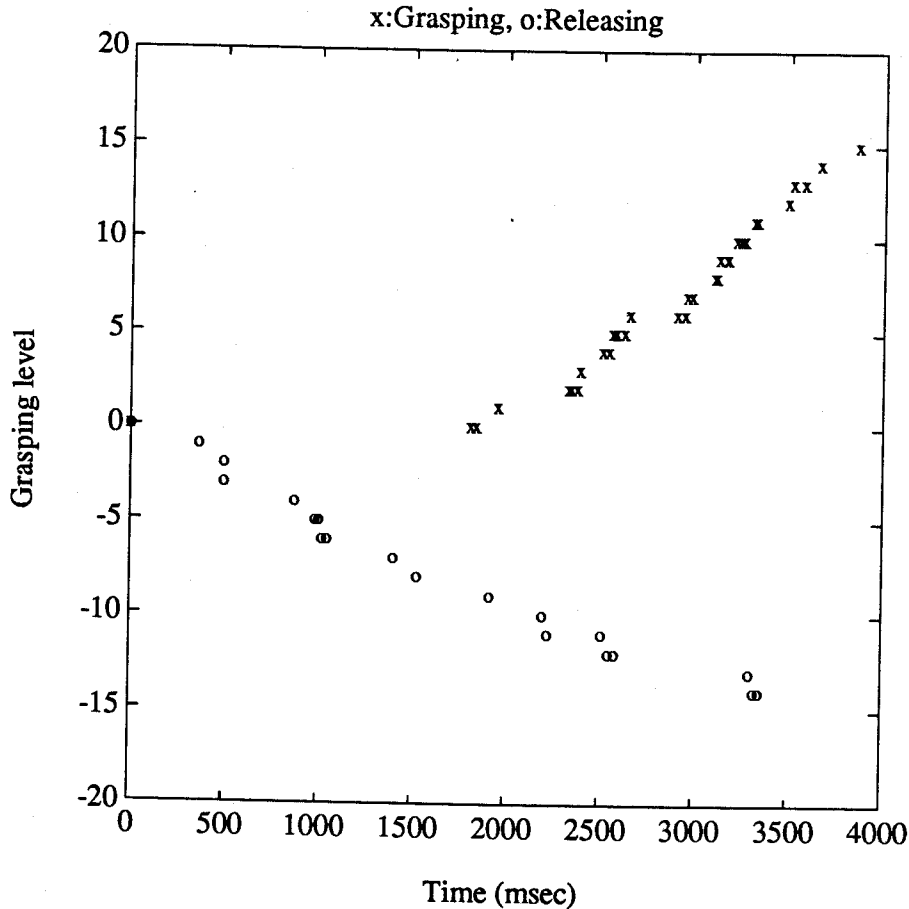


Figure 6.5: Cumulated grasped levels and released levels obtained from the decision filter using grasping data and releasing data

The resolution of the decision parameters was directly related to the resolution of the tactile image, i.e. the inter-threshold range. Larger inter-threshold ranges (i.e. > 0.5 N) might be suitable for heavier objects. Smaller values of threshold ranges were found to increase the transitional uncertainties, thus increasing the image noise which resulted in a larger number of incorrect decisions.

The processing time, that is, the user cpu time required to implement the decision filter, depended on the number of data points to be considered in each block and on the size of the dead band filter. Four different dead bands were tried in an attempt to determine an optimum size to be used to obtain decisions from a tactile image. In each case the plot of the cumulated grasped levels as a function of time was used to determine the number of correct decisions. This information, in conjunction with the processing time

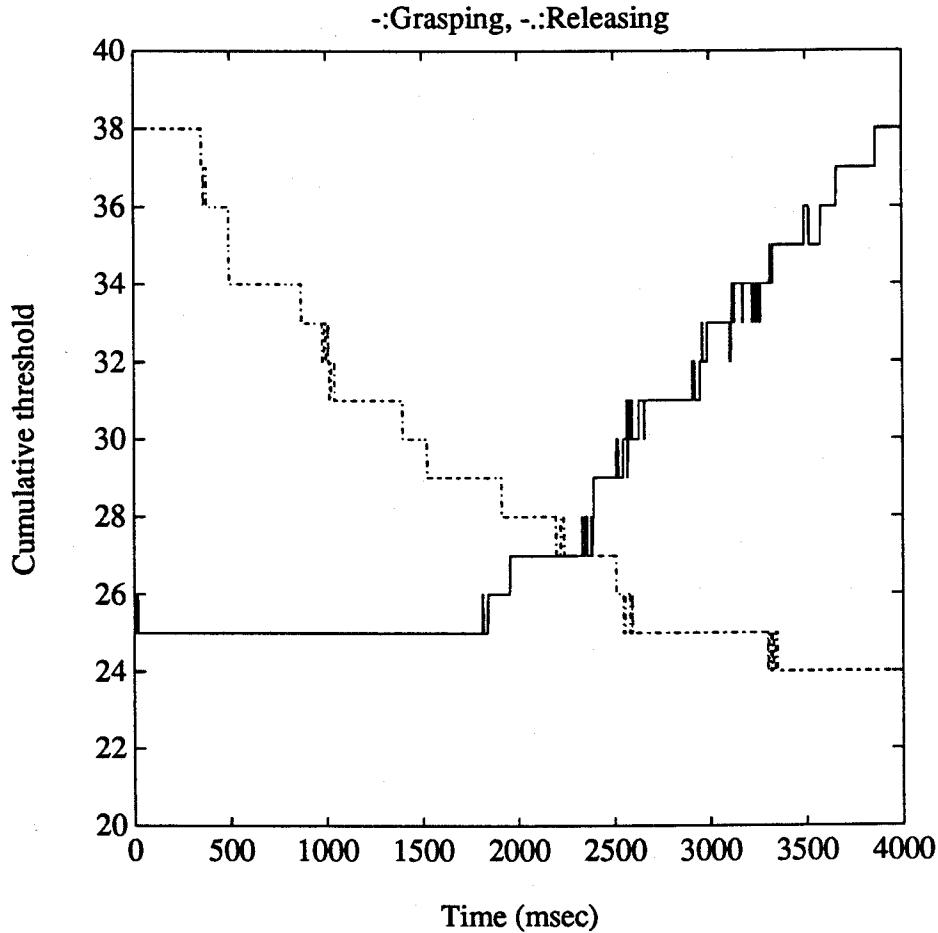


Figure 6.6: Total gripper force during grasping and releasing .

taken by the decision filter when different dead bands were selected, was used to determine the specifications for the dead band filter.

Using a 100-point data block, 4 dead bands of sizes 5 point, 10 point, 15 point, and 20 point were applied in the respective decision filters and the processing time was determined using a program written in the "C" language. This program accessed the decision filter, which was implemented similar to an "m" file of the MATLAB library routine, and used the built in function, 'time', of the UNIX operating system to determine the user time and the system time. The processing times required to implement the various decision filters, which used different dead bands to process the data, were calculated by this program and are shown in Table 6.2. The times indicated in the table represents an average time for five repeated trials in each case. From this table it is evident that the processing time of the decision filter varies with the size of the dead band. Therefore, from a timing point of view, it was desirable to select the largest possible dead band which could retain all the important transitions to enable proper task status determination.

Table 6.2: Processing time taken by the decision filters which used various sizes of dead bands .

Size of the dead band	Total user time to process 4000 points/sensor	Average user time to process 100 points/sensor	Total number of floating point operations	Total system time to process 4000 points/sensor
5 points	241.9 s	6.0475 s	408035	6.1 s
10 points	242.1 s	6.0525 s	404549	6.5 s
15 points	263.6 s	6.5900 s	401215	6.3 s
20 points	236.7 s	5.9175 s	398071	4.7 s

The precise identification of all the major transitions which contained the task status information was very difficult in an interconnected system such as the prototype gripper system. Therefore, a combination of the filter processing time and the decision filter output parameter behaviour were used to select the best size for the dead band. For this purpose, the decision filter output parameters were evaluated for each of the four sizes of the dead band filter. The grasping test data were used to obtain the cumulated grasped levels in each case. The curves showing the cumulated grasped levels, when 5, 10, 15 and 20 point dead bands were used in the decision filter, were plotted as a function of time. The curve for a 10 point is shown in Figure 6.7 and the curves for the 5, 15, and 20 point cases are shown in Figures C.1, C.2 and C.3 in Appendix C. From these curves, the choice of a dead band size equal to 10 sample points appeared to be the most appropriate. Larger sizes were rejected because they were likely to miss some of the important transitions while the smaller size (5 point) was eliminated because of the resulting image noise.

The final part of the analysis of the decision filter performance consisted of the selection of the size of the data block. The size of the data block influenced both the time to form a tactile image and the processing time taken by the decision filter to obtain decision parameters from the image. The latter was calculated for data blocks of different sizes, using the program described earlier in this section. The decision filter was used to process tactile images obtained from data blocks of sizes 30, 50 100 and 200 points and the results are shown in Table 6.3. A 10-point dead band filter was employed in all the cases.

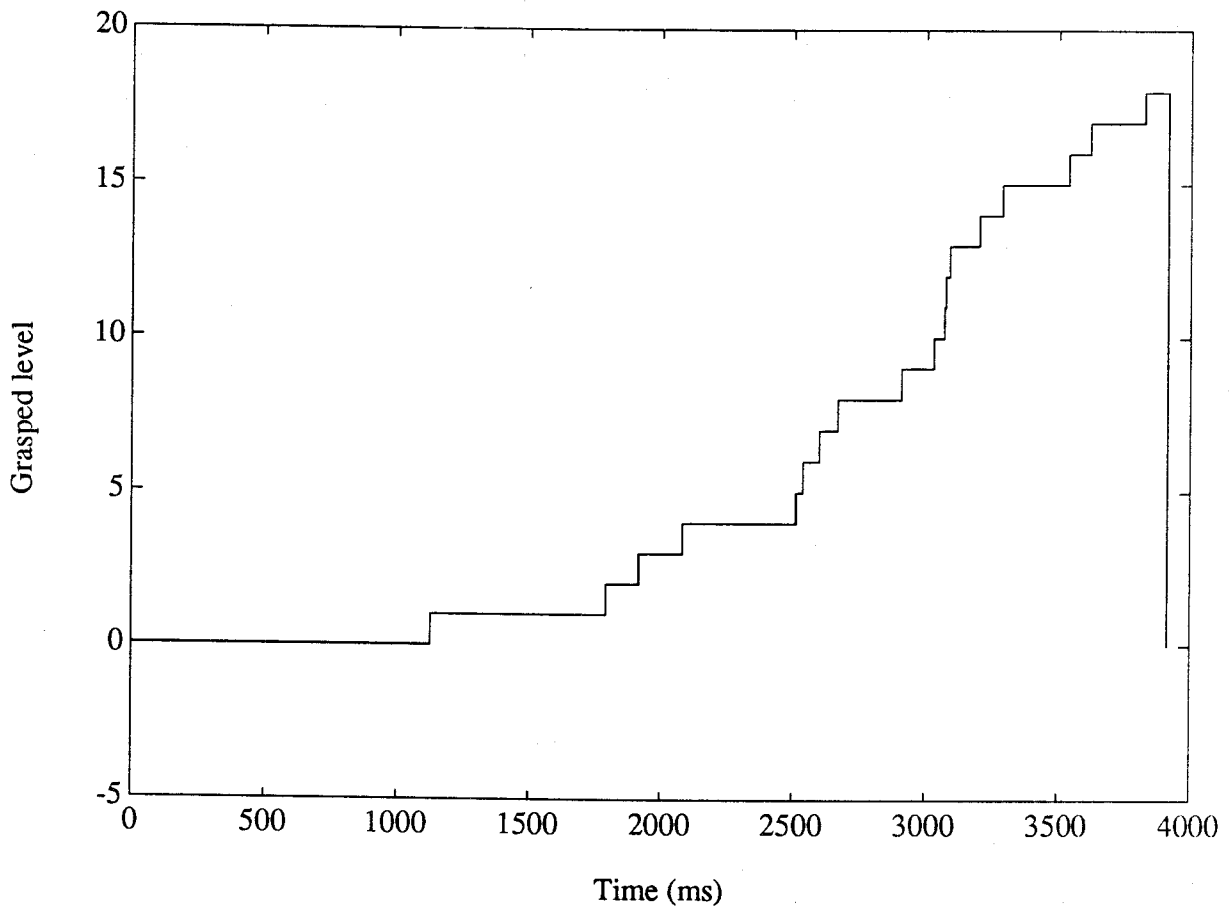


Figure 6.7: Cumulated grasped levels obtained using a 10 point dead band in the decision filter.

The choice of a block size depended on a number of factors which affect the overall process. However, the effect of the processing time for a decision filter when blocks of different sizes were used was determined from Table 6.3. It is clear that the processing time varies with the size of the block. However, the block size is also seen to influence the values of the decision parameters, which are calculated block-wise. To study these effects, the same technique which was used to identify the dead band filter size was used. The cumulated value of grasped level, GL, was obtained using the grasping data and plotted as a function of task time. The plot corresponding to a 100 point block is the same as the curve shown in Figure 6.7. The plots corresponding to three other cases, i.e. data blocks of sizes 30 point, 50 point, and 200 point, are shown in Figures C.4, C.5 and C.6 respectively, in Appendix C. From these plots, it was concluded that to process the data obtained from the tests conducted using the prototype gripper system, uniformly sized

Table 6.3: Processing time taken by the decision filter for different block sizes of data .

Block size	Type of operation	Total user time to process 4000 points/sensor	Average user time to process 100 points/sensor	Total number of floating point operations	Total system time to process 4000 points/sensor
30	Grasping	241.5 s	1.8158 s	373145	4.8 s
50	Grasping	246.8 s	3.0850 s	391226	4.3 s
100	Grasping	237.9 s	5.9475 s	404549	5.1 s
200	Grasping	242.5 s	12.1250 s	412056	3.7 s
30	Releasing	210.6 s	1.5835 s	348038	4.7 s
50	Releasing	239.8 s	2.9975 s	364343	4.3 s
100	Releasing	216.6 s	5.4150 s	376284	3.8 s
200	Releasing	225.4 s	11.2700 s	383012	3.5 s

data blocks containing 100 by 8 points of data was the best choice. The dead band selected for the decision filter, as determined earlier, was 10 points, or 10 ms at the 1 KHz sampling rate.

6.3. Interpretation of the decision parameters

The decision filter output for both the grasping and releasing types of tasks consisted of a set of seven decision parameters obtained from each block consisting of 100 points of data per sensor. Therefore, a 4 s task yielded 40 sets of decision parameters. Table 6.4 shows the decision parameters obtained using the grasping data from the case study, and Table 6.5 shows the same parameters obtained from the releasing data in the case study.

For both types of data, the decision parameters GL and RL obtained from each block show similar levels in many cases. The likely source of this behaviour was attributed to the flexible rubber backing provided in the gripper fingers. The equal values shown for GL and RL had been considered in the formulation of the force decision parameters by way of defining two other parameters, the sensor confidence factor for grasping and the sensor confidence factor for releasing decisions. The behaviour of the decision parameters, GL and RL, confirmed that it was necessary to determine the two sensor confidence factors for every data block.

Table 6.4: Decision parameters from the grasping data .

Time period, ms	Transition points, ms	Cumulated grasped level	Cumulated released level	Sensor conf. factor, %	Sensor # showing trans.
0 - 100	23	0	1	12.5	7
100 - 200	--	0	0	100	--
200 - 300	--	0	0	100	--
300 - 400	338	0	1	12.5	7
400 - 500	422	0	1	25	4,7
500 - 600	--	0	0	75	--
600 - 700	638	0	1	12.5	4
700 - 800	--	0	0	87.5	--
800 - 900	870	0	1	12.5	7
900 - 1000	--	0	0	87.5	--
1000 - 1100	1054	0	1	12.5	7
1100 - 1200	1171	1	0	12.5	4
1200 - 1300	1273	0	1	12.5	7
1300 - 1400	1385	0	1	12.5	7
1400 - 1500	--	0	0	87.5	--
1500 - 1600	1541	0	1	12.5	7
1600 - 1700	1617	0	1	12.5	7
1700 - 1800	--	0	0	100	--
1800 - 1900	1818, 1836	1	1	25 / 25	1,7
1900 - 2000	1907, 1961	1	1	25 / 12.5	4,7
2000 - 2100	2023	0	1	12.5	7
2100 - 2200	2125, 2138	1	1	12.5 / 12.5	7
2200 - 2300	2286	0	1	12.5	7
2300 - 2400	2363	0	1	25	1,7
2400 - 2500	2471	0	1	12.5	7
2500 - 2600	2525, 2556, 2569, 2581	2	2	25 / 25	2,7
2600 - 2700	2605, 2649	1	1	12.5 / 12.5	7
2700 - 2800	2713	1	0	12.5	7
2800 - 2900	--	0	0	100	--
2900 - 3000	2929, 2953	1	1	25 / 12.5	1,8
3000 - 3100	3076	1	0	12.5	8
3100 - 3200	3114, 3119 3133, 3135	3	1	37.5 / 12.5	1,4,8
3200 - 3300	3246	1	0	12.5	8
3300 - 3400	3319, 3333	1	1	25 / 25	1,6
3400 - 3500	--	0	0	100	--
3500 - 3600	3523, 3583	1	1	12.5	4
3600 - 3700	3664	1	0	12.5	1
3700 - 3800	3787	0	1	12.5	6
3800 - 3900	3839, 3869	1	1	25 / 12.5	2,6
3900 - 4000	--	0	0	100	--

Table 6.5: Decision parameters from the releasing data .

Time period, ms	Transition points, ms	Cumulated grasped level	Cumulated released level	Sensor conf. factor, %	Sensor # showing trans.
0 - 100	--	0	0	100	--
100 - 200	--	0	0	100	--
200 - 300	255	1	0	12.5	7
300 - 400	358, 383	0	2	55	7
400 - 500	--	0	0	87.5	--
500 - 600	--	0	0	100	--
600 - 700	--	0	0	100	--
700 - 800	730	1	0	12.5	7
800 - 900	839	1	0	12.5	7
900 - 1000	906, 983	1	1	25 /25	2,7
1000 - 1100	1005, 1006 1048	2	1	25 /25	1,7
1100 - 1200	1133	0	1	12.5	7
1200 - 1300	--	0	0	100	--
1300 - 1400	--	0	0	87.5	--
1400 - 1500	--	0	0	100	--
1500 - 1600	1531	0	1	12.5	2
1600 - 1700	--	0	0	100	--
1700 - 1800	--	0	0	100	--
1800 - 1900	--	0	0	87.5	--
1900 - 2000	1914	0	1	12.5	7
2000 - 2100	--	0	0	100	--
2100 - 2200	--	0	0	100	--
2200 - 2300	2225, 2251	1	1	12.5 /12.5	4
2300 - 2400	--	0	0	100	--
2400 - 2500	--	0	0	100	--
2500 - 2600	2515	0	1	25	2,4
2600 - 2700	--	0	0	100	--
2700 - 2800	--	0	0	100	--
2800 - 2900	--	0	0	100	--
2900 - 3000	--	0	0	100	--
3000 - 3100	--	0	0	100	--
3100 - 3200	--	0	0	100	--
3200 - 3300	--	0	0	87.5	--
3300 - 3400	3329	0	1	12.5	1
3400 - 3500	3415	0	1	12.5	1
3500 - 3600	--	0	0	100	--
3600 - 3700	--	0	0	100	--
3700 - 3800	--	0	0	100	--
3800 - 3900	--	0	0	100	--
3900 - 4000	--	0	0	100	--

A suitable strategy to interpret the decision parameters was considered with an objective to obtain a set of task status decisions. The force decisions of the gripper task status were originally defined to indicate whether an object was being grasped or released during the performance of a task. To confirm the task status decisions associated with the gripper forces, obtained in the above manner, the two identified displacement parameters, static and dynamic object displacements, along with the identified real transitions could be used. By interpreting the two object displacement decision parameters, the displacement of the object which had occurred in the immediate past could be identified. This were included as displacement parameters of the gripper task status.

The interpretation of the force decisions and object displacement decision parameters had to indicate the overall task status of the gripper during different conditions of grasping and releasing objects. The interpretations also had to enable a user to obtain a task status decision from the dynamic force data acquired using the prototype system, such that, by examining the values of the grasping and releasing levels, along with their associated confidence factors, from each block of data, it should be possible to generate the next step in the task. That step could be either to increase the gripper force, or to decrease the gripper force, or to retain the existing level of gripper force. The reasoning logic required to interpret the seven decision parameters in order to determine the task status parameters (both force decisions and the object displacement parameters) was developed by investigating the decision parameters from a single block of data, representing a 100 ms time interval.

From observation of the data from several graspings and releasings, a maximum of four transitions were observed to be appropriate to form task status decisions from each data block. If there were more transitions, the data were considered too noisy to extract useful task status parameters. Therefore, within each block, depending on the number of transitions, the grasped level, GL, and the released level, RL, were allowed to take values ranging from 0 to 4.

During the performance of a task, the decision parameters from a single block could represent any of the following three situations:

1. Category 1 - 0 transition case, where both the cumulated grasped level, GL, and the cumulated released level, RL, were 0,
2. Category 2 - 1, 2, 3, or 4 transition cases in which there was either a pure grasping or a pure releasing, indicated by $GL > 0$ and $RL = 0$, or $GL = 0$ and $RL > 0$, and
3. Category 3 - all cases which exhibited both a cumulated grasped level between 1 and 3 and a cumulated released level between 1 and 3.

The task status indication for the category 1 decision parameters should indicate that

the gripper state was unchanged during the time period corresponding to a specific block. The status indication for the category 2 decision parameters should be that the gripper was either grasping or releasing the object, with no noticeable slip between the object and the gripper, and in the third case the task status should indicate the presence of both grasping and releasing operations within the block. The last case could be further interpreted by a user to denote the presence of slip during grasping or releasing.

The various combinations of GL and RL which have to be considered in a four transition case are: one for Category 1 decision parameter, two for Category 2 parameters, and twelve for Category 3 parameters. In a similar manner, the combinations for three, two, and one transition cases also have to be considered.

Clearly, interpretations of the seven decision parameters in the various combinations, required a reasoning technique which could be readily incorporated into a computer program. It was decided to design and build an expert system for this purpose. To reduce the development time, a restricted number of commercially available expert system development tools was evaluated for suitability. The expert system was designed and built using the KES expert system shell, and was called the "Task Status Indicator" (TSI) expert system. The choice of the KES shell for the development of the TSI expert system was based on its features, which included the facility to embed the expert system as a part of an integrated "C" language program, the availability of three types of inferencing mechanisms, and user friendliness.

6.3.1. Design considerations for the expert system

An expert system was used to provide the capability to incorporate symbolic representation of facts, data and heuristic knowledge into the task oriented tactile sensing software package. The expert system development tool contained the methods by which the knowledge was represented in the expert system; the knowledge itself had to be incorporated by the designer.

In the design of the TSI expert system knowledge base, the facility to embed the system as a part of an integrated program was important. This requirement arose because the system had to interact with the tactile imaging program, the decision filter, and other programs, which were developed and written in the "C" programming language. The other attractive features of the KES tool were the facility provided to incorporate event-driven inferencing in combination with backward chaining, and the type of inferencing mechanism which could be used to obtain decisions from incomplete knowledge. These features of the KES tool will be elaborated in the next section.

6.3.1.1. Requirement specifications

The first step in the design of the expert system was to analyze the requirements. This was done by identifying the external requirements of the expert system, determining the available domain sources, characterizing the end-user, and identifying the real-world-context in which the expert system will operate. The result of this requirement analysis was a functional specification that stated the known inputs and outputs, the knowledge representation, and the inference requirements of the expert system. This functional specification was used as a guideline to select the inference engine, and in the construction of an attribute hierarchy. The detailed explanation of the above aspects are given in the KES Knowledge Base Author's Manual [107]. A brief description of the available inferencing mechanisms and the knowledge representation technique in KES are given below.

6.3.1.2. Inferencing mechanisms and the knowledge representation technique

The inference engine controls the use of the knowledge in the knowledge base, functioning the way a human expert does when solving problems and making decisions. Once the requirements of the expert system were analyzed, the domain knowledge characteristics could be determined. This influenced the choice of an inference engine which depended on the form of knowledge in the domain and the type of reasoning process an expert might use to reach the desired goals.

The KES software provides three types of inference engines: Production rules (PS), Hypothesize and Test (HT) and Statistical Reasoning (BAYES). All of the three inference engines use a similar goal-directed approach (backward chaining) in making inferences. The pursuit of a goal drives a typical expert system session. KES also performs event-driven (forward chaining) inferencing in which the expert system responds to the occurrence of an event rather than pursuing a goal. An "event" in KES corresponds to the assignment of a value to an attribute. An event can cause other events to occur, which can result in forward chaining.

The main purpose of the expert system based on the KES tool is to determine the values of one or more inferred attributes. The **attributes** are used to represent knowledge about a domain. Domain knowledge consists of facts about the domain and the relationships between the facts. In KES, an attribute represents some piece of knowledge such as a fact or characteristic of a domain. The *attributes* section of the knowledge base contains these pieces of knowledge. An attribute is assigned a value which is either entered by an end-user, or asserted in the *actions* section, read from files, or sourced from an embedded interface. The attributes are classified into two types from the manner in which values are assigned to them: **inferred** attributes and **input** attributes. The values assigned to inferred attributes depend on the values of other input attributes. The relationship be-

tween attributes are expressed in the *externals* and *attributes* sections of the knowledge base - these are the sections that influence attribute values. The range of valid values for an attribute is the value set and it varies with the type of attribute. Some attributes can have multiple values.

The inference engine uses an attribute's knowledge sources to determine an attribute's value. Each KES inference engine has its specific knowledge sources and a few common knowledge sources. For HT, **Descriptions** are the specific knowledge sources and the *Default or Calculation* clauses and External programs are the common knowledge sources.

In the goal-directed (backward chaining) method of reasoning, the expert system attempts to obtain a value of a goal attribute by following an attribute hierarchy. A typical attribute hierarchy is shown in Figure 6.8, in which the goal attribute and the input attributes are shown.

The link between the attributes corresponds to the method of assigning a value to the attributes. The inference engine, in a backward chaining process, works its way down the hierarchy, seeking the values of input attributes if necessary, then works its way up the hierarchy, inferring the values of non input attributes as it ascends. The difference between the three inference engine types are in the way knowledge is represented and the way information is processed. A PS inference engine uses production rules to represent knowledge, while a BAYES inference engine performs statistical pattern classification based on Bayes' theorem. A KES HT inference engine implements a hypothesize-and-test approach to problem solving. That is, it reasons through formulation of an hypothesis and its subsequent verification. This technique is similar to the abductive reasoning process used in mathematical logic theories. HT determines the smallest number of causes, represented by 'descriptions' in the knowledge base, that explain all known manifestations of the problem of interest. This concept is known as **minimal set covering** and will be discussed further in the next section.

6.4. The Task Status Indicator Expert System

The input parameters to the expert system were the set of seven decision parameters obtained by processing the tactile images. On-line determination of task status consisted of interpreting the decision parameters in such a way that the interpreted results could be easily analyzed and used to determine control actions for the gripper. For this purpose, a parametric form of task status identification was considered. The behaviour of the seven decision parameters was analyzed within a specified data block in order to formulate the task status in terms of quantifiable task parameters. The result of the analysis was used to select the following task status parameters: the grasped level, the released level, the con-

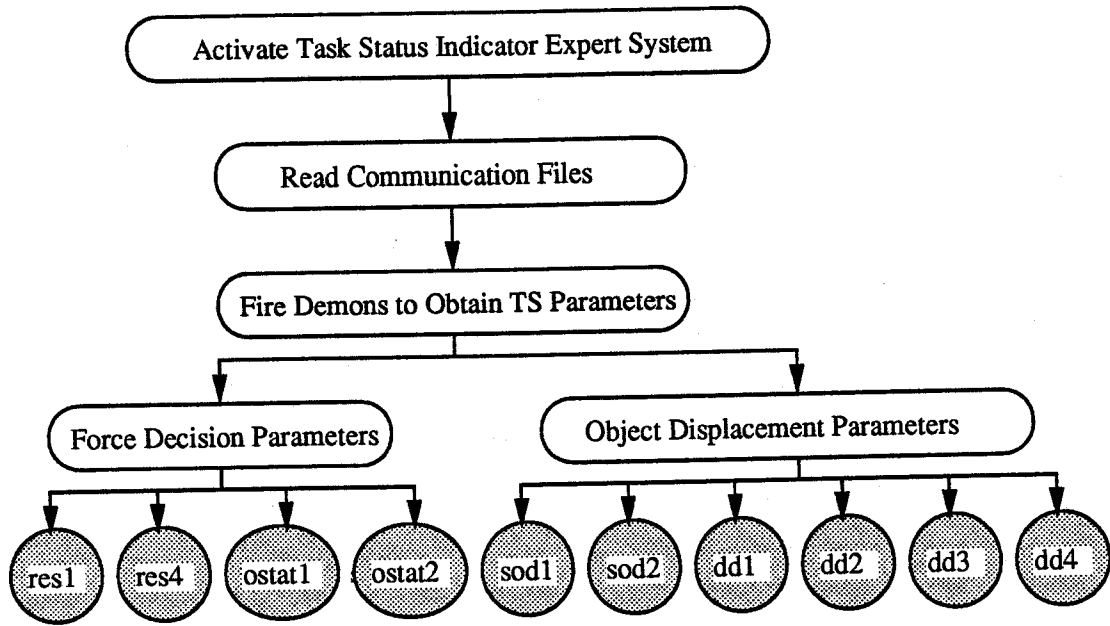


Figure 6.8: A typical attribute hierarchy

confidence level for grasped decisions, the confidence level for released decisions, the dynamic object displacement and the static object displacement. These parameters could be assigned values by the TSI expert system based on the seven decision parameters obtained using the decision filter.

To design the TSI expert system, the following external requirements were formulated. The expert system to be designed was required to:

1. determine a confidence level for each decision based on the relative strengths of the grasped and released levels and their associated sensor confidence factors obtained from each set of decision parameters,
2. interpret the static and dynamic displacements in every block, in such a way that it was possible to assign a specific direction to the object movement relative to the gripper,

3. determine the task status in terms of selected quantifiable parameters which could be accessed by a second expert system to determine the necessary control actions to complete the task successfully, and
4. serve as a friendly user-interface to report the task status in terms of English language descriptions so that the user will be able to easily understand the status of the task

The available domain sources for the expert system essentially consisted of human intuitive reasoning based on engineering judgment under similar circumstances. For example, if the gripper status indicated a progressively increasing released level in the decision parameters obtained from successive blocks, then a human was likely to decide that the object was slipping from the gripper. In a similar manner, if a number of grasped levels were found during a releasing task, then the most likely decision would be that the object was being regripped after a possible slip.

The expert system was integrated into the application software developed for the Sun 4/110 workstation environment. The transfer of information to and from the expert system was through communication files which used the designated KES format to perform read and write operations. The decision-making in the expert system was restricted to normal cases of object handling situations. To ensure quick response from the expert system, it was embedded into an integrated computer program which performed all the steps of the task oriented procedure.

Out of the three methods of inferencing supported by the KES tool [107], the Hypothesize and Test (HT) method was selected. Though many factors affect the selection of an inference engine, the choice depended largely on the characteristics of the available inputs, and the desired outputs. A Production rule-based inference engine (PS in KES) is suited for those expert system applications where the domain knowledge is already in the form of, or is readily translatable to, branching logic, or *if..then* rules. The BAYES engine is useful in situations where there is a large body of pre-existing data that is expressed as probabilities. This pre-existing data is usually based on quantitative data collected in previous cases, or based on an expert's judgment of the likelihood of certain events. BAYES provides an empirically reliable inference process, as long as the data are sufficient.

HT is suited for applications when minimal set covering is appropriate. In the minimal set covering method of inferencing, the inference engine considers all of the available knowledge sources, and arrives at a set of possible decisions which are ranked according to the certainty factor assigned to the decisions. The decision which was evaluated using the most of the dependent attributes is given the largest value of certainty factor.

In HT inferencing, knowledge is represented using frame-like descriptions. Each description consists of a collection of statements related to the domain. In an HT knowledge base, it was possible to attach an estimate of how likely a particular event was likely to occur. These **symbolic certainties** were subjective, non-numeric likelihood indicators classified into five categories: **always, high, medium, low and never**. They provided a means for categorically including or excluding information from the inference process, and a way for the HT inference engine to rank competing probabilities.

An HT inferencing is appropriate to applications where:

1. inputs are not statistically independent,
2. outcomes are not mutually exclusive,
3. outcomes require only a best available solution (minimal set covering),
4. the outcome is a subset selected from a possible set of solutions,
5. multilevel hierarchies are needed,
6. automatic search and question pruning capabilities are required, and
7. event-driven inferencing is required.

Since the desired outcomes and the inputs to the TSI expert system satisfied most of these characteristics, an HT inference engine was selected for the TSI expert system.

Development of the TSI expert system to interpret the decision parameters consisted of first developing a knowledge base with rules formulated to assign symbolic values to a set of pre-defined attributes. The formulation of logical rules to assign values to the task status parameters was primarily based on heuristic reasoning. The design and development of the knowledge base is described in the next section.

6.5. Design and development of the TSI knowledge base

The most important task involved in the design of the knowledge base was to relate the attributes and the knowledge sources through the structure of the knowledge base, so that known information was used to infer attribute values and solve the problem addressed by the expert system. Attributes were linked to one another by an **is inferred from** relation. An attribute whose value was inferred from a knowledge source depends on the attribute(s) used by the knowledge source. An attribute hierarchy, which was a conceptual way of relating attributes in a domain, was developed using the input parameters to the expert system. The hierarchy identified which attributes had to be used to infer the values of others. At the top of the hierarchy was the final goal of the expert system: the attribute representing the solution to the problem that is being addressed. For the TSI expert system, two goal attributes, "result", and "dod/sod", were identified. The attribute "result" obtained the force decisions of the task status, and the attribute dod/sod

determined the object displacement decisions of the task status. The goal attribute's values were inferred from one or more attributes below it in the hierarchy. The bottom of the hierarchy consisted of the input attributes whose values were obtained from **communication** files. The seven decision parameters were used as the input attributes in the TSI knowledge base.

The TSI knowledge base was designed using sections, each of which contained or manipulated domain knowledge. They are included in the following sequential order: *constants*, *text*, *attributes*, *externals*, *demons*, *actions*. Each knowledge base section followed the general format:

name of the knowledge base section:

section contents

*

The *constants* section was used to store long or frequently used phrases as string constants or numbers in numeric expressions. A constant referred to a string of text or a number which was given a name. Subsequently, the name was used elsewhere in the knowledge base. The *text* section was used to provide detailed explanations to the end user in the English language. The information to be displayed to a user was stored in the form of textual attachments, which consisted of one or more strings of text with a given name. The textual attachments were defined both for the knowledge base as whole as well as for specific attributes. The *attributes* section contained the declarations of the attributes represented in the attribute hierarchy. The attribute hierarchy designed for the knowledge base will be described in Section 6.5.1.1. An attribute was assigned a value at run time; the value held data specific to a end-user session with the expert system. In order to communicate with or execute programs outside the expert system, an *external* section was used. To send information to, or receive information from, an external program communication files were used. The inference engine passed attribute values to the other programs through the use of the interface created by the *externals* section. Attribute values themselves were determined by the external programs, thereby becoming a knowledge source for the specific attribute. For event-driven inferencing, *demons* were employed. These performed actions triggered by events, in the form: "when guard then body". The guard of a demon consisted of a set of conditions, and the body contained the sequence of actions to be performed when the guard was satisfied. Though demons could determine the values of attributes, they could not be used as knowledge sources, because they were not executed by backward chaining.

The *actions* section was used to issue instructions to the expert system to control its operation. Commands in the *actions* section displayed messages, prompted for information from the user, and set the goal attributes for the inference engine. The commands

in this section were normally executed in a sequential order. However, provision was made to modify the sequence when it was required to be done.

The last step in the design process consisted of the identification of the portion of the task to be performed under procedural control in order to determine the information to be inferred from the rules and structure of the attribute hierarchy. The major events at the end-user interface were included under procedural control. Procedural controls were incorporated in the *actions* sections of the knowledge base. In the knowledge base, the *attributes* section contained the descriptions that controlled inferencing. The control structure was used to guide the inference process and provide the end-user interaction by determining the order in which the expert system commands were executed. The *actions* section of the knowledge base embodied the control structure and defined the form of interaction with the end user and external programs. The control structure was first conceptualised using process diagrams. To facilitate easy understanding of the expert system decisions, the explanatory texts were made available to the user using *textual* attachments. Once these design decisions were made, the next step in the development of the knowledge base consisted of building the actual control structure and attribute hierarchies. These served as the blueprint for the knowledge base structure of the expert system.

6.5.1. Implementation of the TSI expert system

6.5.1.1. Inferred attributes and the method of evaluation

The input parameters to the expert system were the set of seven decision parameters obtained by processing the tactile image from a block of data. The behaviour of these parameters within each data block was used to define the structure and dependencies of the attributes. A maximum of four transitions was allowed for each data block consisting of 100 consecutive data points per sensor. If there were more than four transitions, the data were considered too noisy to extract useful task status parameters and the expert system displayed this information to a user.

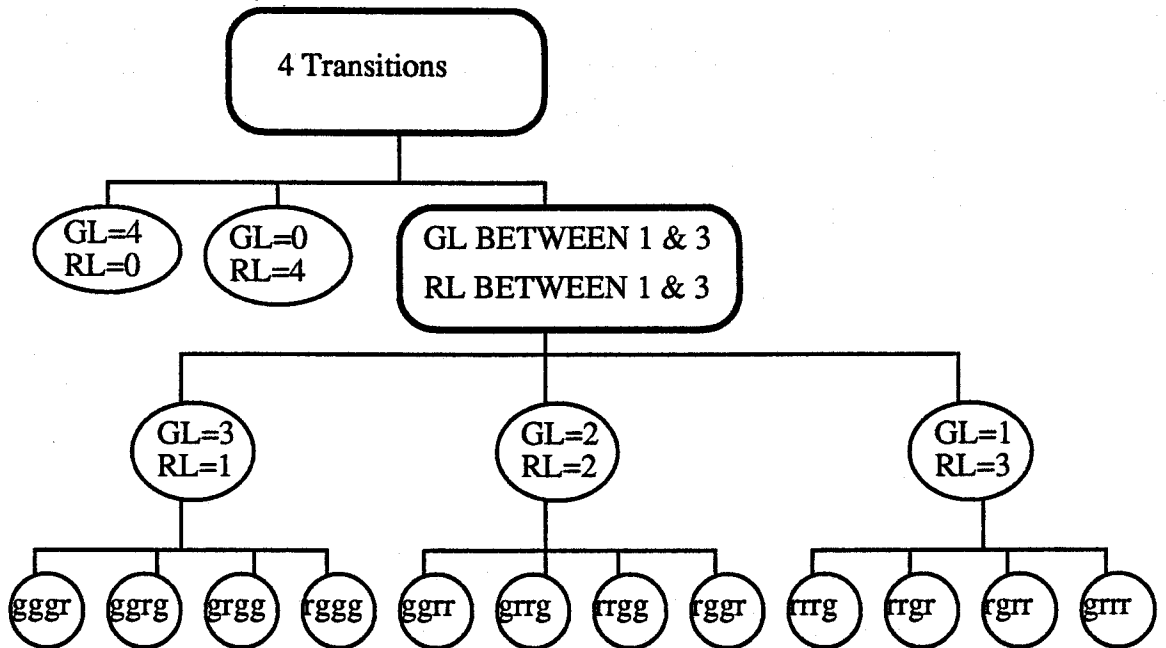
Within a block, depending on the number of transitions, the two force decision parameters of the task status, the grasping level and the releasing level, could take values ranging from 0 to 4. These five cases of transitions were handled separately using event-driven forward chaining rules. In each case, the decision parameters, the grasped level and released level, were identified and were weighted with the sensor confidence factor for the respective decisions. The relative values of the decision parameters (the grasped level and the released level) within each data block were used to determine confidence levels for the task status force decisions.

A typical decision hierarchy used for formulating an event-driven (forward chaining) decision, consisted of the decision parameters, GL and RL, grouped in such a way that all the possible combinations of the two parameters could be identified and used to formulate task status decisions. A typical decision hierarchy for a four transition case is shown in Figure 6.9. In this Figure, GL and RL are the decision parameters obtained from a single block. In a four transition case, all the three possibilities were considered: (a) the case when GL was 4 and RL was 0, (b) the case when GL was 0 and RL was 4, and (c) the case when both GL and RL assumed values between 1 and 3. The case (c) was further classified into three possibilities in which different combinations of the number of grasps, ng , and number of releases, nr were considered. Each subclass in case (c) was classified into four cases in which the sequence of grasping, g , and releasing, r were considered. Thus a total of 14 events were identified to obtain task status from the decision parameters from a block with four identified transitions. Similar decision hierarchies were formed for other cases which consisted of 1, 2 and 3 transitions in a single block. The corresponding hierarchy diagrams were a subset of the four transition case decision hierarchy shown in Figure 6.9. The total number of events identified for a 3 transition case was 8, for a 2 transition case was 4, and for a 1 transition case was 2. A 0 transition case represented a single event when both g and r were 0. The event driven inferencing section of the knowledge base was built using a set of 5 demons to handle the 4, 3, 2, 1 and 0 transition cases. These together handled a total of 29 different possible situations.

The case of a pure grasp ($RL=0$), or a pure release ($GL=0$) was distinctly defined in all the cases. The event-driven decisions obtained by firing the demons were translated into three symbolic categories of task status, one for each of the three categories listed in Section 7.4.1.1. To distinguish between the decision parameters and the task status parameters derived from the decision parameters, the terms "grasping level", and "releasing level" were used in the expert system implementation (to correspond to the grasped level and the released level parameters). The categorization in terms of these parameters incorporated in the TSI expert system were:

1. Category 1 - 0 transition case, where both the grasping level and the releasing level were 0,
2. Category 2 - 1, 2, 3, or 4 transition cases in which there was either a pure grasping or a pure releasing, and
3. Category 3 - all other cases which exhibited both a cumulative grasped level between 1 and 3 and a cumulative released level between 1 and 3.

It is evident that during the performance of a task, category 1 could result when there are no transitions. The second case could result when there is no noticeable slip between the object and the gripper, and the third case will be encountered when the object slipped during grasping or releasing.



Legend

GL: cumulated grasped level within a block
 RL: cumulated released level within a block
 g: grasping, r:releasing

Figure 6.9: Decision hierarchy for a four transition case •

This task categorization was built into the knowledge base using the backward-chaining hierarchy shown in Figure 6.10. Category 1 was independent of the type of task and occurred only when there were no transitions within the data block. Categories 2 and 3 could occur for all the four cases of transitions and for both grasping and releasing type of tasks. In order to represent the categories of task using attributes, four intermediate attributes, "res2", "res4", "ostat1", and "ostat2" were created. These intermediate attributes were assigned values when any of the five demons, which performed event-driven inferencing, fired. The values assigned to these four attributes determined the category of the task and they influenced the values assigned to two other attributes, "res1", and "res3". The latter two intermediate attributes determined the value for the goal attribute "result" in accordance with the main attribute hierarchy of the TSI knowledge base shown in Figure 6.11.

The attribute "result" characterized the gripper status based on the two decision categories. The value for the attribute "result" was assigned a symbolic value 'result2', if the task belonged to a definite class in which there was either no change in task status or the task status could be definitely identified as grasping or releasing. The attribute "result" was assigned with a value 'result1' in all other cases which involved both grasping and releasing within the data block.

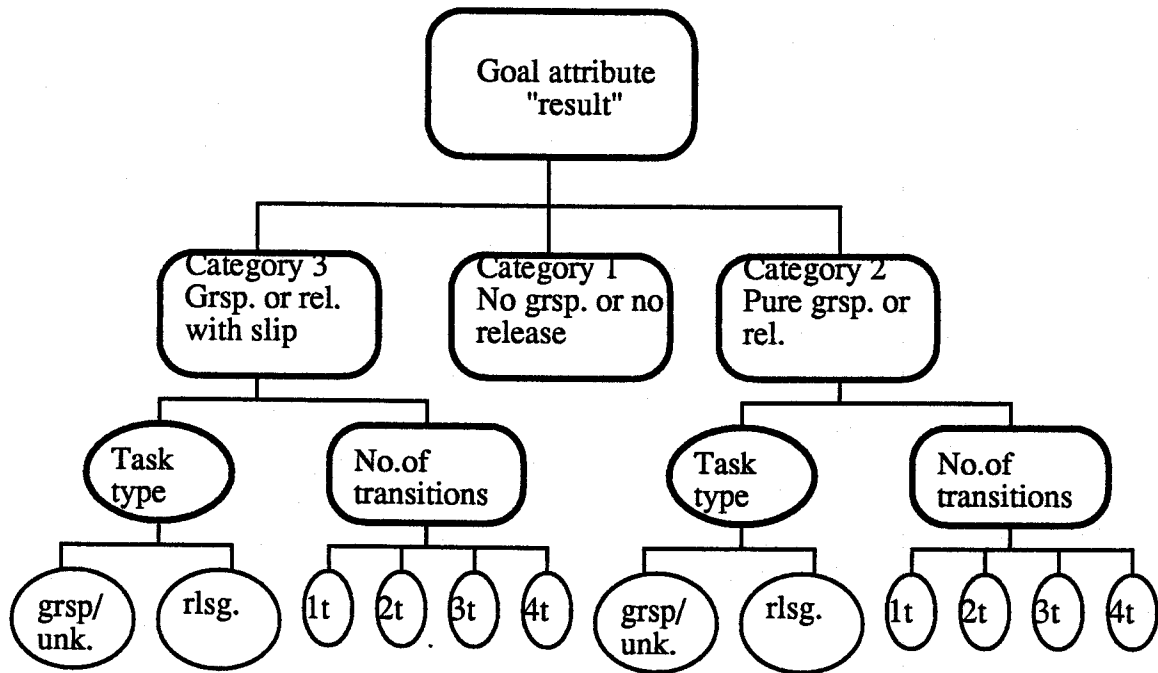


Figure 6.10: Hierarchy to determine task categorization .

6.5.1.2. Confidence level for the grasping and the releasing decisions

Once the value for the attribute "result" was obtained, a confidence level was calculated for both the grasping and releasing decisions in a single block. The confidence level for category 1 was always 100 % because it was a definite case of no change in the gripper status. For categories 2 and 3, the confidence level for a grasping or releasing decision was calculated based on the following considerations.

The decision filter determined a basic sensor confidence factor for the two parameters, GL and RL, defined by Equation (6.1). Thus, for each data block, the fraction of sensors indicating positive transitions gave the value for the grasping confidence factor, while those showing negative transitions contributed to the releasing confidence factor. For the case with the maximum possible transition, i.e. 4, occurring within a block, the situation reflects the maximum confidence in the decision. That is, in a 4 transition case, if either GL or RL equals 4, then the confidence associated with the decision that the task is grasping or releasing, should be equal to the maximum achievable con-

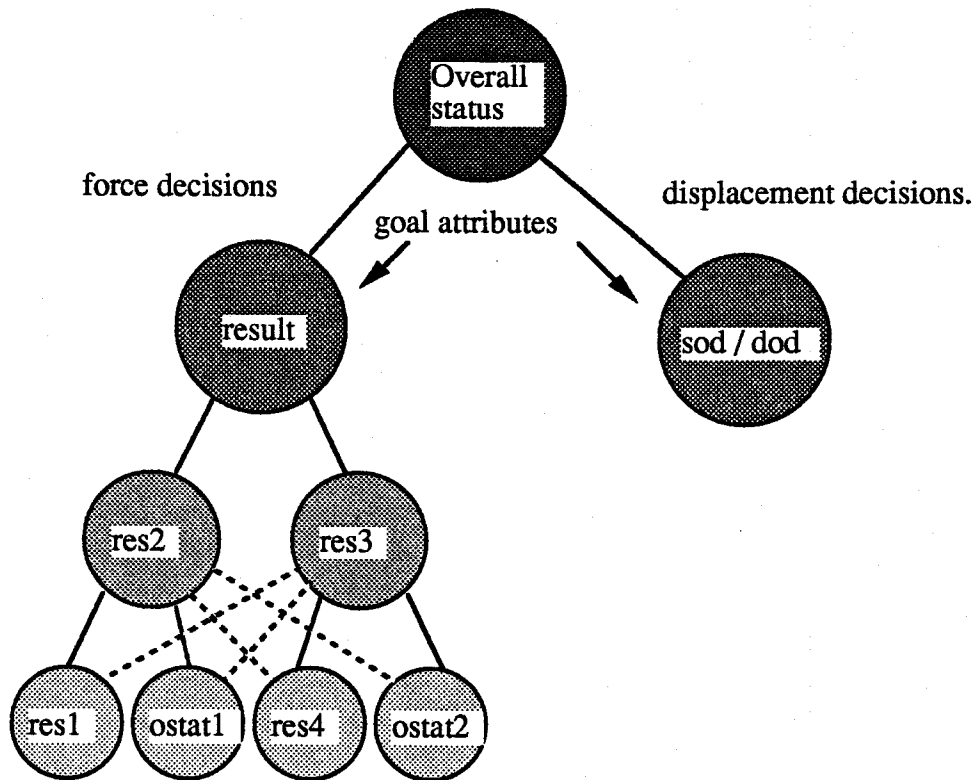


Figure 6.11: Attribute hierarchy for force decisions in the TSI knowledge base .

confidence level. With eight sensors taking part in the task (which was the maximum possible using the prototype gripper system), a maximum value of 100 % would correspond to a 4 transition case in which all the 8 sensors are involved in the task and all of them measure a grasping transition at least once during the time interval of the block.

The decision parameter, defined as sensor confidence factor (SCF), was assigned with a percentage value for every identified positive (grasping) and negative (releasing) transition within a block. Therefore, in a four transition case showing all grasping transitions, the decision parameter grasped level was 4 and the sum of the SCF's was 400 if all the eight sensors showed grasping transitions. The resulting sum of SCF's was multiplied by 1/4 or 0.25 in order to normalize the maximum value obtained for the confidence level to be 100 %. In cases where there were both grasped and released levels within the data block, the respective SCF values were cumulated separately to determine the confidence level for grasping and releasing within the block.

The mathematical formulation of this reasoning consisted of two equations for-

mulated based on the following rule. If there is only one transition within a block, then either GL or RL will have a non zero value. In this case, the strength of the decision is 1 out of a possible value of 4. For a 1 transition case, the confidence level was determined using the relation

$$\text{Conf1 or Conf2} = \text{SCF} \times 0.25 \quad (6.2)$$

where SCF is the basic sensor confidence factor for the grasped level decision parameter, or the released level decision parameter obtained from Equation (6.1). For 2, 3 and 4 transition cases, the confidence levels were given by

$$\text{Conf1} = \sum 0.25 \times \text{SCFG}, \text{ and} \quad (6.3)$$

$$\text{Conf2} = \sum 0.25 \times \text{SCFS}, \quad (6.4)$$

where,

Conf1 = grasping confidence level,

Conf2 = releasing confidence level,

SCFG = sensor confidence factor for positive transitions, and

SCFS = sensor confidence factor for negative transitions.

The confidence level formulated in this way indicated two things about a decision: it gave the strength of the decision in terms of the number of sensors reporting the same type of transitions, and it graded each level with respect to a maximum possible value for a specific system. For example, a grasping decision got a higher value of confidence level if the decision filter parameters showed all 4 out of 4 transitions to be positive compared to a case consisting of 2 out of 2 transitions, both of which are positive. In a similar manner, the confidence level for grasping from a data block which had 3 transitions showing 2 grasping and 1 releasing would be higher than the block which had 2 transitions with 1 grasping and 1 releasing even if the SCF's in both cases were equal.

6.5.1.3. Object displacements

The object displacement information of the task status was determined using both the static and the dynamic displacement parameters determined by the decision filter. Within a block there were possibilities of both types of displacements occurring. In the decision filter, all grouped transitions (displacement transition sets) occurring within the pre-defined dead-band time period, t_{db} , were evaluated and used to determine the dynamic displacement of the object. The resultant direction obtained for the parameter "dynamic object displacement" (dobd), for a data block, was based on majority voting scheme. This decision parameter was in the form of a four element vector in which the resultant direction was encoded numerically. In order to interpret this vector, the

knowledge base of the TSI expert system defined four attributes, dd1, dd2, dd3, and dd4. These attributes were assigned values by forward chaining, and they, in turn, determined the direction of the dynamic displacement by assigning symbolic values to the attribute, dod. The attribute hierarchy which was used in the TSI expert system to obtain the displacement decisions of the task status is shown in Figure 6.12.

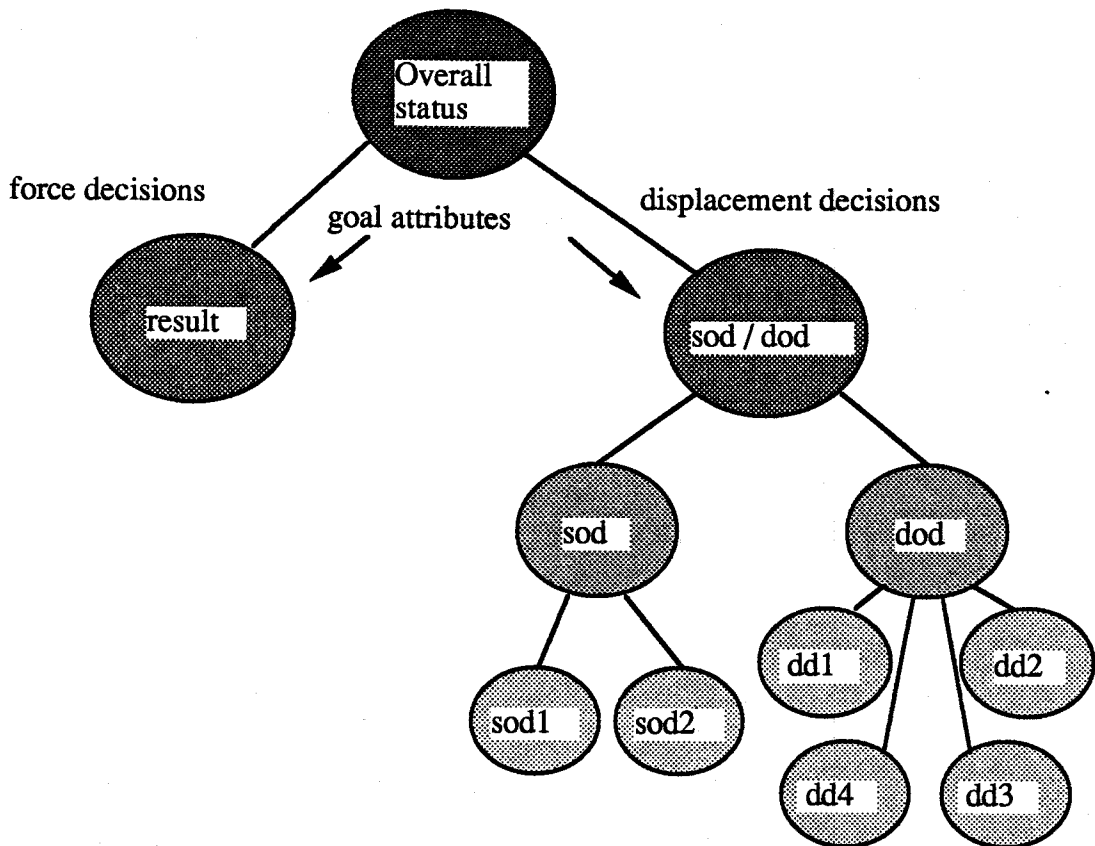


Figure 6.12: Attribute hierarchy for displacement decisions in the TSI knowledge base .

If the displacement transition sets corresponded to a time period exceeding t_{db} , they were identified as the parameter "static object displacement" (sobd). Since the number of transitions considered per data block was limited to four, there could be a maximum of two static object displacements per block, identifiable by the decision filter. Therefore, the parameter, sobd, was a two element vector, with the elements identifying the direc-

tion of the displacement. The direction of displacement was pre-defined in terms of the eight directions shown in Figure 6.4.

The TSI knowledge base used a logic which interpreted the two static displacements within each block to obtain a single decision with an assigned symbolic certainty value. This logic was formulated to assign certainty values depending on the strengthening or weakening characteristics of the two directions. The attribute hierarchy used to obtain the static displacement status of the task is shown in Figure 6.12.

At the beginning of a session, the value of each attribute in the knowledge base was "undetermined". During the session, the value associated with an attribute became "known" either because it was supplied by the end user or because it was determined by the inference engine. If a value is unavailable for an attribute, or could not be inferred, its status changed to "unknown". By identifying the status of the various attributes, it was possible to isolate the error conditions during an expert system session. Textual descriptions of various error conditions were incorporated into the knowledge base.

Using the attribute hierarchies discussed above, the knowledge base for the TSI expert system was built using the KES syntax. User-friendliness was given primary importance by incorporating textual explanations at various stages of the decisions. To display English language descriptions of the various decisions to a user, suitable **messages** were used in the knowledge base design. In summary, the expert system first used event-driven forward chaining to determine the category to which a task belonged, and then used backward chaining to obtain the decisions based on the Hypothesize and Test (HT) method of inferencing [107]. The error conditions were also identified by the expert system and displayed to the user. The task status decisions were indicated in the form of grasped level and/or released level, each with an associated confidence level. The two types of object displacements were also displayed along with the sensing site locations which had indicated transitions. The complete listing of the knowledge base developed for the TSI expert system is given in a separate document [110]. To evaluate its performance, the TSI expert system, developed and implemented in a Sun 4/110 work station, was tested in a stand alone mode using real data.

6.5.2. Performance evaluation of the TSI expert system

A typical object handling experiment consisting of grasping and releasing a sample object was conducted and the dynamic force data was acquired in real time. A total time of 4 s was allocated to each grasping and releasing task. The sample was first grasped and then released. Both grasping and releasing were performed at the same uniform gripper velocity of 7 cm/s. The forces on each of the eight sensing sites were sampled at 1000 Hz. The raw force data measured by the eight sensors and digitized and stored by the

data acquisition system are shown plotted in Figure 6.13. In order to make comparisons, data measured by all 8 sensors are plotted in the figure.

In these plots, the ordinate shows the raw digitized sensor outputs and the abscissa is marked with the time of operation in milliseconds. Clear trends of grasping and releasing are evident in the plots pertaining to data from sensors 1, 2, 3, 4 and 8.

The raw data obtained during the 4 s grasping and the 4 s releasing period were divided into 40 blocks, each block consisting of 100 values of sampled data corresponding to a 100 ms time window. The decision parameters were determined for each block as described in Section 6.2, and these decision parameters were interpreted by the TSI expert system to obtain the task status parameters in terms of force decisions and object displacement decisions. These status parameters were displayed indicating the task status at the end of every block of data. A typical expert system display obtained using the grasping force data from two consecutive blocks, 17 and 18, is shown below:

A Typical Display of the Expert System Output

Task status from block 17

```

*****
Knowledge Engineering System (KES), Release 2.5.
Copyright (C) 1988, Software Architecture & Engineering,
Inc.
Loading the knowledge base 'vkb24.pkb'.
*****
Welcome to the Online Status Indicator Expert designed
by Vaidy. This expert will determine the status of the
task from the dynamic forces acquired by a tactile
sensing system, it will display a confidence factor
for the decisions and will indicate static and
dynamic object displacements. If you want to restart,
type 'n' in the direct question mode.
*****
The object was statically displaced in Nodirection <a>
*****
The object was dynamically displaced North <a>
*****
Released to level 1
Confidence in releasing 6.25
Releasing by sensor 1 at 116 msec
*****
Old data written in 'filetrans3'
*****

```

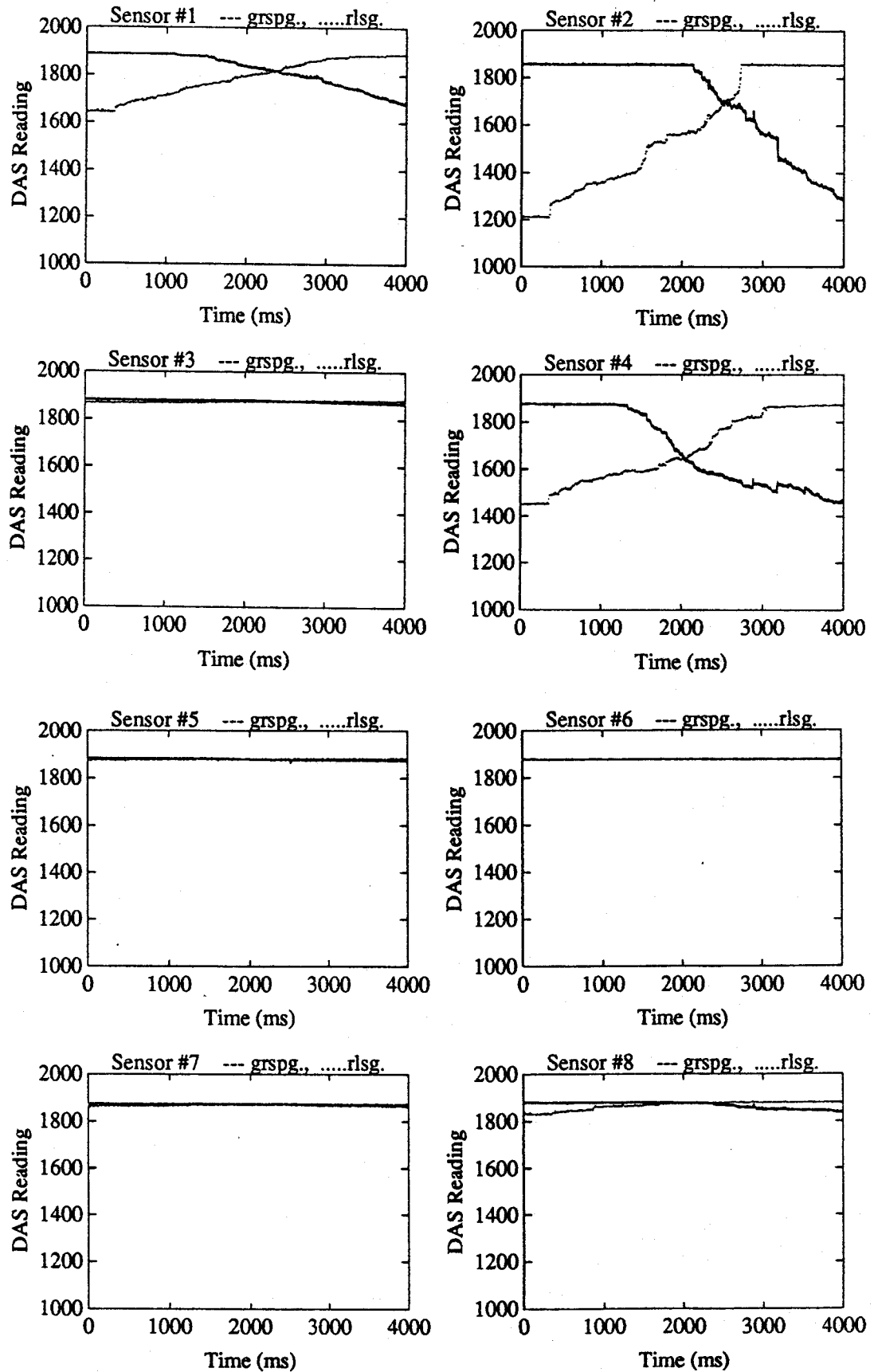


Figure 6.13: Raw force data measured by the 8 sensors of the prototype system during grasping and releasing of the sample .

Task status from block 18

```

*****
The object was statically displaced in Nodirection <a>
The object was not dynamically displaced <a>
*****
There are no transitions, status = unchanged
Grasped to level 0
Released to level 0
*****
New data successfully written in filetrans4
*****
Do you wish to continue ?
  1. yes
  2. no
=? 2
*****
Type 's' to stop
Ready for command: s

```

For the complete duration of the task, similar expert system output was obtained from each block at intervals of 100 ms. The task status results displayed by the expert system were summarized so as to present them in a tabular form as shown in Tables 6.6 and 6.7. Table 6.6 shows the expert system display obtained from the grasping force data, and Table 6.7 shows the display from the releasing force data. The abbreviation 'Nodir' refers to a case when there is no static object displacement. The term 'No' was used to denote the absence of dynamic object displacements.

In order to visualize the performance of the TSI expert system, a graphical representation of the task status could be obtained by dividing the status parameters into those displaying force decisions and those displaying object displacement decisions. The results pertaining to the parameters grasping/releasing levels and their confidence (in %) were plotted as shown in Figure 6.14 and those pertaining to the object displacements were plotted in Figure 6.15. The time of operation of the task is shown on the X-axis. The bar graphs indicate the task status of the gripper contact at all identifiable time instants when a change in the gripper contact state has occurred.

Both the grasping and releasing tasks have been depicted in the same Figure 6.14 to readily illustrate the variation of the confidence level for the grasping level and releasing level decisions. The higher confidence levels seen for grasping level decisions are evident in the expert system decisions for the grasping task. Similarly, the releasing task shows a higher confidence level for the releasing level decisions.

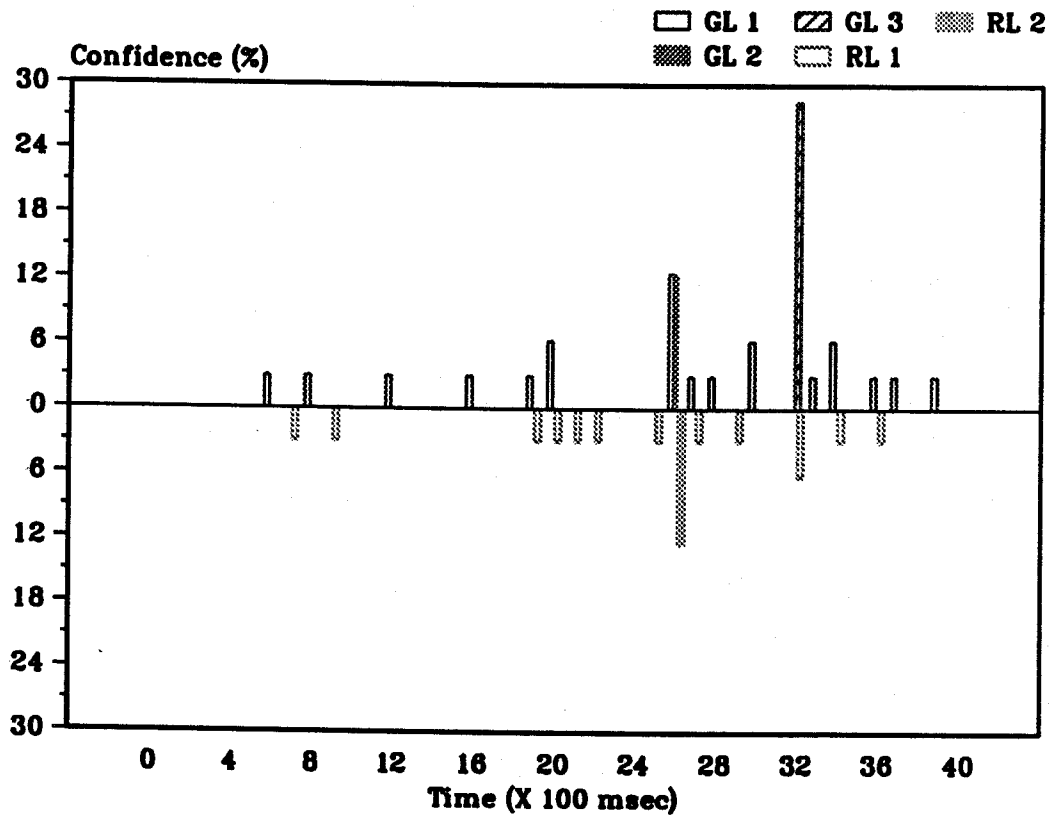
Table 6.6: Summary of the task status determined by the TSI expert system from the grasping data .

Block no.	Unchd. state	Grspg. level	Relsg. level	Conf. level, grspg.	Conf. level, relsg.	Dynamic displt.	Static displt.	Decision correct?
1		0	1	0	3	No	Nodir	No
2	y	0	0	0	0	No	Nodir	Yes
3	y	0	0	0	0	No	Nodir	Yes
4	y	0	0	0	0	No	Nodir	Yes
5		0	1	0	6.25	No	Nodir	No
6	y	0	0	0	0	No	Nodir	Yes
7		0	1	0	3	No	Nodir	No
8	y	0	0	0	0	No	Nodir	Yes
9		0	1	0	3	No	Nodir	No
10	y	0	0	0	0	No	Nodir	Yes
11	y	0	0	0	0	No	Nodir	Yes
12		1	0	3	0	No	Nodir	Yes
13	y	0	0	0	0	No	Nodir	Yes
14	y	0	0	0	0	No	Nodir	Yes
15	y	0	0	0	0	No	Nodir	Yes
16		0	1	0	3	No	Nodir	No
17	y	0	0	0	0	No	Nodir	Yes
18	y	0	0	0	0	No	Nodir	Yes
19		1	1	3	3	No	Nodir	Yes
20		1	1	6.25	3	No	SouWest	Yes
21		0	1	0	3	No	Nodir	No
22		0	1	0	3	No	Nodir	No
23	y	0	0	0	0	No	Nodir	Yes
24		1	1	3	3	No	Nodir	Yes
25		0	1	0	3	No	Nodir	No
26		2	2	12.5	12.5	No	South	Yes
27		1	1	3	3	No	Nodir	Yes
28		1	0	3	0	No	Nodir	Yes
29	y	0	0	0	0	No	Nodir	Yes
30		1	1	6.25	3	No	SouEast	Yes
31	y	0	0	0	0	No	Nodir	Yes
32		3	1	28.5	6.25	South	South	Yes
33		0	1	3	0	No	Nodir	No
34		1	1	6.25	3	No	South	Yes
35	y	0	0	0	0	No	Nodir	Yes
36		1	1	3	3	No	Nodir	Yes
37		1	0	3	0	No	Nodir	Yes
38	y	0	0	0	0	No	Nodir	Yes
39		1	0	3	0	No	Nodir	Yes
40	y	0	0	0	0	No	Nodir	Yes

Table 6.7: Summary of the task status determined by the TSI expert system from the releasing data .

Block no.	Unchd. state	Grspg. level	Relsg. level	Conf. level, grspg.	Conf. level, relsg.	Dynamic displt.	Static displt.	Decision correct?
1	y	0	0	0	0	No	Nodir	Yes
2	y	0	0	0	0	No	Nodir	Yes
3	y	0	0	0	0	No	Nodir	Yes
4		0	1	0	25	No	Nodir	Yes
5	y	0	0	0	0	No	Nodir	Yes
6	y	0	0	0	0	No	Nodir	Yes
7	y	0	0	0	0	No	Nodir	Yes
8	y	0	0	0	0	No	Nodir	Yes
9		1	0	3	0	East	Nodir	No
10		0	2	0	25	West	Nodir	Yes
11		0	2	0	25	South	Nodir	Yes
12		0	1	0	3	No	Nodir	Yes
13	y	0	0	0	0	No	Nodir	Yes
14	y	0	0	0	0	No	Nodir	Yes
15	y	0	0	0	0	No	Nodir	Yes
16		0	1	0	3	No	Nodir	No
17	y	0	0	0	0	No	Nodir	Yes
18	y	0	0	0	0	No	Nodir	Yes
19	y	0	0	0	0	No	Nodir	Yes
20		0	1	0	3	No	Nodir	Yes
21	y	0	0	0	0	No	Nodir	Yes
22	y	0	0	0	0	No	Nodir	Yes
23		1	1	3	3	N0	N0dir	Yes
24	y	0	0	0	0	No	Nodir	Yes
25	y	0	0	0	0	No	Nodir	Yes
26	y	0	0	0	0	No	Nodir	Yes
27	y	0	0	0	0	No	Nodir	Yes
28	y	0	0	0	0	No	Nodir	Yes
29	y	0	0	0	0	No	Nodir	Yes
30	y	0	0	0	0	No	Nodir	Yes
31	y	0	0	0	0	No	Nodir	Yes
32	y	0	0	0	0	No	Nodir	Yes
33	y	0	0	0	0	No	Nodir	Yes
34		1	1	1	3	No	Nodir	Yes
35		0	1	0	3	No	Nodir	Yes
36	y	0	0	0	0	No	Nodir	Yes
37	y	0	0	0	0	No	Nodir	Yes
38	y	0	0	0	0	No	Nodir	Yes
39	y	0	0	0	0	No	Nodir	Yes
40	y	0	0	0	0	No	Nodir	Yes

(a) Force decision parameters - sample 1 grasping .



(b) Force decision parameters - sample 1 releasing .

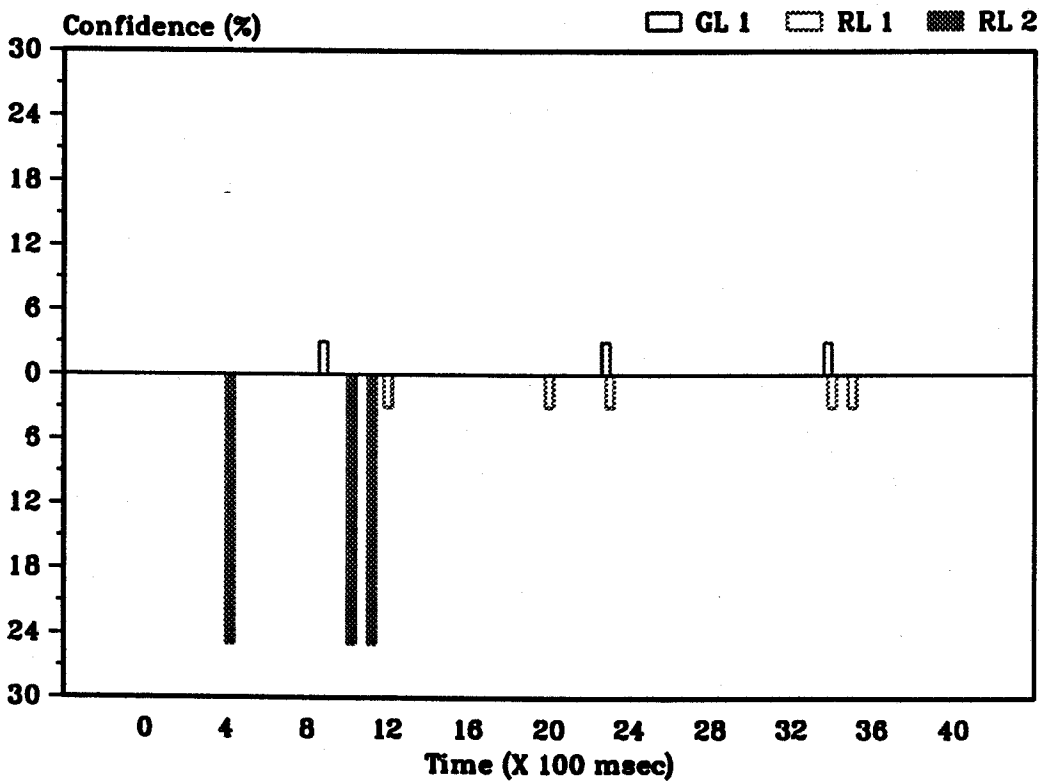
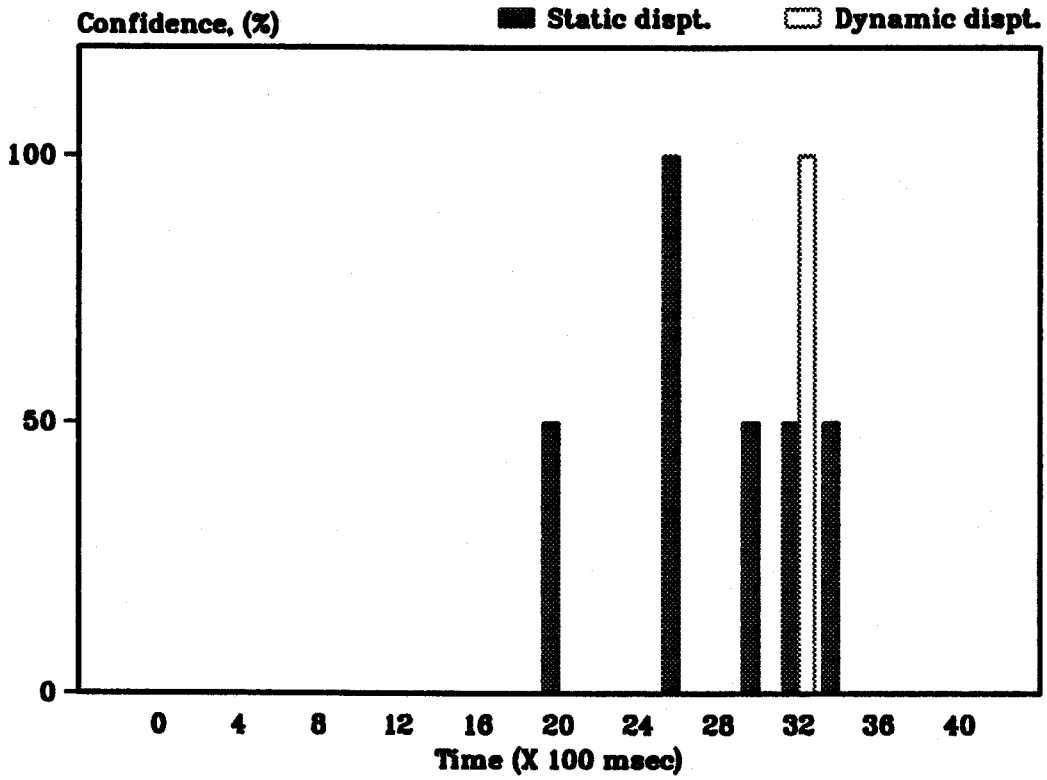


Figure 6.14: Task status parameters obtained from TSI expert system - Test 1.

(a) Object displacement parameters - sample 1, grasping .



(b) Object displacement parameters - sample 1, releasing .

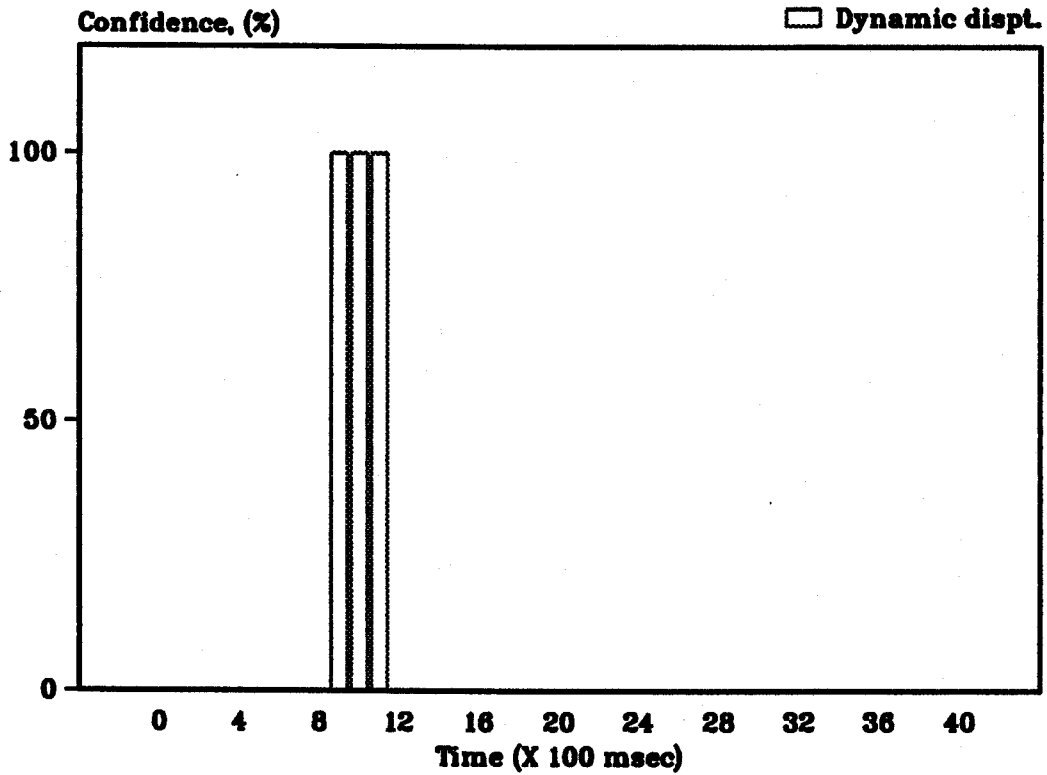


Figure 6.15: Object displacement parameters obtained from TSI expert system - Test 1 .

6.5.3. Interpretation of results

The profile of raw forces in Figure 6.13 clearly shows that grasping and releasing trends of the task were properly captured from the prototype gripper system. Referring to Figure 6.13, it can be seen from the raw data plots that grasping and releasing trends are clearly exhibited by the forces sensed by sensor #1, #2, #3, #4 and #8. The fact that some sensors exhibit a more pronounced variation than others indicates that the dynamic forces are not uniform in spite of using a parallel-jaw gripper for the task. Therefore, interpretation of the tactile sensing data is necessary to identify the task behaviour. The other contributors to dissimilar behaviour of sensor outputs are the position of the object, the sensor characteristics and their orientations, and the noise. The tactile imaging technique helps to compensate for some of these errors with an appropriate choice of force ranges.

The presence of many uncertain transitions in the total gripper force variation (shown in Figure 6.6) shows that a direct interpretation of the total forces from raw data would be erroneous. The effectiveness of the decision filter in reducing the noise in the tactile images is evident from a comparison of Figures 6.5 and 6.6. In Figure 6.5, which shows the plot of cumulated grasped and released levels, it is clear that the decision parameters obtained are in general agreement with the nature of the task. The definite trends displayed by the decision filter outputs confirm the effectiveness of the tactile imaging technique to produce relatively noise-free profiles for grasping and releasing decisions.

The TSI expert system, which determined the task status based on the decision parameters, has yielded correct decisions in a large majority of cases, as demonstrated by the expert system output summary given in Table 6.6 and Table 6.7. Though the task status had indicated both grasping and releasing during a grasping operation, the confidence level for grasping decisions were higher than the corresponding confidence level for the releasing decisions. This indicates that in order to generate control decisions based on the task status, it will be necessary to consider all the four force decision parameters of the task status. Results from the releasing task also emphasize the necessity of using all the four force decision parameters. When the TSI expert system indicates no change in the gripper status, the gripper may be considered to be performing its task satisfactorily without needing additional control actions. When interpreted in this manner, it can be seen that the status parameters have been correctly evaluated in a majority of cases.

6.5.4. Limitations

The behaviour of the seven identified decision parameters within a data block have been used to determine the task status. These parameters have been selected based on human judgment which is subjective in nature. There may be other possible selections of decision parameters which might be easier to interpret. In order to interpret the decision parameters from a 100-point data block, a maximum of only four transitions were considered. This was done since the TSI expert system was developed to test the applicability of the technique rather than to build a commercial product. By restricting the maximum allowable transitions per block, it was possible to restrict the number of decision rules to be used in the expert system. However, this reduced the accuracy of the method and for precision tasks the present accuracy may be insufficient. The selection of the number of possible transitions depends on the size of the pre-filter and the size of the dead band window used in the decision filter. Therefore, for a different choice, the decisions obtained may not be identical. The number of transitions allowable was also based on a fixed gripper speed. Grippers actuated at higher speeds may tend to miss useful transitions.

6.6. Summary and Conclusions

Tactile sensing arrays are suitable for measuring dynamic forces on gripper fingers when the gripper is grasping or releasing an object. The dynamic forces measured and acquired during the performance of a task were converted into tactile images and the images were used to identify the positive and the negative changes in force (transitions) occurring during the performance of the task. A positive transition resulted due to an increase in the measured force at a specific sensing site while a negative transition occurred due to a decrease in the gripper force at that site. The changes in force can be attributed either to actual increases or decreases in the applied force at a site, or to the force moving laterally with respect to the sensing site.

A set of seven decision parameters was identified by analyzing a tactile image in a case study, and a filter was designed to determine these parameters from a tactile image. From a block of data consisting of a fixed number of sampled forces, a set of decision parameters was obtained. In this filter, for a small time window, two types of transitions, positive and negative, were cumulated to define values for two decision parameters, namely, grasped level and released level. The transition points defined the times at which the state of the gripper contact had changed. By evaluating the spatial relationships among the observed transitions and identifying the sensing sites measuring active transitions, the values for the other decision parameters, namely, the sensor confidence factor for the grasping decision, and for the releasing decision, the static and dynamic object displacements, and the transition points were assigned.

The interpretation of the decision parameters was achieved using an expert system, called the TSI expert, in which a component of human decision-making capability was incorporated. To develop a knowledge base for the TSI expert, the possible values for the decision parameters, grasped level and released level, were divided into three categories. These categories covered all possible values which these two decision parameters could take. The first category referred to a case when there was no transition in a single block of force data, which was interpreted as no change in the gripper status. The second category pertained to a situation when it was either a pure grasping or a pure releasing operation without slip and the third category dealt with all cases which showed both non-zero grasped and released levels. The last category was interpreted to mean the presence of slip during grasping or releasing, owing to the fact that some sensors measured increasing forces and some measured decreasing forces. The numerical value of the cumulated grasped and released levels along with the sensor confidence factors were used to determine an overall confidence level for the task status decisions.

Two types of task status parameters were determined and displayed by the user-friendly expert system. The force decision parameters displayed were the grasping and releasing levels with associated confidence levels for the two decisions, obtained from each block of data. The object displacement decisions displayed were the static and dynamic object displacements, determined relative to the gripper position at the beginning of a data block. The work reported thus far has been summarized in Figure 6.16, which shows the steps involved in the task oriented procedure to determine the decision parameters and the task status parameters from dynamic force data.

The TSI expert was tested in a stand alone mode using a set of actual data measured while grasping and releasing a sample object. Using these data, the performance of the decision filter and the expert system were evaluated. It was found that the confidence level parameter of the task status plays an important role in correctly characterizing a grasping or a releasing operation.

For handling objects of different kinds, with varying shapes, sizes and orientations using an intelligent gripper, a typical on-line control decision could be either to increase or decrease the applied gripper forces, or to move the gripper differently to prevent object slippage. By processing the force decision and object displacement decision task status parameters determined by the TSI expert system, it could be possible to obtain such control decisions. For example, the task status parameters from two successive blocks may be grouped and delivered to a second expert system which could process the task status parameters and obtain control decisions for every two block set of data.

Using the static and dynamic displacements of the object occurring within a specified time interval, it is possible to identify slow slippages of the object which have occurred in the recent past (100 ms time in the case study).

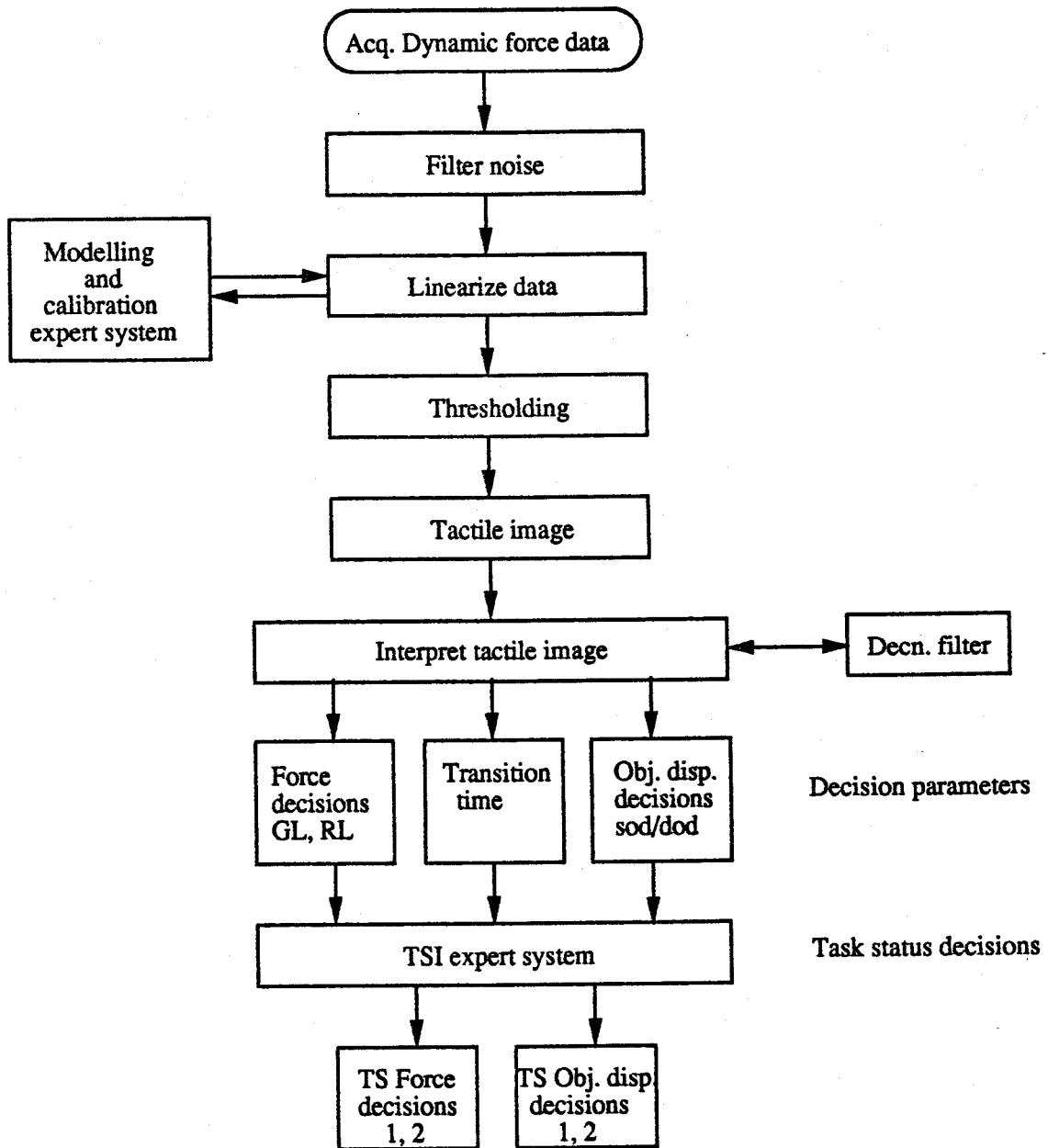


Figure 6.16: A typical flow diagram of the task oriented procedure used to determine the task status parameters from dynamic force data .

Various software modules developed for processing the raw dynamic force data described in Chapters 5 and 6 were integrated into a single application program called the task oriented procedure. The program embedded the TSI expert system so that the task status parameters could be determined from the data obtained while handling different sample objects. The next chapter will describe the development of the integrating software and the various test cases which were used to validate the complete procedure.

7. SYSTEM INTEGRATION, RESULTS AND PERFORMANCE EVALUATION

7.1. Introduction

The development of a task oriented procedure for a tactile sensing gripper would be complete if the various functional modules described in earlier chapters were integrated into a single executable computer program. Such a program, which was called "Interface Program II", was designed to access the MATLAB software package, execute the various processing modules, and embed two expert systems, namely, the TSI expert system (described in Section 6.5), and the Control Decision Indicator" (CDI) expert system described in this chapter. The CDI expert system was designed primarily to test the feasibility of using the task status decision parameters to form suitable on-line control decisions by interpreting task status parameters from two successive blocks. The design of the CDI expert system was carried out in a manner similar to the design of the TSI expert system.

The design, implementation and testing of the CDI expert system using the KES development tool will be described and its salient features will be discussed. The reasoning technique used to infer control decisions from task status parameters was based on human intuitive knowledge. This knowledge was incorporated into the CDI knowledge base using a set of attributes whose values determined the confidence factor for specific types of decisions. The detailed descriptions of these attributes and the manner in which the values assigned to them were interpreted in order to obtain consistent control decisions from the task status will also be discussed.

Interface Program II, which embedded both the TSI expert system and the CDI expert systems, displayed recommended control decisions to successfully complete a task. Once the program obtained the dynamic forces measured by the tactile sensors of the prototype system, it executed all the steps up to and including the formulation of a set of control decisions. To achieve this, considerations for embedding the two expert systems into Interface Program II have been outlined and the method used to embed the two systems have been stated.

The last section of this chapter deals with the performance evaluation of the com-

plete task oriented procedure. Four categories of tests were designed and nine sample objects of varying shapes, dimensions and masses were used. The results obtained from various tests will be described in order to discuss the applicability of the procedure for grasping and releasing tasks.

A summary of the TSI expert system display as well as the preliminary control decisions obtained using the CDI expert will be used to identify the main features of the task oriented procedure. The main limitations of the procedure and recommended areas for further investigation will be outlined at the end of the chapter.

7.2. Software Integration

The requirements for the software integration of various modules that had been designed to perform specific functions on the dynamic force data were first identified. Software integration consisted of development of two programs, Interface Program I, and Interface Program II. Interface Program I, which was designed to carry out the off-line processing was described in Section 4.4.2.1. This program is executed before using Interface Program II. Interface Program II was designed to perform all the on-line tasks using the results from Interface Program I. These results consisted of the definitions of the force thresholds for each sensor used in the prototype gripper system. The thresholds were stored in the designated "MAT" or binary files to facilitate fast access by Interface Program II. The dynamic force data, from which the task status was determined, were assumed to be available in the form of ASCII files. For the purposes of testing and evaluation of the integrated computer program, the dynamic forces encountered during a task were used. The main components of Interface Program II were identified by dividing the task oriented procedure into functional software subsystems.

7.2.1. Software subsystems

The task oriented procedure designed to obtain the task status from the dynamic force data performed three main functions:

1. prefiltering and tactile imaging,
2. determination of the seven decision parameters, and
3. execution of the TSI expert system.

To perform these functions, Interface Program II accessed the software modules which performed the listed tasks. The tasks of prefiltering, tactile imaging and the determination of the decision parameters were performed by modules which were developed using the MATLAB software library routines. Therefore, these modules were combined into a single module called the "Application Program". The TSI expert system was implemented using the KES shell as described in Chapter 6. To integrate this expert system

into Interface Program II, an embedding technique was selected. The first part of Interface Program II was used to load the dynamic force data from ASCII files. This part was designated the "user input" section. In this section, the program displayed messages to a user to enable him/her to enter the necessary information.

The three identified sections which were incorporated in Interface Program II were the user inputs, the application program, and the embedded expert system.

7.2.1.1. User inputs section

In this section of Interface Program II, the user was prompted to enter a set of four parameters. These were the following: the name of the ASCII file which contained the dynamic force data, the type of operation (grasping, releasing, or unknown) to which the data belonged, the size of a data block, and the beginning block number from which task status determination commenced. The requirement for the designated ASCII file was that the force data in the file had to be stored in a flat ASCII format, consisting of fixed record length data consisting of values measured by the eight sensors and stored in an eight-column array. The type of operation information sought from the user was used to identify the file which contained the definition of the force thresholds for each of the eight sensors of the prototype system. The threshold definitions obtained by Interface Program I were different for grasping and releasing type calibration data. If the task type information was unknown, then as a default, the thresholds obtained from the grasping type calibration data for all the eight sensors, were used. The data block size was made user selectable to make the program easily adaptable for various types of tasks. The beginning block number enabled the selection of data for processing from any desired point in the file.

7.2.1.2. Application program section

The application program consisted of the filters designed to perform prefiltering, tactile imaging and the program which determined the seven decision parameters from a tactile image. These filters were separately developed in the form of 'M-files' and tested using the appropriate commands of the Matlab software package. M-files are the disk files containing the MATLAB command statements and are so designated owing to an extension of ".m" used in their file names. Typically an M-file consisted of a sequence of MATLAB statements, possibly including references to other M-files.

A *script* file was used to automate long sequences of MATLAB commands. When a *script* file is invoked, MATLAB simply executes the commands found in the file, instead of waiting for an input from the keyboard. The statements in a script file operate globally on the data in the workspace. A *function* file differs from a *script* file in that a *function* file permits passage of arguments to the function. The variables defined in a

function file are local to the function and do not operate globally on the workspace. The *function* files were used to expand the MATLAB library, by creating new user-specific MATLAB functions.

In order to access the M-files in proper sequence, a main program was written so that a system call to this program will execute the operations shown in the flow chart of Figure 7.1. This application program obtained the seven decision parameters from a set of dynamic force data.

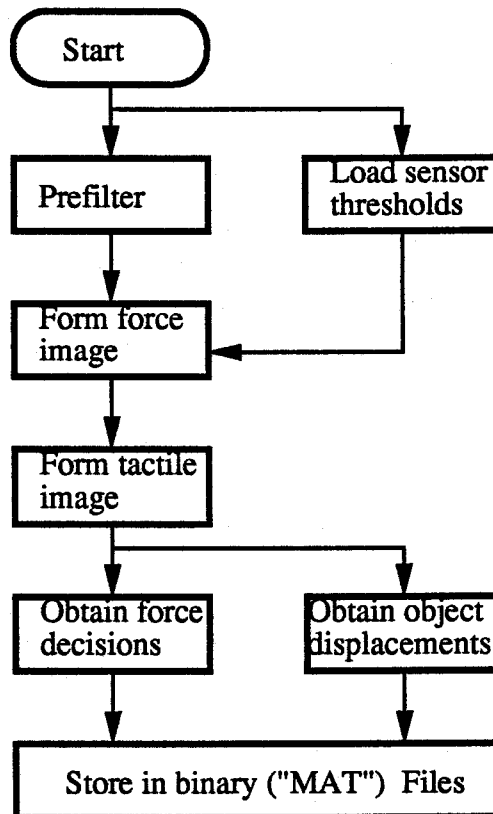


Figure 7.1: Flow chart of the Application program section of Interface Program II .

7.2.1.3. Embedded expert system section

The primary advantage of using the KES shell for developing the TSI expert system was the facility provided by KES to embed the knowledge base as a part of the integrated software. This could be done because the integrating software was written in the C programming language. KES supplied a set of functions and data structures that the program embedded in order to retrieve and manipulate the data, and to gain access to the knowledge stored in a KES knowledge base. A knowledge base used in such an environment is said to be embedded in the program.

Embedding the expert system offered several advantages over a stand-alone system:

1. The embedded expert system operated as a module under the control of the application.

2. By including the expert system techniques in decision making, the design of the decision filter could be simplified. This was because in a knowledge base the problem could be expressed in a simple, straightforward and easily maintainable form.
3. There was a performance gain over the stand-alone KES runtime system. This was tested by determining the total time taken to run the expert system in the embedded and stand-alone modes.
4. The end-user interface could be easily modified to offer additional clarifications or explanations without modifying the knowledge base.

Communication with an external program that was called by the expert system was much slower than an embedded system because of the absence of a direct link between the knowledge base and the program. In the embedded system, all information needed by the C program was accessible through the use of function calls.

The first phase in embedding was the development of the C program without the calls to KES functions. This helped to ease debugging of the program since the number of variable elements was restricted. After the C portion of the program was developed, the second phase involved the development of the knowledge base as described in Chapter 6. The knowledge base designed for use in an embedded system was the same as the one which was designed to operate as a stand-alone system. The knowledge base was separately developed and tested independent of the C program.

The third and final phase of embedding was the integration of the C program with the knowledge base, using the embedded interface shown in Figure 7.2. This consisted of providing an interface that allowed communication between KES and the C program. That is, the C program gave instructions to KES and received and manipulated the data obtained from KES. The KES program received its inputs from the C program and sent messages back to it.

To perform these tasks, the C-functions called by KES had to be included in the C program. The calls to the C-functions provided by KES were also included in the program. The knowledge base developed in phase two was parsed and stored. The C program loaded the parsed knowledge base in order to access it. A header file containing the declarations of the HT functions and data types was included so that calls to HT functions were handled properly. This is the file `ht.h` shown in Figure 7.2. The block `ht.o` refers to a library file containing the object code for the KES functions which were linked with the program.

The C program instructed KES to run the *actions* section, execute KES commands, and obtain the values for the attributes. All these tasks were performed through calls to a set of library functions. These functions allowed the C program to:

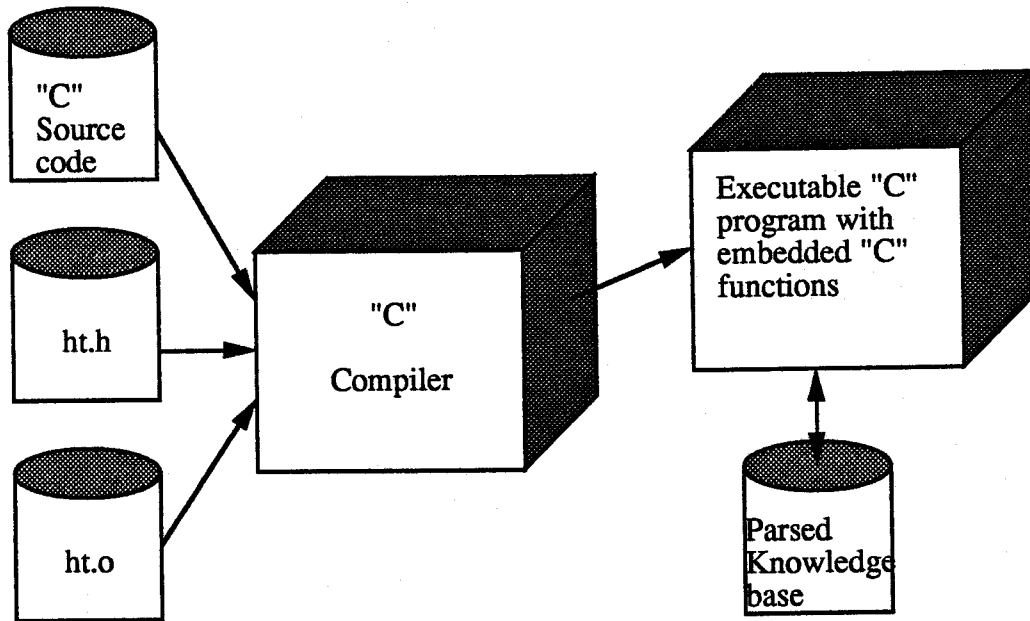


Figure 7.2: Integrating a C program with a Knowledge base [from KES Knowledge Base Author's Manual [107], Fig.12-14, page 12-7] .

1. load and free a parsed knowledge base,
2. send data to the expert system,
3. receive data from the expert system,
4. issue commands to the expert system, and
5. load or save case information from the knowledge base.

During the execution of the program, the expert system could send a message to the C program or seek a value for an attribute. This was facilitated by "callback" functions which allowed KES to ask for an attribute value either from a data base or from an end-user, and to send messages to the C program. These messages were either directly displayed to a user, or reformatted and displayed, or used to trigger a particular action. One function from each of these callback categories was included in the integrated C program.

7.2.1.4. Levels of embedding

There were three levels of embedding provided in KES. Level 1 was the simplest level to work with and Level 3 was the most complex. The levels differed in the number of functions offered, the flexibility of manipulating the variables in the knowledge base, and the complexity of the data types and functions provided. Each level contained a set of library and callback functions. Different data types were used at each level. However,

functions from all three levels could be used in a single program without speed or space penalties. Each level was independent, that is, a knowledge base could be embedded using functions from a single level. The functionality provided by each level was either duplicated or replaced by the functionality at another level. However, there was no one-to-one correspondence between the functions provided at different levels. For example, each level provided a way of performing the **obtain** command but the functions used to obtain a value differed in the data type used and in the method used to access the information. The choice of a level was governed by the needs of the application. The main features of the three levels [107] were analyzed in order to select the level of embedding to be used in Interface Program II.

Level 1 provided all the necessary functions to embed the TSI knowledge base. It provided access to the expert system in a manner similar to that of an end-user. The functions provided the capability to execute the run-time commands. Level 1 included basic functions to load a knowledge base, run the *actions* section, and execute all the run-time KES commands. All input and output to KES had to be passed in the form of strings.

Though the Level 2 functions offered more functionality by providing facility to incorporate the procedural knowledge in terms of C functions, and the Level 3 functions could retrieve "static" data, which includes information such as the number and the type of attributes, these functions required cumbersome procedures for embedding specific sections of a knowledge base. For determining the task status from separately acquired and stored data, a simple basic control of the expert system was sufficient. Level 1 contained eight functions which could be used to start and stop the system, execute KES commands, display messages and get inputs. Therefore, Level 1 was selected for embedding the TSI and the CDI expert systems.

7.2.2. Development of Interface Program II

After analyzing the requirement specifications of each of the three sections, and the features of the MATLAB software and KES, the development of Interface Program II was undertaken on a Sun 4/110 workstation. The program development was done in four stages. In each stage, a specific functional section of the program was independently designed and tested. Consequently, the program consisted of five parts in which the first four parts performed the tasks listed below.

1. Access the user input section.
2. Execute the application and process timing programs.
3. Translate the decision parameters stored in "mat" files into ASCII parameters and store them in KES communication files.
4. Embed the TSI expert system using Level 1 functions.

The last part of Interface program II consisted of the subroutines used by the other sections.

The first part performed the tasks selected for the user input section. It loaded the user-designated file and selected two successive blocks of data. The beginning data block, *nb*, and the number of points per block, *nn*, entered by the user were used to determine the two sets of data. These two sets were then written into two pre-designated files. The format of these files was such that they could be directly accessed by the "load" command of the MATLAB software. In this format, which is also termed as "flat ASCII format", the data were stored in ASCII form, with fixed length rows terminated with carriage returns, and with spaces separating the numbers. The task type was separately stored in a third flat ASCII file. The program also identified error conditions and displayed them to the user. The two data blocks were identified to the user as confirmation of the selection.

The second part performed the execution of the application program and the calculation of the time required to execute the complete procedure. To execute the Application program, a *script* file called "try`matt`" was created. This consisted of the MATLAB commands which loaded the three files created in part 1 and assigned values to three parameters, *n1*, *n2*, and *n3*. These parameters specified the size of the moving average low pass filter, the size of the dead band to be used in the decision filter, and the size of the data block, respectively. The next step was to execute the main application program, called "Stat`filt.m`", which was developed in the form of a *function* file. This M-file accessed three other M-files, which were developed to perform the three tasks of prefiltering the raw data, obtaining a tactile image from the filtered data, and determining the seven decision parameters from the tactile image. The seven decision parameters obtained from the first block of data were stored in a "MAT" file. The same procedure was repeated using the force data from the second block of data and its decision parameters were stored in a second "MAT" file.

The timing calculations were done using the utility function "time" provided in the UNIX operating system. The time to obtain the decision parameters from the raw force data was evaluated using this timing function. Two calls were made to this function: the first one was made before accessing the MATLAB script file and the other was made after the control returned back to Interface Program II after the decision parameters were determined and stored in "MAT" files.

The third section of Interface Program II performed file transformations. This consisted of writing the seven parameters obtained from each "MAT" file in two new files, "file`trans1`" and "file`trans2`". The format used to write these two files conformed to the communication file format specified by the KES software. Each parameter was written

on a separate line terminated by a period. At the end of the file, the section termination character used in KES, namely %, was written in each of the files.

The development of the fourth part of Interface Program II consisted of embedding the KES knowledge base using Level 1 functions. Level 1 functions represented information in the form of character strings and used the following five data types: HT_boolean_type, HT_command_type, HT_error_type, HT_msg_class_type, and HT_string_type. The HT_boolean_type represented the values *true* and *false*. For example, HT_true_c was defined as 1 and HT_false_c was defined as 0. The HT_command_type enumerated the commands which were executed by the function HT_command(). The name of each value of this type corresponded to the name of its associated command. For example, HT_askfor_cmd_c had a value corresponding to the "askfor" command of KES. HT_error_type enumerated the errors that occurred when calling a KES embedded function. For example, HT_success_c indicated that there were no errors and any other value represented an error. The HT_message_class_type enumerated the kinds of messages passed to the function HT_receive_mesg() and HT_string_type represented a standard C language character string.

For activating and deactivating the expert system, the following three functions were used: HT_ld_kb(), HT_run_actions() and HT_free_kb(). To execute the KES commands from the C program, the function HT_command() was used. Definition and detailed descriptions of these functions and data types are given in the KES Reference Manual [111].

7.2.3. Summary of software integration

Two integrating programs, namely, Interface Programs I and II were developed and implemented. Interface Program I performed characterization of the prototype gripper system using a simple model and obtained the force thresholds for each of the eight sensors. Interface Program II used these threshold definitions for each sensor to form a tactile image and then developed a set of decision parameters which were used by an expert system to determine the task status. The time required to execute Interface Program II was evaluated to indicate the processing time required to perform all of the operations. To test the performance of the scheme, a testing and validation procedure was designed and implemented as described in the next section.

7.3. Testing, Validation and Performance Evaluation

The integrated computer program developed to determine the on-line task status was centered around the laboratory prototype gripper system. In order to evaluate the performance of the task oriented procedure, the validity of the raw force data was first established. To perform this validation, the performance of the prototype gripper system and the VAXlab data acquisition system were evaluated using a set of standard tests. This was done to confirm that the raw data was not excessively corrupted with the hardware system components and the data acquisition procedures. Thereafter, the validity of the task data were ascertained by acquiring raw force data during the real time tests and observing the plots of the raw data measured by all the eight sensors as a function of task time.

Two types of test procedures, Test Procedure 1 and Test Procedure 2, were designed to acquire real time raw data while carrying out different categories of tasks. The test procedures accommodated a number of typical object handling situations for which the prototype gripper might be used. Therefore, the design of these procedures considered the limitations of the prototype system.

In the case of Test Procedure 1, a set of nine sample objects was prepared. The term "task" was defined such that the definition was applicable to all the object handling situations considered in the tests. The procedure was implemented to obtain raw force data from three different categories of grasping and releasing operations. In contrast to this, the second procedure was implemented to obtain raw data from a set of pre-defined artificial slip tests. All test data were acquired using the laboratory prototype gripper system.

The performance evaluation of the integrated computer program consisted of using the authenticated raw force data as inputs to Interface Program II and observing the display of the TSI expert system. The task status determined and displayed by the TSI expert system was used to verify the validity of the decisions. The task status decisions were also used to determine a set of control decisions using the embedded Control decision indicator (CDI) expert system. The above mentioned performance evaluation procedure was carried out using the raw force data from a selected number of tasks belonging to different categories.

7.3.1. Performance of the VAXlab data acquisition system

In order to authenticate the raw force data which were used to evaluate Interface Program II, the performance of the VAXlab data acquisition system which was used to obtain the raw data during a task was evaluated using a set of three standard tests. These tests were used to determine the behaviour of the digitized output data from the DAS

when different types of inputs were connected to the eight channels. The design procedure and the salient features of the hardware and associated software of the DAS and the prototype gripper system have been described in Chapter 3.

Test 1 consisted of determining the switching delays and time constants in the eight-channel system. To determine these quantities, the characteristics of the output from the eight channels of the DAS were obtained when voltages of V_{\max} and V_{\min} were input to alternate channels. That is, channels 1, 3, 5 and 7 were connected to V_{\max} , and channels 2, 4, 6, and 8 were connected to V_{\min} . The unloaded sensor output, which corresponded to a voltage V_{\max} in the shunt mode of FSR operation, from one of the eight sensors, was connected to channels 1,3, 5 and 7, while the other 4 channels were grounded (corresponding to an input V_{\min}). A sampling rate of 1 KHz was used and 100 sampled data values were obtained for each of the eight channels. The channel outputs were plotted and are shown in Figure 7.3. It is evident from the plots that the outputs from the eight channels closely correspond to the inputs with negligible switching delays between channels. The curves also show that the inter-sampling delay is negligibly small.

In test 2, the cross-talk between channels was investigated. In this test, the four channels,1,3,5,and 7 were connected to the respective inputs of the tactile sensors 1,3,5, and 7, while maintaining the other four channels at ground potential. The resulting data acquired by the DAS were plotted as a function of time as shown in Figure 7.4. This curve shows that the cross-talk between channels in a situation when a maximum force variation existed between any two adjacent sensors, is negligible.

In order to determine the linearity of the DAS, a 100 Hz ramp signal from a signal generator was connected to all the eight channels. The corresponding output plotted from the DAS data acquired in channel 1 is shown in Figure 7.5. The sampling method used in all the cases was the maximum allowable frequency in the system which guaranteed 12 bit accuracy (using the burst mode triggering discussed in Section 3.4.1.1, Chapter 3). It can be seen from Figure 7.5, that the ramp was reproduced without any visible distortion. Therefore, it was concluded that a linear model assumed for the VAXlab DAS was appropriate. The error in the output was considered to be limited to the A to D conversion quantization errors.

The results from these three tests indicated that the data acquisition system used in the prototype gripper system performed data conversions with a linear input-output relationship and the quantization error in the A to D converter was limited to ± 1 LSB [95]. This error was assumed to be negligible to justify the use of a linear relationship between the analog sensor outputs and their corresponding digitized values.

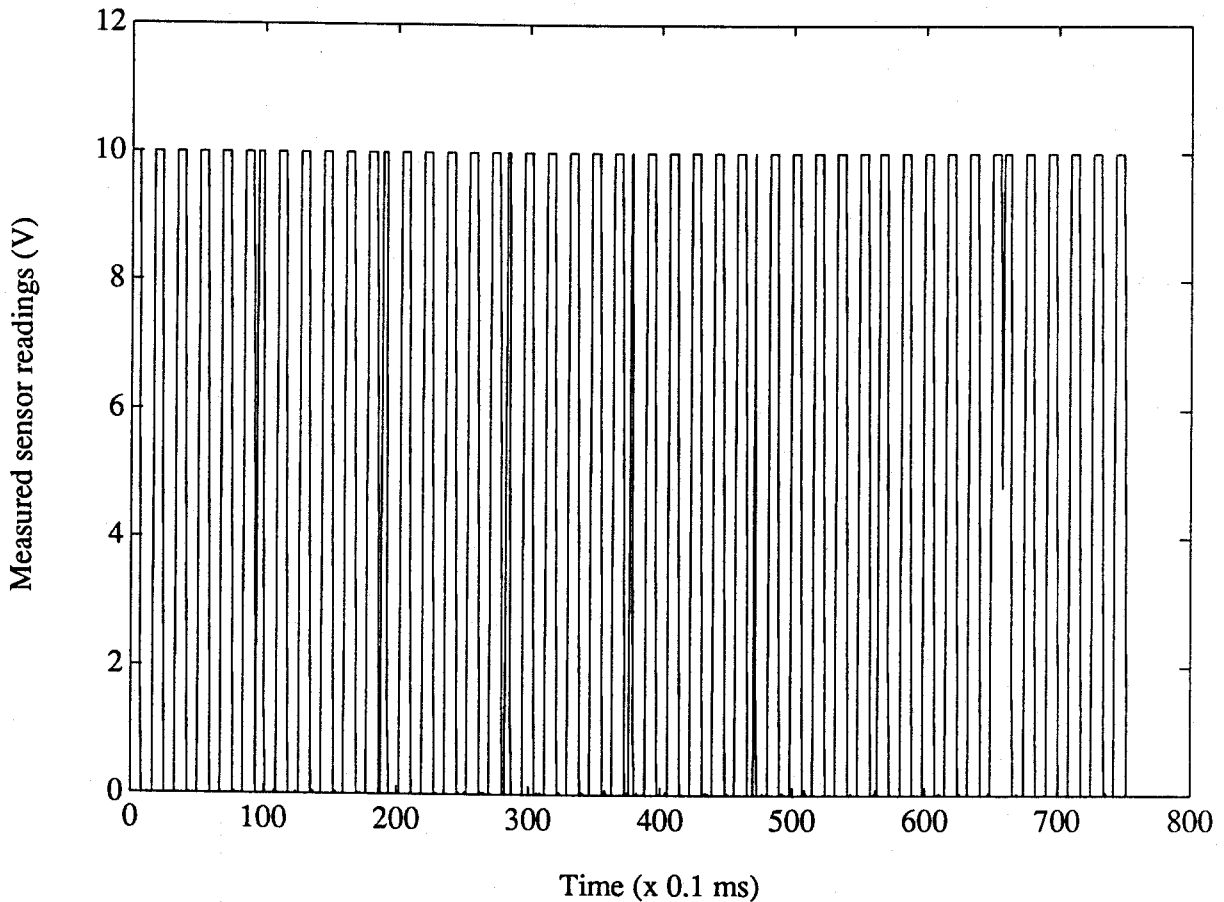


Figure 7.3: The outputs from channels 1 to 8 to test for switching delays in the DAS .

7.3.2. Procedures to obtain real time task data

7.3.2.1. Apparatus for the Test Procedure 1

The prototype gripper system which was used to carry out the tests in this category was actuated at a constant jaw speed of 7 cm/s. Mechanical fixtures were built to hold the objects in the space between the gripper fingers. These fixtures were mounted on a vice fastened to a horizontal surface. The robot gripper was equipped with a mechanical spring-operated limit switch which prevented application of excessive gripper forces to the object. A push-button switch was used to activate the gripper motor to signal starting and stopping of the gripping action.

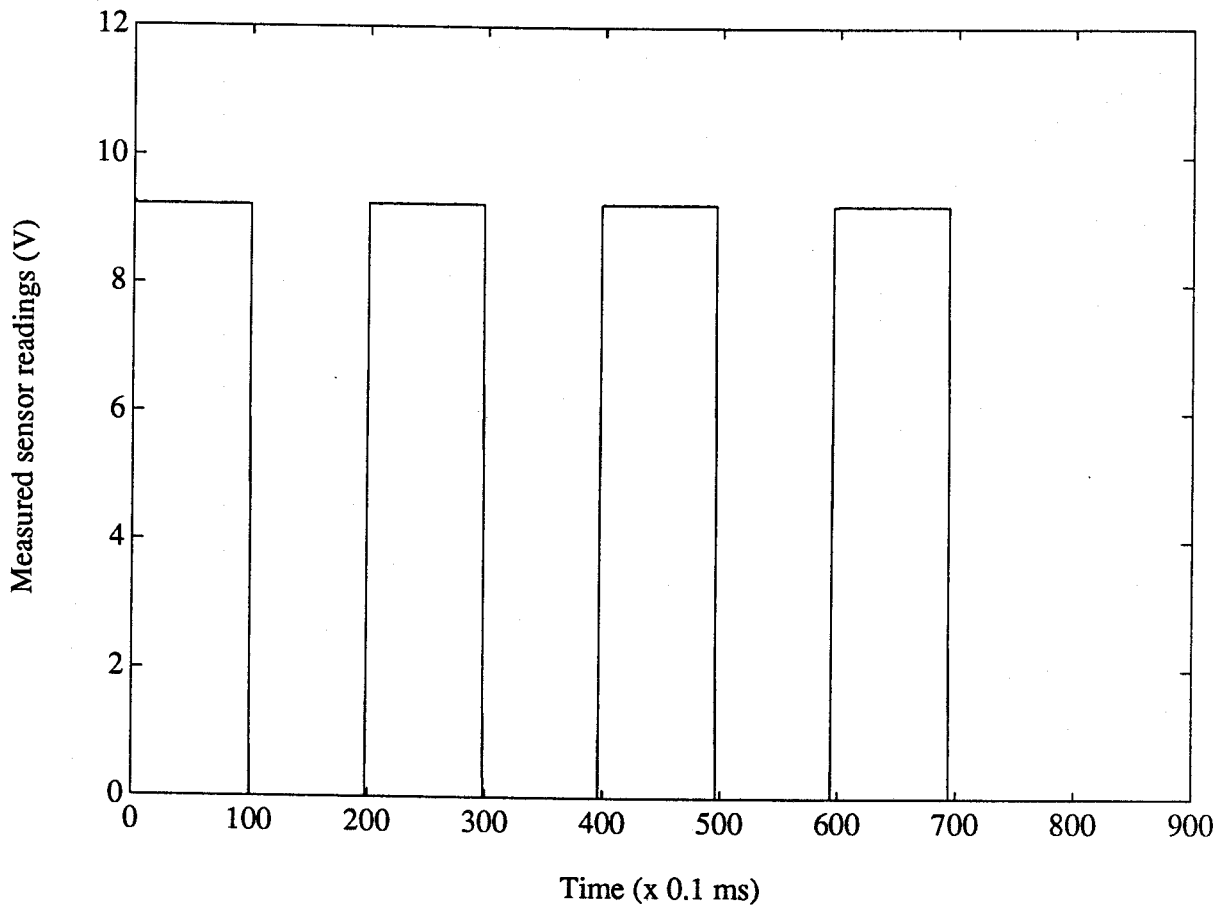


Figure 7.4: The outputs from channels 1 to 8 to test for channel cross-talk in the DAS .

The measured signals from the eight tactile sensors were connected to the eight channel data acquisition system (DAS) installed in a MicroVAX 3600 computer. A program was written to sample all the eight channels at a uniform rate of 1 KHz or 500 Hz depending on the category of the task (to be discussed in a later section). The execution of the program was initiated through the keyboard and was terminated automatically after completion of the specified total task time. A set of nine samples was fabricated for acquiring raw data in Test Procedure 1.

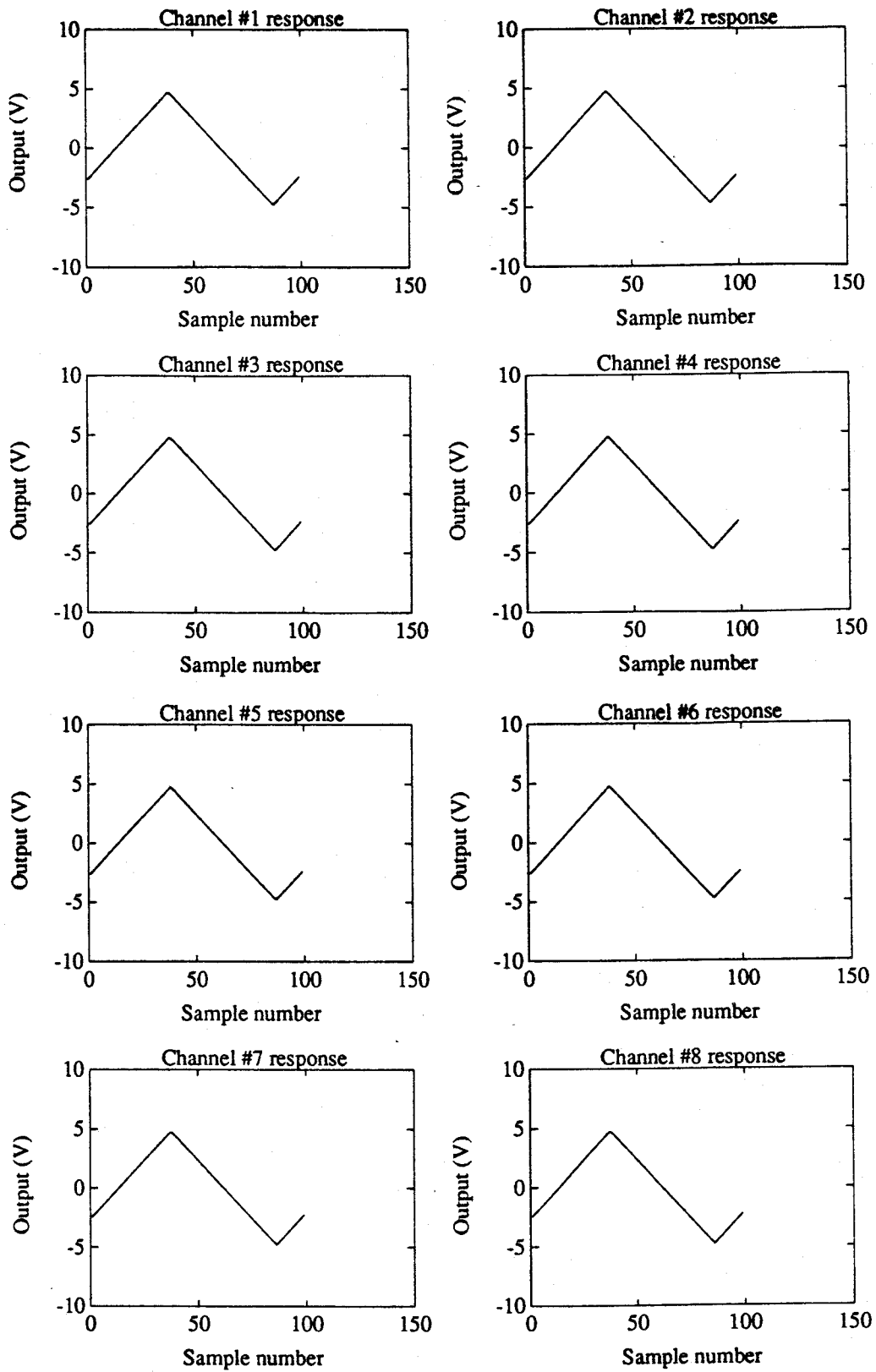


Figure 7.5: The measured output from channels 1 to 8 of the DAS .

7.3.2.2. Selection and specifications of samples

The nine samples used in Test Procedure 1 belonged to one of three shape categories, namely, disc, sphere and cylinder. Four different materials, brass, aluminum, steel and plastic were used in their fabrication. The samples had approximately similar dimensions. The size and weight of the samples were selected so they could be accommodated by the gripper. The mechanical specifications of the nine samples used for testing are listed in Table 7.1.

Table 7.1: Mechanical specifications of the samples used in grasping and releasing tests.

Sample number	Type	Weight, g	diameter, mm	height/width,mm
1	small aluminum disc	22.0	17	20
2	small aluminum cylinder	22.0	17	20
3	aluminum sphere	21.5	24	--
4	large aluminum disc	30.0	24	16
5	large aluminum cylinder	30.0	24	16
6	large brass disc	58.5	24	12
7	heavy steel sphere	80.2	27	
8	heavy steel cylinder	57.0	24	15
9	light plastic sphere	7.3	25	--

7.3.2.3. Definition of task

The validation of the task oriented procedure involved the determination of the correctness of task status decisions obtained from the TSI expert system during the performance of a task. In the Test Procedure 1, a task was defined as the grasping or releasing of one of the selected nine sample objects using the prototype gripper system. A grasping type task commenced when the gripper motor was started to activate the fingers to close on the sample suspended between the parallel jaws. It ended when the limit switch operated causing the the jaw movement to stop. A releasing task commenced when a release command was given to the gripper motors and ended when the sample was fully released and fell free under the force of gravity. The force signals acquired during the

grasping and releasing operations of the gripper constituted the dynamic grasping and releasing forces.

7.3.2.4. Task time and sampling rate selection

In this procedure, the time to perform the complete task was chosen based on the following criterion. The real time data which could be stored for each run of the test was limited by the buffer capacity, 64 Kbytes, allowed by the VAXlab software package. Therefore, a maximum of 4000 values of forces per sensor could be measured and stored. To complete the grasping or releasing operation of a sample at the selected gripper speed, a mean value of the actual time required was 4 s. This was determined from a number of repeated trials of grasping and releasing experiments performed using all the selected samples. Therefore, the maximum sampling rate for data acquisition was limited to 1 KHz for acquiring complete task data for grasping and releasing operations. For performing a combined grasping followed by releasing operation, a total task time of 8 s was allowed. Therefore, the sampling rate for these tests was chosen to be 500 Hz.

7.3.3. Artificial slip and the Test procedure 2

An artificial slip was defined as the slippage occurring at a sensing site due to the sliding motion of a selected sample with respect to the sensors. Test Procedure 2 was designed to perform artificial slip tests using two selected samples. The task in this case was defined as the sliding motion of a sample object on the surface of a horizontal finger pad. The sample moved with a uniform velocity and travelled the full length of the pad. To obtain raw force data during an artificial slip, separate hardware was designed and built.

The arrangement consisted of a robot finger mounted horizontally on a platform with eight tactile sensors mounted on the surface of the finger. The transducer, flexible backing and other mechanical components used for the tactile sensors were the same ones which were used in the prototype gripper system. A set of three new samples were built by attaching light aluminum plates to the plane surfaces of three discs. The plate was equipped with a lead screw as shown in in Figure 7.6.

This arrangement facilitated mounting of weights on the samples in order to apply different forces while the sample moved over the sensors. In order to move the sample over the sensors, a string was attached to the sample. The string could be pulled horizontally by hanging weights at the other end. The arrangement used is shown in Figure 7.7.

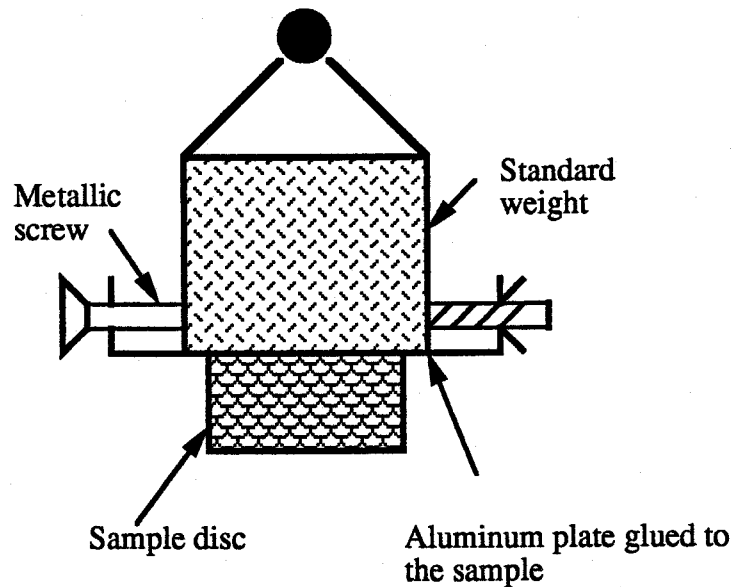


Figure 7.6: A typical sample built for the artificial slip tests .

7.3.4. Implementation of the two test procedures

The raw data required for the performance validation were obtained by implementing the two test procedures. For the purposes of analyzing the results, the data obtained using Test Procedure 1 were divided into three categories. The data from the slip tests obtained using Test Procedure 2 were designated as the fourth category. The implementation procedures used in each of the four categories, and the analysis of the results obtained from them are described in the following section.

7.3.4.1. Category 1: Independent grasping followed by releasing test

In this category, all the samples listed in Table 7.1 were used to obtain dynamic force data using Test Procedure 1. The forces measured by all the eight sensors of the prototype system were acquired while grasping the sample. The task lasted for a time duration of 4 s. The forces measured by the sensors were first stored in the buffer and later separated into eight individual arrays. The sensor outputs were plotted on a graphics terminal and the trends of the raw force data were observed to confirm whether the nature of the task had been indicated by the sensor outputs. After confirming the validity of the raw data in this manner, the sensor outputs were stored in designated files before conducting the next test, which was to perform a task of releasing the held sample.

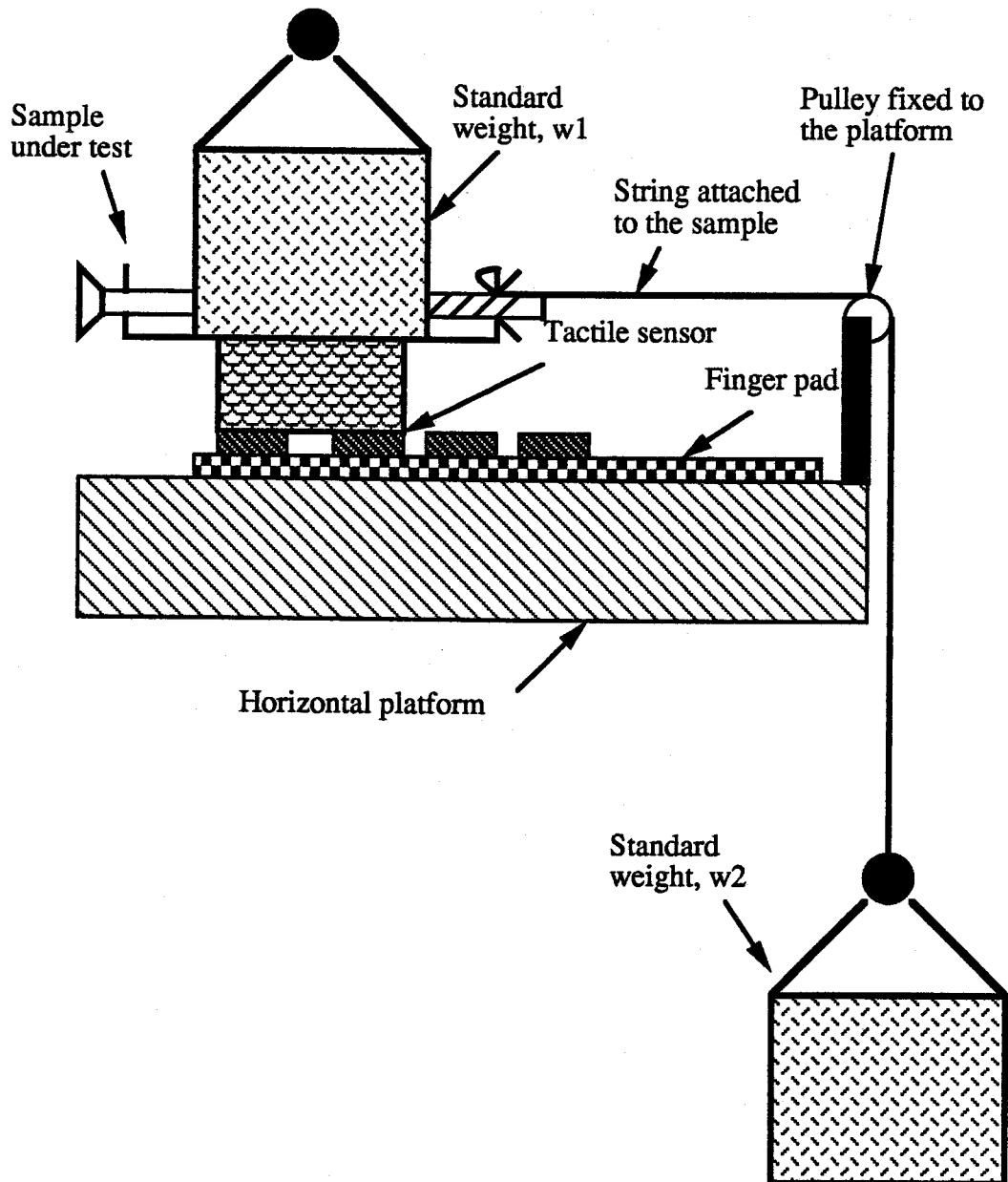


Figure 7.7: Test set up used to perform artificial slip tests .

To perform releasing of the sample, the vertical support was released from the vice so that the object was held freely by the gripper jaws. The releasing operation commenced when the gripper motor was commanded to operate in a reverse direction and the data acquisition program was directed to acquire data as the sample was released. The releasing continued for a period of 4 s. As in the previous case, the raw data were validated by visually observing the sensor outputs before storing them in files. These tests were designated as the independent grasping and releasing tests because the dynamic force data were obtained using independent runs of the data acquisition program at the maximum allowed sampling rate of 1 KHz.

7.3.4.2. Results from test Category 1

Two types of plots were obtained from the raw data. The first type plotted the digitized sensor output from each of the eight sensors as a function of task time. The task time was evaluated from the sampling time information. For each channel, at a sampling frequency of 1 KHz, each data point was assumed to represent the force at the sampling instant (ignoring the delay of 6.4 μ s between samples from each channel). The task time was plotted on the abscissa and the measured value of output from each sensor, as stored by the DAS, was plotted on the Y-axis. In the second type of plot representing the raw data, the four sensor outputs from the left finger and the right finger of the gripper were separately grouped. The grouped raw data were plotted as a function of task time in the form of a mesh plot. Each sensor output was identified in the mesh which had a common time axis for all sensors.

As an example, the raw data plots obtained from category 1 tests using sample 2 (which is the small aluminum cylinder), is shown in Figure 7.8. Both the grasping and releasing curves are shown in the same plot in Figure 7.8 so that the trends in each case can be observed and compared. These plots indicate the grasping and releasing task trends in each case. Some sensors were not contacted during the task and hence did not show significant force variations.

The raw data were stored and then used in Interface Program II to determine the decision parameters and the task status. The typical specifications of one set of parameters entered through the keyboard to process the sample 2 grasping data using Interface Program II were:

1. File name: s21g.dat,
2. Type of data: 1,
3. Number of data points per block: 100, and
4. Beginning block number: 1.

The program was executed to determine the task status parameters and displayed them on the terminal screen. The status parameters were obtained from the decision parameters,

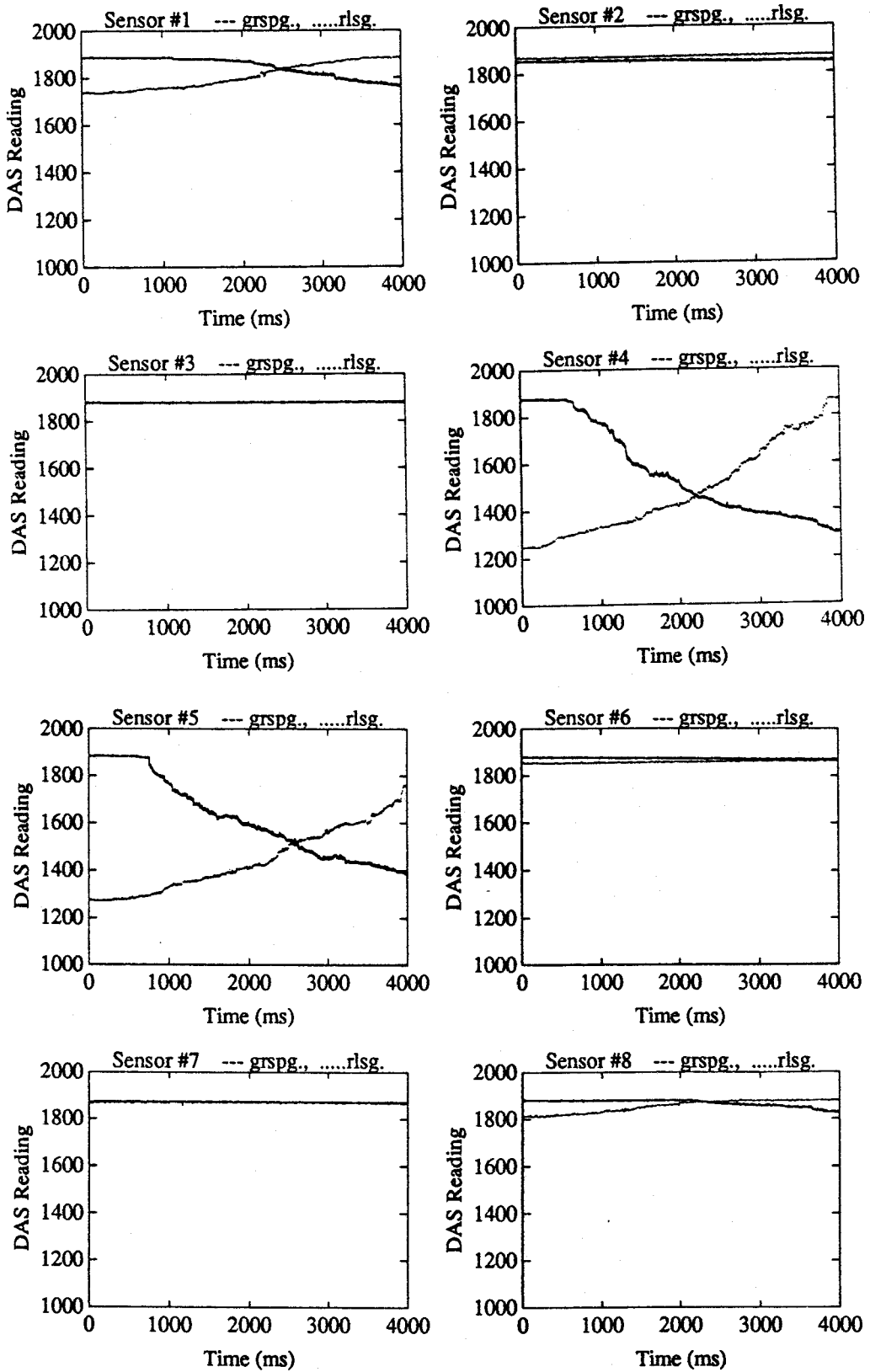


Figure 7.8: Raw force data measured by the tactile sensors during independent grasping and releasing operations performed on sample 2 .

which in turn were obtained from the tactile image formed from each block of data. To confirm the correctness of the decision parameters, these were also displayed in the form of intermediate results. The decision parameters and the cumulated primitive value of gripper forces were determined from the same raw data. Curves were plotted to show the variation of the cumulated grasped and released levels and the cumulated force primitive values as a function of task times. These are shown in Figure 7.9.

The transitional uncertainties are clearly evident in the cumulated primitive values obtained from both grasping and releasing data. The cumulated primitive values represented a measure of total gripper force during the task and their variation with task time are shown in Figure 7.9(a). The curves for both grasping and releasing tasks are plotted in the same graph. The trend shown by the two curves indicate that the tactile imaging procedure implemented has retained most of the dynamic information contained in the raw data. The presence of the transitional uncertainties in the two curves justify the necessity for a decision filter. The cumulated grasped levels and cumulated released levels, determined after partitioning the raw data obtained during grasping and releasing, are shown plotted as a function of task time in Figure 7.9(b). The decision filter outputs obtained in these two graphs could be contrasted with the corresponding variation of total gripper force shown in Figure 7.9(a), to observe the effectiveness of the decision filter in reducing the noise and the transitional uncertainties. It can be seen in Figure 7.9(a), that the transitional uncertainties in the case of releasing data are lower than those encountered during grasping. This occurred because of the compliant rubber material placed over the FSR elements. During grasping, the sample was compressed by the gripper fingers. The elasticity of the rubber causes reaction forces, which result in a negative transition to follow a positive transition. The large transitional uncertainties observed in the total gripper force variation, during releasing in the initial part of the task, and the same effect observed during the later part of a grasping task, justifies this inference. Further, it can be seen from Figure 7.9(b), that in the case of releasing, the decision parameter released level may be directly interpreted to obtain the task status while in the case of grasping the parameter grasped level alone will be inadequate. Moreover, during the course of an operation, the future behaviour of the decision parameter grasped level or released level will be difficult to predict. This factor necessitated the development of the TSI expert system to interpret all the selected seven decision parameters to obtain task status decisions valid for both grasping and releasing tasks.

To investigate the performance of the TSI expert system Interface Program II was executed in two separate sessions using the grasping and releasing data pertaining to sample 2. A copy of the output messages that appeared on the terminal display was directed to file. The task status indications at the end of every data block consisting of 100 points of data per sensor, were compiled manually from the stored results. A summary of the resulting task status obtained by using the grasping data of sample 2 is shown in Table 7.2.

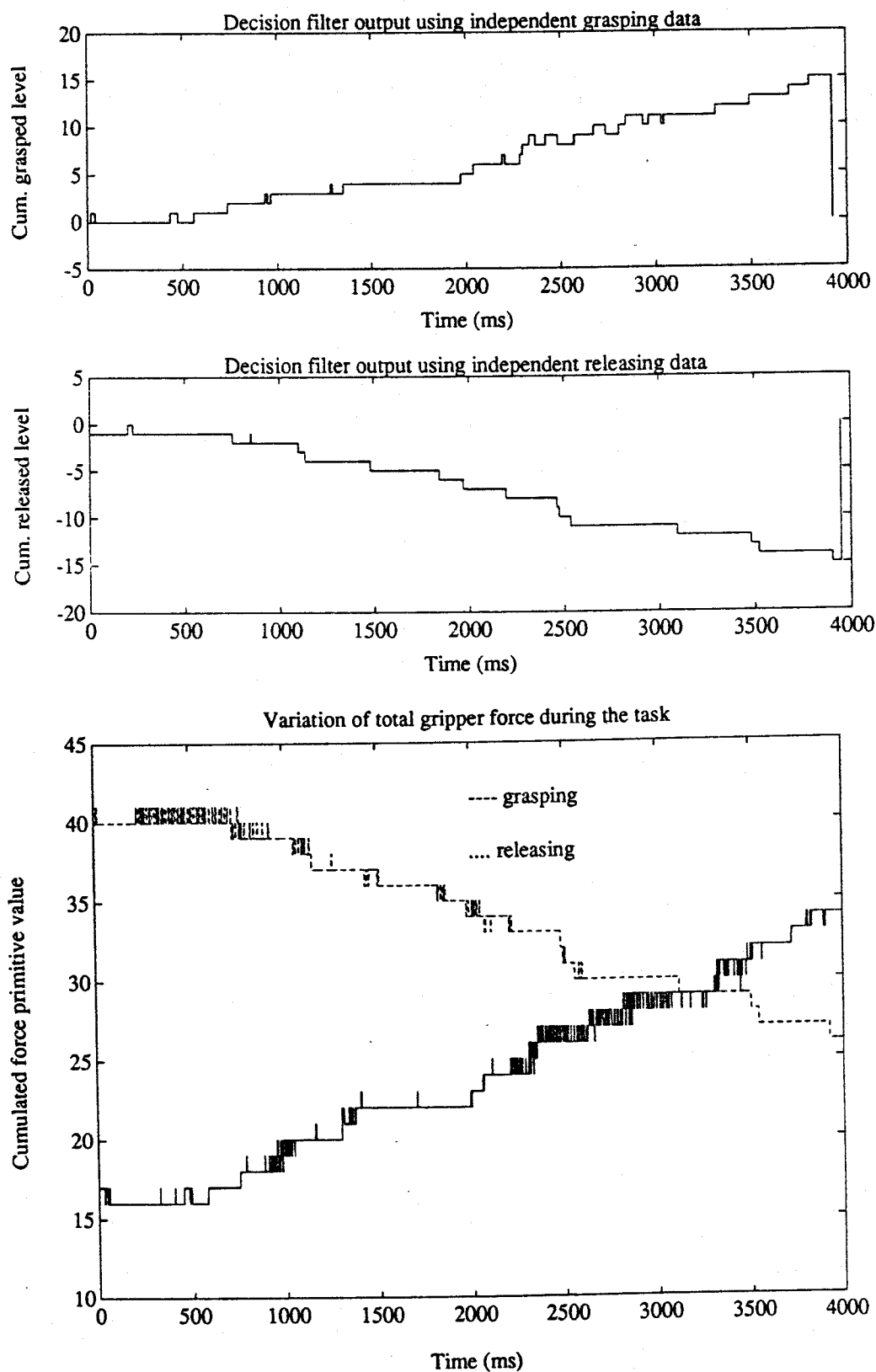


Figure 7.9: Cumulated grasped levels and primitive force variations from grasping and releasing data of sample 2 .

Table 7.2: A summary of the task status parameters obtained from the TSI expert system using sample 2 grasping data .

Block no.	Unchanged state	Grasping level	Releasing level	Grasping con. level	Releasing con. level	Dynamic displacement	Static displacement	Decision correct ?
1		1	1	3	3	No	Nodir	Yes
2	y	0	0	0	0	No	Nodir	Yes
3	y	0	0	0	0	No	Nodir	Yes
4		0	1	0	3	No	Nodir	No
5		1	1	3	3	No	Nodir	Yes
6		1	0	3	0	No	Nodir	Yes
7	y	0	0	0	0	No	Nodir	Yes
8		1	0	6.25	0	No	Nodir	Yes
9		0	1	0	3	No	Nodir	No
10		2	2	19	19	West	West	Yes
11		1	0	3	0	No	Nodir	Yes
12		0	1	0	3	No	Nodir	No
13	y	0	0	0	0	No	Nodir	Yes
14		1	1	3	3	No	Nodir	Yes
15	y	0	0	0	0	No	Nodir	Yes
16	y	0	0	0	0	No	Nodir	Yes
17	y	0	0	0	0	No	Nodir	Yes
18	y	0	0	0	0	No	Nodir	Yes
19	y	0	0	0	0	No	Nodir	Yes
20	y	0	0	0	0	No	Nodir	Yes
21		1	0	3	0	No	Nodir	Yes
22	y	0	0	0	0	No	Nodir	Yes
23		1	1	3	3	No	Nodir	Yes
24		3	1	28.5	6.25	South	Nodir	Yes
25		1	1	3	3	No	Nodir	Yes
26		1	1	3	3	No	Nodir	Yes
27		2	1	12.5	6.25	West	West	Yes
28		1	1	3	3	No	Nodir	Yes
29		1	0	6.25	0	South	Nodir	Yes
30		1	1	3	3	No	Nodir	Yes
31		2	1	6	3	No	Nodir	Yes
32		1	0	3	0	No	Nodir	Yes
33		1	0	3	0	No	Nodir	Yes
34		1	1	9.5	9.5	North	Nodir	Yes
35		1	0	9.5	0	East	Nodir	Yes
36		1	0	6.25	0	No	Nodir	Yes
37	y	0	0	0	0	No	Nodir	Yes
38		1	0	3	0	No	Nodir	Yes
39		1	1	3	3	No	Nodir	Yes
40	y	0	0	0	0	No	Nodir	Yes

Table 7.2 shows the seven task status parameters (six defined earlier in Section 7.4.4.1 and the seventh parameter, unchanged state) obtained from each of the 40 blocks of test data. In addition, Interface Program II also calculated the total time to obtain these seven task status parameters from the raw force data, using the "time" function of the UNIX operating system. The total time determined was used to examine the real time applicability of the procedure and will be discussed in Section 7.4.5.1.

The last column in Table 7.2 gives an indication of the correctness of the task status decision as perceived by a human subject. This decision is based on the following logic: During a grasping type of task, if the status parameters from any block show a non-zero released level and a zero grasped level, then the decision was considered incorrect. This is because during the task the sample object never fell from the gripper during grasping. In a similar manner, during a releasing operation, if the task status parameters showed a non-zero grasped level and a zero released level, then the decision was considered incorrect. Such criteria were applied to the all three categories of tests: category 1, category 2, and category 3. The percentage of correct status decisions during a task was used as a figure of merit of the complete task oriented procedure.

For visual display of the task status parameters, the six task status parameters (defined in Section 7.4.4.1) were divided into 4 force decision parameters and two object displacement parameters. The force decision parameters were the grasping level, the releasing level, and the confidence levels for grasping and releasing. The two object displacement parameters were the static object displacement and the dynamic object displacement. The four force decision parameters, obtained from the grasping test data of sample 2 were plotted in the form of a bar chart as shown in Figure 7.10. In this diagram, the height of the bar indicates the calculated confidence level and the type of fill inside the bar represents the different grasped and released levels. The released levels have been plotted showing the confidence levels on the negative Y-axis. In Figure 7.10 it can be seen that task status decisions from grasping data results in higher grasped levels with higher confidence factors when compared to the released levels and their confidence factors. The dominating task parameters in this case are the grasped level and the confidence factor for the grasped level decisions.

The two object displacement parameters obtained from the grasping data are shown in Figure 7.11. In this figure, the static and dynamic object displacements relative to the gripper fingers, have been plotted as bars. The heights of the bars show the certainty factors associated with the displacement decisions. This was indicated by the expert system which obtained the certainty factor based on the Hypothesize and Test procedure described in Chapter 6. The times at which both static and dynamic displacements were identified agreed with those times when a higher released level with a higher confidence factor (when compared with the corresponding grasped level and its confidence factor)

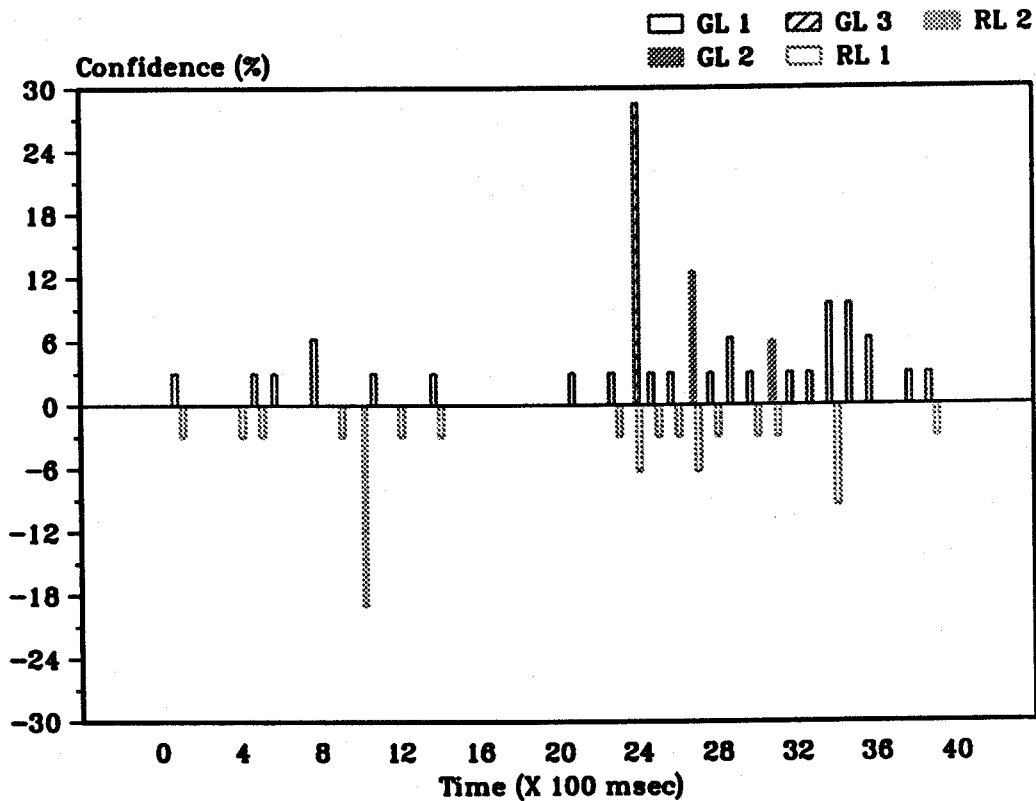


Figure 7.10: The force decision parameters of the task status obtained from the TSI expert system using sample 2 grasping data .

were obtained from the TSI expert system. Therefore, at these task times (i.e. task time =1000 ms, and 2700 ms in Figures 7.10 and 7.11) it is likely that the sample might have experienced temporary slip. This demonstrated that it was possible to identify slip using the force decision and displacement decision parameters of the task status. The dynamic displacements identified at other times during the task may have occurred because of lateral transient movements of the sample. This effect could be seen from the behaviour of the force decision parameters at the corresponding times at which both the grasped level and released level have been assigned a value of unity with nearly equal confidence in the two decisions.

A summary of the task status parameters obtained from the releasing data of sample 2 is shown Table 7.3. The corresponding bar charts of the force decision and the object displacement parameters obtained using the releasing data were plotted in the manner

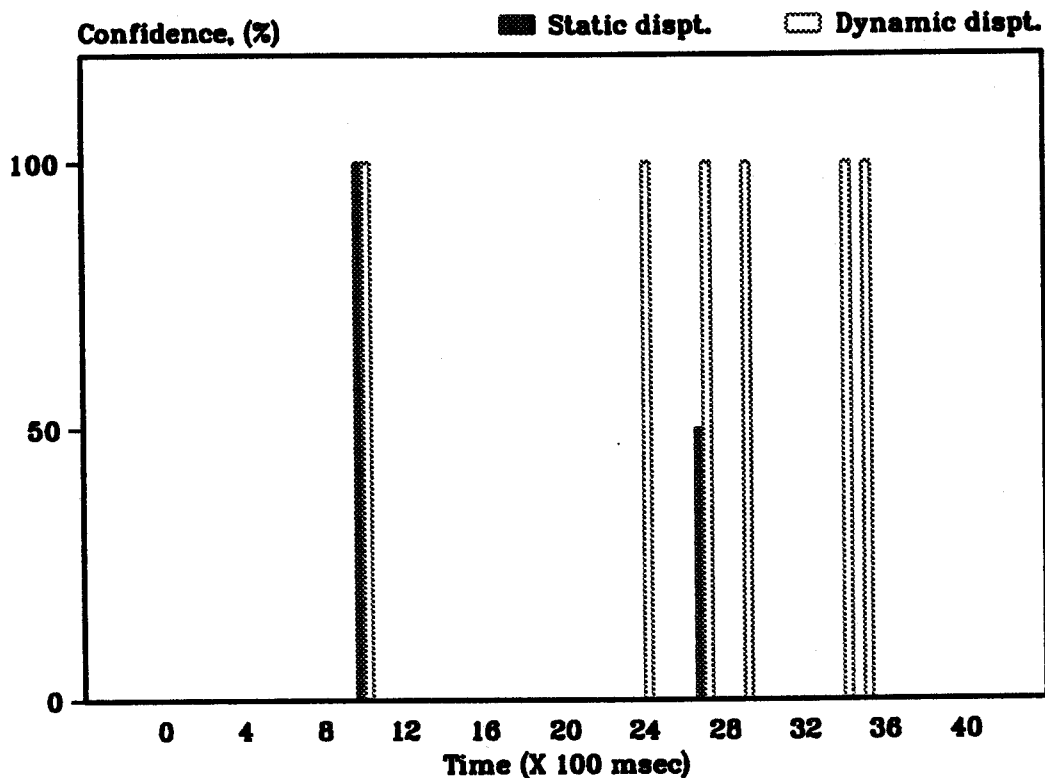


Figure 7.11: The object displacement parameters of the task status obtained from the TSI expert system using sample 2 grasping data.

described above and are shown in Figures 7.12 and 7.13 respectively. If the above mentioned logic is applied to identify slip, it can be seen from these figures that the sample has experienced a definite slip at a task time = 900 ms. Since releasing of the object did not involve re-grasping once the sample was released, for task times greater than 900 ms, the grasped level decisions are seen to be far fewer compared to the released level decisions and the confidence for grasping either equal or less than the confidence for releasing.

For each of the eight samples used in Category 1 type of tests, the above procedure was repeated to obtain a validation package consisting of the following graphs plotted as a function of the task time.

1. A plot showing the variation of the raw force data from each of the eight sensors during grasping and releasing of the samples.

Table 7.3: A summary of the task status parameters obtained from the TSI expert system using sample 2 releasing data .

Block no.	Unchanged state	Grasping level	Releasing level	Grasping con. level	Releasing con. level	Dynamic displacement	Static displacement	Decision correct ?
1		0	1	0	3	No	Nodir	Yes
2	y	0	0	0	0	No	Nodir	Yes
3		1	1	3	3	No	Nodir	Yes
4		0	1	0	3	No	Nodir	Yes
5		0	1	0	3	No	Nodir	Yes
6		0	1	0	3	No	Nodir	Yes
7		0	1	0	3	No	Nodir	Yes
8		0	2	0	25	North	Nodir	Yes
9		1	2	6.25	12.5	North	South	Yes
10		0	1	0	3	No	Nodir	Yes
11		1	0	3	0	No	Nodir	No
12		0	1	0	3	No	Nodir	Yes
13		0	1	0	3	No	Nodir	Yes
14	y	0	0	0	0	No	Nodir	Yes
15		1	0	3	0	No	Nodir	No
16		0	1	0	3	No	Nodir	Yes
17	y	0	0	0	0	No	Nodir	Yes
18	y	0	0	0	0	No	Nodir	Yes
19		1	1	3	3	No	Nodir	Yes
20	y	0	0	0	0	No	Nodir	Yes
21		0	1	0	3	No	Nodir	Yes
22	y	0	0	0	0	No	Nodir	Yes
23		0	1	0	3	No	Nodir	Yes
24	y	0	0	0	0	No	Nodir	Yes
25		0	1	0	3	No	Nodir	Yes
26		0	1	0	6.25	No	Nodir	Yes
27	y	0	0	0	0	No	Nodir	Yes
28	y	0	0	0	0	No	Nodir	Yes
29	y	0	0	0	0	No	Nodir	Yes
30	y	0	0	0	0	No	Nodir	Yes
31	y	0	0	0	0	No	Nodir	Yes
32		0	1	0	3	No	Nodir	Yes
33	y	0	0	0	0	No	Nodir	Yes
34	y	0	0	0	0	No	Nodir	Yes
35	y	0	0	0	0	No	Nodir	Yes
36		0	1	0	3	No	Nodir	Yes
37	y	0	0	0	0	No	Nodir	Yes
38	y	0	0	0	0	No	Nodir	Yes
39	y	0	0	0	0	No	Nodir	Yes
40		0	1	0	3	No	Nodir	Yes

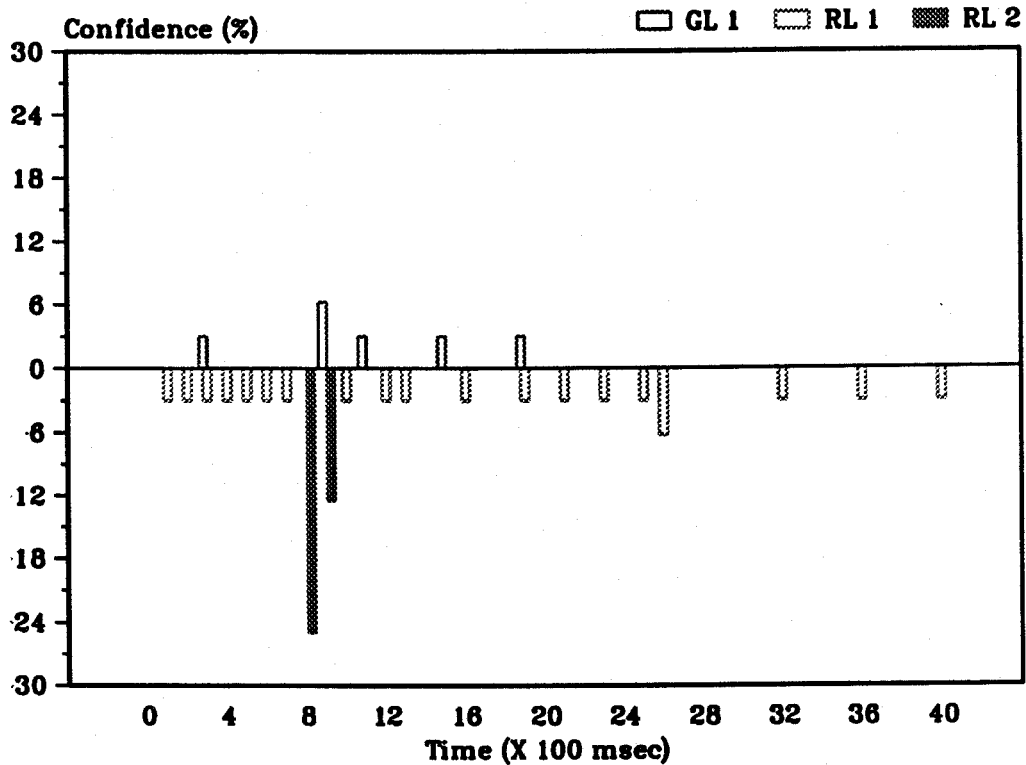


Figure 7.12: The force decision parameters of the task status obtained from the TSI expert system using sample 2 releasing data .

2. Four mesh plots showing the force profile in the left and right jaws of the gripper during grasping and releasing of the samples.
3. Two intermediate result plots showing the variation of cumulated grasped and released levels and cumulated primitive force values obtained using the grasping and releasing sample data.
4. Two result plots showing the four force decision parameters indicated by the TSI expert system plotted in the form of a bar graph using the grasping and releasing sample data.
5. Two result plots showing the object displacement parameters indicated by the TSI expert system plotted in the form of bar graphs using the grasping and releasing sample data.

In addition to the above, two sample performance tables were also obtained using the summary of the task status decisions displayed by Interface Program II. The various

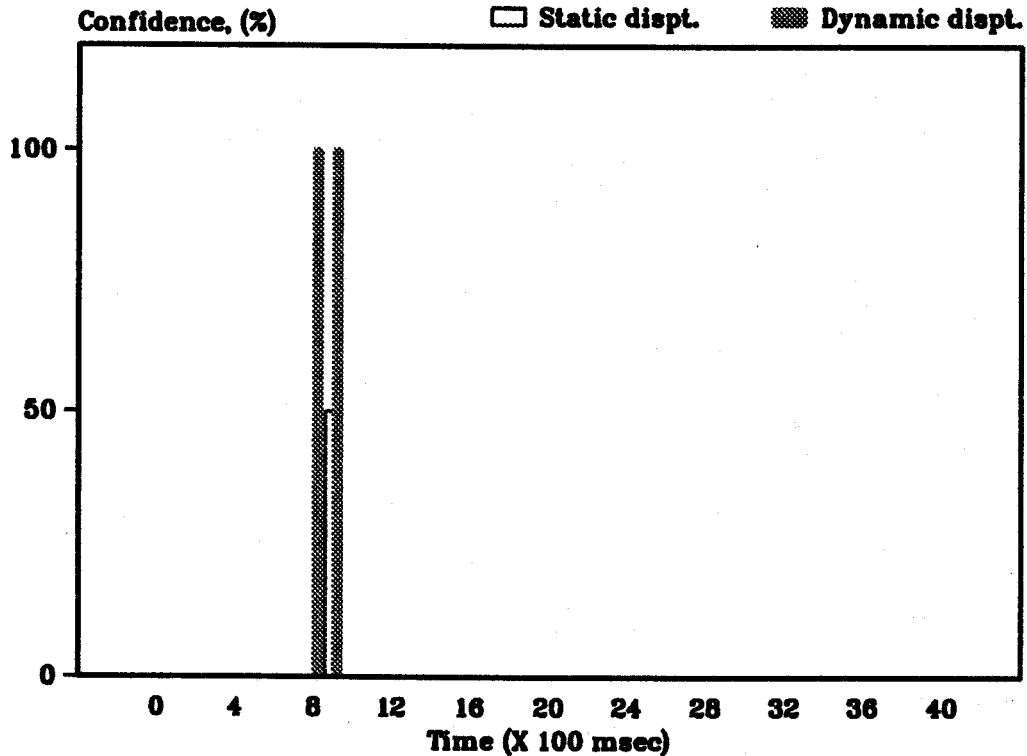


Figure 7.13: The object displacement parameters of the task status obtained from the TSI expert system using sample 2 releasing data .

graphs included in the validation package for sample 1 were depicted as example plots during the description of the development of the individual stages of the integrated procedure in Chapters 3, 4, 5, and 6. The two performance tables obtained using the sample 1 grasping and releasing data were also shown in Chapter 6 where these were used to validate the output of the TSI expert system in the stand-alone mode. Similar task status results were obtained when the sample 1 grasping and releasing data were used in Interface Program II.

The raw force data plots, the intermediate plots, and the force decision plots described in the validation package for samples 5 and 7 are shown in Appendix D. The four performance tables obtained using sample 5 and sample 7 grasping and releasing data are also shown in Appendix D. The three samples, 2, 5, and 7 were chosen arbitrarily to represent the different shapes and materials of the sample objects used in the investigation in Category 1 tests.

7.3.4.3. Category 2: Combined grasping followed by releasing test

In these tests, the grasping and releasing operations were combined in a single test run. Due to the limitations of the buffer capacity discussed earlier, the maximum sampling rate for these tests was limited to 500 Hz. In these tests, the sample was mounted using the vertical fixture and held between the gripper jaws. Data acquisition commenced when the gripper was commanded to close in on the sample. When the sample was held by the gripper with the maximum force allowed by the limit switch, the direction of the gripper motor was reversed. The data acquisition continued without interruption. At the chosen sampling rate of 500 Hz, the data acquisition proceeded for a time period of 8 s. Within this period, the object was fully released. Similar to the category 1 test, the raw data was validated by inspecting the variation of the data from each sensor as a function of the task time. The raw data were subsequently stored.

7.3.4.4. Results from test Category 2

In this category of tests, the same nine samples were used to determine the dynamic forces during a different type of task. The task consisted of a combined grasping followed by releasing operation without stopping the acquisition of the force data. A similar validation package was identified to obtain results from this category of tests. The sampling rate used for these tests was 500 Hz. Therefore, the task time for plotting the various graphs was from 0 to 8 s. A typical validation package for these type of tasks were identified and this consisted of the following components:

1. A plot showing the variation of raw force data from each of the eight sensors during the combined grasping and releasing of the samples.
2. Two mesh plots showing the force profile in the left and right jaws of the gripper during the task.
3. An intermediate result plot showing the variation of cumulated grasped and released levels and cumulated primitive force values obtained using the combined grasping and releasing sample data.
4. A result plot showing the four force decision parameters indicated by the TSI expert system plotted in the form of a bar graph using the combined grasping and releasing sample data.
5. A result plot showing the object displacement parameters indicated by the TSI expert system plotted in the form of bar graphs using the combined grasping and releasing sample data.

The sample performance table consisted of a summary of the TSI expert system displays that were obtained using the force data acquired during the combined task. The input specifications used in Interface Program II were similar to the ones used for category 1 tests. However, in these tests, a block consisting of 100 points of data corresponded to a real time window of 200 ms instead of 100 ms in the earlier case. For all

of the nine samples, the graphs included in the validation package were obtained and the sample performance tables were generated using the results from Interface Program II. A set of validation plots for sample 2 are shown in Figures 7.14, 7.15, 7.16, and 7.17. The raw force data plotted as a function of the task time is shown in Figure 7.14. The plots showing the cumulated grasped and released levels plotted against the task time are shown in Figure 7.15. Figures 7.16 and 7.17 display the task status parameters in the form of bar graphs. It can be seen from Figure 7.14 that the sensor #3, #4, #5 and #8 were actively involved in the task. The raw data obtained from all of them show a pronounced flat region which had occurred almost at the same time. The curves in Figure 7.15 indicate the presence of many transitional uncertainties and noise in the total gripper force as well as in the decision filter output. The inability of the decision filter to remove all noise and uncertainties is evident. The ability of the TSI expert system to interpret even noisy decision parameters is shown by the bar graph in Figure 7.16. The grasping and releasing operation on the sample is truly reflected in the task status parameters pertaining to the force decisions. The noisy nature of the data manifested in the form of a large number of dynamic object displacements shown in Figure 7.17. However, in this case, the sample has experienced slip only once at the point where the static displacement of the object has been identified.

The performance of the integrated scheme has been summarized in the sample 2 performance table shown in Table 7.4. This table lists all the task status parameters and assigns a figure of merit to each set of decisions obtained from each block of force data.

The plots listed in the validation package were obtained for all the nine samples. The results for the sample performance tables were also obtained using Interface Program II. The set of plots included in the validation package for samples 5 and 7 are shown in Appendix E. The corresponding sample performance tables obtained from the combined grasping and releasing data of samples 5 and 7 are also shown in Appendix E.

7.3.4.5. Category 3: Repeatability test

The repeatability tests were aimed at determining the consistency of the raw data as well as the subsequent decisions obtained from them. The repeatability tests consisted of repeated tasks using the same sample for a fixed number of trials. Each of the nine samples were independently grasped and released five times. During each trial, the sample was manually repositioned before actuating the gripper and obtaining the forces during the task. The raw force data were acquired during each trial.

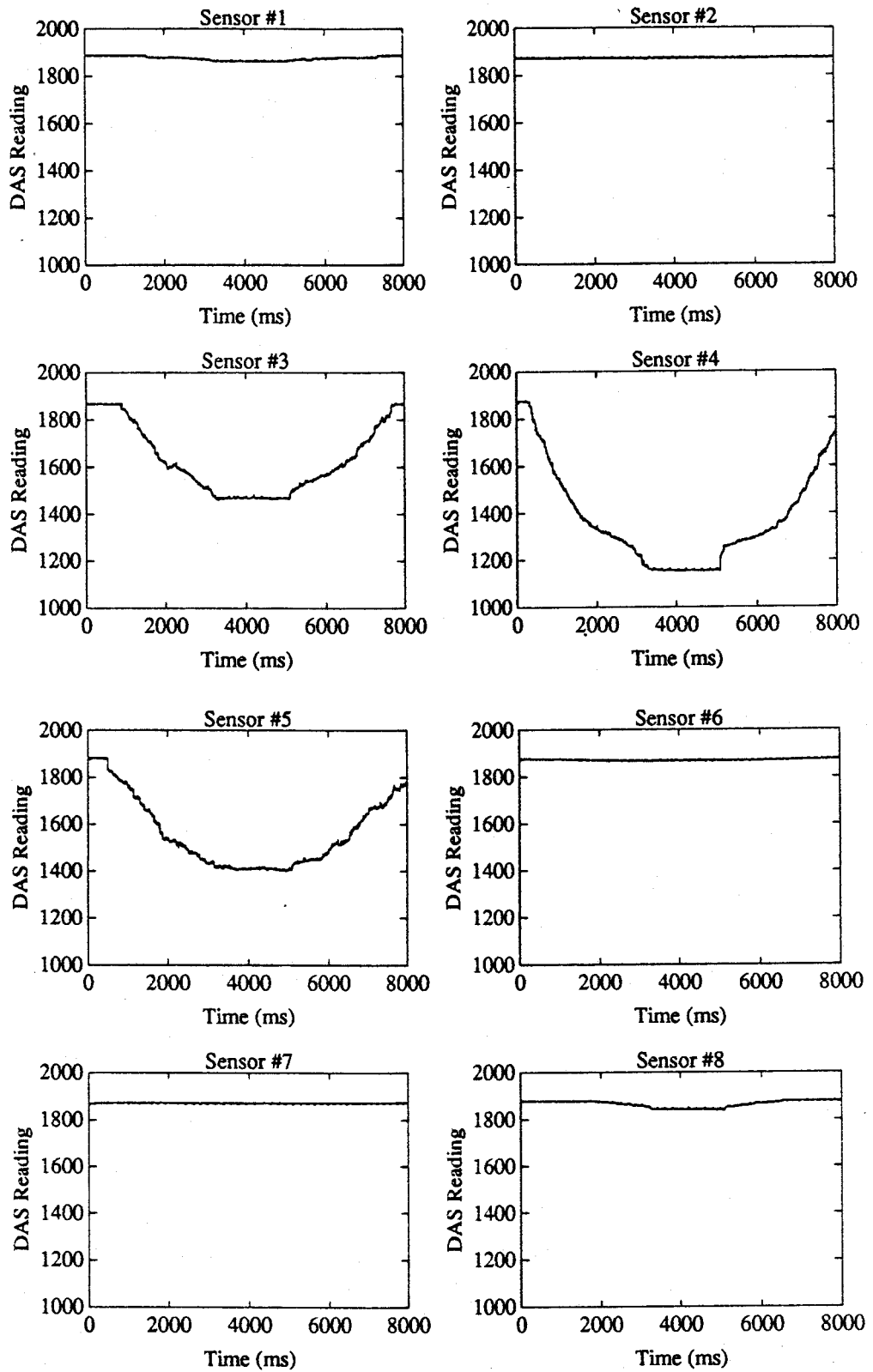


Figure 7.14: Raw force data measured by the tactile sensors during the combined grasping and releasing operation performed on sample 2 .

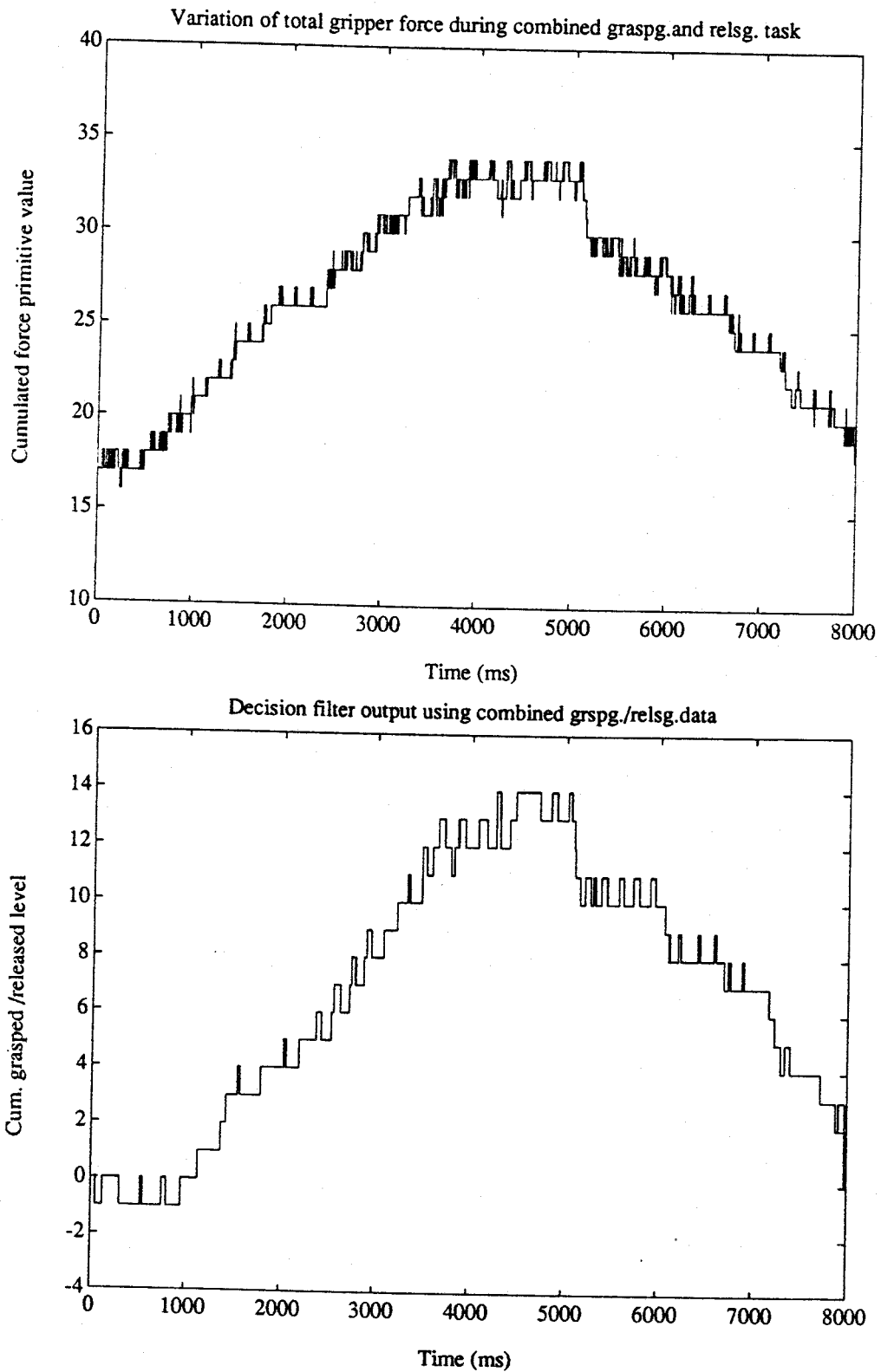


Figure 7.15: Cumulated grasped levels and primitive force variations from the combined grasping and releasing data of sample 2 .

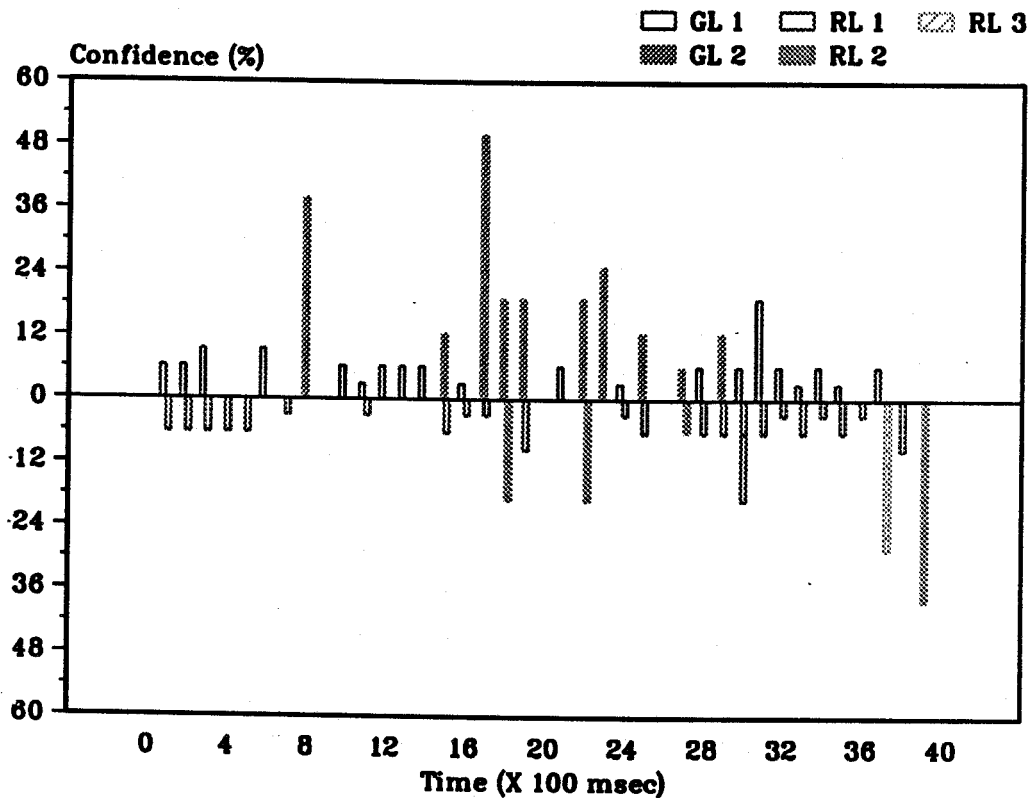


Figure 7.16: The force decision parameters of the task status obtained from the TSI expert system using the combined grasping and releasing data of sample 2 .

7.3.4.6. Results from test Category 3

To interpret and discuss results from this test category, validation packages consisting of the following plots were obtained for three of the nine samples.

1. A plot showing the variation of raw force data from each of the eight sensors during independent grasping and releasing of the samples.
2. Two result plots showing the four force decision parameters indicated by the TSI expert system drawn in the form of a bar graph using the independent grasping and releasing sample data.
3. Two result plots showing the object displacement parameters indicated by the TSI expert system drawn in the form of bar graphs using the independent grasping and releasing sample data.

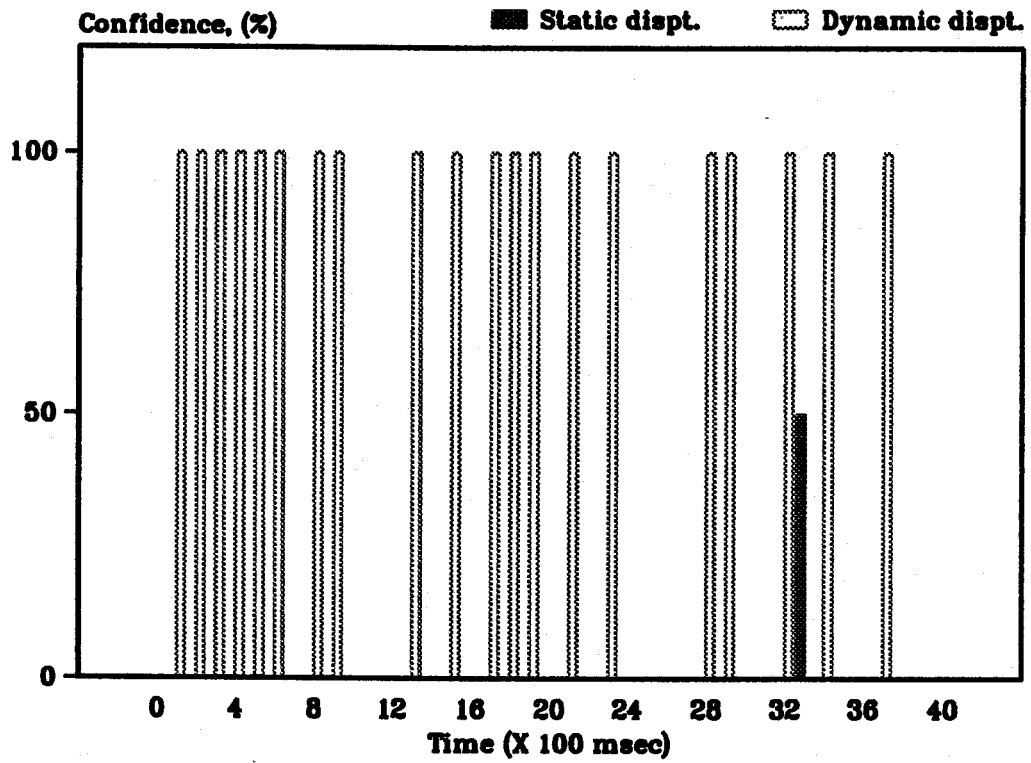


Figure 7.17: The object displacement parameters of the task status obtained from the TSI expert system using the combined grasping and releasing data of sample 2 .

Table 7.4: A summary of the task status parameters obtained from the TSI expert system using sample 2 combined grasping and releasing data .

Block no.	Unchanged state	Grasping level	Releasing level	Grasping con. level	Releasing con. level	Dynamic displacement	Static displacement	Decision correct ?
1		1	1	6.25	6.25	Northeast	Nodir	Yes
2		1	1	6.25	6.25	Southwest	Nodir	Yes
3		1	1	9.5	6.25	West	Nodir	Yes
4		0	1	0	6.25	Southwest	Nodir	Yes
5		0	1	0	6.25	West	Nodir	Yes
6		1	0	9.5	0	Southwest	Nodir	Yes
7		0	1	0	3	No	Nodir	Yes
8		2	0	38	0	West	Nodir	Yes
9	y	0	0	0	0	Northeast	Nodir	Yes
10		1	0	6.25	0	No	Nodir	Yes
11		1	1	3	3	No	Nodir	Yes
12		1	0	6.25	0	No	Nodir	Yes
13		1	1	6.25	6.25	West	Nodir	Yes
14		1	0	6.25	0	No	Nodir	Yes
15		2	1	12.5	3	Southwest	Nodir	Yes
16		1	1	3	3	No	Nodir	Yes
17		2	0	50	0	South	Nodir	Yes
18		2	2	19	19	West	Nodir	Yes
19		2	1	19	9.5	North	Nodir	Yes
20	y	0	0	0	0	No	Nodir	No
21		1	0	6.25	0	West	Nodir	Yes
22		2	2	19	19	No	Nodir	Yes
23		2	0	25	0	West	Nodir	Yes
24		1	1	3	3	No	Nodir	Yes
25		2	1	12.5	6.25	No	Nodir	Yes
26	y	0	0	0	0	No	Nodir	No
27		2	2	6	6	No	Nodir	Yes
28		1	1	6.25	6.25	Northeast	Nodir	Yes
29		1	1	19	19	Southwest	Nodir	Yes
30		1	1	6.25	6.25	No	Nodir	Yes
31		1	1	3	3	No	East	Yes
32		1	1	6.25	6.25	East	Nodir	Yes
33		1	1	3	3	No	Nodir	Yes
34		1	1	6.25	6.25	East	Nodir	Yes
35		1	1	3	3	No	Nodir	Yes
36		0	1	0	6.25	No	Nodir	Yes
37		1	3	6.25	28.5	Northeast	Nodir	Yes
38		0	1	0	9.5	No	Nodir	Yes
39		0	2	0	38	No	Nodir	Yes
40		0	1	0	9.5	No	Nodir	Yes

The sample performance tables for this category summarize the task status decisions obtained from the results displayed by the TSI expert system using the grasping and releasing sample data. Some of the validation plots obtained from four trials of independent grasping and releasing operations performed using sample 1 are given in Appendix F. For each trial, the raw force data plots and the force decision plots are shown. Appendix F also shows the corresponding performance tables obtained from the four trials of grasping and releasing of sample 1.

7.3.4.7. Category 4: Artificial slip test

In the slip test, the objective was to determine whether it is possible identify the occurrence of slip from the task status parameters. The sample object was placed on top of the robot finger pad placed horizontally on a X-Y translation table. A selected weight, w_1 , was placed on top of the aluminum plate and second weight, w_2 , was attached to the free end of the string. Before commencing the task, the weight, w_2 , was supported so that the sample remained at one end of the finger pad. This support was released in synchronism with the initiation of the data acquisition process which was signalled by operating a key of the computer keyboard. The task data for a total period of 4 s were acquired from all the eight sensors. The raw data was validated by observing the plots of the measured sensor forces as a function of the task time on a computer graphic screen. When the sample passed over a sensor at a slow speed, a dip could be seen on the the measured sensor force. A number of tests were conducted using different weights for w_1 , and w_2 , using the two samples prepared for this test.

7.3.4.8. Results from test Category 4

A set of two selected samples was tested in this category using different weights for w_1 and w_2 . The combinations of weights, w_1 , and w_2 were chosen such that the sample slid slowly enough to enable the acquisition system to record a change in the forces. From an observation of the raw data, which was plotted on a terminal screen after the every test was completed, a set of 5 tests involving the two samples were selected for the purposes of performance evaluation. Table 7.5 shows the details of the samples and the different weights, w_1 and w_2 , chosen for the eight tests.

For each of these five tests, a validation package was identified. A typical validation package for these types of tasks consisted of the following components:

1. A plot showing the variation of raw force data from each of the eight sensors during each simulated slip test.
2. An intermediate result plot showing the variation of cumulated grasped and released levels and cumulated primitive force values obtained using the simulated slip test data.
3. A result plot showing the four force decision parameters indicated by the

Table 7.5: Summary of parameters used in test category 4.

Test number	Sample type	Weight, w1, on the sample	Weight, w2, attached to the string
1	small aluminum disc	500 g	300 g
2	small aluminum disc	1000 g	500 g
3	large aluminum disc	500 g	200 g
4	large aluminum disc	1000 g	500 g
5	small aluminum disc	500 g	200 g

TSI expert system drawn in the form of a bar graph using the force data from the slip test.

4. A result plot showing the object displacement parameters indicated by the TSI expert system drawn in the form of bar graphs using the force data from the slip test

The sample performance table for these cases consisted of a summary of the TSI expert system displays obtained using the force data acquired during the slip test. The input specifications used in Interface Program II were similar to the ones used for the test category 1. In these tests, a block consisting of 100 points of data corresponded to a real time window of 100 ms. For all the eight test cases, the graphs defined in the validation package were obtained and the sample performance table was generated using the results from Interface Program II. A set of validation plots obtained from the data from test 1 are shown in Figures 7.18, 7.19 and 7.20. The raw force data plotted as a function of the task time is shown in Figure 7.18. The motion of the sample over the sensors was captured by the measured forces which are shown in the form of a dip in the force value in Figure 7.18 on sensors at different times. The plots showing the cumulated grasped and released levels plotted against the task time are shown in Figure 7.19. Since the variation of the total force on all the sensors remained constant for most part of the test except toward the end of the task, the corresponding plots of cumulated primitive value and the decision filter output show such a characteristic in Figure 7.19. Figure 7.20 shows the force decision parameters obtained by executing Interface Program II using the slip test 1 data. The grasped and released levels (mostly 0) shown in this figure emphasizes that if the total

force on the tactile sensors were to remain constant, then the task oriented procedure will not yield any task status decisions. The object displacement parameters obtained from this test did not indicate either a static or a dynamic displacement anytime during the task. This was considered reasonable because in the absence of total sensing system force variations the procedure will not be able to identify any real transitions.

The performance of Interface Program II when used with the data from artificial slip test 1 has been summarized in the test 1 performance table shown in Table 7.6. This table lists all the task status parameters and assigns a figure of merit to each set of decisions obtained from each block of force data.

The plots listed in the validation package were obtained using the data from the eight artificial slip tests listed in Table 7.5. The results for the eight test performance tables were also obtained using Interface Program II. The raw force plots and the force decision plots described in the validation package for the artificial slip tests 2,3, and 4 are given in Appendix G. The corresponding sample performance tables obtained from the TSI expert system results which used data from tests 2, 3, and 4 are also given in Appendix G.

7.3.5. Performance of the task oriented procedure

The four specific categories of tests were selected in order to substantiate a number of inferences about the complete task oriented tactile sensing procedure.

The raw data plots from the first three categories of tests clearly show the grasping and releasing trends observed during the task. This demonstrates the effectiveness of the tactile sensing and the data acquisition hardware of the prototype gripper system to obtain data which contain the important dynamic characteristics of a task. The raw data plots have also indicated in test category 1 the variations in grasping and releasing forces that were recorded by the same sensors. This emphasizes the fact that using non uniform sensors it is possible to characterize the dynamic force data as long as the relative values of forces at different times are used for tactile imaging. This tends to validate the technique of tactile imaging used in the task oriented procedure.

In the raw data from the category 2 tests, it was seen that at the time of switching from a grasping operation to a releasing operation, the curves become horizontal. The switching and other noise do not corrupt the data, probably because of the flexible backing used in the tactile sensors. The behaviour of the raw forces shows good repeatability and stable, primarily monotonic responses, as evident from the raw plots of the repeatability tests. The raw data plots from the artificial slip tests indicate a dip in the force measured by some of the sensors when the sample passes over it. The depth of the

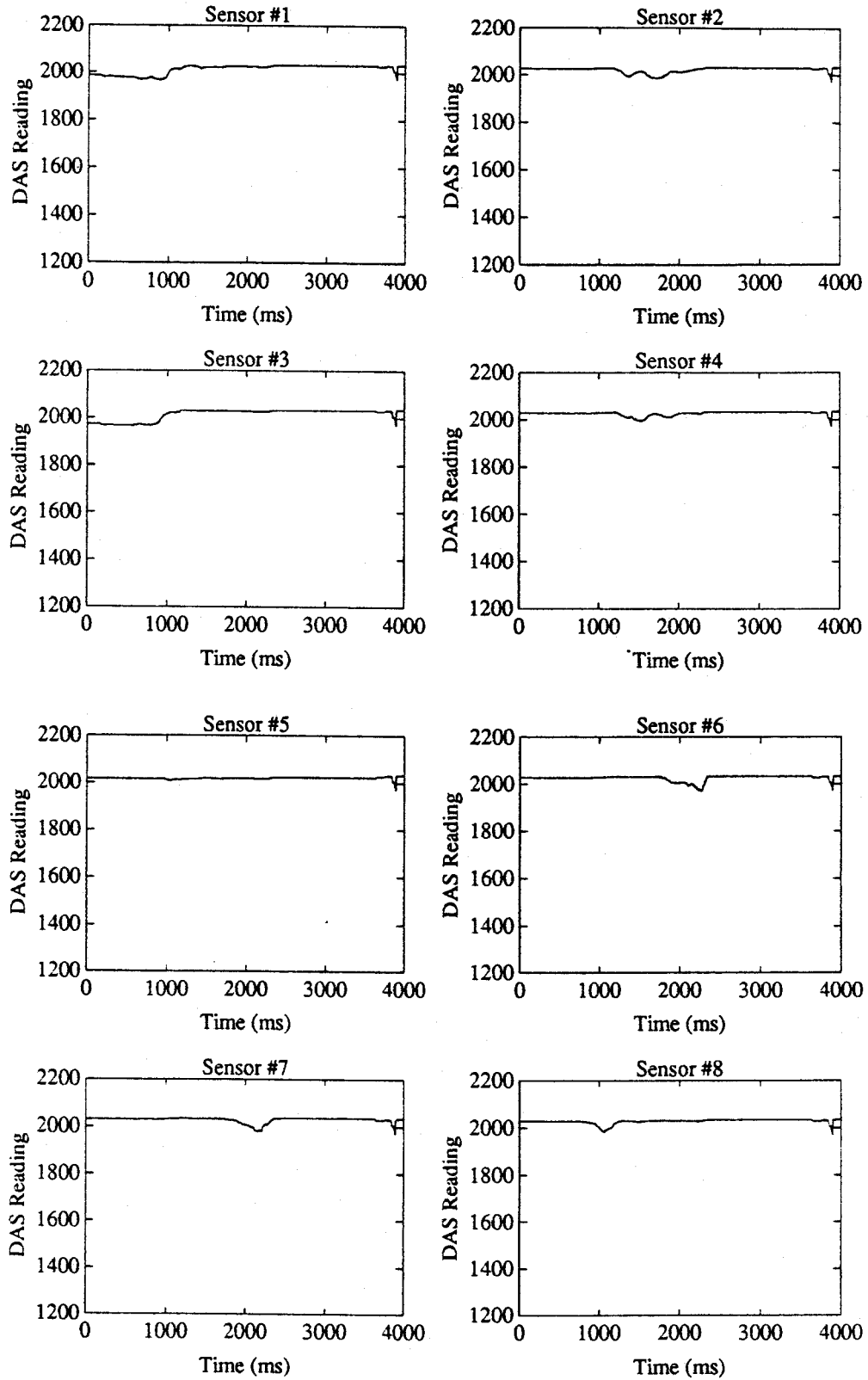


Figure 7.18: Raw force data measured by the tactile sensors during the artificial slip test 1 .

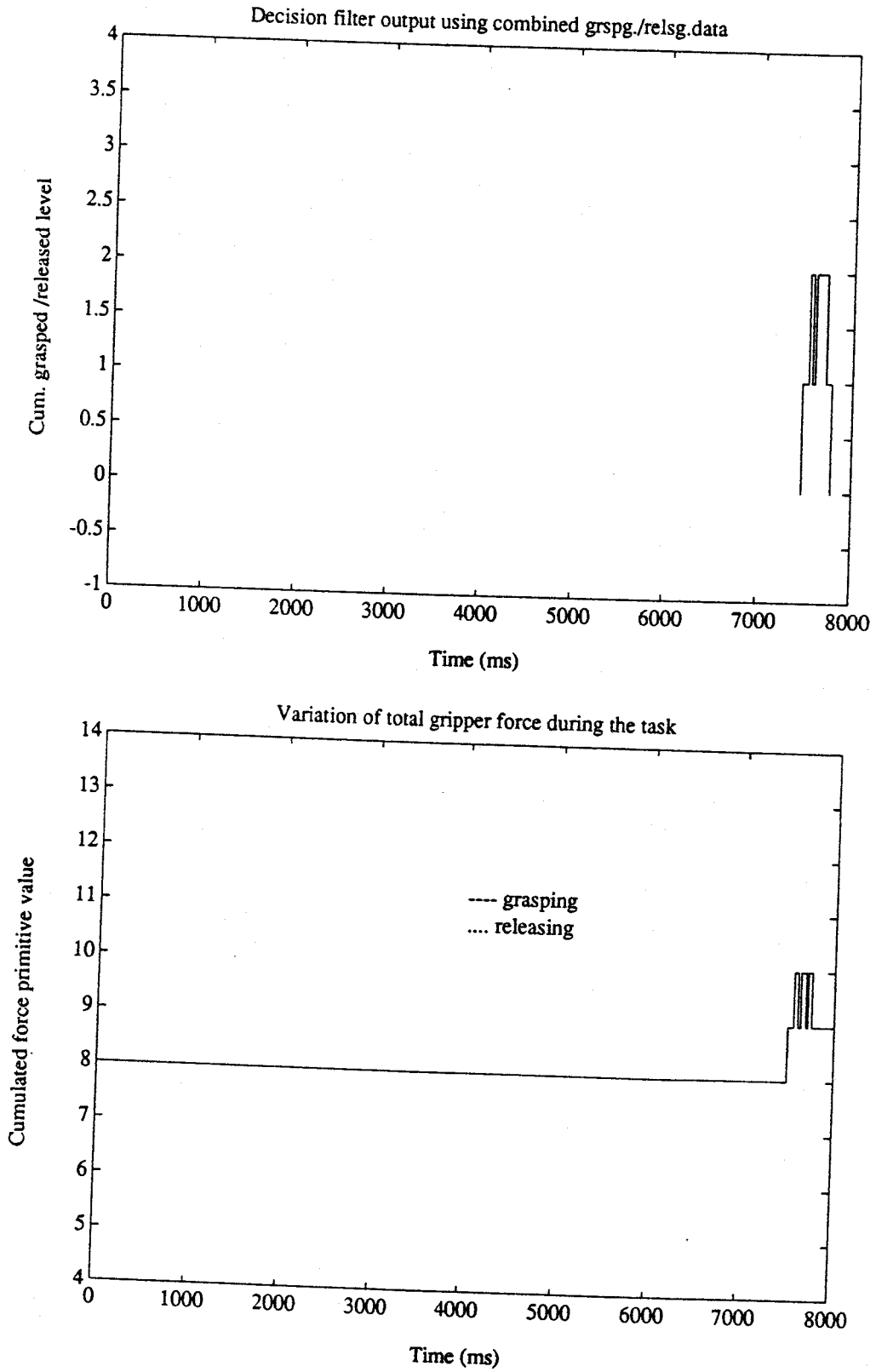


Figure 7.19: Cumulated grasped levels and primitive force variations obtained from the artificial slip test 1 data •

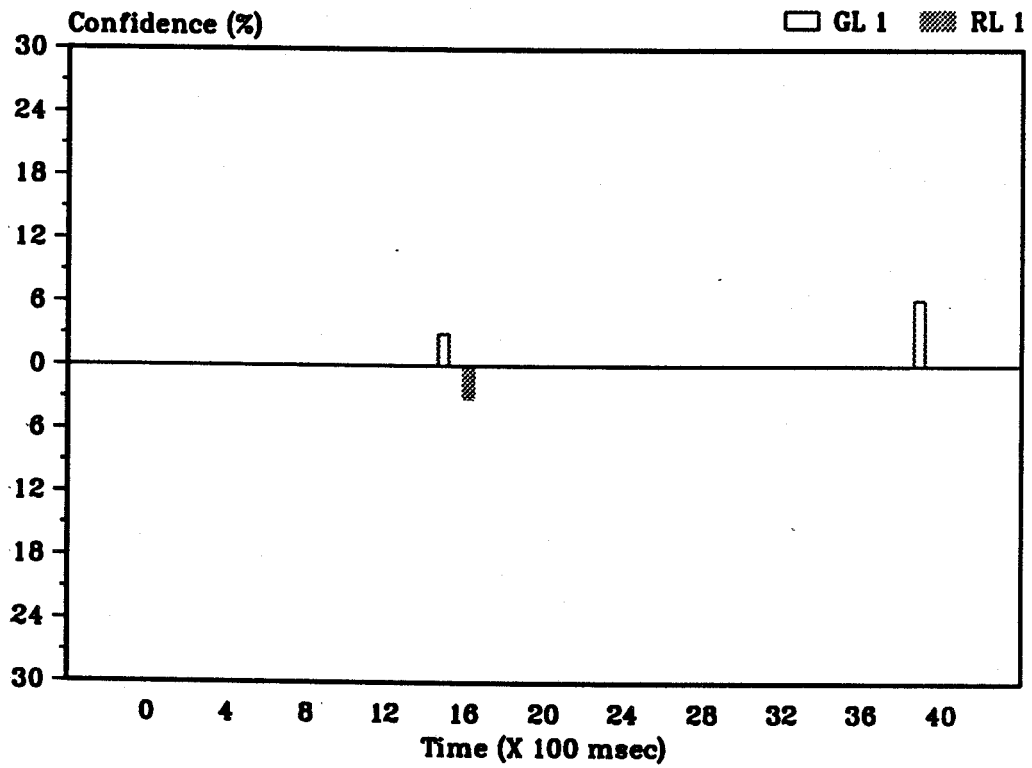


Figure 7.20: The force decision parameters of the task status obtained from the TSI expert system using the data from the artificial slip test 1 •

Table 7.6: A summary of the task status parameters obtained from the TSI expert system using the data from the artificial slip test 1.

Block no.	Unchanged state	Grasping level	Releasing level	Grasping con. level	Releasing con. level	Dynamic displacement	Static displacement	Decision correct ?
1	y	0	0	0	0	No	Nodir	Yes
2	y	0	0	0	0	No	Nodir	Yes
3	y	0	0	0	0	No	Nodir	Yes
4	y	0	0	0	0	No	Nodir	Yes
5	y	0	0	0	0	No	Nodir	Yes
6	y	0	0	0	0	No	Nodir	Yes
7	y	0	0	0	0	No	Nodir	Yes
8	y	0	0	0	0	No	Nodir	Yes
9	y	0	0	0	0	No	Nodir	Yes
10	y	0	0	0	0	No	Nodir	Yes
11	y	0	0	0	0	No	Nodir	Yes
12	Y	0	0	0	0	No	Nodir	Yes
13	y	0	0	0	0	No	Nodir	Yes
14	y	0	0	0	0	No	Nodir	Yes
15		1	0	3	0	No	Nodir	Yes
16		0	1	0	3	No	Nodir	Yes
17	y	0	0	0	0	No	Nodir	Yes
18	y	0	0	0	0	No	Nodir	Yes
19	y	0	0	0	0	No	Nodir	Yes
20	y	0	0	0	0	No	Nodir	Yes
21	y	0	0	0	0	No	Nodir	Yes
22	y	0	0	0	0	No	Nodir	Yes
23	y	0	0	0	0	No	Nodir	Yes
24	y	0	0	0	0	No	Nodir	Yes
25	y	0	0	0	0	No	Nodir	Yes
26	y	0	0	0	0	No	Nodir	Yes
27	y	0	0	0	0	No	Nodir	Yes
28	y	0	0	0	0	No	Nodir	Yes
29	y	0	0	0	0	No	Nodir	Yes
30	y	0	0	0	0	No	Nodir	Yes
31	y	0	0	0	0	No	Nodir	Yes
32	y	0	0	0	0	No	Nodir	Yes
33	y	0	0	0	0	No	Nodir	Yes
34	y	0	0	0	0	No	Nodir	Yes
35	y	0	0	0	0	No	Nodir	Yes
36	y	0	0	0	0	No	Nodir	Yes
37	y	0	0	0	0	No	Nodir	Yes
38	y	0	0	0	0	No	Nodir	Yes
39		1	0	6.25	0	No	Nodir	Yes
40	y	0	0	0	0	No	Nodir	Yes

dip in the raw data curve depends on the weights w_1 , and w_2 . The weight w_1 determines the applied force on the sensor and w_2 determines the speed at which the sample passes over the sensor.

Considering the raw data plots from all the tests in categories 1 to 4, it was concluded that the prototype gripper system hardware was suitable for measuring the dynamic force data during the performance of the type of tasks examined in this project.

The intermediate results were used to validate the tactile imaging and the decision filter performances. In the results obtained from test category 1, the plot of cumulated grasped level is seen to be relatively less noisy when compared with the corresponding plot showing the cumulated force primitives plotted as a function of task time. Similar behaviour is seen from the intermediate result plots from tests in categories 2 and 4 also. These show that the tactile imaging filter and the decision filter implementations are appropriate for the type of tasks investigated.

The performance tables obtained by summarizing the task status decisions arrived at by the TSI expert system provide a means to identify the correctness of the procedure. Considering the performance reported in Tables 7.2 and 7.3, the last column indicates the correctness of the task status decisions obtained from each block of data according to the criteria established in Section 7.4.4.1. This information was used to infer two main characteristics of the task oriented procedure:

1. to determine a quantifiable performance index for the task oriented procedure, and
2. to identify the type of tasks for which the technique could be applied.

The performance index was defined as the percentage of correct task status decisions obtained during a single test run. For tests in categories 1 and 3, a single test run consisted of a grasping or a releasing operation performed on any of the nine samples, whereas for tests in category 2, the combined grasping and releasing operation on any one sample constituted a single test run. For artificial slip tests, each test included in Table 7.5 was considered a test run.

The performance index was evaluated from the sample performance tables determined from the data in each of the four test categories 1, 2, 3, and 4. The index was tabulated in the form of four tables, each corresponding to the test category from which the indices were determined.

Table 7.7 shows the performance indices obtained from the nine grasping and nine releasing tests in category 1. The performance indices which were evaluated using the sample performance tables obtained from the tests in Categories 2 and 3 are shown in

Tables 7.8 and 7.9 respectively. The performance indices for the procedure in case of the artificial slip tests are shown in Table 7.10.

Table 7.7: Performance index of the task oriented procedure using results from independent grasping and releasing [Category 1] tests.

Serial number	Sample tested	Type of the task performed	Percentage of correct decisions
1	Sample 1	Grasping	80.0
2	Sample 1	Releasing	97.5
3	Sample 2	Grasping	92.5
4	Sample 2	Releasing	95.0
5	Sample 3	Grasping	92.5
6	Sample 3	Releasing	97.5
7	Sample 4	Grasping	82.5
8	Sample 4	Releasing	97.5
9	Sample 5	Grasping	80.0
10	Sample 5	Releasing	87.5
11	Sample 6	Grasping	57.5
12	Sample 6	Releasing	97.5
13	Sample 7	Grasping	62.5
14	Sample 7	Releasing	85.0
15	Sample 8	Grasping	62.5
16	Sample 8	Releasing	92.5
17	Sample 9	Grasping	72.5
18	Sample 9	Releasing	87.5

The tables showing the performance indices for the task oriented approach indicate that the task status decisions in a majority of cases have been correct with varying degrees of accuracy. The mean value of the percentage of correct decisions were found to be 84.3 % for category 1 tests, 82.7 % for category 2 tests, 75.2 % for category 3 tests and 100 % for category 4 tests. The 100 % accuracy obtained in the case of category 4 tests was not considered because the decision making employed in the task oriented procedure relied on the variation of forces with task time. Therefore, this was dismissed as a trivial case. An overall index for the task oriented procedure was evaluated by taking the mean value of the performance indices obtained from the tests in categories 1, 2, and 3 and this value was found to be 80.4 %. Therefore, it can be concluded for a general purpose grasping or releasing task, the task oriented procedure defined here will be able to identify the correct task status of the gripper with an accuracy of 80.4 %.

Table 7.8: Performance index of the task oriented procedure using results from Combined grasping and releasing [Category 2] tests .

Serial number	Sample tested	Type of the task performed	Percentage of correct decisions
1	Sample number 1	Grasp then release	100.0
2	Sample number 2	Grasp then release	87.5
3	Sample number 3	Grasp then release	95.0
4	Sample number 4	Grasp then release	75.0
5	Sample number 5	Grasp then release	82.5
6	Sample number 6	Grasp then release	75.0
7	Sample number 7	Grasp then release	90.0
8	Sample number 8	Grasp then release	75.0
9	Sample number 9	Grasp then release	85.0

Table 7.9: Performance index of the task oriented procedure using results from Repeatability [Category 3] tests .

Serial number	Trial number	Type of task performed	Percentage of correct decisions
1	1	Grasping	85.0
2	1	Releasing	97.5
3	2	Grasping	77.5
4	2	Releasing	85.0
5	3	Grasping	67.5
6	3	Releasing	62.5
7	4	Grasping	57.5
8	4	Releasing	70.0

Table 7.10: Performance index of the task oriented procedure using results from artificial slip [Category 4] tests .

Serial number	Simulated slip test type	Sample used	Percentage of correct decisions
1	Test 1	Sample 1:Small aluminum disc	100.0
2	Test 2	Sample 1:Small aluminum disc	100.0
3	Test 3	Sample 1:Small aluminum disc	100.0
4	Test 4	Sample 2:Large aluminum disc	100.0
5	Test 5	Sample 2:Large aluminum disc	100.0

The next logical step after the task status had been identified was to investigate the possibility of designing a control scheme which could interpret the task status to obtain a set of control decisions. The strategy for determining the control decisions should take into account the nature of the task status parameters, their accuracy, and the time availability during a task. The task status decision parameters, grasped level and released level often displayed similar values and therefore, a method was needed to extract consistent control parameters. The confidence factor associated with the task status parameters was shown to be useful for proper task status interpretation. These parameters could be used in arriving at control decisions which would be meaningful. The mean value of performance index obtained for the task status indications were about 80 %. Therefore, the control decisions should consider the variation of relative task status parameters rather than their absolute values.

Using these requirements, a preliminary control scheme was designed, developed and tested. As the control scheme was primarily used to demonstrate the feasibility of using the task status parameters in a meaningful way, control schemes which could be integrated into Interface Program II were explored. The details are described in the next section.

7.4. Control Decisions From Task Status

When a robot hand has to grasp an object or release a held object, the gripper contact forces may be used to guide the successful accomplishment of the task. For a task oriented grasp, the hand should grasp the object such that it is stable and the grasping scheme proposed should be able to guide the gripper controller to complete the task effectively.

7.4.1. Scope of the work

For a real time task, two possible control actions which could be initiated on-line to improve the contact state of the gripper were identified. While grasping an object using parallel jaws, the gripper fingers may be activated so as to grip with an increased force, or the fingers may be moved relative to the object position in any direction. Similarly, in the case of a releasing operation, either the gripper force can be maintained or reduced, or the grippers may be moved to prevent dropping of the object.

In order to formulate the correct control decision, based on the task status obtained in terms of the parameters discussed earlier, two control decisions were identified at the top level: "Conaction" and "Movcond", for force 'control action' and gripper 'movement condition', respectively. The parameter "Conaction" was used to decide whether there should be an increase or no change in the gripping force, and the parameter "Movcond" was used to decide whether the gripper should be moved relative to the last object position.

7.4.1.1. Hierarchy of the control decision parameters

Since the control decisions were to be determined solely from the force data, the most direct approach was to compare the task status of the gripper from adjacent time intervals. The choices for the values taken by the two main control decision parameters were governed by the values taken by the task status parameters. Using this information, hierarchies of parameters used to identify the two control decision parameters, Conaction and Movcond were determined. These are shown in Figures 7.21 and 7.22 respectively. The formulation of these hierarchy diagrams were based on the following rules: 1. any control action should be a function of the force variations identified between two successive blocks of data, and, 2. any movement action of the gripper should be a function of the identified relative object displacements determined from two successive blocks of data. These rules were incorporated in the hierarchy diagrams shown in Figures 7.21 and 7.22 by making the Conaction parameter a function of two other parameters, "Forcinc", and "Relcond". The Movcond parameter was a function of the two parameters, "Stamov" and "Dynmov". These four parameters, Forcinc, Relcond, Stamov, and Dynmov were

defined to represent conditions which indicate 'force increase', 'relative task status conditions', 'static movement', and 'dynamic movement' between two successive data blocks, respectively.

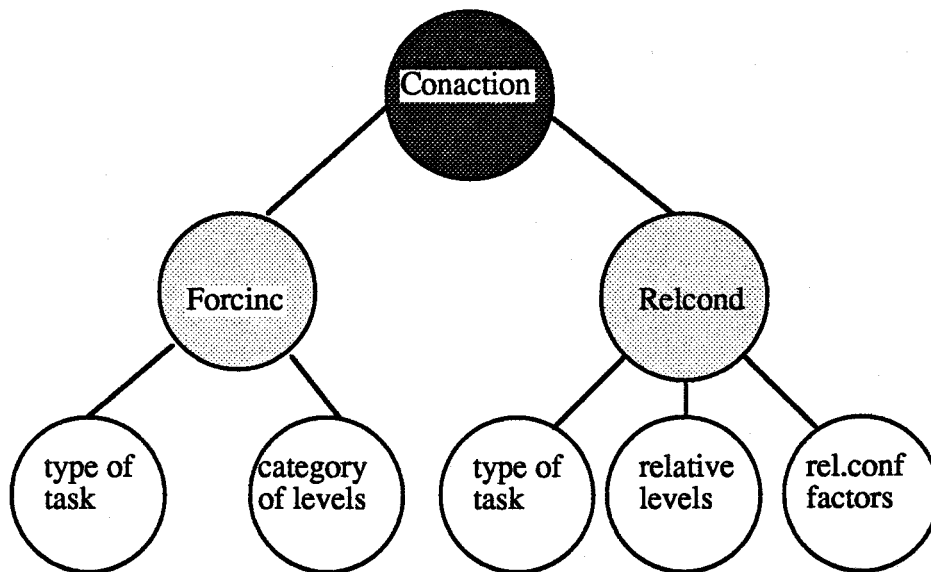


Figure 7.21: Hierarchy diagram for the parameter "Conaction" .

The dependencies of the two parameters, Forcinc and Relcond are also shown in Figure 7.21. The parameter Forcinc depended on the type of task being performed and the category of levels exhibited by the task status parameters. The type of task was one of grasping, releasing, or none. Within each time interval for which task status parameters have been determined, the levels of grasping and releasing were categorized. For example, if the task status parameters were determined from the force data acquired during a 100 ms time period, then, the reference grasping and releasing level at the beginning of this time interval was set to 0 and the cumulated grasping and releasing levels at the end of the 100 ms period were indicated by the TSI expert system. To categorize this information, the following criteria were used. A pure grasp with no releasing levels was differentiated from a grasp with one or more releasing levels within the same time interval. Further sub-categorization consisted of identifying the number of graspings and releasings and assigning different values of confidence factors for each type of task behaviour. The number of sensing sites reporting the specified task type data were considered in

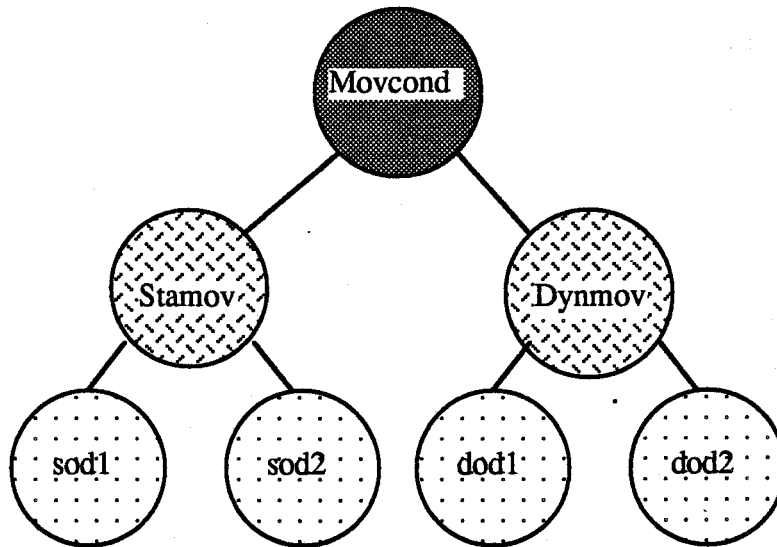


Figure 7.22: Hierarchy diagram for the parameter "Movcond".

calculating the composite confidence levels. Thus, in summary, the category of levels assigned to the parameter Forcinc depended on the combined effects of the four task status parameters, namely, grasping and releasing levels, and their associated confidence factors.

The parameter Relcond determined the relative behaviour of the gripper states during two consecutive time periods. This was a function of the task type, which could be grasping, releasing or unknown, the relative cumulated grasping and releasing levels, and the relative confidence factors calculated for each type of task behaviour.

In order to restrict the possible values which the parameter Conaction can take, it was necessary to identify those situations which would be commonly encountered in a real task. This was done using intuitive reasoning tools, which could eliminate a number of combinations of the dependent parameters. This is explained in the next section.

7.4.1.2. Heuristic reasoning

The task status parameters were determined using data either from a 100 ms or a 200 ms time window and a maximum allowance of four possible transitions was set. If there were more than four transitions, then the data were deemed to be too noisy to interpret. The resulting task status parameters identified both grasping and releasing types of

task behaviour using levels zero to four only. This resulted in 20 independent combinations of grasping and releasing levels for identification. Within the block of data pertaining to a set time window, the instants at which the grasping and releasing levels were reported were ignored for determining the parameter Conaction. However, this information was used to determine the static and dynamic displacements of the object relative to gripper fingers.

The parameter Movcond determined whether the gripper should be instructed to move relative to the current object location. As shown in Figure 7.22, this parameter depends on the two displacement parameters "Stamov" and "Dynmov". Stamov was determined from the task status parameters, sod1 and sod2, which were the reported static object displacements during two successive time windows (of 100 ms or 200 ms duration). The parameter Dynmov was determined from the corresponding dynamic displacements, dod1 and dod2. The static displacements were given a higher priority and weight while determining the resultant recommended movement. The parameter Movcond indicated the direction of movement in terms of North, South, East, West, North east, North west, South east and South west as defined in Section 6.2.4, in Chapter 6.

In the assignment of symbolic values to the control decision parameters, Conaction and Movcond, a measure of confidence level had to be embedded in each value to enable correct interpretation of the control decisions. The criteria for allocation of confidence levels for various values of the two parameters are outlined in the following paragraph.

7.4.2. Assignment of confidence levels

The magnitudes of the grasping/releasing levels were considered in calculating the confidence factors for specific status decision parameters. For example, in the case of two time intervals which have indicated task status parameters as follows; the first one reports four transitions, in which the task status parameters, the grasping level and the releasing level, were assigned a value 2, and the second one reports one transition, in which the task status parameter grasping level was assigned a value 1. The latter was assigned a higher value of confidence factor compared to the former, because, the status indication in the second case, namely, a pure grasping, was a better form of confirmation compared to the first one in which both grasping and releasing were identified. If four transitions were reported and all four of them indicated grasping, then the confidence factor for grasping was higher.

The confidence levels assigned to the parameters were based on the confidence levels of their dependent parameters. For Conaction, the allocation considered the levels assigned for Forcinc and Relcond, while for Movcond, the confidence levels of Stamov and Dynmov were considered.

The possible symbolic values resulting for the parameter Forcinc were divided into 23 categories, and those for Relcond were divided into 7 categories. The contribution of the two parameter confidence levels to the confidence level of Conaction was equal. In the case of Movcond, the contribution of the confidence level associated with Stamov was given a higher weight and priority over the one associated with Dynmov. Using these ideas, tables were formed to indicate the confidence level associated with the control decision parameters when they have a particular symbolic value.

In order to incorporate the features described above, the development of a conventional program to determine the control parameters was considered. Because of a number of different rule based conditional inferences present in the decision hierarchies, the implementation of the reasoning mechanisms were found to be too complex. In addition, the need to consider the accuracy of the task status parameters required an excessive number of function calls to perform simple operations.

A knowledge based expert system implementation proved to be a better alternative to the conventional program. In this case, the control decision parameters could be readily identified using hierarchy diagrams and the various reasonings and interpretations could be performed with relative ease. Since the knowledge sources were separated from the algorithms, an expert system was easier to debug than a conventional program. The accuracy of the task status parameters could be readily included in the expert system decisions by way of certainty factors. In order to reduce development time, the expert system was designed using the KES tool. The implementation of the expert system designed and built to obtain the control decision parameters from task status are described in the following section.

7.4.3. Preliminary design of a Control decision indicator expert system

In order to determine the control decision parameters using the task status parameters, a knowledge base was designed and built. The expert system which used this knowledge base to determine the control actions was called the "Control decision indicator" (CDI) expert system.

The control decision logic, most of which was based on human heuristic knowledge, was formulated and implemented in the expert system. Since the CDI expert system was also developed using the KES tool, it could also be embedded into Interface Program II.

The parameter "Conaction" was evaluated based on its symbolic value assigned by the expert system. The symbolic value, in turn, was assigned based on the values of the dependent parameters, Forcinc and Relcond. The parameters Forcinc and Relcond were given values using the backward chaining rules incorporated in the knowledge base. For-

cinc considered the task type (grasping or releasing) and the category (1, 2 or 3 defined in Section 7.4.1.1) to which the task status parameter, "result", belonged, as determined from the last two successive data blocks. If the task type was unknown, it was taken as grasping, by default.

The parameter Relcond accounted for the changes in the task status between two successive data blocks by comparing the four task status parameters, namely, the grasping level, the releasing level, and the confidence factors associated with each of these two decisions, as determined by the TSI expert system. The parameter Forcinc could be assigned with 23 different symbolic values (11 for a grasping type of task, 11 for releasing, and 1 for no change of status) and Relcond was assigned with 6 different symbolic values (3 each for grasping and releasing type tasks).

The contribution of the two parameters, Forcinc and Relcond, towards strengthening or weakening of the two control decisions, namely "increase the gripper force" or "do not increase the gripper force" was considered first. Based on their contributions, look up tables were formulated to assign a percentage confidence value for each symbolic value of the two parameters, Forcinc and Relcond. The assigned confidence values for the parameter Forcinc are shown in Table 7.11, and those for the parameter Relcond are shown in Table 7.12. Based on the criterion of equal weight to its two dependent parameters, the parameter Conaction obtained a resultant confidence value for each of its assigned symbolic values. This was calculated by averaging the confidence values assigned to the respective symbolic values of the two parameters Forcinc and Relcond. Table 7.13 shows the confidence values for the parameter Conaction when it is assigned with different symbolic values, which are indicated in the first column.

In a similar manner, the parameter "Movcond" was determined using the two displacement parameters "Stamov" and "Dynmov". In this case, a typical gripper movement decision consisted of two possible alternatives: "do not move the gripper" and "move gripper in a particular direction". The symbolic value assigned to the parameter Movcond was based on the values taken by the dependent parameters, Stamov and Dynmov. The parameters Stamov and Dynmov were determined using the forward chaining rule incorporated in the HT knowledge base. Based on the symbolic value assigned to these two parameters, Movcond was assigned one or more symbolic values. The value taken by the parameter Movcond showed the direction in which the gripper should move. The confidence value associated with Movcond was based on the symbolic certainty factor assigned to it by the HT inference engine. The symbolic values assigned to Movcond consisted of the eight directions of gripper movement, namely, North, South, East, West, North east, North west, South east and South west, defined in Section 6.2.4, and a condition corresponding to no movement (Nodir). The values assigned to Stamov and Dynmov were based on the static and dynamic object displacement parameters determined by

Table 7.11: Assigned confidence values for symbolic values of the parameter "Forcinc"

Decision: Increase gripping force		Decision: Do not increase gripg.force	
Symbolic value	Confidence level, %	Symbolic value	Confidence level, %
forcinc1	80	forcinc13	80
forcinc2	70	forcinc14	70
forcinc3	60	forcinc15	60
forcinc4	40	forcinc16	40
forcinc5	36	forcinc17	36
forcinc6	33	forcinc18	33
forcinc7	30	forcinc19	30
forcinc8	20	forcinc20	20
forcinc9	16	forcinc21	16
forcinc10	13	forcinc22	13
forcinc11	10	forcinc23	10
forcinc12	0		

the TSI expert system. For evaluating the value for the parameter Movcond, static displacements were given a higher weight than the dynamic displacements. This was based on the inference obtained in Section 7.3.4.2, in which it was found that in a majority of cases, the static object displacements represented object slip while the dynamic object displacements (alone) represented transient object movements. Table 7.14 shows the confidence levels for the parameter Movcond when its dependent parameters take various symbolic values. Table 7.15 shows the relationship between the Inferred Direction (ID) and the Other Direction (OD), which are used in the Table 7.14. In Tables 7.13 and 7.14, the corresponding control decisions are also indicated. The interpretation of the various parameter values are clarified in Section 7.4.4.1.

7.4.4. Control decisions from sample test data

To test the control decisions, the task status parameters obtained from the nine independent grasping and releasing sample data from the tests in category 1, and the nine combined grasping and releasing data obtained from the tests in category 2, were used to formulate a set of control decision tables for the various tasks.

The input for the CDI expert system consisted of task status parameters evaluated

Table 7.12: Assigned confidence values for symbolic values of the parameter "Relcond".

Decision: Increase gripping force		Decision: Do not increase gripg.force	
Symbolic value	Confidence level, %	Symbolic value	Confidence level, %
rcon1g	80	rcon1r	80
rcon2g	60	rcon2r	60
rcon3g	40	rcon3r	40
rcond0	0	rcond0	0

on-line and stored in two designated files. These files were set up so as to permit communication with the CDI expert system. The task status parameters were obtained using the data from 100 ms time window containing dynamic force data from the eight tactile sensors.

The task status parameters from the 40 blocks were used to formulate control decisions using the CDI expert system. The task status parameters from two successive blocks were grouped and delivered to the CDI expert system. The CDI expert system processed the task parameters and obtained the control decisions for every 2 block set of data. The two main control decision parameters determined by the CDI expert system from each set of task status parameters were Conaction and Movcond. The dependent control parameters, Forcinc, Relcond, Stamov and Dynmov were also determined and displayed.

Figure 7.23 shows the complete flow chart of the task oriented procedure used to obtain control decisions from dynamic force data. The various modules and system developed for the project, were integrated into a single program which executed the main stages shown in this diagram.

Table 7.13: Assigned confidence values for symbolic values of the parameter "Conaction"

Decision: Increase gripping force		Decision: Do not increase gripping force	
Symbolic value	Confidence level, %	Symbolic value	Confidence level, %
Conact 00	0	Conact 00	0
Conact g10	40	Conact r10	40
Conact g11	80	Conact r11	80
Conact g12	70	Conact r12	70
Conact g13	60	Conact r13	60
Conact g20	35	Conact r20	35
Conact g21	75	Conact r21	75
Conact g22	65	Conact r22	65
Conact g23	55	Conact r23	55
Conact g30	30	Conact r30	30
Conact g31	70	Conact r31	70
Conact g32	60	Conact r32	60
Conact g33	50	Conact r33	50
Conact g40	17.5	Conact r40	17.5
Conact g41	57.5	Conact r41	57.5
Conact g42	47.5	Conact r42	47.5
Conact g43	37.5	Conact r43	37.5
Conact g50	7.5	Conact r50	7.5
Conact g51	47.5	Conact r51	47.5
Conact g52	37.5	Conact r52	37.5
Conact g53	27.5	Conact r53	27.5

7.4.4.1. A preliminary analysis of the control decisions

A summary of control decisions formulated by the CDI expert system using the data from test Category 1, obtained while performing independent grasping and releasing operations on sample 2, are shown in Tables 7.16 and 7.17 respectively. The control decisions formulated using the data from test Category 2, which involved the combined grasping and releasing operation performed on sample 2, are shown in Table 7.18. The control decisions obtained from test 1 in Category 4 are shown in Table 7.19. These tables contain the decisions from 20 consecutive block sets of data. Each block set accounts for a 200 ms time period of the task in case of the results from test Category 1, and a 400 ms time period in case of the results from test Category 2.

Table 7.14: Confidence level assignment for the parameter "Movcond" and its associated decisions .

Stamov	Dynmov	Movcond	Decision	Confidence, %
No direction	None	Cond m0	Do not move	100
Indicated direction	Indicated direction	Opposite direction	Move in Opp. direction	100
Indicated direction	None	Opposite direction	Move in Opp. direction	75
No direction	Indicated direction	Opposite direction	Move in Opp. direction	50
Indicated direction	Opposite direction	Opposite direction	Do not move	50

Table 7.15: Relationship between the "Indicated direction" and the "Opposite direction" used in CDI knowledge base .

Indicated direction	Opposite direction
North	South, Southeast, Southwest
South	North, Northeast, Northwest
East	West, Northwest, Southwest
West	East, Northeast, Southeast
Northeast	West, South, Southwest
Northwest	South, East, Southeast
Southeast	North, West, Northwest
Southwest	North, East, Northeast

The control decisions were obtained from the task status parameters obtained from two successive data blocks. Each decision was associated with a confidence level which was used to interpret the decision so as to make a final choice.

The results obtained in Table 7.16 were evaluated for accuracy. The task status parameters corresponding to the two blocks 19 and 20 showed that there was no change in the gripper contact states and the corresponding control decision was in favour of no

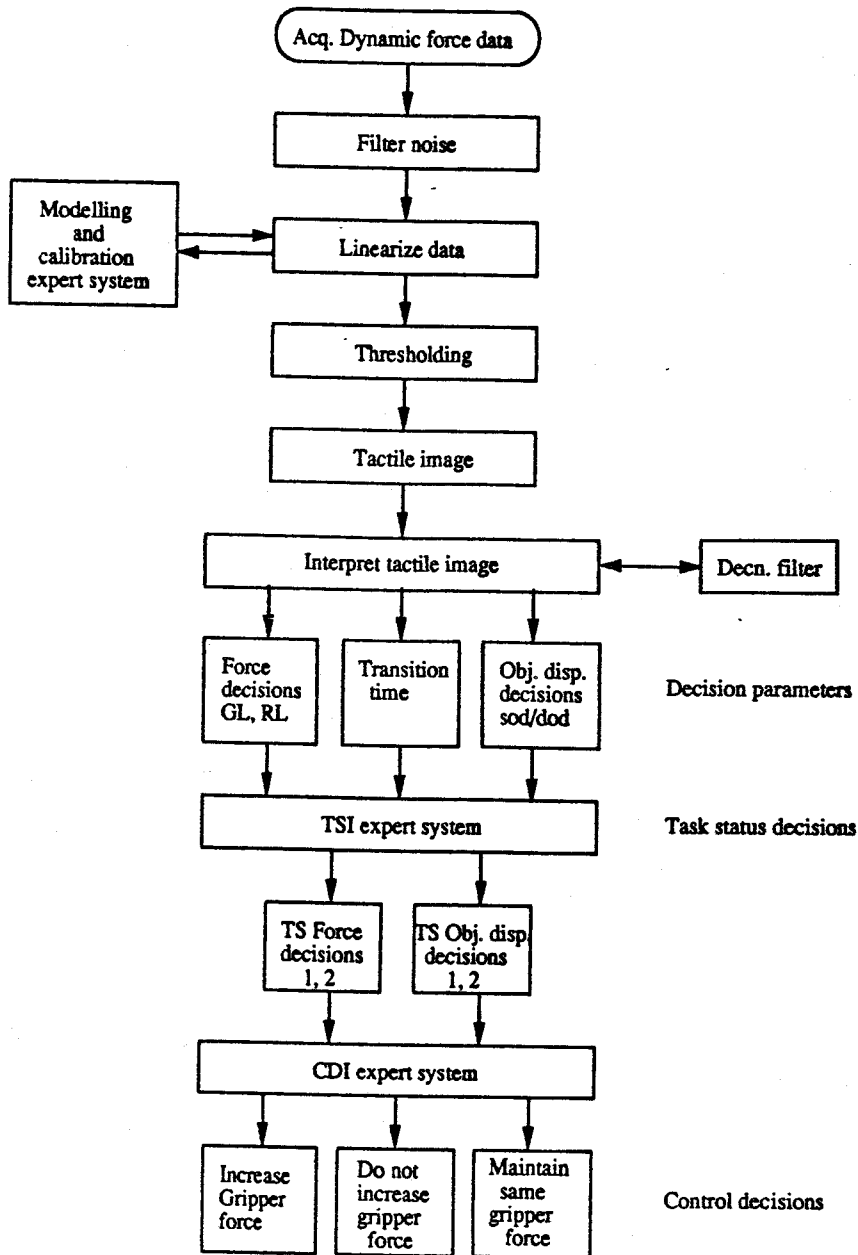


Figure 7.23: Complete flow chart of the task oriented procedure •

action to be taken either to increase the gripper force or to move the gripper fingers. The task status from the subsequent two blocks, 21 and 22, showed that the task status data from the first block displayed a grasping level of 1 and releasing level of zero, with the confidence level being higher for the grasping decision. This was indicated in the corresponding control decision which was to take no action. Likewise, the task status data from blocks 9 and 10, showed releasing levels of 1 and 2 for the two blocks, with corresponding levels of 0 and 2 for grasping. Therefore, the corresponding control action

Table 7.16: Summary of the results displayed by the CDI expert system - Test Category 1: sample 2 grasping.

Blk.no	Time period,ms	Force decision	Confidence %	Mov.decision	Confidence %	Remarks
1,2	0 to 200	maintain same	100	do not move	100	--
3,4	201 to 400	do not increase	43	do not move	100	--
5,6	401 to 600	do not increase	66	do not move	100	--
7,8	601 to 800	do not increase	54	do not move	100	--
9,10	801 to 1000	increase force	67	move East	100	large slip in West direction
11,12	1001 to 1200	increase force	28	do not move	100	--
13,14	1201 to 1400	do not increase	78	do not move	100	--
15,16	1401 to 1600	maintain same	100	do not move	100	--
17,18	1601 to 1800	maintain same	100	do not move	100	--
19,20	1801 to 2000	maintain same	100	do not move	100	--
21,22	2001 to 2200	maintain same	100	do not move	100	--
23,24	2201 to 2400	do not increase	78	move North	50	small slip in South direction
25,26	2401 to 2600	do not increase	84	do not move	100	--
27,28	2601 to 2800	do not increase	100	move East	75	slip in West direction
29,30	2801 to 3000	do not increase	100	move North	75	slip in South direction
31,32	3001 to 3200	do not increase	77	do not move	100	--
33,34	3201 to 3400		96	move South	50	small slip in North direction
35,36	3401 to 3600	maintain same	100	move West	75	slip in East direction
37,38	3601 to 3800	maintain same	100	do not move	100	--
39,40	3801 to 4000	maintain same	100	do not move	100	--

recommended was to increase the gripper force to prevent slippage. The direction of movement suggested for the gripper was East, since the object had experienced both static and dynamic displacements in the West direction, according to the TSI expert system display.

Table 7.17: Summary of the results displayed by the CDI expert system - Test Category 1: sample 2 releasing .

Blk.no	Time period,ms	Force decision	Confidence %	Mov.decision	Confidence %	Remarks
1,2	0 to 200	maintain same	100	do not move	100	--
3,4	201 to 400	increase force	85	do not move	100	--
5,6	401 to 600	maintain same	75	do not move	100	--
7,8	601 to 800	maintain same	75	move South	50	small slip in North direction
9,10	801 to 1000	increase force	85	move South	75	slip in North direction
11,12	1001 to 1200	increase force	28	do not move	100	--
13,14	1201 to 1400	maintain same	100	do not move	100	--
15,16	1401 to 1600	increase force	28	do not move	100	--
17,18	1601 to 1800	maintain same	100	do not move	100	--
19,20	1801 to 2000	maintain same	100	do not move	100	--
21,22	2001 to 2200	maintain same	100	do not move	100	--
23,24	2201 to 2400	maintain same	100	do not move	100	--
25,26	2401 to 2600	maintain same	75	do not move	100	--
27,28	2601 to 2800	maintain same	100	do not move	100	--
29,30	2801 to 3000	maintain same	100	do not move	100	--
31,32	3001 to 3200	maintain same	100	do not move	100	--
33,34	3201 to 3400	maintain same	100	do not move	100	--
35,36	3401 to 3600	maintain same	75	do not move	100	--
37,38	3601 to 3800	maintain same	100	do not move	100	--
39,40	3801 to 4000	maintain same	75	do not move	100	--

Table 7.18: Summary of the results displayed by the CDI expert system - Test Category 2: sample 2 combined grasping and releasing .

Blk.no	Time period,ms	Force decision	Confidence %	Mov.decision	Confidence %	Remarks
1,2	0 to 200	do not increase	79	move Northeast	75	slip in North & SW directions
3,4	201 to 400	increase force	80	move Northeast	50	small slip in SW direction
5,6	401 to 600	increase force	38	move Northeast	50	small slip in SW direction
7,8	601 to 800	increase force	38	move East	50	small slip in West direction
9,10	801 to 1000	maintain same	75	move Southwest	75	slip in NE direction
11,12	1001 to 1200	do not increase	85	do not move	100	--
13,14	1201 to 1400	do not increase	85	move East	75	slip in West direction
15,16	1401 to 1600	do not increase	84	move Northeast	75	slip in S & W direction
17,18	1601 to 1800	do not increase	100	move Northeast	75	slip in S & W direction
19,20	1801 to 2000	do not increase	57	do not move	100	--
21,22	2001 to 2200	do not increase	86	move East	75	slip in West direction
23,24	2201 to 2400	do not increase	97	move East	75	slip in West direction
25,26	2401 to 2600	do not increase	56	do not move	100	--
27,28	2601 to 2800	increase force	87	move Southwest	50	small slip in NE direction
29,30	2801 to 3000	do not increase	81	move Northeast	75	slip in SW direction
31,32	3001 to 3200	increase force	86	move West	50	small slip in East direction
33,34	3201 to 3400	increase force	77	move West	100	large slip in East direction
35,36	3401 to 3600	increase force	51	do not move	100	--
37,38	3601 to 3800	increase force	51	move Southwest	75	slip in NE direction
39,40	3801 to 4000	do not increase	43	do not move	100	--

Table 7.19: Summary of the results displayed by the CDI expert system - Test Category 4: artificial slip test 1 .

Blk.no	Time period,ms	Force decision	Confidence %	Mov.decision	Confidence %	Remarks
1,2	0 to 200	maintain same	100	do not move	100	--
3,4	201 to 400	maintain same	100	do not move	100	--
5,6	401 to 600	maintain same	100	do not move	100	--
7,8	601 to 800	maintain same	100	do not move	100	--
9,10	801 to 1000	maintain same	100	do not move	100	--
11,12	1001 to 1200	maintain same	100	do not move	100	--
13,14	1201 to 1400	maintain same	100	do not move	100	--
15,16	1401 to 1600	increase force	28	do not move	100	--
17,18	1601 to 1800	maintain same	100	do not move	100	--
19,20	1801 to 2000	maintain same	100	do not move	100	--
21,22	2001 to 2200	maintain same	100	do not move	100	--
23,24	2201 to 2400	maintain same	100	do not move	100	--
25,26	2401 to 2600	maintain same	100	do not move	100	--
27,28	2601 to 2800	maintain same	100	do not move	100	--
29,30	2801 to 3000	maintain same	100	do not move	100	--
31,32	3001 to 3200	maintain same	100	do not move	100	--
33,34	3201 to 3400	maintain same	100	do not move	100	--
35,36	3401 to 3600	maintain same	100	do not move	100	--
37,38	3601 to 3800	maintain same	100	do not move	100	--
39,40	3801 to 4000	maintain same	100	do not move	100	--

Similar accuracy studies were conducted using the results obtained in the other summary tables. These tests were used to confirm the two main objectives of the investigation, namely, the adequacy of the chosen control parameters for performing real time tasks and the correctness of the proposed evaluation technique.

Thus it was inferred that a simple rule of selecting the decision based on the highest value of confidence level may be used to obtain appropriate control decisions. Applying this rule, it was evident that the decisions obtained in Table 7.16 were appropriate for the successful completion of a grasping task, and the decisions in Table 7.17 were appropriate for a releasing task. Similar interpretations of the control decisions shown in Table 7.18 showed that appropriate control decisions were obtained for tasks which involve both grasping and releasing operations.

It was also clear from the results shown in Tables 7.16 and 7.17 that whenever a noticeable slip (which has been denoted as a large slip to distinguish it from a small slip) occurred, as evidenced by a static object displacement, the CDI expert system recommended an increase in the gripper force as well as a movement of the gripper.

The control decisions were obtained for all the other 8 sample tests in test categories 1 and 2. A summary of the control decisions obtained from the tests which involved the samples 1, 5, and 7, in both the test categories, 1 and 2, are given in Appendix H. It can be seen that in all the cases, concurring results similar to the ones obtained in the case of sample 2, have been obtained.

The control decision parameter values displayed by the expert system provided correct recommendations in about 70 % of the tested cases. The direction of gripper movement to compensate for the static and dynamic displacements of the object relative to the grippers were also indicated. These decisions can be used to proceed with the task in the presence of slip. This indirect method of slip detection and initiation of corrective action appears to be suitable for general purpose gripping operations. However, for precision tasks, this technique may have to be modified using additional sensors to detect slip in a shorter time.

7.4.5. Limitations and recommendations

In the proposed task oriented procedure, during the performance of a grasping or releasing operation, the real time data were first acquired, then on-line tactile images were formed from the dynamic force data, and these images were processed to obtain a set of decision parameters. These decision parameters were subsequently interpreted to yield task status and control decision parameters. If such a system is to be designed for a real time operation, an important factor to be considered is the time taken to do the various operations. In the proposed procedure, the timing considerations were given secondary importance in the design because of a primary need to study the feasibility of the procedure before fine tuning the design.

Since timing considerations play a vital role in the real time execution of a task oriented procedure, the times taken to perform all the operations envisaged in Interface Program II were evaluated using the "time" utility function of the UNIX operating system.

7.4.5.1. Timing analysis

The performance tables obtained from the various tests included the data about the timing requirements to process the raw data in order to achieve the task status and control decisions. For every two block set of data, the user time and the system time were computed by Interface Program II. The user time is defined as the cpu time spent in the application program while the system time refers to the time spent in the operating system kernel on behalf of the application program. These times were affected by the load on a multi-tasking system, such as the one used to execute Interface Program II. Therefore, to arrive at an average value for the system time and CPU time, the times taken to process two blocks of data were averaged over all the blocks. The averaged time values are shown in Table 7.20. These are the average times to process the data obtained using the nine grasping and releasing tests belonging to Category 1.

Table 7.20: Average time to execute Interface Program II to process two blocks of data .

Serial number	Test category	Sample / test type	Mean user time,s	Mean system time, ms
1	Category 1 graspg.	Sample 1	46.36	640.0
2	Category 1 releasg.	Sample 1	35.16	596.0
3	Category 1 graspg.	Sample 2	45.84	610.5
4	Category 1 releasg.	Sample 2	38.62	591.5
5	Category 1 graspg.	Sample 3	45.82	767.0
6	Category 1 releasg.	Sample 3	36.54	673.5
7	Category 1 graspg.	Sample 4	48.86	558.0
8	Category 1 releasg.	Sample 4	34.70	655.5
9	Category 1 graspg.	Sample 5	46.72	730.5
10	Category 1 releasg.	Sample 5	28.56	542.5
11	Category 1 graspg.	Sample 6	48.14	714.5
12	Category 1 releasg.	Sample 6	34.94	683.0
13	Category 1 graspg.	Sample 7	50.16	739.5
14	Category 1 releasg.	Sample 7	39.42	703.5
15	Category 1 graspg.	Sample 8	48.16	540.5
16	Category 1 releasg.	Sample 8	35.58	515.0
17	Category 1 graspg.	Sample 9	44.38	778.5
18	Category 1 releasg.	Sample 9	36.76	519.0
19	Cat. 2, graspg+rel.	Sample 1	43.96	585.0
20	Cat. 2, graspg+rel.	Sample 2	46.32	584.5
21	Cat. 2, graspg+rel.	Sample 3	44.46	568.0
22	Cat. 2, graspg+rel.	Sample 4	61.54	603.0
23	Cat. 2, graspg+rel.	Sample 5	49.62	551.5

Table 7.20: Average time to execute Interface Program II to process two blocks of data (continued).

24	Cat. 2, grasp+rel.	Sample 6	53.26	546.5
25	Cat. 2, grasp+rel.	Sample 7	45.88	560.0
26	Cat. 2, grasp+rel.	Sample 8	49.10	592.0
27	Cat. 2, grasp+rel.	Sample 9	53.18	724.0
28	Category 3 graspg.	Sample 1, trial 1	48.28	686.0
29	Category 3 releasg.	Sample 1, trial 1	36.06	667.5
30	Category 3 graspg.	Sample 1, trial 2	52.62	761.5
31	Category 3 releasg.	Sample 1, trial 2	36.20	680.0
32	Category 3 graspg.	Sample 1, trial 3	53.37	757.0
33	Category 3 releasg.	Sample 1, trial 3	36.12	714.5
34	Category 3 graspg.	Sample 1, trial 4	57.48	638.0
35	Category 3 releasg.	Sample 1, trial 4	36.98	516.0
36	Cat. 4, artificial slip	Test type 1	38.54	570.5
37	Cat. 4, artificial slip	Test type 2	39.18	587.5
38	Cat. 4, artificial slip	Test type 3	40.84	655.0
39	Cat. 4, artificial slip	Test type 4	42.96	674.5
40	Cat. 4, artificial slip	Test type 5	41.35	705.5

From Table 7.20, it is evident that the average system time for all the cases is a small fraction of the user time. This suggests that by optimizing the codes used in the program implemented for digital filtering and other operations carried out by Interface Program II, it should be possible to speed up the task oriented procedure. It was also observed that further optimization of the procedure was possible by optimizing the design

of the tactile imaging, the decision making and the dead band filters. The design of the two expert systems, TSI, and CDI, could also be improved by using advanced development tools.

In the case of a pure slip occurring during a task, the technique will be able to reliably recognize slip only after the object has moved from the contacting sensor area. This is seen as another limitation of the proposed method. Nevertheless, the proposed method of slip characterization was seen to be sufficient for many general purpose gripping tasks. For accurate slip detection, other techniques such as measuring vibrations at the contact surface [112] or measuring object acceleration [113] may be used.

7.5. Conclusion

This Chapter described the software integration of the task oriented tactile sensing procedure and the implementation and testing of the complete scheme. The procedure was validated using experimental data obtained while performing a variety of grasping and releasing tasks using a laboratory prototype system. A technique to formulate control decisions from on-line task data was developed and the control decisions obtained were found to be in agreement with human decisions which would have been taken under similar circumstances.

The integrated computer program was able to determine the status of the gripper contact from dynamic force data by suitably interpreting a set of decision parameters. The interpretation of the decision parameters was achieved using an embedded expert system in which a form of human-like decision making capability was incorporated.

The task status parameters obtained by the expert system were in the form of grasping and releasing levels and associated confidence levels for the two decisions, obtained from each block of data. The two object displacement parameters were the static and dynamic object displacements, determined relative to the gripper position at the beginning of a data block. These parameters, evaluated from two successive data blocks, were used to determine two control decision parameters, namely, Conaction and Movcond. Conaction indicated three type of decisions, each with its associated confidence level. They were:

1. increase gripper force,
2. do not increase gripper force, and
3. maintain the same status

The parameter Movcond indicated the direction of gripper movement recommended to compensate for either the slippage or the twisting of the object while it was being grasped. For the purposes of investigations in this project, the effect of slipping and

twisting were considered to be the same. Combinations of the two decisions, Conaction and Movcond, were found to be useful to guide the completion of the task. The validity of the decisions from the TSI and CDI expert systems were demonstrated using summary tables showing the expert system displays after processing every two-block set of experimental data obtained while grasping and releasing nine different sample objects. The detailed steps of the integration of the processing software and the embedding of the expert system to form a single integrated program were discussed.

The results obtained at various stages of system implementation using four different categories of test, were obtained in the form of validation packages and performance tables. These were defined separately for each category of test. The validation package and performance table for one sample test from each category were used to represent the results obtained and to validate the task oriented procedure. The significant results from each test category were presented to relate them to the various features of the integrated procedure. The limitations of the procedure and future directions for the investigation have been identified.

In order to perform a task oriented gripping operation, the contact status of the gripper displayed by the TSI expert system provides a complete set of information about the task including the direction of object displacement relative to the gripper. Using this information, it has been shown that an on-line task can be carried out successfully by initiating an appropriate corrective action determined from the contact status of the gripper. The static and dynamic displacements of the object occurring within a specified time interval may be used to identify slippages of the object which had occurred in the recent past (100 ms time in the case study), and to initiate corrective action in order to proceed with the task.

8. SUMMARY, CONCLUSIONS AND FUTURE DIRECTIONS

8.1. Summary

This thesis has described the design, development and implementation of a computer-aided task oriented implementation procedure to determine the status of a robotic gripper during a grasping or releasing operation. In this procedure, the dynamic forces measured during grasping and releasing operations were used to determine the status of the gripping task. A prototype gripper system was used to determine the real time dynamic forces. These forces were stored in data files, partitioned into blocks each containing 100 points of sampled force values. These data were processed by an integrated computer program which performed tactile imaging and image interpretation to facilitate decision making based on the force data. The decisions obtained from each block of data were in the form of a set of task status parameters describing the grasping and releasing levels with associated confidence factors and the object displacements which could be identified based on a set of criteria.

Using the task status information, a method was also designed and implemented to determine a set of control decisions which could be used to complete a task successfully. The task status displayed by an expert system provided information which were used to identify slippages of the object and to recommend corrective action.

To establish the suitability of the task oriented technique, it was first tested using grasping and releasing data obtained from nine different samples. The results from these tests were used to demonstrate the correctness of the task status decisions. Two additional experiments were conducted to obtain sample data to check for consistency of decisions and to test for slip detection. Consistency of decisions was checked using four independent sets of test data using the same object. Robustness of the scheme has been tested using a "combined grasping followed by releasing" type of test to obtain the task data for each sample.

The slip test data were obtained from tests using different apparatus in a fourth experiment. The apparatus consisted of a finger pad fitted with eight tactile sensors laid horizontally on a platform. Sample objects, which were loaded with different weights, were dragged across so that the motion could represent a slipping situation. The sensor

outputs were recorded during the motion of the sample between two fixed points. Two different sample objects were used with different combinations of weights.

The raw grasping and releasing data from each sensing site was plotted for each test, and visually verified before storing. This examination of the data was performed using the menu-driven graphical interface, Interactive Data Acquisition Tool (IDAT), of VAX-lab. The raw force data were pre-filtered before partitioning into 40 blocks of data, each block consisting of 100 sampled values of force per sensing site. To account for the nonlinearities of the sensor assembly, each sensor was modelled and calibrated using an expert system-based modelling and calibration technique. In this technique, three types of mathematical functions were fit to a set of input-output data, and the mean modelling error based on a least error square method was determined and displayed to the user. The embedded expert system component provided facilities to remodel or re-calibrate the system. The model parameters for all eight sensors were stored in the form of ASCII files. Using the sensor model parameters, the measured values of forces on each sensing site were converted to their corresponding values of applied force. From this data, force images were formed by thresholding the applied force values to obtain force primitives at each sensing site. The force images from the sensors were combined to form a tactile image.

After obtaining a tactile image, decision parameters were formulated to facilitate interpretation of the task status. For this purpose, a decision filter was designed and implemented using the MATLAB software library. The main factors considered for designing the decision filter were the transitional uncertainties, the number of sensors, and timing and accuracy considerations. It was found from the tests conducted on the prototype gripper system that there was a mean variation of about 8 % in the sensor readings for the same applied force for changes in the FSR material, the compliant backing, and the point of application of the force. These errors contributed to the transitional uncertainties. The time constraints and error tolerance were two factors which were very complex to determine for a practical system. The tradeoff between the pre-filter width (for a moving average type low pass filter) and the allowable loss of dynamic force information was investigated to design the low pass filter.

To select a suitable filter width, the decision parameters were obtained from a case study using grasping and releasing test data pertaining to one of the samples. Filters of different widths, namely, 5, 10, 15 and 20 points were applied to the same data and the decision parameters were analyzed to identify errors. The residual noise levels and the processing time to obtain the tactile image, were used as criteria to select a 10 point filter width for prefiltering. After considering noise and uncertainty criteria, a value of 50 g in the force domain was selected as the inter-threshold range with an allowable margin of 4 g (which is 8 % of 50) around each threshold point. To identify the real transitions

caused by a definite increase in the sensed force from those caused by noise and uncertainties, a dead band of 10 in terms of the number of samples was also created. In a separate case study, four arbitrarily selected dead bands (in time) of widths 5, 10, 15 and 20 points were incorporated in a decision filter and the decision parameters obtained in each case were analyzed to determine a trade-off among the following: the ability of the filter to reduce uncertain transitions, the loss of some of the real transitions, and the time taken to arrive at a decision. Out of the four filters selected, it was found that a 10-point dead band was suitable for the decision filter.

By incorporating the above factors, a decision filter was designed and implemented in two stages. The first stage of the decision filter obtained the following information from a tactile image: the positive and negative transitions in the tactile image, the sensors reporting positive and negative transitions, and the cumulative sum of forces on all the eight sensors expressed in terms of a cumulated primitive value.

The second stage of the filter used this information along with the spatial displacement of the object, reflected in the form of force gradients (with respect to time) at successive transitions, to determine whether the data belonged to a grasping, a releasing or an unclassified category. This produced a result in the form of an overall task status along with an estimated sensor confidence factor. During the operation, the percentage of sensors indicating positive transitions was used to assign a value for a grasping confidence factor, while the percentage showing negative transitions was used to obtain a value for a releasing confidence factor.

The object displacement was identified in the form of two distinct categories, static and dynamic. A static object displacement was defined as detected motion of the object occurring after the dead band period (10 msec) as against a dynamic displacement which was determined by the object displacement detected within the dead band time period. These two displacements were interpreted differently by the task status expert system.

The results obtained from the decision filter were validated by comparing cumulated values of grasped/released levels with the corresponding variations of cumulative primitive values of forces from all the sensors. The cumulative primitive force value is an indication of the total force on the gripper during the task.

After identifying the task status parameters to be displayed to a user, an on-line expert system was designed using KES [107], and implemented. The expert system determined a set of four force decision parameters and two object displacement parameters and displayed them to a user. From these decisions, it was possible for the user to know the status of an on-line operation. The force decision of the task status was derived from the maximum grasped and released levels identified during the immediate past, and from

the confidence levels in these decisions. The object displacement decisions were in the form of identified static and dynamic displacements obtained from the same block of data.

In order to integrate the various functional modules, two interface programs were designed and implemented. The first program performed the off-line tasks of modelling and calibration of the prototype tactile sensors. The second interface program was designed to integrate the following on-line functions: filtering the raw data, assigning force primitives and obtaining the tactile image, applying the decision filter to determine the status parameters, storing these parameters in files in a suitable form to enable access by the expert system, executing the Task status indicator expert system to display the task status, and optionally executing a second expert system which recommends the control action for successful completion of the task. Both interface programs were coded in the "C" programming language.

For sensor calibration and modelling, Interface Program I was executed. This program requested the user to input the modelling data in the form of pairs of input force and resultant analog sensor outputs for each sensor. These data were transferred to the modelling program which fitted suitable polynomials and stored the coefficients in designated files. If a remodelling or calibration was requested, the program sought new data from the user in the same format before activating the modelling/calibration expert system. The expert system displayed the modelling error in each case and compared it with the sensor uncertainty value which was determined and stored separately.

For task status identification, Interface Program II was used. The dynamic force data in four different categories of tests which involved nine selected samples were acquired in real time and the data were stored in ASCII files. Interface Program II first accepted a filename from which the real time data were obtained, as well as the number of data points to be used per block, the beginning block number, and the type of task attempted. Control was then transferred to the processing section of the program written using MATLAB library files. This program loaded the relevant files containing the sensor models and formed the tactile images for two blocks, each containing the designated number of points of data. The two images were then successively applied to the decision filter and two sets of task status parameters were evaluated and stored. The TSI (Task status indicator) expert system was then activated to read the decision parameters and interpret them in the form of force decision and object displacement parameters to a user. The two sets of task status parameters were successively displayed. The expert system stored the status parameters in separate files, which could be accessed by another expert system, or user, or another program. Interface Program II finally executed the CDI (Control decision indicator) expert system to display the recommended control actions for proceeding with the task. The complete sequence of operations described above was

tested with real time data obtained from four categories of tests, namely, independent grasping and releasing of nine samples, combined grasping and releasing of the nine samples, four repeatability tests, and four artificial slip tests.

To determine the suitability of the proposed scheme for real time tasks, performance validation packages were obtained from each set of grasping and/or releasing test data. A typical validation package consisted of the following information:

1. plots of raw sensor outputs from all the sensors,
2. plots of decision filter parameters and cumulated force primitives,
3. bar charts of TSI expert system outputs showing the force decision and object displacement decisions,
4. summary tables of TSI expert system display's for each block of data, and
5. summary table of CDI expert system output from two successive blocks of data.

The task status parameters obtained by the expert system were in the form of grasping and releasing levels and associated confidence levels for the two decisions, obtained from each block of data. The two object displacement parameters were the static and dynamic object displacements, determined relative to the gripper position at the beginning of a data block. These parameters evaluated from two successive data blocks were used to determine two control decision parameters, namely, "Conaction" and "Movcond".

A typical recommendation of the CDI expert system consisted of a "control action" and a "movement action". In the preliminary version of the CDI expert system, these were indicated by the two attributes, Conaction and Movcond, each specified with a corresponding value of confidence level. Using the concept of human-like interpretation of tactile information, a number of heuristic rules were incorporated in the CDI expert system.

Conaction indicated three types of decisions, each with its associated confidence level. They were: increase gripper force, do not increase gripper force, and maintain the same status. Movcond indicated the desired direction of movement of the gripper relative to the object in terms of a set of pre-defined directions. A confidence factor associated with the movement decision was also displayed. Using the test data from three samples, the control decisions were obtained for each of the three categories of tests. The recommended control actions were found to be consistent with the nature of the task.

By comparing the task status decisions determined by the TSI expert with plots showing the variation of forces on the gripper, and the raw force data plots, the correctness of the procedure was established. Using the task status information from the tables

showing the summary of the results displayed to the user, it was confirmed that the computer-aided procedure could be used to determine the on-line task status by processing the real time dynamic force data measured by the tactile sensors.

8.2. Conclusions

The goal of the project was to design develop and test a task oriented procedure to determine the status of a tactile sensing gripper during a task. This objective was achieved by analyzing the dynamic forces acquired during the task. The forces were obtained using a prototype gripper system and the force signals were utilized to produce a tactile image. The changing tactile images identified during a task were interpreted to reveal the status of a gripper.

The instantaneous normal forces measured by the prototype gripper system were found to represent the force impulses acting on the gripper fingers during a task. The variation of raw force data observed in the various test cases demonstrated the effectiveness of the prototype gripper system in capturing the grasping and releasing trends of the task. The filtering of the raw data using a 5 point moving average filter was found to be sufficient to eliminate random noise while preserving the dynamic information contained in the force data. The multi-level tactile imaging was found to be appropriate to identify variation of forces as small as 0.5 N and this was adequate to obtain discernible quantitative decision parameters for a set of selected tasks.

The contact status of the gripper displayed by the TSI expert system in the form of task status parameters provided a complete set of information about the task including the direction of object displacement relative to the gripper. Using this information, it was shown that an on-line task could be carried out successfully by initiating an appropriate corrective action determined from the contact status of the gripper. The static and dynamic displacements of the object occurring within a specified time interval were used to identify slippages of the object which had occurred in the recent past (100 ms time in the case study), and initiate corrective action in order to proceed with the task.

The integrated computer program developed to determine the task status was validated using experimental data obtained while performing a variety of grasping and releasing tasks using a laboratory prototype system. The results showed that the task status determined in various cases gave correct displays in 80 % of the tested cases. The interpretation of the decision parameters was performed by an embedded expert system in which a form of human decision making capability was incorporated. The task status obtained by using the task oriented procedure provided a sufficient set of information about the task which included the direction of object displacement relative to the gripper.

The technique used to formulate control decisions from on-line task data yielded control decisions which were found to be in agreement with human decisions which would have been taken under similar circumstances. In the case of a pure slip, this technique was able to recognize slip after the object had moved from the contacting sensor area. This was identified as the limitation of the procedure. Nevertheless, use of the integrated procedure for slip characterization was observed to be applicable for general purpose gripping tasks such as those used in the test cases.

From the test results, it was possible to determine control actions that a gripper would need to take to carry out the task. The control decision parameters indicated whether it was necessary to increase the gripper force, to decrease the gripper force, or to maintain the same force. The direction of gripper movement necessary to compensate for identified object movements with respect to the gripper was also indicated by the control decision parameters. The validity of the decisions from the TSI and CDI expert systems was demonstrated using summary tables showing the expert system displays after processing every two-block set of experimental data obtained while grasping and releasing nine different sample objects.

The results obtained at various stages of system implementation using four different categories of tests, were obtained in the form of validation packages and performance tables. The validation packages were defined separately for each category of test. The results from the validation packages demonstrated the correctness of the task oriented procedure. The significant results from each test category were used to highlight the various features of the integrated procedure.

8.3. Major Contributions

In achieving objectives of the project, the contributions in the area of robotic tactile sensing and data interpretation are evident. The first contribution is the development of a method to measure and store dynamic tactile forces during the performance of a task. The sensing of forces was achieved using a commercial piezoresistive transducer, called Force Sensing Resistor, used in its shunt mode of operation.

The method of dynamic force characterization using the tactile imaging technique is the second significant contribution in the area of tactile sensing. Tactile imaging techniques which have been attempted earlier obtained binary tactile images using a simple two-level thresholding technique. The main disadvantage of this technique was the inability of the images to identify small but definite variations in the gripper forces. By measuring the resultant value of normal gripper forces and using a multilevel thresholding, the method suggested in this thesis was able to extract additional information from finer variations of forces than those achieved by the binary imaging technique.

The modelling and calibration technique used to define the behaviour of the tactile sensors is a novel method of combining the powerful digital signal processing tools and the decision-making capability of the expert system into a single executable computer program. The knowledge required to model and calibrate complex systems, such as the tactile sensors, using a set of mathematical functions, have been captured in the expert system knowledge base so that a user can perform these tasks with relative ease. This method of modelling and calibration, which accepts a set of numerical input-output system data, is applicable to other practical systems which are very complex to model because of inherent interactions among various components of the system.

The development of a computer-aided integrated procedure to identify the task status from dynamic force data using an embedded expert system is a major contribution to the development of intelligent grippers. The suitability of the procedure, which has been demonstrated using a set of control decisions obtained from the CDI expert system, indicates the possibility of employing the task oriented procedure to achieve real time intelligent gripping of objects. Since the procedure was validated using experimental data obtained while performing real tasks on a set of selected laboratory samples, its applicability in a practical unstructured environment appears to be promising.

The task status obtained using the task oriented procedure provides a complete set of information about the task including the direction of object displacement relative to the gripper. The displacement of the object with respect to the gripper fingers was used to characterize slip. The slippage during grasping was assessed by observing the displacement of the object as well as any noticeable release of the object, as indicated by a decrease in the force primitive value in the tactile image. Slippage during releasing was characterized by an increase in the force primitive value of the tactile image during a releasing process along with the object displacement.

8.4. Future Directions

A definite first step in extending the work reported in this thesis is to study the recommendations of the control decision expert system using real data from some typical cases in which the task behaviour is abnormal. Examples of such situations may include the tasks using the parallel jaw gripper when the gripper speed is made unequal during grasping and releasing of objects. This will assist in identifying the maximum and minimum gripper velocities at which the procedure will be applicable. The recommended control actions may be translated into appropriate logic signals which may be implemented in hardware so as to develop a closed loop intelligent gripper system. The performance of such a system may be evaluated using bench mark tests designed to identify the task characteristics of the object twisting and rotation during grasping.

A second possible direction of investigation could be to develop a single expert system to perform functions of the TSI and CDI expert systems. Use of an object oriented programming language C++, may be considered to build this expert system. This might result in considerable savings in time necessary to arrive at a suitable control decision based on dynamic force data. This will expand the area of application of the task oriented procedure to include special purpose precision tasks.

The plots of raw data obtained from the artificial slip tests have shown the force gradients recorded by the sensors when the sample passed over them. In cases where the sample velocity was small, the TSI was able to detect the changing status. If the sample travelled faster so that force changes occurred in a time period less than 100 msec, then the task status indication was ambiguous. Increasing the sampling rate and reducing the block size are two suggested modifications to the proposed scheme to handle such cases. Further analysis in this direction will be required to determine the maximum speed at which slip is identifiable.

REFERENCES

1. Johansson, R. S. and Westling G. K. , "Roles of Glabrous Skin Receptors and Sensori-Motor Memory in Automatic Control of Precision Grip when Lifting Rougher or More Slippery Objects", *Experimental Brain Research*, Vol. 56, 1984, pp. 550-564.
2. Churchill, M., *Tactile Sensors for Robotics and Medicine* , John Wiley & Sons, New York, 1989, pp. 1-12.
3. Bolsinger, P. P. and Mai, N. , "A Microcomputer System for the Measurement of Finger Forces", *Journal of Biomedical Engineering*, Vol. 7, 1985, pp. 51-55.
4. Cooney, W. P. and Chao, E. Y. S. , "Biomechanical Analysis of Static Forces in the Thumb During Hand Function", *Journal of Bone Joint Surgery*, Vol. 59, 1977, pp. 28-36.
5. Neuman, M. R., Berec, A. and O'Connor, E., "Capacitive Sensors for Measuring Finger and Thumb Tip Forces", *IEEE Frontiers in Engineering and Comp. Health Care*, 1984, pp. 436-439.
6. Matlin, Margaret W., *Perception*, Allyn and Bacon Inc., Massachussets 02159, 1983, pp. 199-223, ch. 9.
7. Melzack, R. and Wall, P. D., "On the Nature of Cutaneous Sensory Mechanisms", *Brain*, Vol. 85 1962, pp. 331-352.
8. Melzack, R. and Wall, P. D., "Pain Mechanisms: A new Theory", *Science*, Vol. 150 1965, pp. 971-979.
9. Kenshalo, D., editor, *The Skin Senses*, Thomas, Springfield, Illinois, 1968.
10. Melzack, R. and Dennis, S. G., "Neurophysiological Foundations of Pain", in *The Psychology of Pain*, Sternbach, R. A., ed., Raven, New York, 1978.
11. Johansson, R. S. and Valbo, A. B. , "Tactile Sensory Coding in the Glabrous Skin of the Human Hand", *Trend in Neurosciences*, Vol. 6, 1983, pp. 27-31.
12. Johansson, R. S. and Westling G. K. , "Signals in Tactile Afferents from the Fingers Eliciting Adaptive Motor Responses during Precise Grip", *Experimental Brain Research*, Vol. 66, 1986, pp. 141-154.
13. Johansson, R. S. and Westling G. K. , "Coordinated Isometric Muscle Commands Adequately and Erroneously Programmed for the Weight during Lifting Task with Precision Grip", *Experimental Brain Research*, Vol. 71, 1988, pp. 59-71.
14. Harmon, Leon D, "Automated Tactile Sensing", *International Journal of Robotic Research*, Vol. 1, No. 2, Summer 1982..
15. Bejczy, Anatol K, "Sensory Systems For Automated Grasping and Object Handling", International Conference on Telemanipulators for the Physically Handicapped Rocquencourt, France, September, 4-6, 1978.
16. Hill, J. W. , MCGovern, D. E. and Sword, A. J., "Study to Design and Develop Remote Manipulator System", Tech. report NAS2-7507, NASA, 1973.

17. Vaidyanathan, Chelakara S., "A Tactile Sensing System for an Industrial Robot", *M.Sc. Thesis*, Department of Electrical Engineering, University of Saskatchewan, SK, Canada., 1987.
18. Westling, G. K., "Sensori-Motor Mechanisms during Precision Grip in Man", *UMEA Medical Dissertations*, Department of Physiology, University of Umea Sweden, 1986.
19. Westling, G. K. and Johansson, R. S. , "Factors Influencing Force Control during Precision Grip", *Experimental Brain Research*, Vol. 53, 1984, pp. 277-284.
20. Hillis, William Daniel., "Active Touch sensing", Tech. report A. I. Memo 629, Massachussets Institute of Technology, April 1981.
21. Dario, Paola, and Danillo De Rossi, "Tactile Sensors and the Gripping Challenge", *IEEE Spectrum*, August 1985.
22. Harmon Leon D, *Tactile Sensing*, Springer Verlag, NATO-ASI 1984..
23. Jacobsen, Stephen C, McCammon, Ian D., Biggers, Klaus B., and Phillips, Richard P., "Design of Tactile Sensing Systems for Dextrous Manipulators", *IEEE Control Systems Magazine*, Vol. 8, No. 1, February 1988, pp. 3-13.
24. Clark, James J., "A Magnetic Field Based Compliance Matching Sensor for High Resolution, High Compliance Tactile Sensing", *Proceedings of 1988 International Conference on Robotics and Automation*, Philadelphia, Pennsylvania, April 24-29 1988.
25. Jameson, J. W., "Analytic Techniques for Automated Grasp", *Ph.D. Thesis*, Department of Mechanical Engineering, Stanford University, CA, 1985.
26. Jameson, W. and Leifer, L.J., "Automatic Grasping : An Optimization Approach", *IEEE Transactions on Systems, Man and Cybernetics*, Vol. SMC-17(5), 1985, pp. 806-814.
27. Nguyen, V. D., "The Synthesis of Stable Grasps in the Plane", *Proceedings of IEEE Conference on Robotics and Automation*, 1986, pp. 884-889.
28. Nguyen, V. D., "Constructing Stable Grasps in 3D", *Proceedings of IEEE Conference on Robotics and Automation*, 1987, pp. 240-245.
29. Nguyen, Van-Duc, "Constructing Force Closure Grasps", *The International Journal of Robotic Research*, Vol. 3, No. 3, June 1988.
30. Berkemeier, M. and Fearing, R. S., "Determining the Axis of a Surface of Revolution Using Tactile Sensing", *Proceedings of 1990 IEEE International Conference on Robotics and Automation*, 1990, pp. 974-979.
31. Fearing, R. S., "Simplified Grasping and Manipulation with Dextrous Robot Hands", *IEEE Journal of Robotics and Automation*, Vol. RA-2(4), 1986, pp. 188-195.
32. Fearing, R. S., "Implementing a Force Strategy for Object Re-orientation", *Proceedings of IEEE Conference on Robotics and Automation*, 1986, pp. 96-102.

33. Sladek, E. and Fearing, R. S., "The Dynamic Response of a Tactile Sensor", *Proceedings of 1990 IEEE International Conference on Robotics and Automation*, 1990, pp. 962-967.
34. Kerr, J. and Roth, B., "Analysis of Multifingered Hands", *International Journal of Robotic Research*, Vol. 4(4), Winter 1986, pp. 3-17.
35. Feddema, J. T. and Ahmad, S., "Determining a Static Robot Grasp for Automated Assembly", *Proceedings of IEEE Conference on Robotics and Automation*, 1986, pp. 918-924.
36. Kerr, J. and Roth, B., "Special Grasping Configurations with Dextrous Hands", *Proceedings of IEEE Conference on Robotics and Automation*, 1986, pp. 1361-1367.
37. Yoshikawa, T., *Analysis and Control of Robot Manipulators with Redundancy*, MIT Press, 1984, pp. 735-747.
38. Yoshikawa, T. and Zheng, X., "Coordinated Dynamic Hybrid Position/Force Control for Multiple Robot Manipulators Handling One Constrained Object", *Proceedings of 1990 IEEE International Conference on Robotics and Automation*, 1990, pp. 1178-1183.
39. Dudar, A. M. and Eltimsahy, A. H., "A Near-Minimum Time Controller for Two Coordinating Robots Grasping an Object", *Proceedings of 1990 IEEE International Conference on Robotics and Automation*, 1990, pp. 1184-1189.
40. Lyons, D. , "A Process-Based Approach to Task Plan Representation", *Proceedings of 1990 IEEE International Conference on Robotics and Automation*, 1990, pp. 2142-2147.
41. Kumar, V. and Waldron, K. J., "Sub-optimal Algorithms for Force Distribution in Multifingered Grippers", *Proceedings of IEEE Conference on Robotics and Automation*, 1987, pp. 252-257.
42. Cutkosky, M. R. and Wright, P. k., "Friction Stability and Design of Robotic Fingers", *International Journal of Robotic Research*, Vol. 5(4), Winter 1987, pp. 20-37.
43. Kenaley, G. L. and Cutkosky, M. R., "Electrorheological Fluid-based Robotic Fingers with Tactile Sensing", *Proceedings of 1989 IEEE International Conference on Robotics and Automation*, 1989.
44. Prasad, A. and Cutkosky, M. R., "Manipulating with Soft Fingers: Modelling Contacts and Dynamics", *Proceedings of 1989 IEEE International Conference on Robotics and Automation*, 1989.
45. Li, Z. and Sastry, S., "Task Oriented Optimal Grasping by Multifingered Robot Hands", *Proceedings of IEEE Conference on Robotics and Automation*, 1987, pp. 389-394.
46. Zhuang, H. , Roth, Z. and Hamano, F., "A Complete and Parametrically Continuous Kinematic Model for Robot Manipulators", *Proceedings of 1990 IEEE International Conference on Robotics and Automation*, 1990, pp. 92-97.

47. Tomovic, R., Bekey, G. A. and Karplus, W. J., "A Strategy for Grasp Synthesis with Multifingered Robot Hands", *Proceedings of IEEE Conference on Robotics and Automation*, 1987, pp. 83-89.
48. Lyons, D. M., "A Simple Set of Grasps for Dextrous Hand", *Proceedings of IEEE Conference on Robotics and Automation*, 1985, pp. 588-593.
49. Stephanou, H. K. and Erkman, A.M., "Evidential Classification of Dextrous Grasps for the Integration of Perception and Action", *Journal of Robotic Systems*, Vol. 5(4) 1988, pp. 309-336.
50. Biggers, K. G., Jacobsen, S. C. and Gerpheide, G. E., "Low level Control of the Utah/MIT Dextrous Hand", *Proceedings of IEEE Conference on Robotics and Automation*, 1986, pp. 61-66.
51. Iberall, T., "The Nature of Human Prehension : Three Dextrous Hands in One", *Proceedings of IEEE Conference on Robotics and Automation*, 1987, pp. 396-401.
52. Lyons, D. M., "Tagged Potential Fields : An Approach to Specification of Complex Manipulator Configurations", *Proceedings of IEEE Conference on Robotics and Automation*, 1986, pp. 1749-1754.
53. Ahmad, S. and Lee, C., "Shape Recovery from Contour-Tracking with Force Feedback", *Proceedings of 1990 IEEE International Conference on Robotics and Automation*, 1990, pp. 447-452.
54. Allen, P. K. and Bajczy, *Two Sensors are Better than One: Example of Integration of Vision and Touch*, MIT Press, 1986, pp. 59-64.
55. Roberts, K., "Robot Active Touch Exploration: Constraints and Strategies ", *Proceedings of 1990 IEEE International Conference on Robotics and Automation*, 1990, pp. 980-985.
56. Dario, P. and Butazzo, G., "An Anthropomorphic Robot Finger for Investigating Artificial Tactile Perception", *International Journal of Robotic Research*, Vol. 6(3), Fall 1987, pp. 25-48.
57. Dario, P., Bergamasco, M., Femi, D., Fiorillo, A., Vaccarelli, A., "Tactile Perception in Unstructured Environments: A Case Study for Rehabilitative Robotics Applications", *Proceedings of IEEE Conference on Robotics and Automation*, 1987, pp. 2047-2054.
58. Jacobsen, S. C., McCammon, I. D., Biggers, K. B. and Phillips, R. P., "Tactile Sensing System Design Issues in Machine Manipulation", *Proceedings of IEEE Conference on Robotics and Automation*, 1987, pp. 2087-2096.
59. Allen, P. , "Mapping Haptic Exploratory Procedures to Multiple Shape Representations", *Proceedings of 1990 IEEE International Conference on Robotics and Automation*, 1990, pp. 1679-1684.
60. Paul, R. P., Durrant-Whyte, H. F. and Mintz, M., *A Robot Distributed Sensor and Actuation Robot Control System*, MIT Press, 1986, pp. 93-100.
61. Durrant_Whyte, H. F., Rao, B. Y. S. and Hu, H. , "Toward a Fully Decentralized

- Architecture for Multi-Sensor Data Fusion”, *Proceedings of 1990 IEEE International Conference on Robotics and Automation*, 1990, pp. 1331-1336.
62. Hackett, J. K. and Shah, M. , “Multi-Sensor Fusion: A Perspective”, *Proceedings of 1990 IEEE International Conference on Robotics and Automation*, 1990, pp. 1324-1330.
 63. Durrant-Whyte, H. F., “Consistent Integration and Propagation of Disparate Sensor Observations”, *International Journal of Robotic Research*, Vol. 6(3), Fall 1987, pp. 3-24.
 64. Smith, R. C. and Cheeseman, P., “On the representation and Estimation of Spatial Uncertainty”, *International Journal of Robotic Research*, Vol. 5(4), Winter 1987, pp. 56-68.
 65. Brost, R. C., “Automatic Grasp Planning in Presence of Uncertainty”, *Proceedings of IEEE Conference on Robotics and Automation*, 1986, pp. 1575-1581.
 66. Donald, B. R., “Robot Motion Planning with Uncertainty in the Geometric Models of the Robot and Environment: A Formal Framework for Error Detection and Recovery”, *Proceedings of IEEE Conference on Robotics and Automation*, 1987, pp. 1588-1593.
 67. Cameron, Alec., David, Ron and Durrant-Whyte, Hugh, “Touch and Motion”, *Proceedings of 1988 International Conference on Robotics and Automation*, Philadelphia, Pennsylvania, April 1988, pp. 1062-1067.
 68. Kazerooni, H., “Direct- Drive Active Compliant End Effector (Active RCC)”, *IEEE Journal of Robotics and Automation*, Vol. 4, No. 3, June 1988.
 69. Montana, David J., “ The Kinematics of Contact and Grasp”, *The International Journal of Robotic Research*, Vol. 7, No. 3, June 1988, pp. 17-32.
 70. Hollerbach, J. M., Narasmhan, S. and Wood, J. E., “Finger Force Computation without the Grip Jacobian”, *Proceedings of IEEE Conference on Robotics and Automation*, 1986, pp. 871-875.
 71. Luo, Ren C. and Loh Horng-Hai, “ Tactile array Sensor for Object Identification Using Complex Moments”, *Journal of Robotic Systems*, Vol. 5(1), 1988, pp. 1-12.
 72. Howe, R. D. and Cutkosky, M. R., “Sensing Skin Acceleration for Slip and Texture Perception”, *Proceedings of 1989 IEEE International Conference on Robotics and Automation*, 1989.
 73. Howe, R. D., Popp, N., Akella, P., Kao, I. and Cutkosky, M. R. , “Grasping, Manipulation, and Control with Tactile Sensing ”, *Proceedings of 1990 IEEE International Conference on Robotics and Automation*, 1990, pp. 1258-1263.
 74. Falcidieno, B. and Giannini, F. , “A System for Extracting and Representing Feature Information Driven by the Application Context”, *Proceedings of 1990 IEEE International Conference on Robotics and Automation*, 1990, pp. 1672-1678.
 75. Ellis, R. E., Riseman, E. M. and Hanson, A. R., “Tactile Recognition by Probing: Identifying a Polygon on a Plane”, *Proceedings of National Conference on Artificial Intelligence*, 1986, pp. 632-637.

76. Grimson, W. E. L., Lozano-Perez, T., "Model-Based Recognition and Localization from Sparse Range or Tactile Data", *International Journal of Robotic Research*, Vol. 3(3), Fall 1984, pp. 3-35.
77. Salisbury, J. K., *Interpretations of Contact Geometries from Force Measurements*, MIT Press, 1984, pp. 565- 577.
78. Lee, S. and Hahn, H. , "An Optimal Sensing Strategy of a Proximity Sensor System for Recognition and Localization of Polyhedral Objects", *Proceedings of 1990 IEEE International Conference on Robotics and Automation*, 1990, pp. 1666-1671.
79. Erdmann, M. , "Randomization in Robot Tasks", *Proceedings of 1990 IEEE International Conference on Robotics and Automation*, 1990, pp. 1744-1749.
80. Nguyen, T. and Stephanou, H., "A Topological Algorithm for Continuous Grasp Planning", *Proceedings of 1990 IEEE International Conference on Robotics and Automation*, 1990, pp. 670-675.
81. Stewart, D., Schmitz, D. and Khosla, P. , "Implementing Real-Time Robotic Systems Using CHIMERA II", *Proceedings of 1990 IEEE International Conference on Robotics and Automation*, 1990, pp. 598-603.
82. Houshangi, N. , "Control of a Robotic Manipulator to Grasp a Moving Target Using Vision", *Proceedings of 1990 IEEE International Conference on Robotics and Automation*, 1990, pp. 604-609.
83. Walker, I. , "The Use of Kinematic Redundancy in Reducing Impact and Contact Effects in Manipulation", *Proceedings of 1990 IEEE International Conference on Robotics and Automation*, 1990, pp. 434-439.
84. Mills, J. , "Manipulator Transition To and From Contact Tasks: A Discontinuous Control Approach", *Proceedings of 1990 IEEE International Conference on Robotics and Automation*, 1990, pp. 440-446.
85. Newman, W. and Branicky, M. , "Experiments in Reflex Control for Industrial Manipulators", *Proceedings of 1990 IEEE International Conference on Robotics and Automation*, 1990, pp. 266-272.
86. Goldberg, K. Y. and Mason, M. T. , "Bayesian Grasping", *Proceedings of 1990 IEEE International Conference on Robotics and Automation*, 1990, pp. 1264-1269.
87. Stansfield, S. A. , "Knowledge-Based Robotic Grasping", *Proceedings of 1990 IEEE International Conference on Robotics and Automation*, 1990, pp. 1270-1276.
88. Tan, M. , "CSL: A Cost Sensitive Learning System for Sensing and Grasping Objects", *Proceedings of 1990 IEEE International Conference on Robotics and Automation*, 1990, pp. 858-863.
89. Kaneko, M. and Tanie, K. , "Contact-Point Detection for Grasping of an Unknown Object Using Self-Posture Changeability (SPC)", *Proceedings of 1990 IEEE International Conference on Robotics and Automation*, 1990, pp. 864-869.

90. Laugier, C. , Ijel, A and Trocazz, J. , "Combining Vision Based Information and Partial Geometric Models in Automatic Grasping", *Proceedings of 1990 IEEE International Conference on Robotics and Automation*, 1990, pp. 676-682.
91. Park, Y. and Starr, G. , "Optimal Grasping Using a Multifingered Robot Hand", *Proceedings of 1990 IEEE International Conference on Robotics and Automation*, 1990, pp. 689-694.
92. Purbick, John A, "A Force Transducer Employing Conductive Silicone Rubber", *Proceedings of the First International conference on Robot Vision and Sensory controls*, Stanford-upon-Avon, England, April 1981., 1-3
93. *Force Sensing Resistors*, Interlink Electronics, Santa Barbara, CA 93103, 1986.
94. Tise, Bert, "A Compact High Resolution Piezoresistive Digital Tactile Sensor", *Proceedings of IEEE Conference on Robotics and Automation*, 1988, pp. 760-764.
95. Digital Equipment Corporation, Massachussetts, U.S.A., *ADQ32 A/D Converter Module User's Guide* , 1990.
96. Digital Equipment Corporation, Massachussetts, U.S.A., *VAXlab - A guide to Laboratory I/O routines*, 1990.
97. Mitsubishi Corp., Japan., *Move master Micro-robot RM 101 - Instruction Manual*, 1983.
98. Sladek, E. M. and Fearing, R. S. , "The dynamic Response of a Tactile Sensor ", *Proceedings of the 1990 IEEE International Conference on Robotics and Automation*, 1990, pp. 962-967.
99. Dinnar, U., *A Note on the Theory of Deformation in Compressed Skin Tissues*, American Elsevier Publishing Company, New York, 1970.
100. Mase, G. E., *Schaum's Outline of Theory and and Problems in Continuum Mechanics*, McGraw-Hill Book Company, New York, NY, 1970.
101. Ziegler, B. P., *Theory of Modelling and Simulation*, John Wiley and Sons, New York, NY, 1976.
102. Lastman, G. J. and Sinha, N. K., *Approximation of Functions: Interpolation and Curve Fitting*, Saunders College Publishing, HRW Inc., New York, 1989.
103. Todd, J, *A Survey of Numerical Analysis*, McGraw-Hill Book Company, New York, NY, 1962.
104. de Boor, Carl, *A Practical Guide to Splines*, Springer-Verlag, New York , 1978, Applied Mathematical Sciences Series - 27
105. Woods, D. J. , "Department of Mathematical Sciences Report", Tech. report 85-5 , Rice University, 1985.
106. Berenson, M. L. and Levine, D. M., *Basic Business Statitics, Concepts and Applications*, Prentice Hall, New Jersey, 1989, Fourth edition.
107. Software Architecture & Engineering Inc., *KES Knowledge Base Author's Manual*, 1989.

108. Vaidyanathan, C. S., "Uncertainties in a Tactile Sensing System for an Industrial Robot", Term Project Report, Department of Electrical Engineering, University of Saskatchewan, SK, Canada, April 1988.
109. The Mathworks Inc., *PRO-MATLAB for Sun workstations - user's Guide*, 1987.
110. Vaidyanathan, C. S., "Listing of the Task Status Indicator Expert System Knowledge Base", Project Report, Department of Electrical Engineering, University of Saskatchewan, SK, Canada, Dec. 1990.
111. Software Architecture & Engineering Inc., *KES Knowledge Base Reference Manual*, 1989.
112. Patterson, Robert W., "Development of a Dynamic Touch Sensor", *Ph.D Dissertation*, Aug. 1985.
113. Prasad, A. and Cutkosky, M. R. , "Manipulating with Soft Fingers: Modelling Contacts and Dynamics ", *Proceedings of IEEE Conference on Robotics and Automation*, Scottsdale, Arizona, 1989, pp. 764-769.
114. Sidhu, T. S., "Protection of Power Transformers", *Ph.D Thesis*, Department of Electrical Engineering, University of Saskatchewan, Saskatoon, Canada., 1989.
115. Newman, M., *Industrial Electronics and Controls* , John Wiley & Sons, New York, 1986, pp. 443-446.
116. Siegel, R.E., *Galen on Sense Perception, Chapter V*, 1970.
117. Vallbo, A.B, and Johansson, R. S., *The Tactile Sensory Innervation of the Glabrous Skin of the Human Hand*, Pergamon Press, New York , 1978.
118. Weber, E. H. , "Uber den Tastsinn", *Arch. Anat. Physiol.*, Vol. , No. 1835, pp. 152-159.
119. Harmon, L. D. , "Touch-Sensing Technology: A Review", Tech. report MSR80-83, SME Report, 1980.
120. Mehdian, M. and Rahnejat, H. , "A Sensory Gripper Using Tactile Sensors for Object Recognition, Orientation Control, and Stable Manipulation", *IEEE Transactions on Systems, Man and Cybernetics*, Vol. 19, No. 51989, pp. 1250-1261.
121. Snyder, W. E. and St. Clair, J. , "Conductive Elastomers as Sensors for Industrial Parts Handling Equipment", *IEEE Transactions on Instrumentation and Measurement*, Vol. IM-27, No. 11978, pp. 94-99.
122. Pati, Y. C., Friedman, D., Krishnaprasad, P. S., Yao, C. T., Peckerar, Yang, R., and Marrian, C. R. K. , "Neural Networks for Tactile Perception", Tech. report 88 , University of Maryland, U.S. Naval Research Laboratory, Washington, D.C., 1988.

A. Specifications of the Prototype Gripper System Hardware

Table A.1: Specifications of RM-101 MICROBOT Robot .

Construction	Jointed, metal plate
Degrees of freedom	5
Operational angular coverage ²	
Rotation of body	240°
Rotation of shoulder	150° (75° forward, 75° back)
Rotation of elbow	120° (75° forward, 45° back)
Bending of wrist	180°
Rotation of wrist	360°
Grasp of hand ³	80 mm (maximum)
Lifting capacity	500 g excluding the weight of hand
Maximum operating speed	7 cm/s
Positioning precision ⁴	0.3 mm
Control section	
Drive motors	6 stepper motors
Speed control	Trapezoidal waveform control
Axial control	Simultaneous control of all 6 axes
Interfaces	Centronix type
Programming languages	Assembler, M-ROLY, BASIC
Power supply	115 V AC, 50/60 Hz, 60 W
Weight	Approximately 10 Kg
Accessories	2 Hand attachments

- Notes: 1. These specifications are based on the use of the standard hand.
2. The specifications in parentheses are with the home position as base.
3. The gripping force of the hand without tactile sensors is approximately 800 g.
4. The rated positioning precision is when the arm is at 80° and the forearm is perpendicular to the surface on which the robot base is placed.

A.1. Implementation of an ARIEL DSP-16 DAS for Force Data Acquisition

The DSP-16 based DAS consists of a module equipped with a TMS 320C25 microprocessor capable of executing 5 million instructions per second. It is provided with a large (256K) dynamic RAM to store and display real time data. The DAS allows full data buffer (of 5.2 s) to be loaded with a signal at a sampling rate ranging from 1 KHz to 50 KHz. The signal may be displayed either numerically or graphically, before saving the acquired data into a disk. The Analog to Digital (A/D) converter has a 10 μ s conversion time and the front end is provided with signal conditioning and prefiltering to ensure 16 bit accuracy of the A/D converter. For testing the suitability of this DAS for acquiring dynamic forces, a test apparatus was built in the laboratory. The main constituents of data acquisition are shown in the block diagram of Figure A.1. The outputs from eight tactile

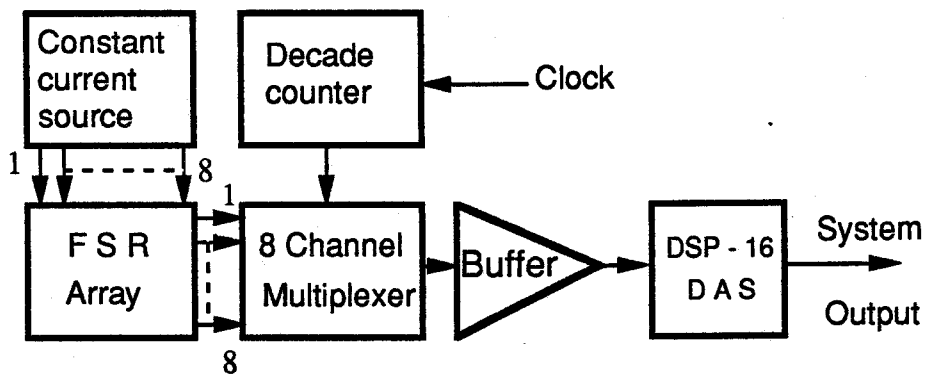


Figure A.1: Block diagram of data acquisition system using DSP-16 system .

sensing sites were multiplexed using an 8 channel CMOS multiplexer (CD 8051 device) and the resulting analog voltages were input to the DAS using a buffer stage. The multiplexer channel selection was asynchronously performed using a decade counter driven by a separate clock. The eight sensing sites were distributed equally between the two jaws of a parallel jaw robotic gripper which was used to hold a sample object. The dynamic forces were recorded while the object was being grasped. A profile of raw data was obtained by measuring the digitized voltage values. Since the input to the DAS was via a serial port, the multiplexer channels were switched cyclically which resulted in the sequential acquisition of (from channel 0 to channel 7) data from sensors. The individual sensor data were separated into files and the dynamic forces recorded by each of the eight sensors were plotted. Figure A.2 shows the dynamic forces measured by sensor #1 plotted against the time of the grasping operation. This data showed some unexpected behaviour and was thoroughly investigated. The inferences are described in the next section.

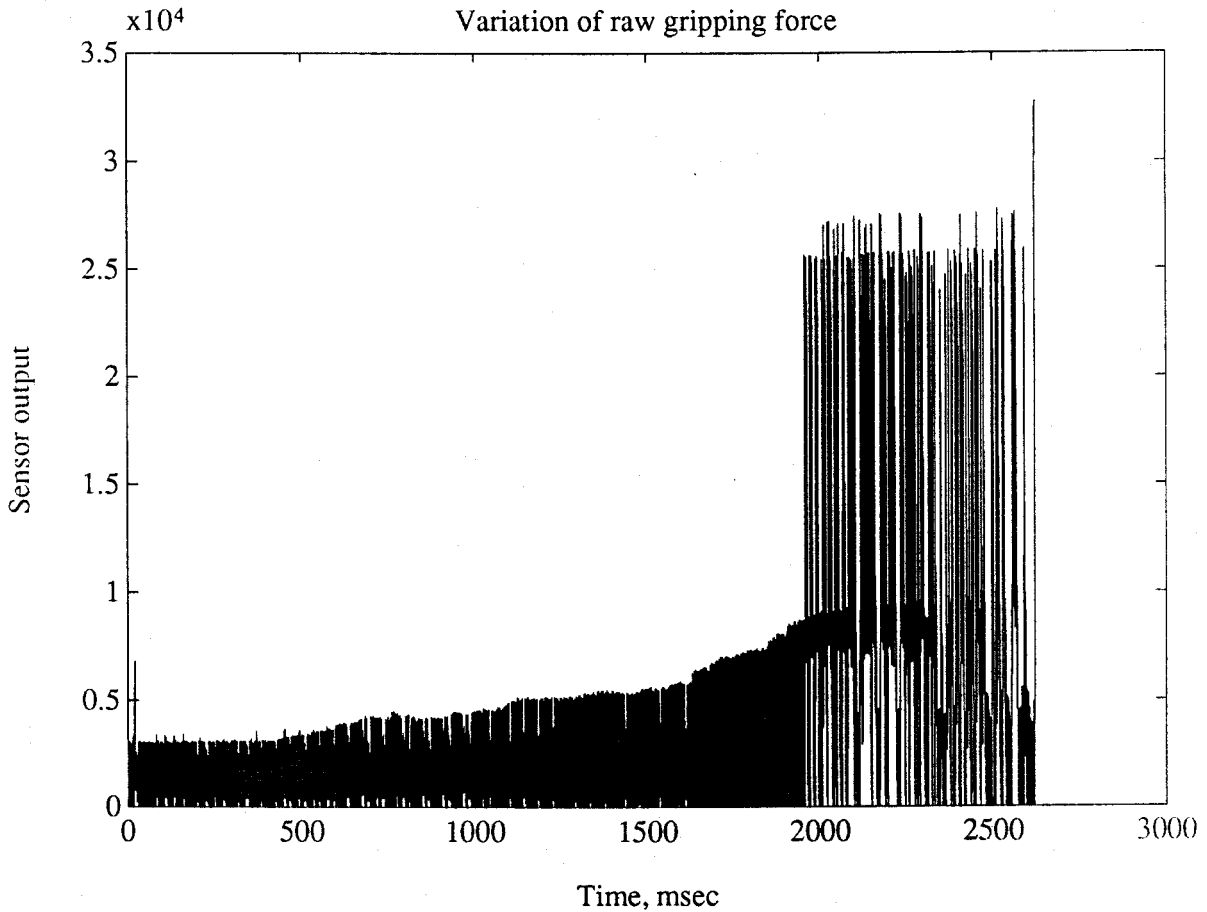
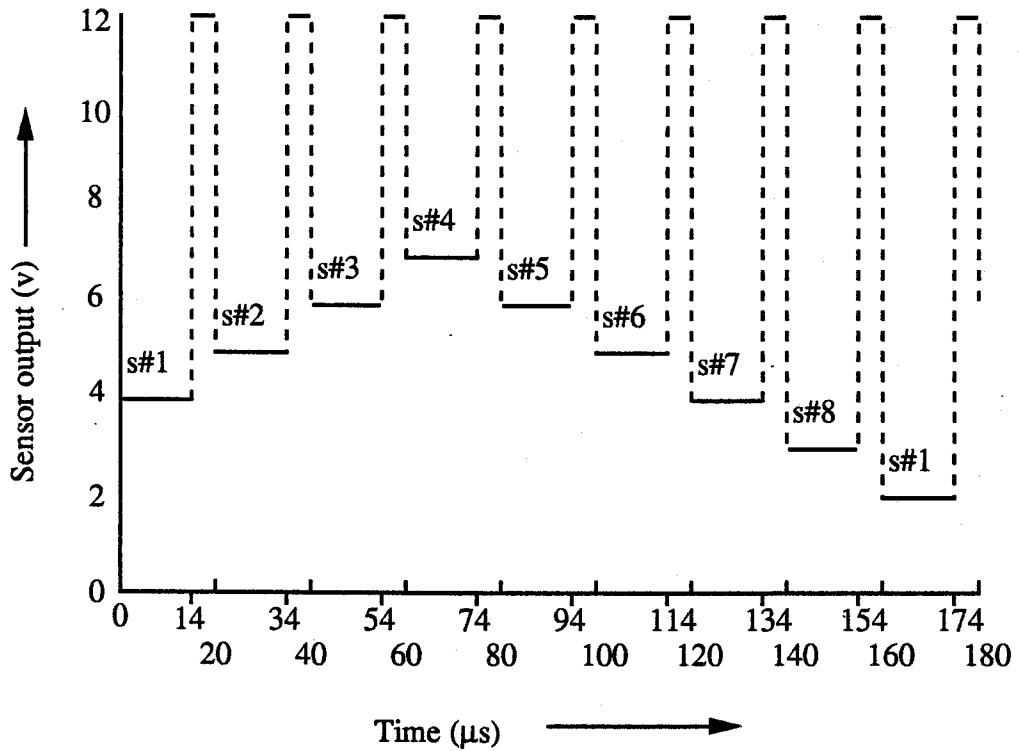
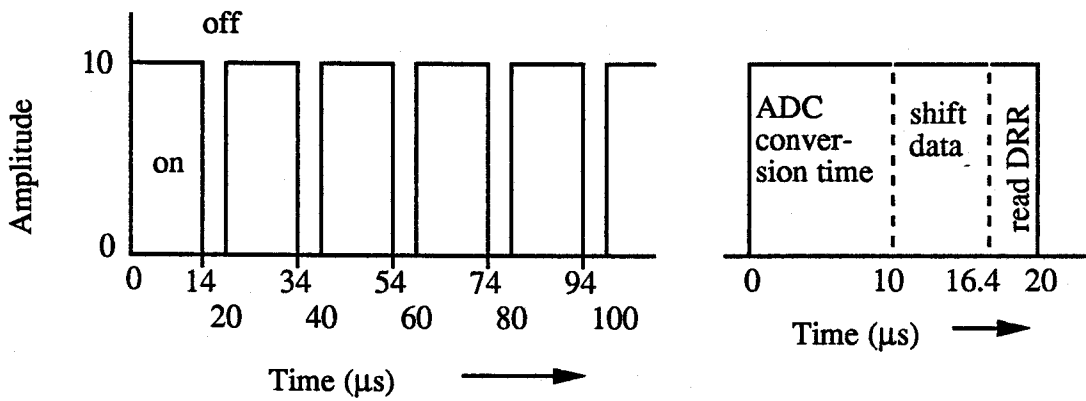


Figure A.2: Grasping forces measured by sensor #1 using DSP-16 system .

It was found that the serial mode of data acquisition using asynchronous switching of eight channels introduced additional noise. Figure A.3(a) shows the analog output from the eight-channel multiplexer which switches sensors 1 to 8 sequentially. The switching instant was controlled by an "enable clock pulse" whose waveform is shown in Figure A.3(b). This pulse shape was selected to ensure good isolation between the channels. In the ARIEL DSP-16 data acquisition system, the two channel A/D converter's 16-bit serial output was connected to the serial input of the TMS320 processor. When properly initialized, an internal interrupt, RINT, is generated whenever the TMS320's serial port Data receive register (DRR) is full. The RINT interrupt indicates that a new sample is available for the TMS320 program. The time available to read a sample is dependent on the sample rate and the time required to shift in a sample. The latter is fixed at $6.4 \mu\text{s}$ (32 instructions). At a sample rate of 50 KHz ($20 \mu\text{s}$), an interrupt is generated every $10 \mu\text{s}$, leaving $10 - 6.4 = 3.6 \mu\text{s}$ to read the DRR. These are shown in Figure A.3(c).



(a) : Analog output from the multiplexer



(b) : Waveform of "Enable" clock

(c) : DSP-16 DAS sample timing

Figure A.3: Analog output from the multiplexer, typical clock waveform and timing partition diagram of DSP-16 DAS .

The data acquired using such a system would not be corrupted if synchronous sam-

pling is employed. This would require additional hardware to be attached to the system [114] and development of a program to read and store the acquired data after digitization. In the asynchronous method of sampling, the the sampling clock of the DSP-16 DAS started the sampling after a preset time delay. If the first point of sampling occurred within the $14 \mu\text{s}$ 'ON' time of the enable clock pulse, then the acquired data was relatively clean. However, if the first sampling occurred anytime within the $6 \mu\text{s}$ 'OFF' time of the pulse, then the signal obtained was contaminated with noise.

A.2. Design of the gripper motor controller

A stepper motor used was a pulsed electric motor whose shaft incrementally rotated through a specified angle for each input pulse applied. Figure A.4 shows the block diagram of the logic and drive circuitry used for controlling the gripper motor. Two

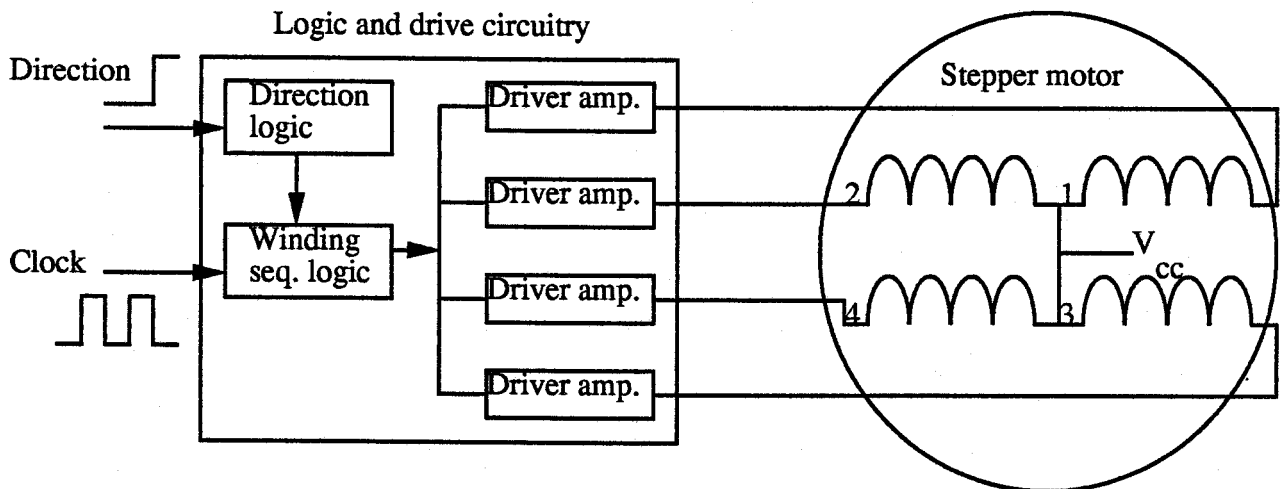


Figure A.4: Block diagram of logic and drive circuitry for a stepper motor [from Martin [115], Fig. K.1, page 443].

inputs were used to control the stepper motor; a stepping (clock) pulse and a logic level that determined the direction of rotation. The logic circuit shown in Figure A.4 converted each clock pulse into four output pulses with a specific phase relationship, which was necessary for correct motor rotation. The output pulses controlled the four driver amplifiers connected to the motor windings (1, 2, 3 and 4).

Figure A.5 shows the current pulse sequence used to rotate the two-phase four-winding stepper motor (provided in the robot RM-101). Logic 1 (ON) corresponds to the

presence of current excitation, and logic 0 (OFF) denotes the absence of current excitation. A 50 % overlap was used between windings 1 and 3, as well as between windings 2 and 4. The pulse train sequence shown is for clockwise rotation of the motor; for counter-clockwise rotation, the sequence was reversed.

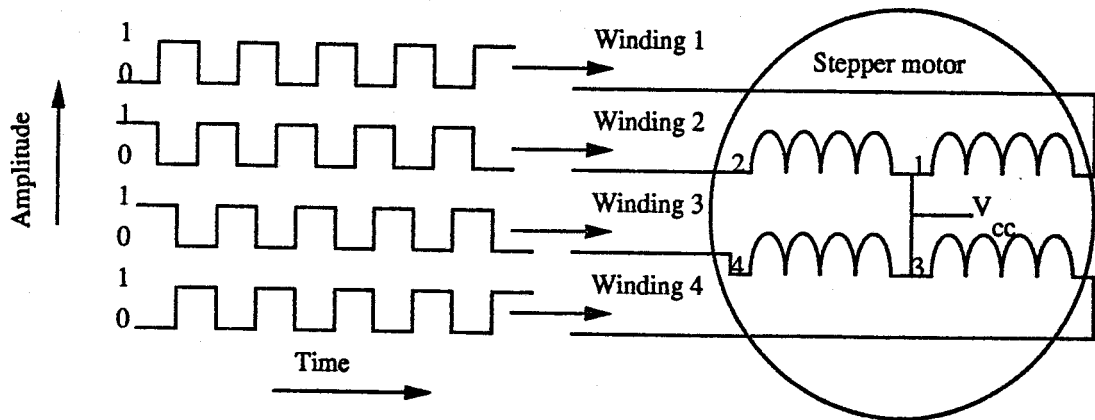


Figure A.5: Current pulse sequence for a two-phase, four winding stepper motor [from Martin [115], Fig. K.2, page 444].

Another important consideration in the design of the controller was the current delivering capability of the driver amplifier stage. The driver amplifier used was a power switch shown in Figure A.6.

The 18 K resistor was used as a current limiting resistor, and the diode was used to provide a path to dissipate the energy stored in the motor winding when the power transistor was switched from ON to OFF. In the absence of this diode, a large transient voltage spike appearing across the motor winding could result in damage to the transistor. To enhance the current delivery to the windings, a Darlington connection was used.

The complete block diagram of the motor controller designed for the prototype system is shown in Figure A.7. The logic required to generate the four overlapping square waves was realized using two J-K flip-flops. The direction input to the logic circuit, indicated in Figure A.7 controls the logic sequence into the four driver amplifiers. The sequencing continued as long as the input (clock) pulses were present. When the pulses were interrupted, the shaft remained at the last commanded position. A double-pole push-button switch was connected to facilitate change of direction of rotation. This feature

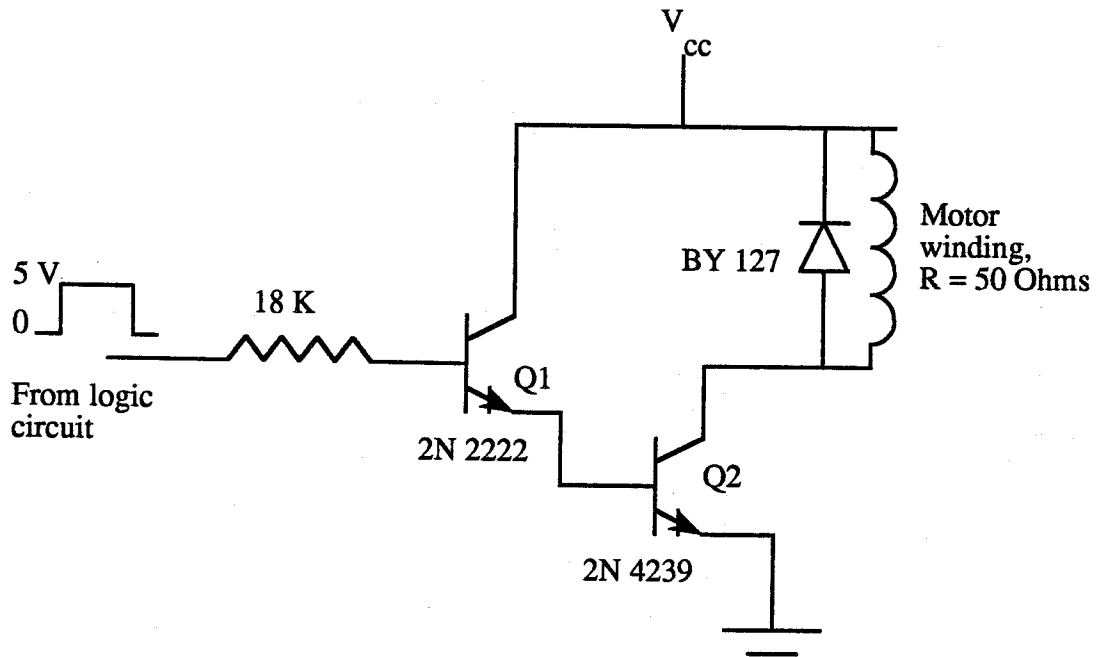


Figure A.6: A driver amplifier for stepper motor control .

enabled the combined grasping and releasing tests to be conducted on sample objects without interruptions. A Darlington driver stage was designed to provide the 250 mA load current per phase required for operating the motor at the rated speed of 7 cm/s.

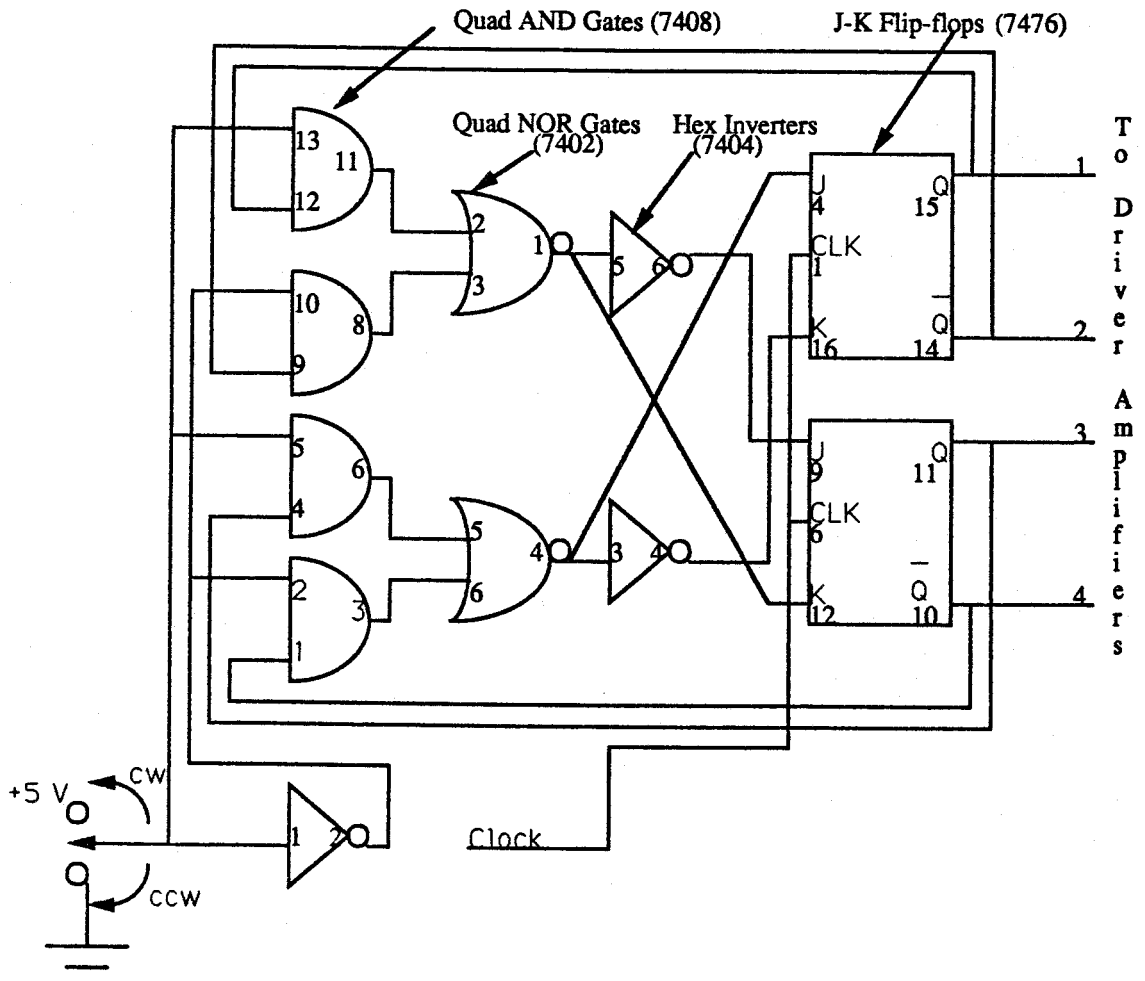


Figure A.7: The complete diagram of the stepper motor control for actuating the grippers of the RM-101 robot

B. Results of Model Development for the Prototype Gripper System

B.1. Listing of the Modelling and Calibration Expert System Knowledge Base

constants:

banner: "*****"

b11: "",
"The system will be treated as a single",
"block and will be modelled using a set of",
"five mathematical functions",
"".

b12: "",
"The data will be used to validate the five models",
"to determine normalized errors. Using these",
"errors as criterion, the best choice of the model",
"will be recommended for your system".

b13: "",
"Please show the errors in using other models".

b14: "",
"Please continue and show error in using this model".

nne: "",
"The Modelling/Calibration is completed".

%

text:

```
{purpose: banner,  
  "",  
  "Welcome to the online Modelling and Calibration ",  
  "knowledge base",  
  "",  
  "This Expert System will guide you to develop",  
  "the best possible model for your system.",
```

```

    "It will determine the best model based",
    "on the normalized mean square error criterion",
    "",
    banner}

```

```

{user1: banner,
  "Your system will be characterized using five",
  "selected functions to determine the best choice",
  "",
  "The data format is assumed to be the following:",
  "",
  "System input-output data Format:.",
  "",
  "Paired values of input( force) ",
  "versus the output (analog sensor output), one set",
  "per line, each set terminated with a <cr>.",
  "Data stored as an ASCII file",
  banner}

```

```

{user2: banner,
  "Your system will be calibrated using all the five",
  "models to determine the best choice.",
  "",
  "The data format is assumed to be the following:",
  "",
  "System input-output data Format:.",
  "",
  "Paired values of input( force) ",
  "versus the output (analog sensor output), one set",
  "per line, each set terminated with a <cr>.",
  "Data stored as an ASCII file",
  banner}

```

```

%
attributes:

```

```

\system control attributes

```

```

  trace_option: sgl (yes, *no)

```

```

    {question: "",
      "Do you wish to see a trace of the",
      "expert system's execution for the duration",
      "of this session"}.

```

```

  what_next: sgl (yes, *no)

```

```

    {question: "",
      "Do you wish to remodel or recalibrate your",
      "tactile sensing system with a new set of data ?",
      ""}.

```

```

\input attributes

```

```

sysaction: sgl (modelling{explain: bl1},
               calibration{explain:bl2},
               none{explain:nne})
{question: "",
  "What do you want to do"}
{explain:"",
  bl1,
  "",
  bl2,
  "",
  nne}.

useroption: sgl (showothers{explain: bl3},
                dontbother{explain:bl4})
{question: "",
  "What do you want to do"}
{explain:"",
  bl3,
  "",
  bl4}.

uncert: real
[constraint : uncert ge 0 and uncert le 100]
{question: "",
  "Enter a value for the system uncertainty.",
  "If unknown enter 0"}.

err1: real
[constraint : err1 ge 0 and err1 le 10000].

err2: real
[constraint : err2 ge 0 and err2 le 10000].

err3: real
[constraint : err3 ge 0 and err3 le 10000].

err4: real
[constraint : err4 ge 0 and err4 le 10000].

err5: real
[constraint : err5 ge 0 and err5 le 10000].

errmin: real
[constraint : errmin ge 0 and errmin le 10000].

modtype: real
[constraint : modtype ge 0 and modtype le 10].

flag : truth (*false).
flag1 : truth (*false).
flag2 : truth (*false).

```

\inferred attributes

```
lowererror: mlt(one, two, three, four, five, zero).
```

```
bestmodel: mlt
```

```
(model1 [ description: lowerror = one;],
model2 [ description: lowerror = two;],
model3 [ description: lowerror = three;],
model4 [ description: lowerror = four;],
model5 [ description: lowerror = five;],
none [ description: lowerror = zero;]).
```

```
%
```

```
demons:
```

```
  Demon1:
```

```
  when
```

```
    determined(uncert)
```

```
  then
```

```
    if uncert = 0 then
```

```
      reassert uncert = 8.08.
```

```
    endif.
```

```
    if uncert le errmin then
```

```
      reassert flag = true.
```

```
    else
```

```
      reassert flag = false.
```

```
    endif.
```

```
  endwhen.
```

```
  Demon2:
```

```
  when
```

```
    err4 = 0
```

```
  then
```

```
    flag1 = true.
```

```
    lowerror = four.
```

```
  endwhen.
```

```
  Demon3:
```

```
  when
```

```
    err5 le errmin
```

```
  then
```

```
    flag2 = true.
```

```
    lowerror = five.
```

```
  endwhen.
```

```
  Demon4:
```

```
  when
```

```
    err1 = errmin
```

```
  then
```

```
    lowerror = one.
```

```
  endwhen.
```

```
  Demon5:
```

```
  when
```

```
    err2 = errmin
```

```
  then
```

```

    lowerror = two.
endwhen.

```

```

Demon6:

```

```

when
    err3 = errmin
then
    lowerror = three.
endwhen.

```

```

Demon7:

```

```

when
    err4 = errmin
then
    reassert lowerror = four.
endwhen.

```

```

%
```

```

actions:

```

```

    display attach purpose of kb.
    message "", "Type 'c' to begin".
    break.
    obtain trace_option.
    if trace_option = yes then
        trace.
    else
        untrace.
    endif.

```

```

\read the file modtrans1 to get the errors in using models 1 to 5

```

```

    erase err1, err2, err3, err4, err5, errmin, modtype.
    read "modtrans1", err1, err2, err3, err4, err5, errmin, modtype.
    if determined(lowerror) = false then
        lowerror = zero.
    endif.
    obtain uncert.

```

```

\determine whether the purpose of using the system is to
\model or calibrate

```

```

if determined(modtype) = true then
    if modtype = 1 then
        sysaction = modelling.
    else if modtype = 0 then
        sysaction = calibration.
    else
        message"",
            "Error in determining the type of action",
            ""
    endif.
endif.
endif.

```

```

else
    message " Error in reading a value for 'modtype'".
endif.
    if sysaction = modelling then
\modelling section
display attach user1 of kb.
if determined(flag1) = true then
    if (flag1) then
        message "",
            banner,
            "Model 4 appears to be the best choice, however, you are cautioned",
            "against using it because the splines will yield",
            "incorrect results when the range of data is different",
            "from the one used for modelling",
            "To confirm its suitability, please use a set of calibration",
            "data and run the expert system again",
            "",
            "You may look into the rrors of other models if you like",
            banner,
            "" .
askfor useroption.
        endif.
endif.
if determined(flag2) = true then
    if (flag2) then
        message "",
            banner,
            "Model 5 appears to be the best, but it is also the ",
            "the most complex and computation-intensive",
            "If the other models have yielded comparable mean square",
            "errors, they should be preferred over this choice".
askfor useroption.
        endif.
endif.
\determine the best model using the error criteria
if determined(useroption) = true then
    if useroption = dontbother then
        obtain bestmodel.

        message "",
            banner.
message combine ("The best model for your system is ", bestmodel).
if determined(flag) = true then

    if (flag) then
message combine ("However, mod. error is
higher than uncert = ", uncert ).
        message "",
            "Please consider remodelling the system",
            "" .

```

```
endif.  
message "",  
    banner.  
endif.  
else  
    bestmodel = model1 | model2 | model3 | model4 | model5.  
endif.  
endif.  
if bestmodel = model1 then  
    message "",  
        banner.  
    message "The model parameters are stored in model1.mat ".  
    message "The model plot is stored in modplot1.met ".  
    message combine ("The RMS error in percent in is ", err1).  
    message "",  
        banner.  
endif.  
if bestmodel = model2 then  
    message "",  
        banner.  
    message "The model parameters are stored in model2.mat ".  
    message "The model plot is stored in modplot2.met ".  
    message combine ("The RMS error in percent in is ", err2).  
    message "",  
        banner.  
endif.  
if bestmodel = model3 then  
    message "",  
        banner.  
    message "The model parameters are stored in model3.mat ".  
    message "The model plot is stored in modplot3.met ".  
    message combine ("The RMS error in percent in is ", err3).  
    message "",  
        banner.  
endif.  
if bestmodel = model4 then  
    message "",  
        banner.  
    message "The model parameters are stored in model4.mat ".  
    message "The model plot is stored in modplot4.met ".  
    message combine ("The RMS error in percent in is ", err4).  
    message "",  
        banner.  
endif.  
if bestmodel = model5 then  
    message "",  
        banner.  
    message "The model parameters are stored in model5.mat ".  
    message "The model plot is stored in modplot5.met ".  
    message combine ("The RMS error in percent in is ", err5).
```

```

message "",
    banner.
endif.
if bestmodel = none then
message "",
    banner.
message "The best model could not be found. check the program ".
message "",
    banner.
endif.

else if sysaction = calibration then
\Calibration section
display attach user2 of kb.
if determined (flag2) = true then
if (flag2) then
message "",
    banner,
    " Model 5 appears to be the best, but it is also the ",
    " the most complex and computation-intensive.",
    " If the other models have yielded comparable mean square",
    " errors, they should be preferred over this choice.".

endif.
endif.

\determine the best model using the error criteria

obtain bestmodel.

message "",
    banner.
message combine ("The best model for your system is ", bestmodel).
if determined (flag) = true then
if (flag) then
message combine ("However, calib. error is
higher than uncert. = ", uncert).
message "",
    "Please consider recalibrating the system",
    ""
endif.
message "",
    banner.
endif.
if bestmodel = model1 then
message "",
    banner.
message "The model parameters are stored in model1.mat ".
message "The calibration plot is stored in calibplot1.met ".

```

```
message combine ("The RMS error in percent in is ", err1).
message "",
    banner.
endif.
```

```
if bestmodel = model2 then
message "",
    banner.
message "The model parameters are stored in model2.mat ".
message "The calibration plot is stored in calibplot2.met ".
message combine ("The RMS error in percent in is ", err2).
message "",
    banner.
endif.
```

```
if bestmodel = model3 then
message "",
    banner.
message "The model parameters are stored in model3.mat ".
message "The calibration plot is stored in calibplot3.met ".
message combine ("The RMS error in percent in is ", err3).
message "",
    banner.
endif.
```

```
if bestmodel = model4 then
message "",
    banner.
message "The model parameters are stored in model4.mat ".
message "The calibration plot is stored in calibplot4.met ".
message combine ("The RMS error in percent in is ", err4).
message "",
    banner.
endif.
```

```
if bestmodel = model5 then
message "",
    banner.
message "The model parameters are stored in model5.mat ".
message "The calibration plot is stored in calibplot5.met ".
message combine ("The RMS error in percent in is ", err5).
message "",
    banner.
endif.
```

```
if bestmodel = none then
message "",
    banner.
message "The best model could not be found. check the program ".
message "",
    banner.
```

```

endif.
else
  stop.

endif.
endif.
  obtain what_next.
    if what_next = yes then
      nextcase.
    else
      stop.
endif.
%
```

B.2. A Typical User Session with the Interface Program I

Enter name of the file, no. of data points, and 1
for modelling and 0 for calibration

Now let us fit a 3rd order polynomial to the data

Do you want to store this plot ? Y/N :

n =

quit

The model parameters will be stored in model1.mat
Now let us fit a 4th order polynomial to the data

Do you want to store this plot ? Y/N :

n =

The model parameters will be stored in model2.mat
Now let us fit a 5th order polynomial to the data

Do you want to store this plot ? Y/N :

n =

The model parameters will be stored in model3.mat
Next let us fit a piecewise cubic polynomials to the data

Do you want to store this plot ? Y/N :

n =

□

The model parameters will be stored in model4.mat
 Finally let us fit a 5th degree nonlinear
 function (sum of 5 exponential functions) to the data

Do you want to store this plot ? Y/N :

n =

□

The model parameters will be stored in model5.mat
 Copy modplot*.met to other files before rerunning
 The value of ns1 is 0
 The value of ne1 is 13
 The file moddata2.dat is written, action type = 1
 user time 0 microsec
 system time 0 microsec
 user time 64290000 microsec
 system time 11790000 microsec

foo3.mat successfully translated to modtrans1
 Loading the knowledge base 'modkb00.pkb'.

Welcome to the online Modelling and Calibration
 knowledge base

This Expert System will guide you to develop
 the best possible model for your system.
 It will determine the best model based
 on the normalized mean square error criterion

Type 'c' to begin

Do you wish to see a trace of the
 expert system's execution for the duration
 of this session

1. yes
2. no

=?

2

Tracing facility off...

Enter a value for the system uncertainty.

If unknown enter 0

[constraint: uncertainty 0 and uncertainty 100]

(Enter a number)

0

Your system will be characterized using five selected functions to determine the best choice

The data format is assumed to be the following:

System input-output data Format::

Paired values of input(force)

versus the output (analog sensor output), one set per line, each set terminated with a <cr>.

Data stored as an ASCII file

Model 4 appears to be the best choice, however, you are cautioned against using it because the splines will yield incorrect results when the range of data is different from the one used for modelling

To confirm its suitability, please use a set of calibration data and run the expert system again

You may look into the errors of other models if you like

What do you want to do

1. show others

2. dont bother

=?

1

The model parameters are stored in model1.mat

The model plot is stored in modplot1.met

The RMS error in percent in is 3.338665

The model parameters are stored in model2.mat

The model plot is stored in modplot2.met

The RMS error in percent in is 2.933939

The model parameters are stored in model3.mat

The model plot is stored in modplot3.met

The RMS error in percent in is 134.59259

The model parameters are stored in model4.mat

The model plot is stored in modplot4.met

The RMS error in percent in is 0

The model parameters are stored in model5.mat

The model plot is stored in modplot5.met

The RMS error in percent in is 5.1186872

Do you wish to remodel or recalibrate your
tactile sensing system with a new set of data ?

- 1. yes
 - 2. no
- =?
2

C. Performance Evaluation of Decision Filter Output

C.1. Effect of dead band size on filter output

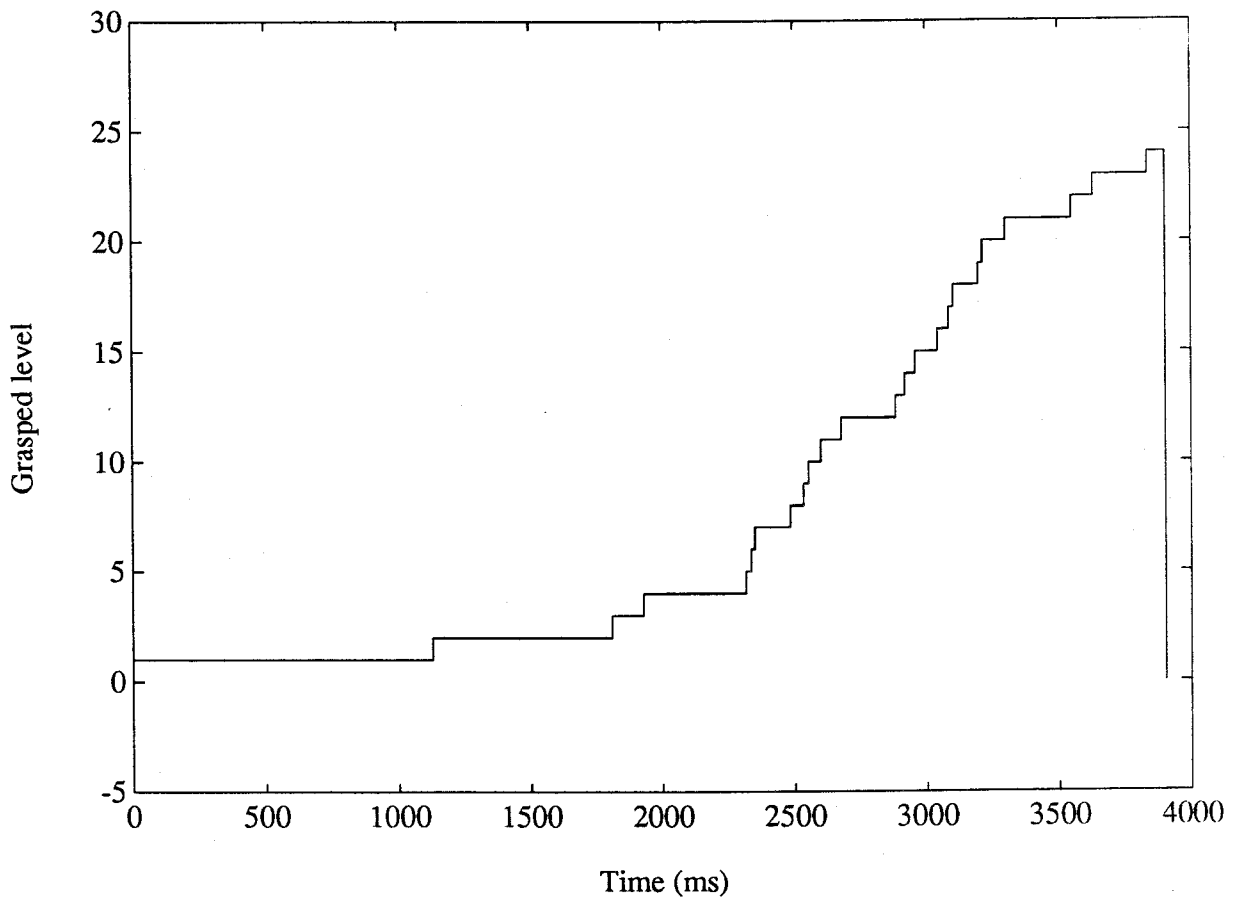


Figure C.1: Cumulated grasped levels using a 5-point dead band filter.

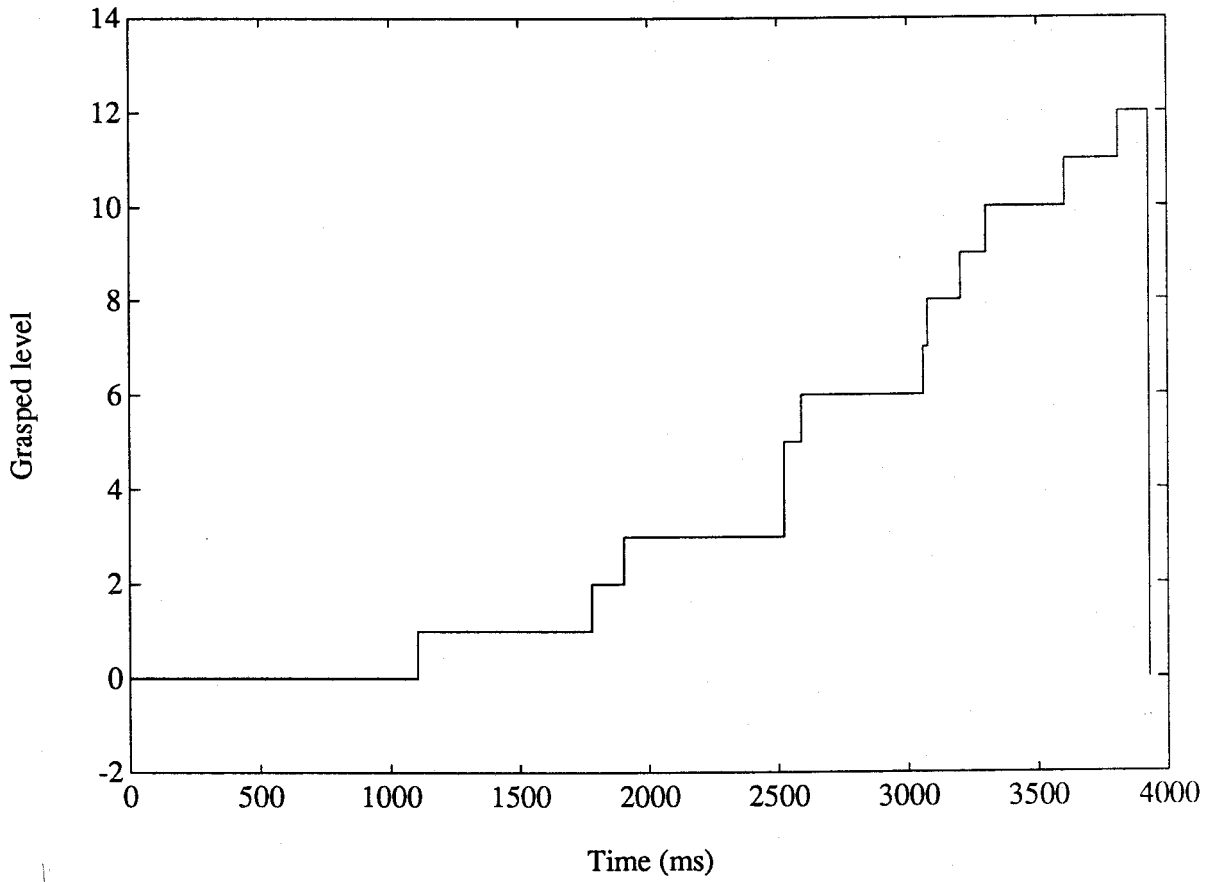


Figure C.2: Cumulated grasped levels using a 15-point dead band filter .

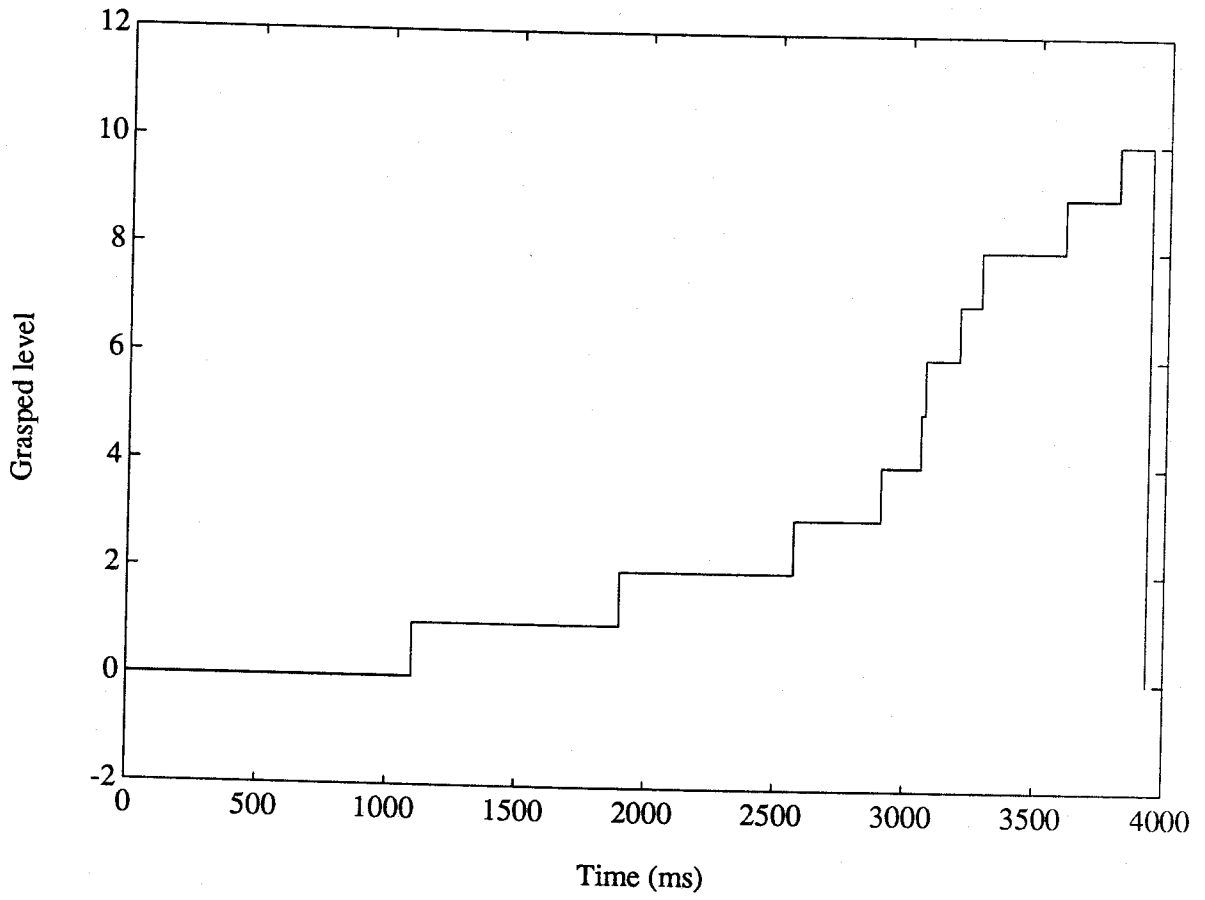


Figure C.3: Cumulated grasped levels using a 20-point dead band filter .

C.2. Effect of block size on filter output

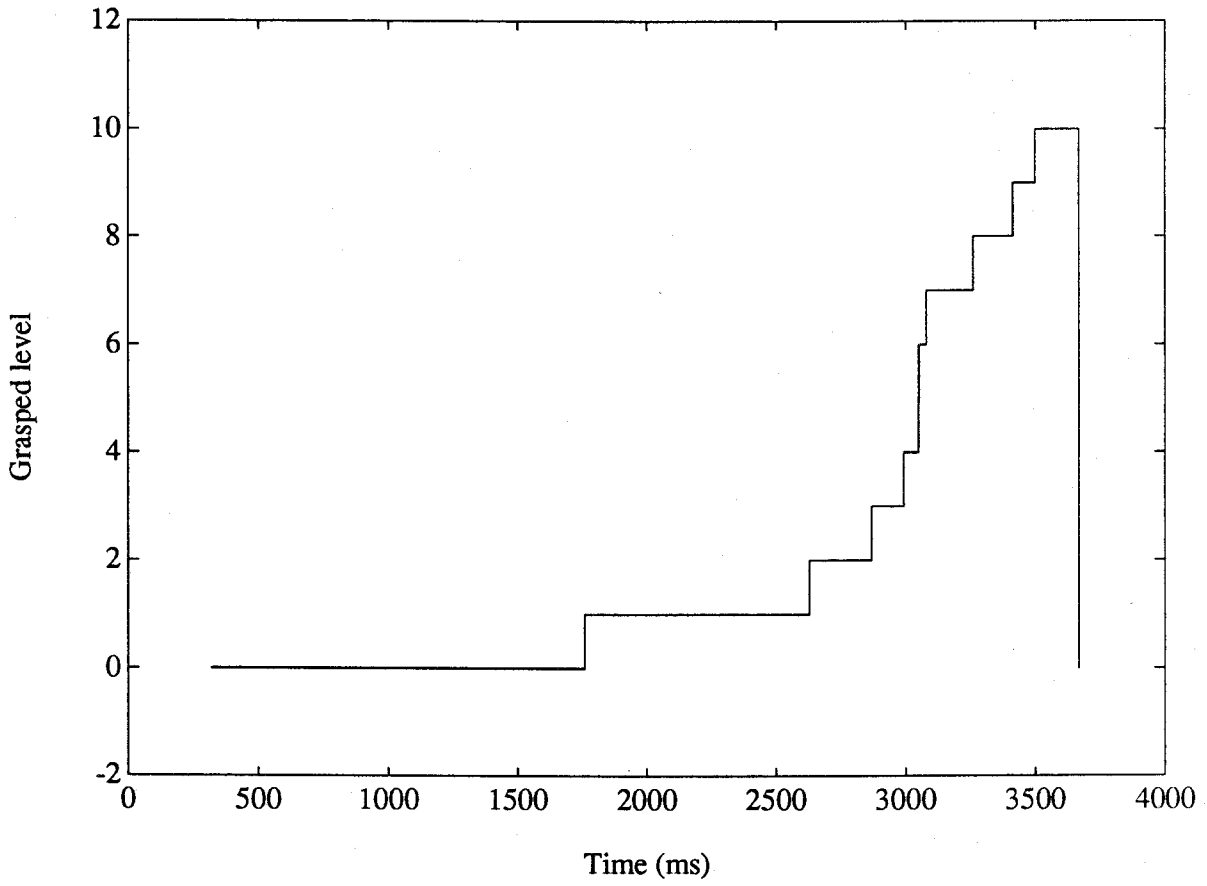


Figure C.4: Cumulated grasped levels using 30-point data blocks .

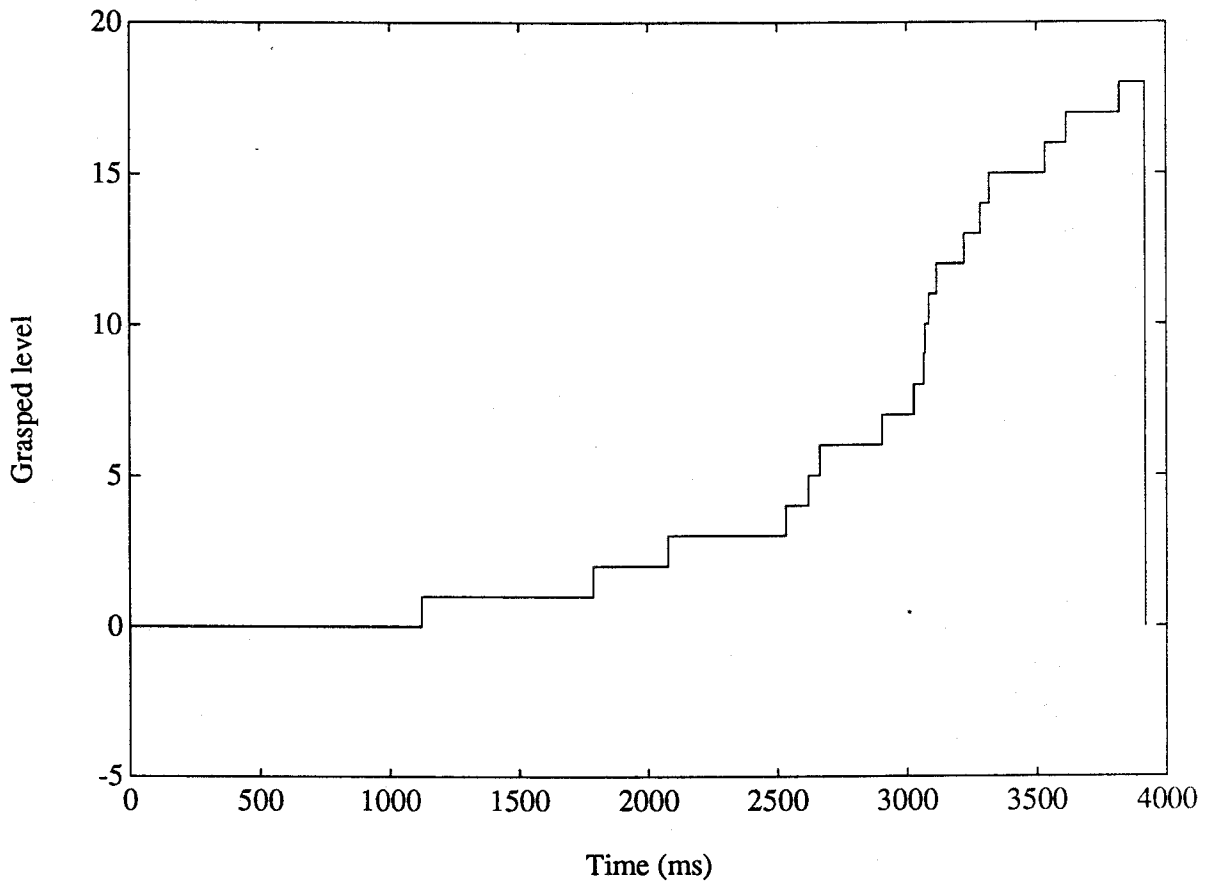


Figure C.5: Cumulated grasped levels using 50-point data blocks .

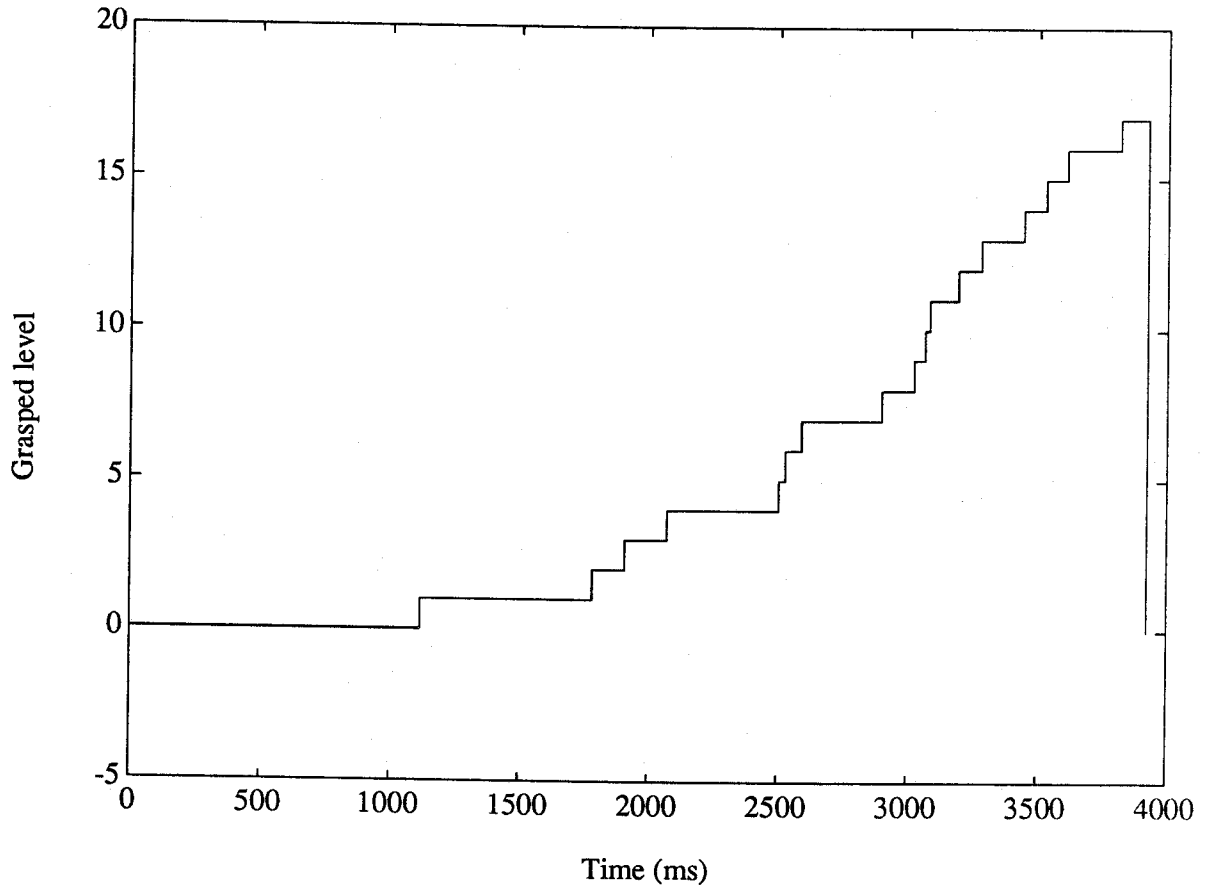


Figure C.6: Cumulated grasped levels using a 200-point data blocks .

D. Performance Evaluation of Interface Program II Using Data from Test Category 1: Independent Grasping and Releasing Tasks

D.1. Validation results from Sample 5 and Sample 7 test data

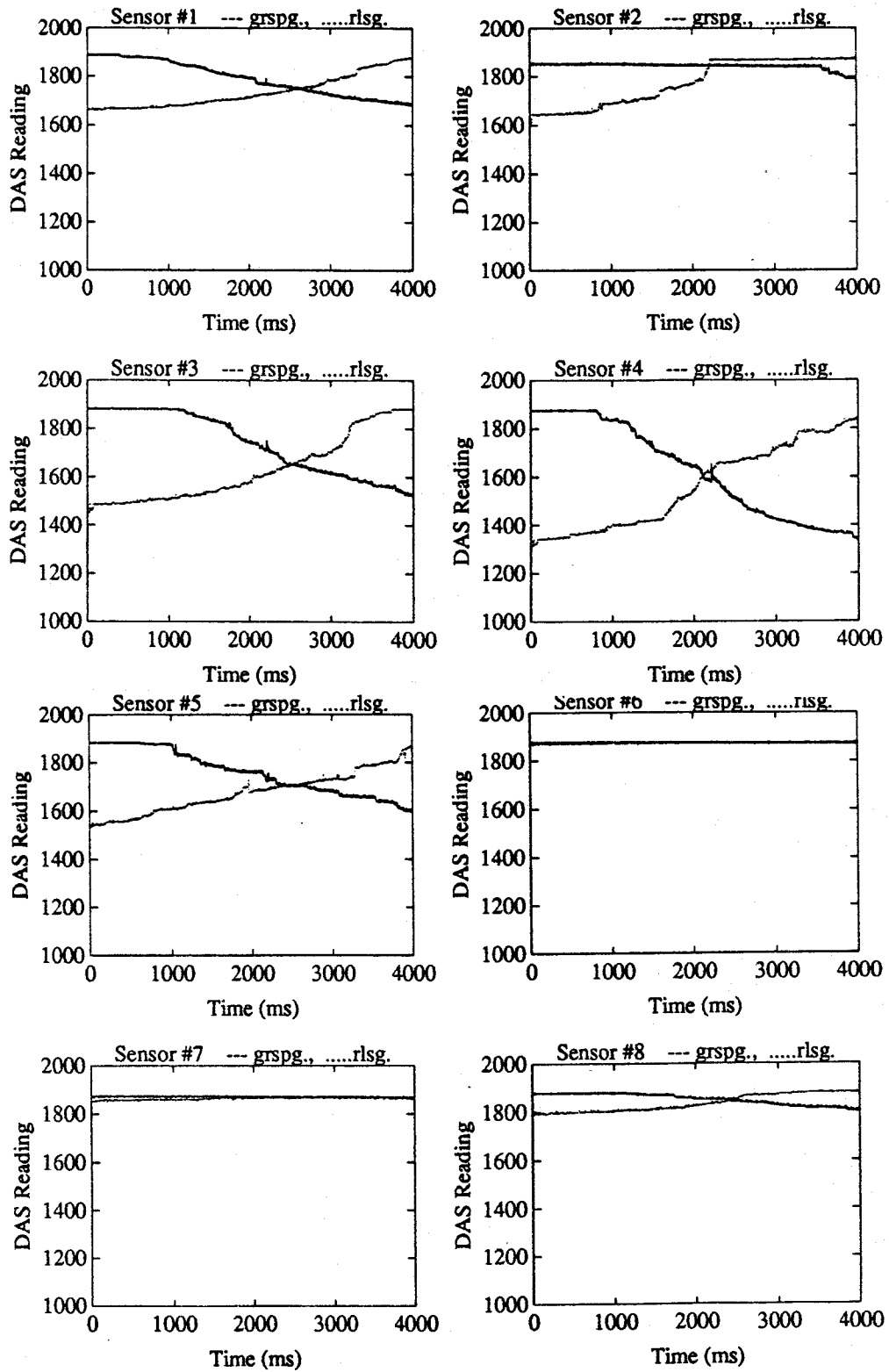


Figure D.1: Raw force data measured by the tactile sensors during independent grasping and releasing operations performed on sample 5 .

Variation of total gripper force during the task

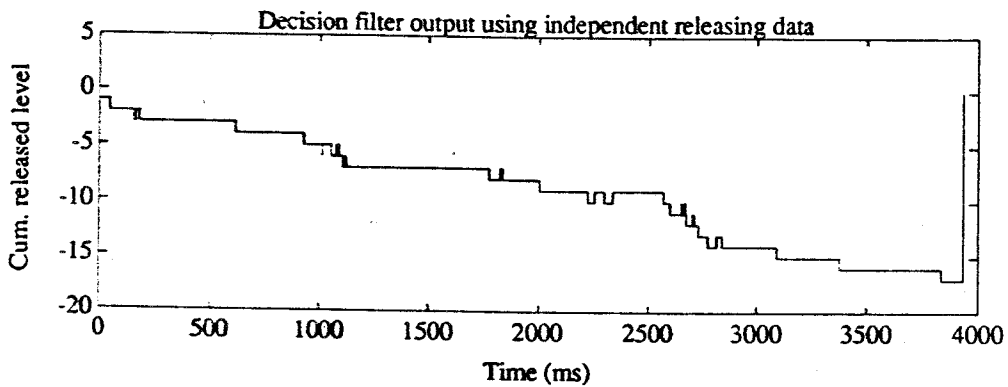
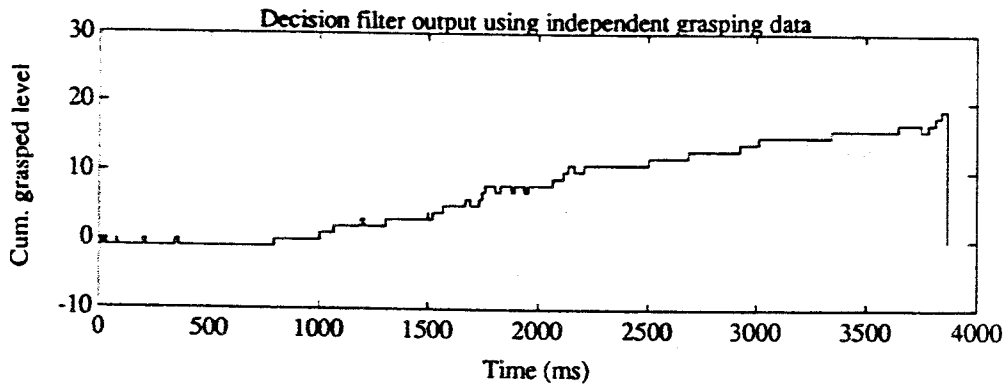
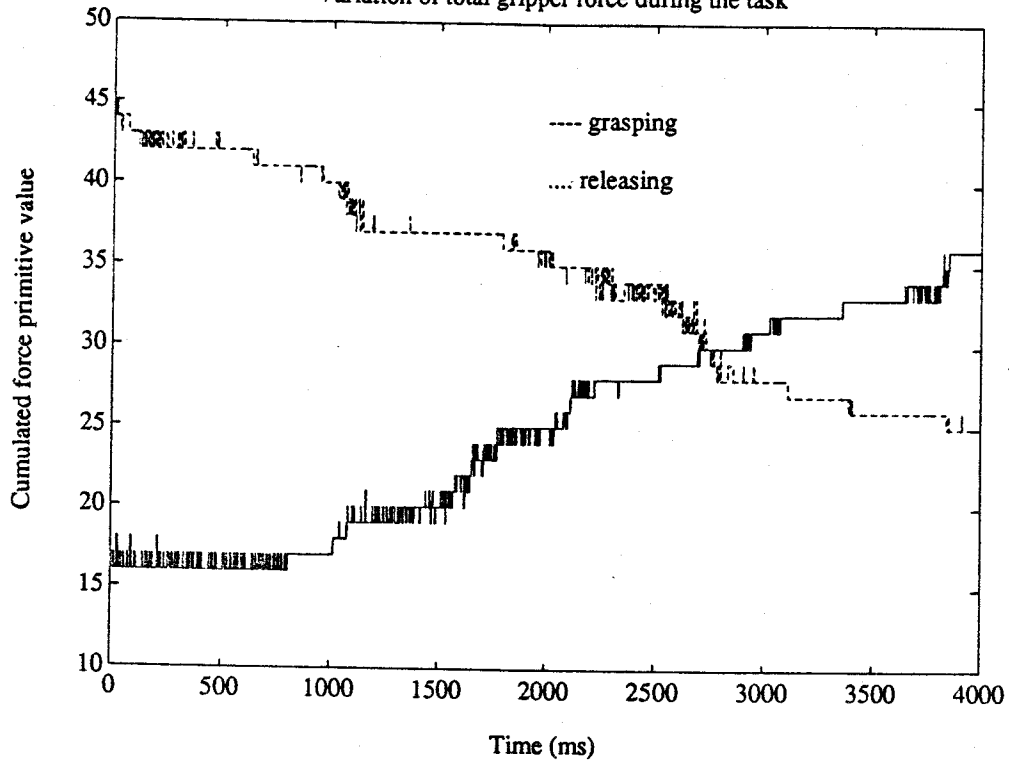
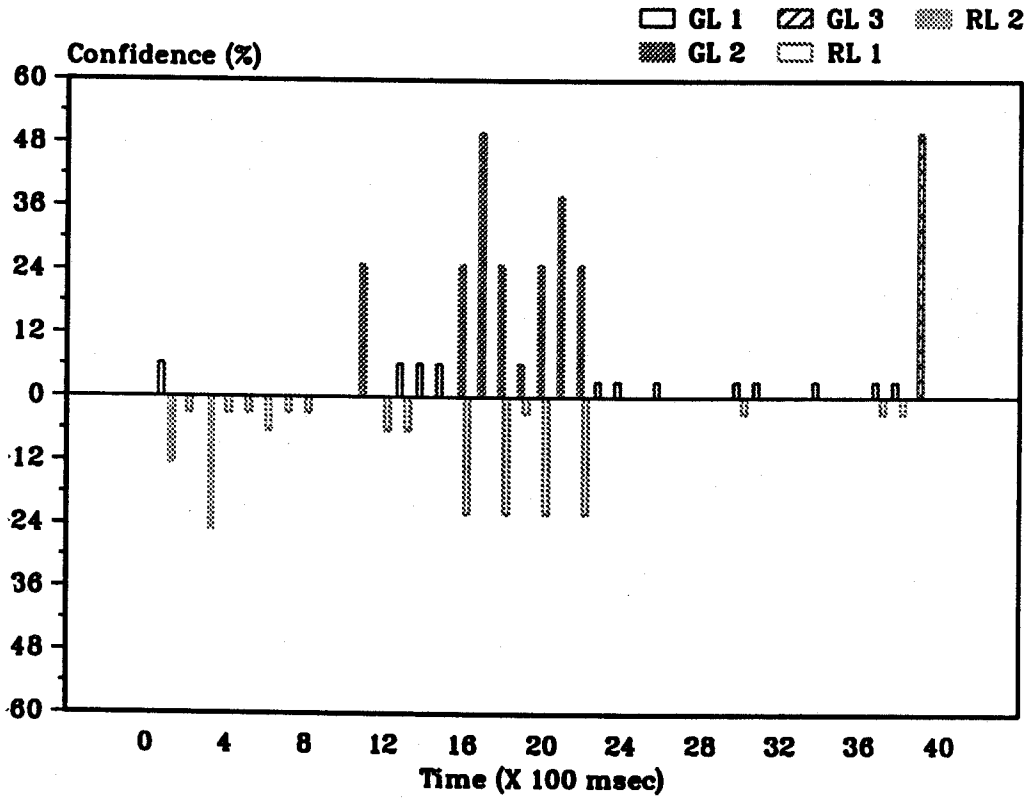


Figure D.2: Cumulated grasped levels and primitive force variations from grasping and releasing data of sample 5 •

(a) Force decision parameters - sample 5 grasping



(b) Force decision parameters - sample 5 releasing

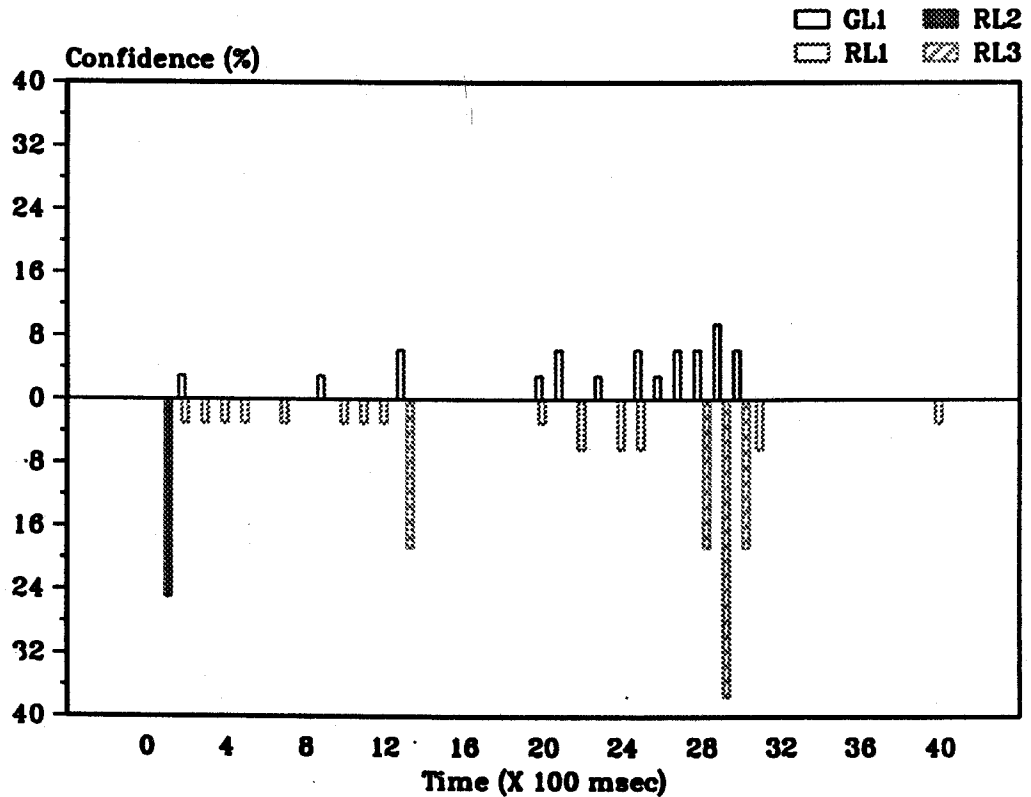


Figure D.3: The force decision parameters of the task status obtained from the TSI expert system using sample 5 grasping and releasing data .

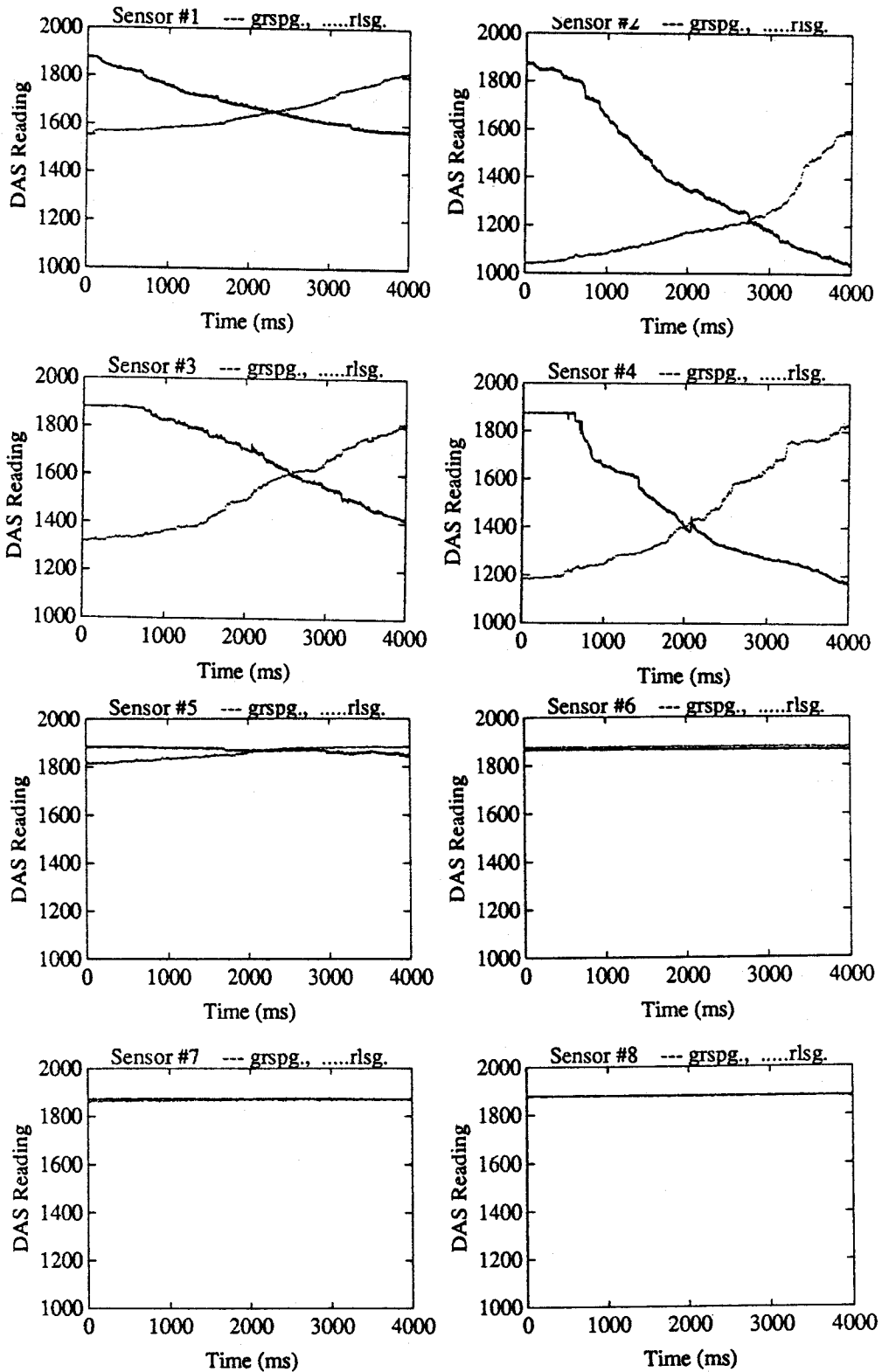


Figure D.4: Raw force data measured by the tactile sensors during independent grasping and releasing operations performed on sample 7.

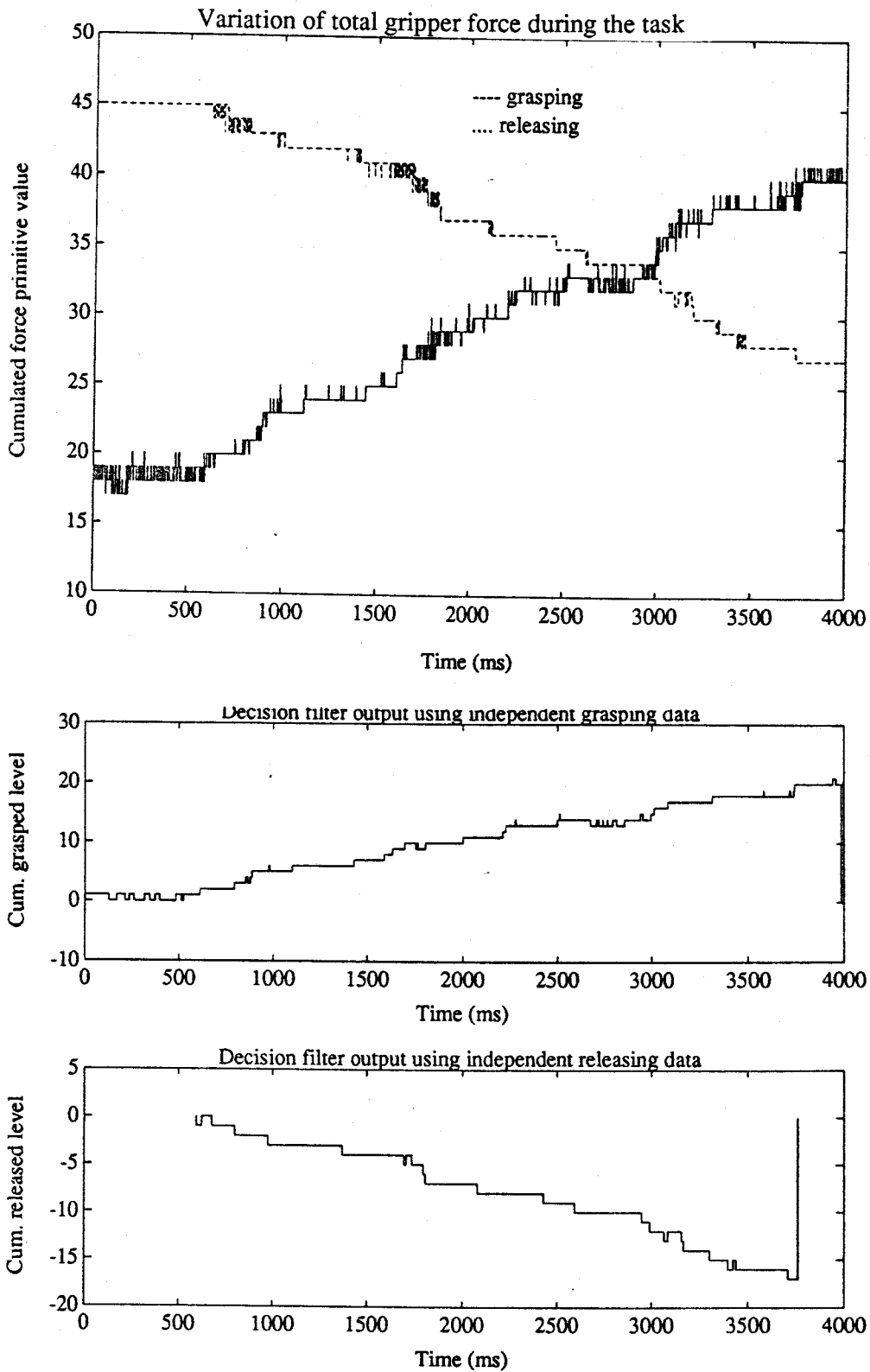
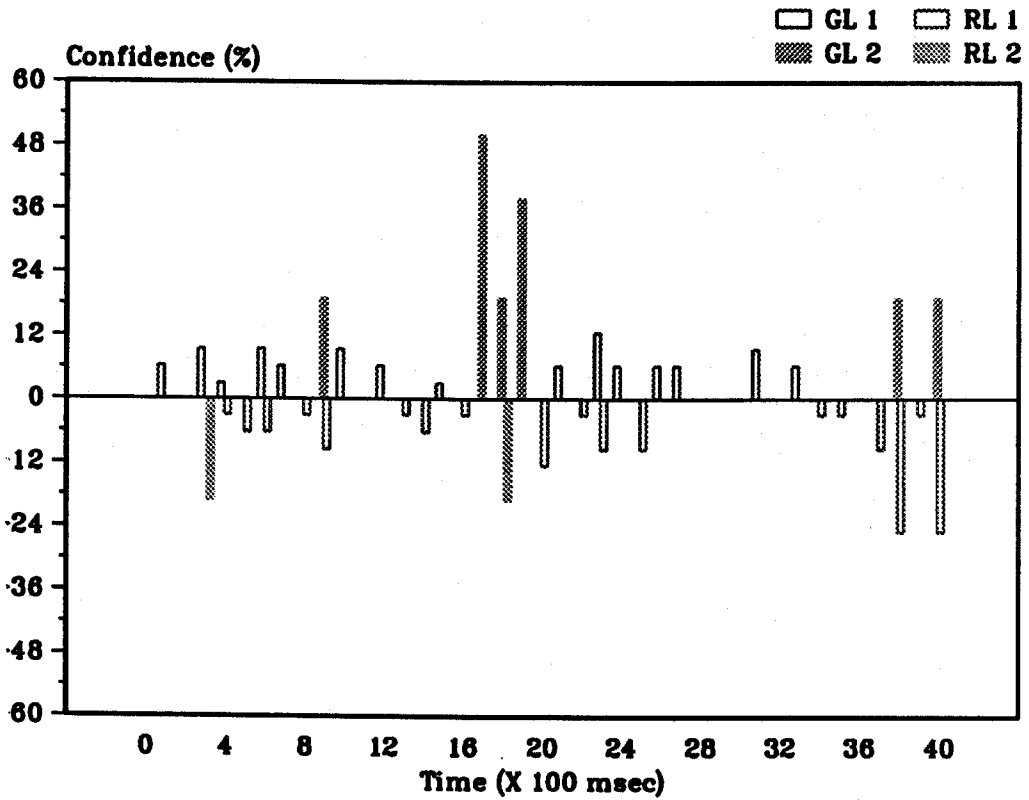


Figure D.5: Cumulated grasped levels and primitive force variations from grasping and releasing data of sample 7 .

(a) Force decision parameters - sample 7 grasping



(b) Force decision parameters - sample 7 releasing

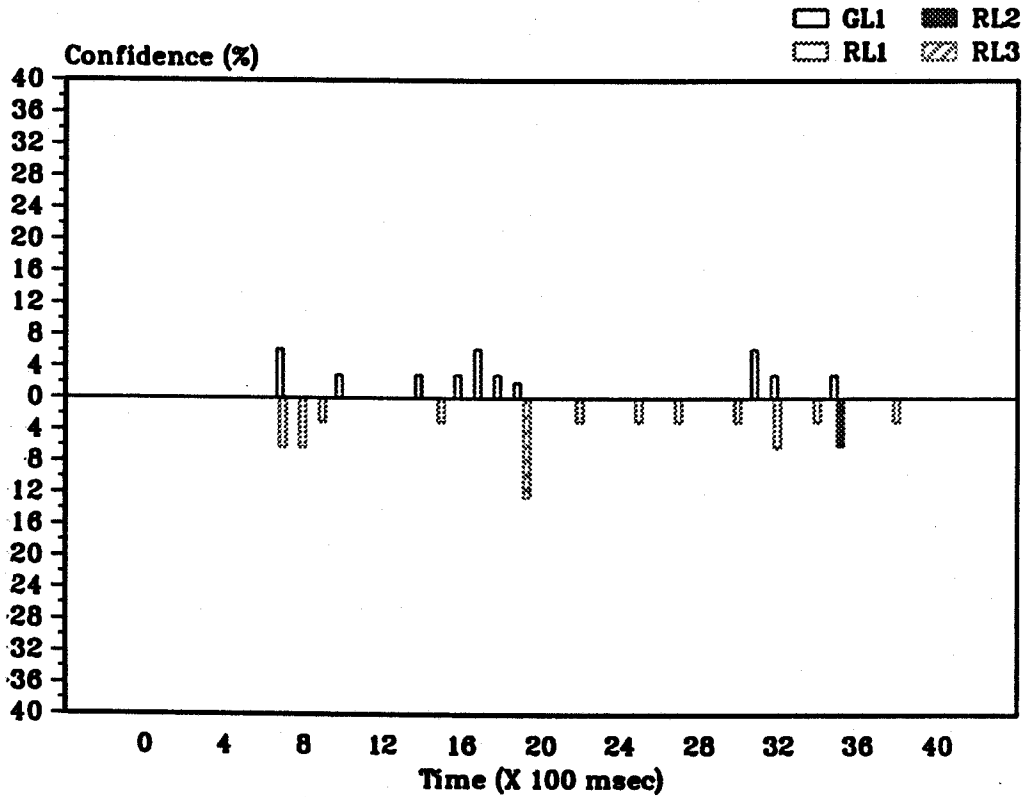


Figure D.6: The force decision parameters of the task status obtained from the TSI expert system using sample 7 grasping and releasing data .

D.2. Performance tables using Sample 5 and Sample 7 test data

Table D.1: A summary of the task status parameters obtained from the TSI expert system using sample 5 grasping data .

Block no.	Unchanged state	Grasping level	Releasing level	Grasping con. level	Releasing con. level	Dynamic displacement	Static displacement	Decision correct ?
1		1	2	6.25	12.5	Northeast	Northeast	Yes
2		0	1	0	3	No	Nodir	No
3		0	2	0	25	Northeast	Nodir	No
4		0	1	0	3	No	Nodir	No
5		0	1	0	3	No	Nodir	No
6		0	1	0	6.25	Northeast	Nodir	No
7		0	1	0	3	No	Nodir	No
8		0	1	0	3	No	Nodir	No
9	y	0	0	0	0	No	Nodir	Yes
10	y	0	0	0	0	No	Nodir	Yes
11		2	0	38	0	South	Nodir	Yes
12		0	1	0	6.25	No	Nodir	No
13		1	1	6.25	6.25	No	Nodir	Yes
14		1	0	3	0	No	Nodir	Yes
15		1	0	6.25	0	West	Nodir	Yes
16		2	1	25	22	South	West	Yes
17		2	0	50	0	East	Nodir	Yes
18		2	1	25	22	South	West	Yes
19		2	1	6	3	No	Nodir	Yes
20		2	1	25	22	South	West	Yes
21		2	0	38	0	East	Nodir	Yes
22		2	1	25	22	South	West	Yes
23		1	0	3	0	No	Nodir	Yes
24		1	0	3	0	No	Nodir	Yes
25	y	0	0	0	0	No	Nodir	Yes
26		1	0	3	0	No	Nodir	Yes
27	y	0	0	0	0	No	Nodir	Yes
28	y	0	0	0	0	No	Nodir	Yes
29	y	0	0	0	0	No	Nodir	Yes
30		1	1	3	3	No	Nodir	Yes
31		1	0	3	0	No	Nodir	Yes
32	y	0	0	0	0	No	Nodir	Yes
33	y	0	0	0	0	No	Nodir	Yes
34		1	0	3	0	No	Nodir	Yes
35	y	0	0	0	0	No	Nodir	Yes
36	y	0	0	0	0	No	Nodir	Yes
37		1	1	3	3	No	Nodir	Yes
38		1	1	3	3	No	Nodir	Yes
39		3	0	85	0	No	Nodir	Yes
40	y	0	0	0	0	No	Nodir	Yes

Table D.2: A summary of the task status parameters obtained from the TSI expert system using sample 5 releasing data .

Block no.	Unchanged state	Grasping level	Releasing level	Grasping con. level	Releasing con. level	Dynamic displacement	Static displacement	Decision correct ?
1		0	2	0	25	No	Nodir	Yes
2		1	1	3	3	No	Nodir	Yes
3		0	1	0	3	No	Nodir	Yes
4		0	1	0	3	No	Nodir	Yes
5		0	1	0	3	No	Nodir	Yes
6	y	0	0	0	0	No	Nodir	Yes
7		0	1	0	3	No	Nodir	Yes
8	y	0	0	0	0	No	Nodir	Yes
9		1	0	3	0	No	Nodir	No
10		0	1	0	3	No	Nodir	Yes
11		0	1	0	3	No	Nodir	Yes
12		0	1	0	3	No	Nodir	Yes
13		1	3	6.25	18.75	No	Nodir	Yes
14	y	0	0	0	0	No	Nodir	Yes
15		0	1	0	3	No	Nodir	Yes
16	y	0	0	0	0	No	Nodir	Yes
17	y	0	0	0	0	No	Nodir	Yes
18	y	0	0	0	0	No	Nodir	Yes
19	y	0	0	0	0	No	Nodir	Yes
20		1	1	3	3	No	Nodir	Yes
21		1	0	6.25	0	No	Nodir	No
22		0	1	0	6.25	No	Nodir	Yes
23		1	0	3	0	No	Nodir	No
24		0	1	0	6.25	No	Nodir	Yes
25		1	1	6.25	6.25	No	Nodir	Yes
26		1	0	3	0	No	Nodir	No
27		1	0	6.25	0	East	Nodir	No
28		1	3	6.25	18.75	North	South	Yes
29		1	3	9.5	37.5	West	West	Yes
30		1	3	6.25	18.75	North	South	Yes
31		1	1	0	6.25	No	Nodir	Yes
32	y	0	0	0	0	No	Nodir	Yes
33	y	0	0	0	0	No	Nodir	Yes
34	y	0	0	0	0	No	Nodir	Yes
35	y	0	0	0	0	No	Nodir	Yes
36	y	0	0	0	0	No	Nodir	Yes
37	y	0	0	0	0	No	Nodir	Yes
38	y	0	0	0	0	No	Nodir	Yes
39	y	0	0	0	0	No	Nodir	Yes
40		0	1	0	3	No	Nodir	Yes

Table D.3: A summary of the task status parameters obtained from the TSI expert system using sample 5 grasping data .

Block no.	Unchanged state	Grasping level	Releasing level	Grasping con. level	Releasing con. level	Dynamic displacement	Static displacement	Decision correct ?
1		1	0	6.25	0	Noreast	Nodir	Yes
2	y	0	0	0	0	No	Nodir	Yes
3		1	2	9.5	19	Noreast	Nodir	Yes
4		1	1	1	3	No	Nodir	Yes
5		0	1	0	6.25	Noreast	Nodir	No
6		1	1	9.5	6.25	South	Nodir	Yes
7		1	0	6.25	0	No	Nodir	Yes
8		0	1	0	3	No	Nodir	No
9		2	1	19	9.5	Souwest	Nodir	Yes
10		1	0	9.5	0	No	Nodir	Yes
11	y	0	0	0	0	No	Nodir	Yes
12		1	0	6.25	0	No	Nodir	Yes
13		0	1	0	3	No	Nodir	No
14		0	1	6.25	0	No	Nodir	Yes
15		1	0	3	0	No	Nodir	Yes
16		0	1	0	3	No	Nodir	No
17		2	0	50	0	No	Nodir	Yes
18		2	2	19	19	No	Nodir	Yes
19		2	0	38	0	No	Nodir	Yes
20		0	1	0	12.5	No	Nodir	No
21		1	0	6.25	0	No	Nodir	Yes
22		0	1	0	3	No	Nodir	No
23		1	1	12.5	9.5	South	Souwest	Yes
24		1	0	6.25	0	No	Nodir	Yes
25		0	1	0	9.5	West	Nodir	No
26		0	1	0	6.25	No	Nodir	No
27		0	1	0	6.25	No	Nodir	No
28		--	--	--	--	No	Nodir	No
29		--	--	--	--	East	Nodir	No
30		--	--	--	--	No	Nodir	No
31		1	0	9.5	0	No	Nodir	Yes
32	y	0	0	0	0	North	Nodir	Yes
33		1	0	6.25	0	Souwest	Nodir	Yes
34		0	1	0	3	No	Nodir	No
35		0	1	0	3	No	Nodir	No
36	y	0	0	0	0	North	Nodir	Yes
37		0	1	0	9.5	North	Nodir	No
38		2	1	19	25	South	Nodir	Yes
39		0	1	0	9.5	No	Nodir	No
40		2	1	19	25	South	Nodir	Yes

Table D.4: A summary of the task status parameters obtained from the TSI expert system using sample 5 releasing data .

Block no.	Unchanged state	Grasping level	Releasing level	Grasping con. level	Releasing con. level	Dynamic displacement	Static displacement	Decision correct ?
1	y	0	0	0	0	No	Nodir	Yes
2	y	0	0	0	0	No	Nodir	Yes
3	y	0	0	0	0	No	Nodir	Yes
4	y	0	0	0	0	No	Nodir	Yes
5	y	0	0	0	0	No	Nodir	Yes
6	y	0	0	0	0	No	Nodir	Yes
7		1	1	6.25	6.25	Norwest	Nodir	Yes
8		0	1	0	6.25	Norwest	Nodir	Yes
9		0	1	0	3	No	Nodir	Yes
10		1	0	3	0	No	Nodir	No
11	y	0	0	0	0	No	Nodir	Yes
12	y	0	0	0	0	No	Nodir	Yes
13	y	0	0	0	0	No	Nodir	Yes
14		1	0	3	0	No	Nodir	No
15		0	1	0	3	No	Nodir	Yes
16		1	0	3	0	No	Nodir	No
17		1	0	6.25	0	North	Nodir	No
18		1	0	3	0	No	Nodir	No
19		1	3	2	12.5	Norwest	Nodir	Yes
20	y	0	0	0	0	No	Nodir	Yes
21	y	0	0	0	0	No	Nodir	Yes
22		0	1	0	3	No	Nodir	Yes
23	y	0	0	0	0	No	Nodir	Yes
24	y	0	0	0	0	No	Nodir	Yes
25		0	1	0	3	No	Nodir	Yes
26	y	0	0	0	0	No	Nodir	Yes
27		0	1	0	3	No	Nodir	Yes
28	y	0	0	0	0	No	Nodir	Yes
29	y	0	0	0	0	No	Nodir	Yes
30		0	1	0	3	No	Nodir	Yes
31		1	0	6.25	0	No	Nodir	No
32		1	1	3	6.25	No	Nodir	Yes
33	y	0	0	0	0	No	Nodir	Yes
34		0	1	0	3	No	Nodir	Yes
35		1	2	3	6	No	Nodir	Yes
36	y	0	0	0	0	No	Nodir	Yes
37	y	0	0	0	0	No	Nodir	Yes
38		0	1	0	3	No	Nodir	Yes
39	y	0	0	0	0	No	Nodir	Yes
40	y	0	0	0	0	No	Nodir	Yes

**E. Performance Evaluation of Interface Program II
using data from test Category 2: Combined Grasping
and Releasing Tasks**

E.1. Validation results from Sample 5 and Sample 7 test data

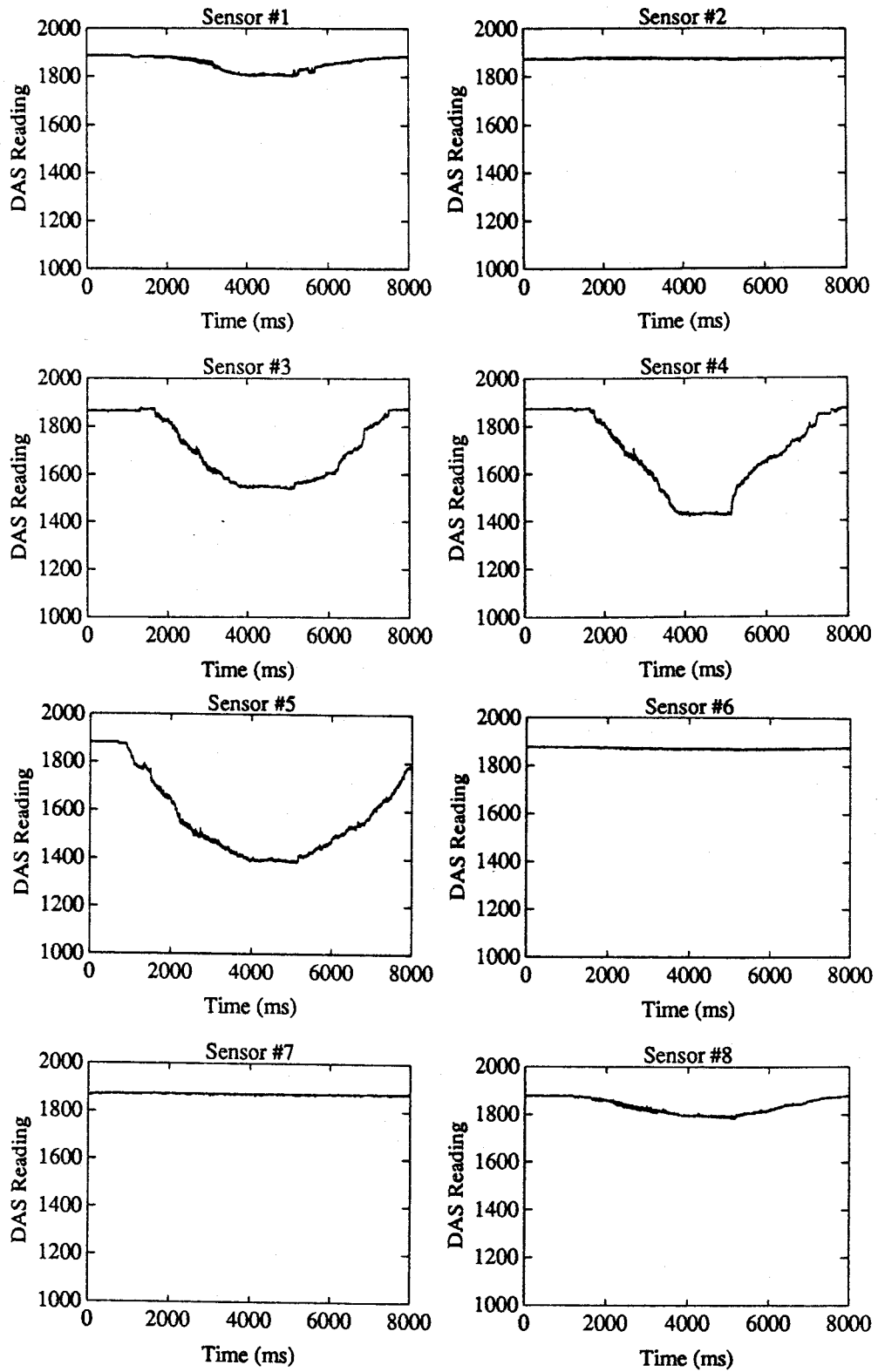


Figure E.1: Raw force data measured by the tactile sensors during the combined grasping and releasing operations performed on sample 5.

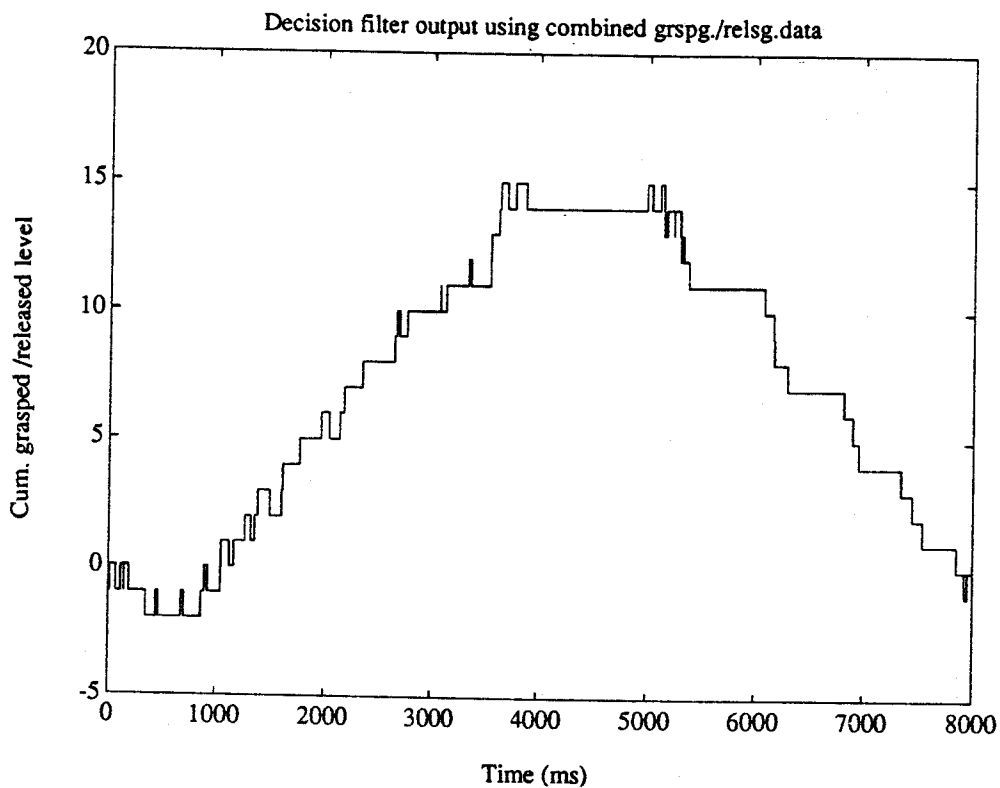
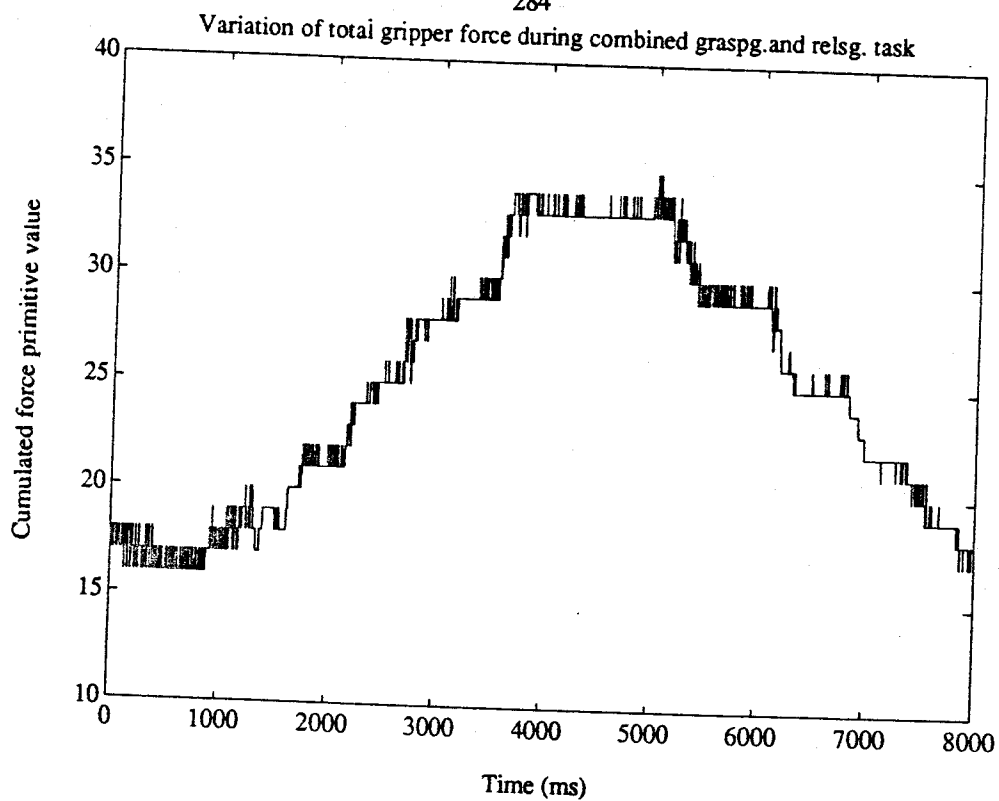
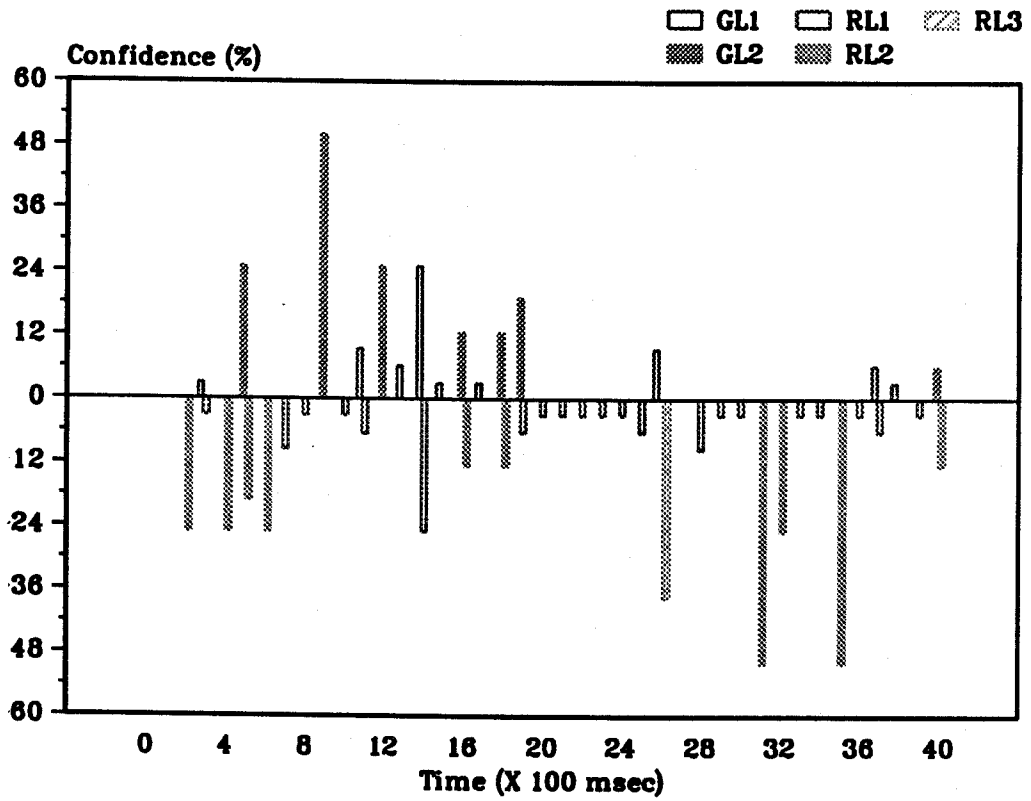


Figure E.2: Cumulated grasped levels and primitive force variations from sample 5 test data .

(a) Force decision parameters - sample 5 combined grasping and releasing



Object displacement parameters - sample 5 combined grasping and releasing

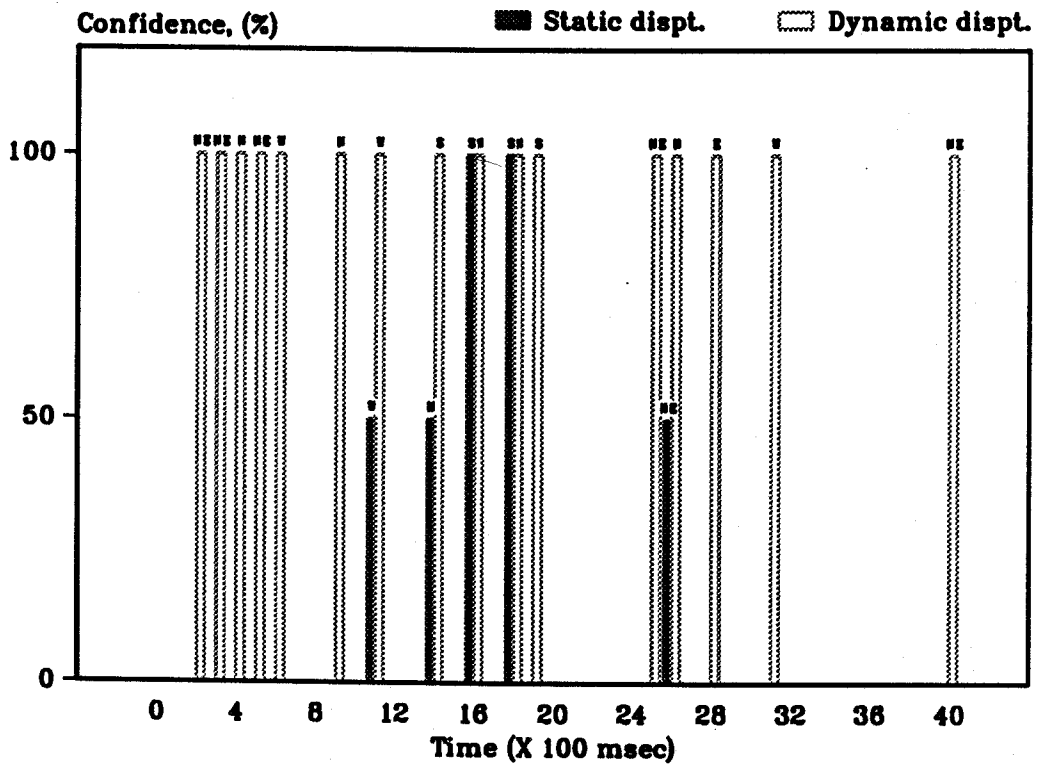


Figure E.3: The force decision and the object displacement parameters of the task status obtained from the TSI expert system using sample 5 test data .

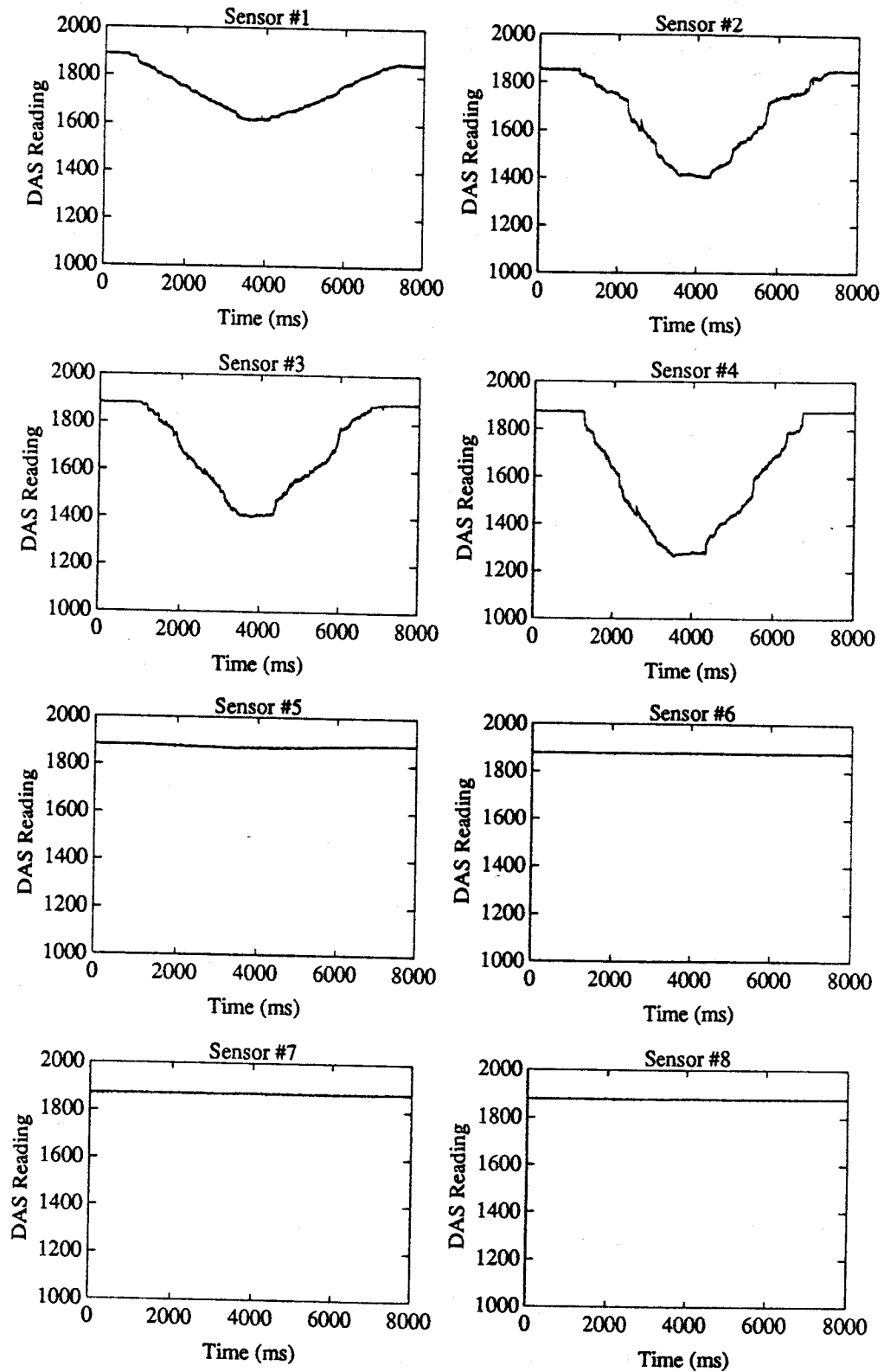


Figure E.4: Raw force data measured by the tactile sensors during the combined grasping and releasing operations performed on sample 7.

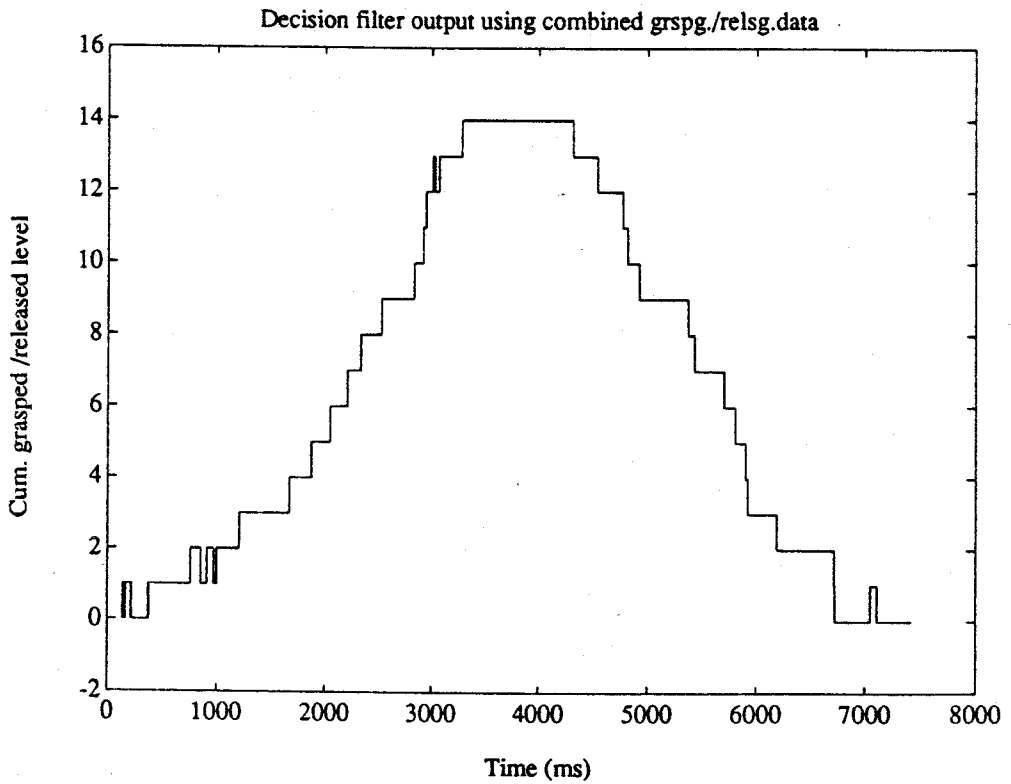
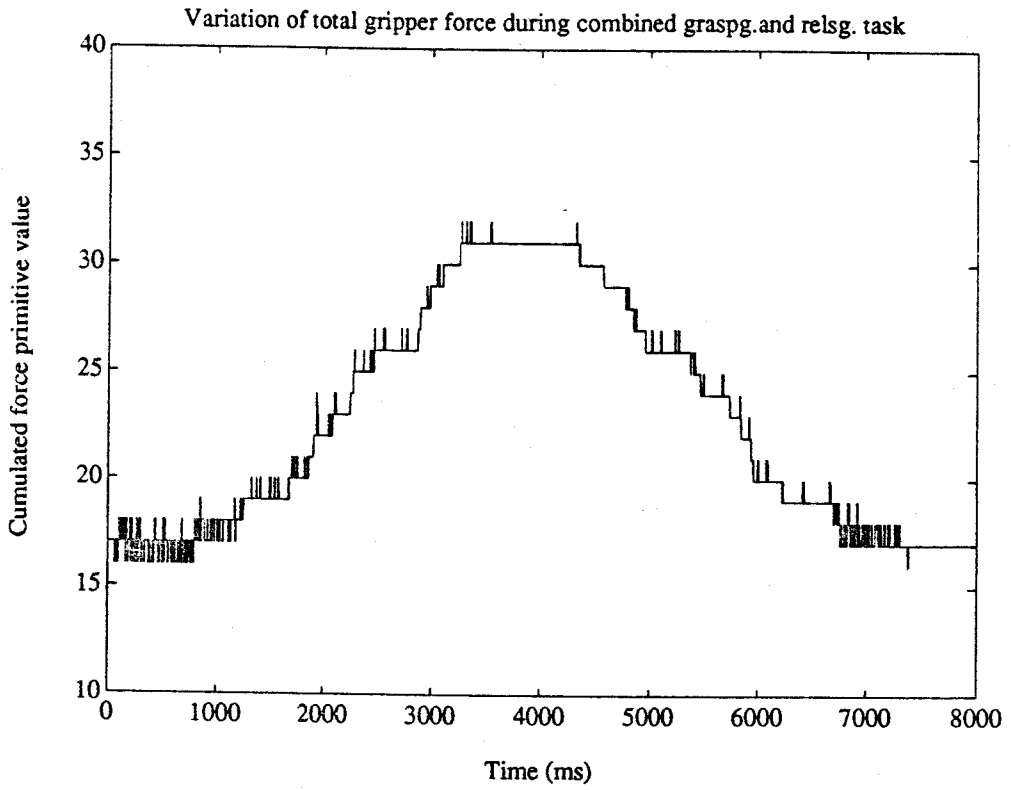
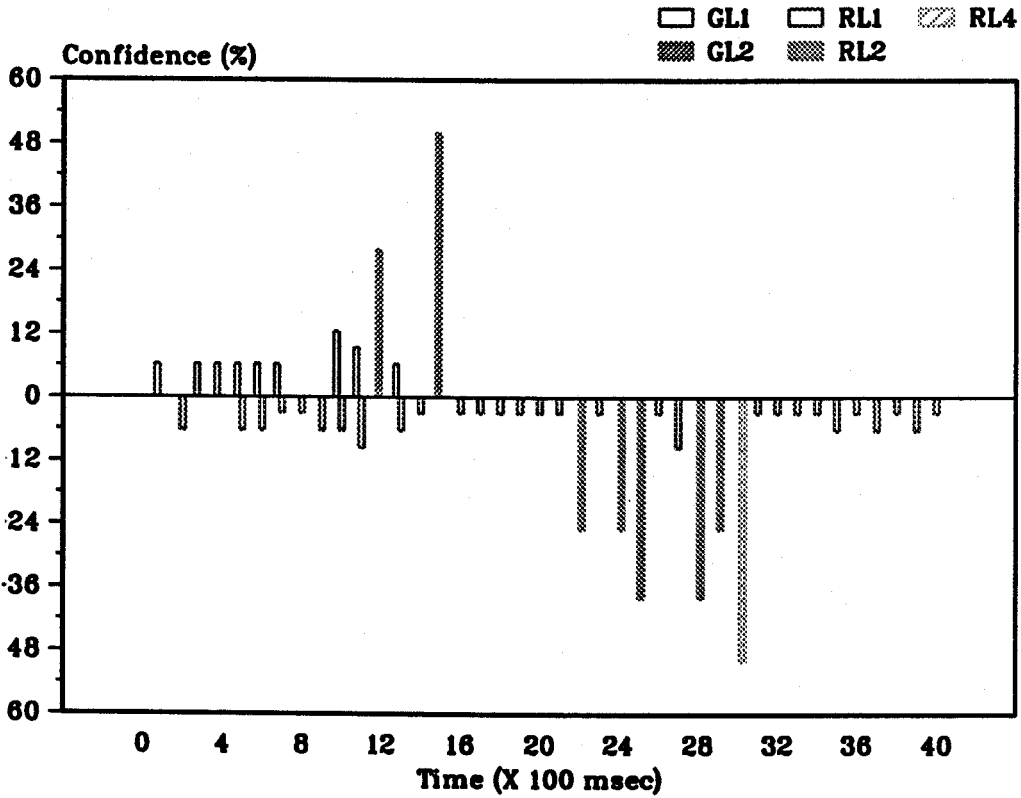


Figure E.5: Cumulated grasped levels and primitive force variations from sample 7 test data .

(a) Force decision parameters - sample 7 combined grasping and releasing



Object displacement parameters - sample 7 combined grasping and releasing

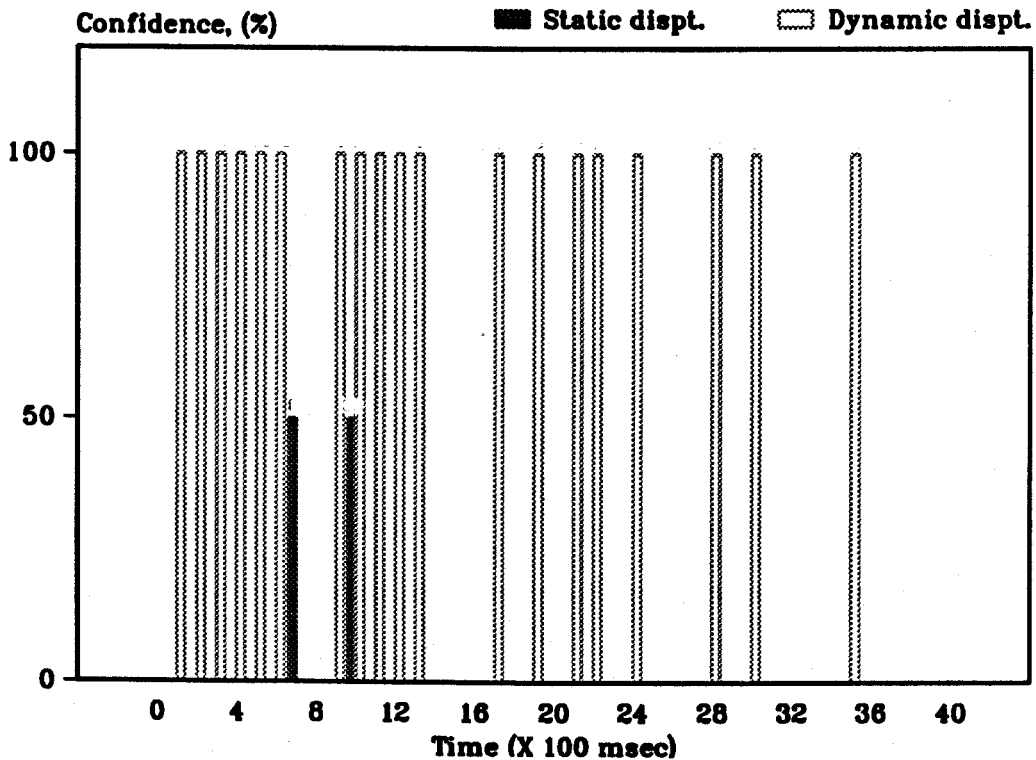


Figure E.6: The force decision and object displacement parameters of the task status obtained from the TSI expert system using sample 7 test data .

E.2. Performance tables using Sample 5 and Sample 7 test data

Table E.1: A summary of the task status parameters obtained from the TSI expert system using sample 5 test data .

Block no.	Unchanged state	Grasping level	Releasing level	Grasping con. level	Releasing con. level	Dynamic displacement	Static displacement	Decision correct ?
1		--	--	--	--	No	Nodir	Yes
2		0	2	0	25	Noreast	Nodir	No
3		1	1	3	3	No	Nodir	Yes
4		0	2	0	25	Noreast	Nodir	No
5		2	2	25	19	North	Nodir	Yes
6		0	2	0	25	Noreast	Nodir	No
7		3	1	28.5	9.5	West	Nodir	Yes
8		0	1	0	3	No	Nodir	No
9		2	0	50	0	North	Nodir	Yes
10		0	1	0	3	No	Nodir	No
11		1	1	9.5	6.25	West	West	Yes
12		2	0	25	0	No	Nodir	Yes
13		1	0	6.25	0	No	Nodir	Yes
14		1	1	25	25	South	North	Yes
15		1	0	3	0	No	Nodir	Yes
16		2	2	12.5	12.5	North	South	Yes
17		1	0	3	0	No	Nodir	Yes
18		2	2	12.5	12.5	North	South	Yes
19		2	1	19	6.25	South	Nodir	Yes
20		0	1	0	3	No	Nodir	Yes
21		0	1	0	3	No	Nodir	Yes
22		0	1	0	3	No	Nodir	Yes
23		0	1	0	3	No	Nodir	Yes
24		0	1	0	3	No	Nodir	Yes
25		0	1	0	6.25	Noreast	Nodir	Yes
26		1	3	9.5	37.5	North	Noreast	Yes
27		--	--	--	--	No	Nodir	Yes
28		0	1	0	9.5	East	Nodir	Yes
29		0	1	0	3	No	Nodir	Yes
30		0	1	0	3	No	Nodir	Yes
31		0	2	0	50	West	East	Yes
32		0	2	0	25	Noreast	Nodir	Yes
33		0	1	0	3	No	Nodir	Yes
34		0	1	0	3	No	Nodir	Yes
35		0	2	0	50	No	Nodir	Yes
36		0	1	0	3	No	Nodir	Yes
37		1	1	6.25	6.25	No	Nodir	Yes
38		1	0	3	0	No	Nodir	No
39		0	1	0	3	No	Nodir	Yes
40		2	2	6.25	12.5	South	Nodir	Yes

Table E.2: A summary of the task status parameters obtained from the TSI expert system using sample 7 test data .

Block no.	Unchanged state	Grasping level	Releasing level	Grasping con. level	Releasing con. level	Dynamic displacement	Static displacement	Decision correct ?
1		1	0	6.25	0	Noreast	Nodir	Yes
2		0	1	0	6.25	Noreast	Nodir	No
3		1	0	6.25	0	Noreast	Nodir	Yes
4		1	0	6.25	0	Noreast	Nodir	Yes
5		1	1	6.25	6.25	Noreast	Nodir	Yes
6		1	1	6.25	6.25	Noreast	Nodir	Yes
7		1	1	6.25	3	No	South	Yes
8		0	1	0	3	No	Nodir	No
9		0	1	0	6.25	South	Nodir	No
10		1	1	12.5	6.25	Souwest	Souwest	Yes
11		1	1	9.5	9.5	South	Nodir	Yes
12		2	0	38	0	Souwest	Nodir	Yes
13		1	1	6.25	6.25	South	Nodir	Yes
14		0	1	0	3	No	North	Yes
15		2	0	50	0	No	Nodir	Yes
16		0	1	0	3	No	Nodir	Yes
17		0	1	0	3	South	Nodir	Yes
18		0	1	0	3	No	Nodir	Yes
19		0	1	0	3	South	Nodir	Yes
20		0	1	0	3	No	Nodir	Yes
21		0	1	0	3	South	Nodir	Yes
22		0	2	0	25	North	Nodir	Yes
23		0	1	0	3	No	Nodir	Yes
24		0	2	0	25	North	Nodir	Yes
25		0	2	0	38	No	Nodir	Yes
26		0	1	0	3	No	Nodir	Yes
27		0	1	0	9.5	No	Nodir	Yes
28		0	2	0	38	Noreast	Nodir	Yes
29		0	2	0	25	No	Nodir	Yes
30		0	4	0	50	North	Nodir	Yes
31		0	1	0	3	No	Nodir	Yes
32		0	1	0	3	No	Nodir	Yes
33		0	1	0	3	No	Nodir	Yes
34		0	1	0	3	No	Nodir	Yes
35		0	1	0	6.25	Noreast	Nodir	Yes
36		0	1	0	3	No	Nodir	Yes
37		0	1	0	6.25	No	Nodir	Yes
38		0	1	0	3	No	Nodir	No
39		0	1	0	6.25	No	Nodir	Yes
40		0	1	0	3	No	Nodir	Yes

F. Performance Evaluation of Interface Program II Using Data from Test Category 3: Repeatability Tests

F.1. Validation package obtained using sample 1 test data

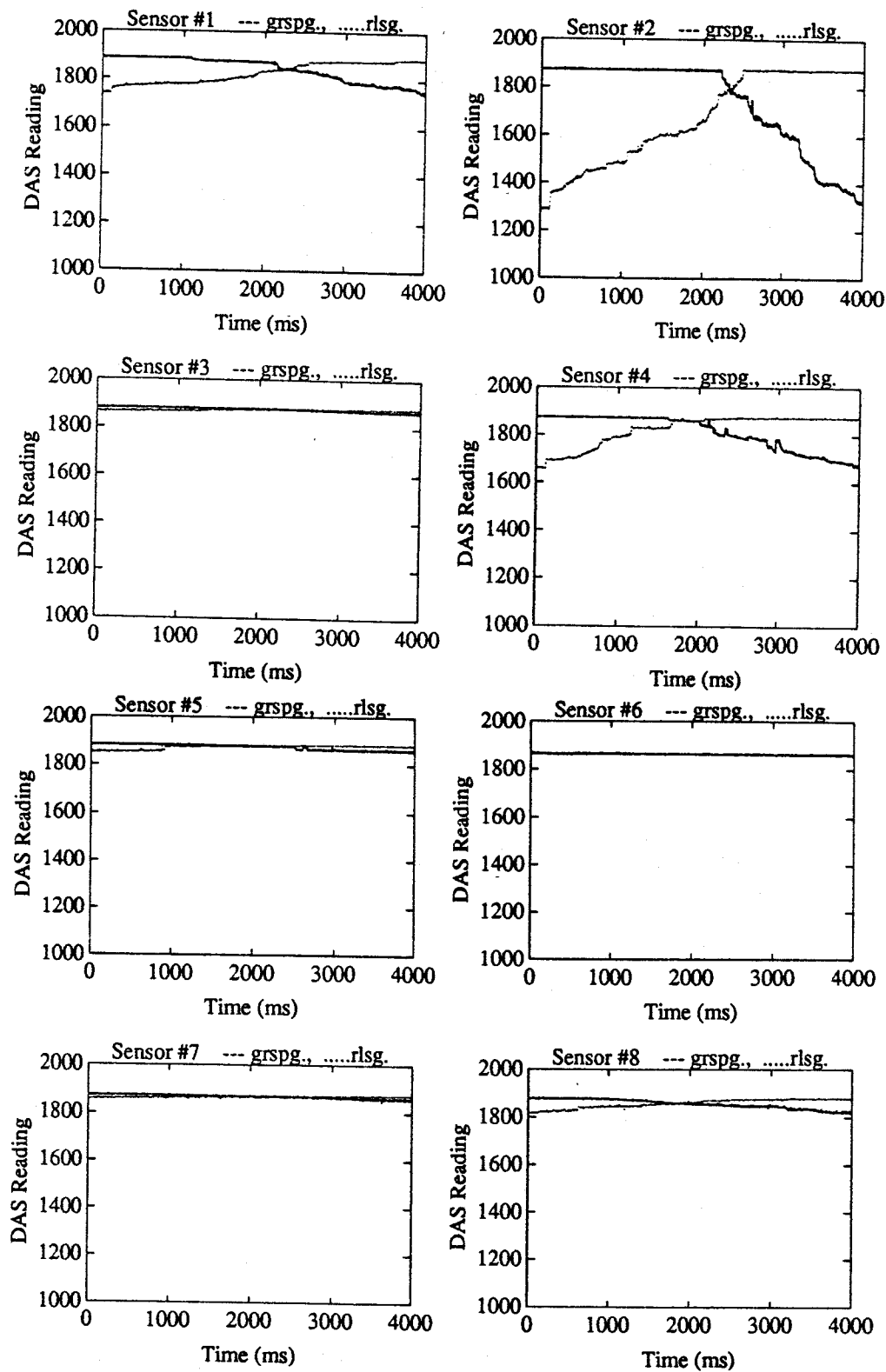
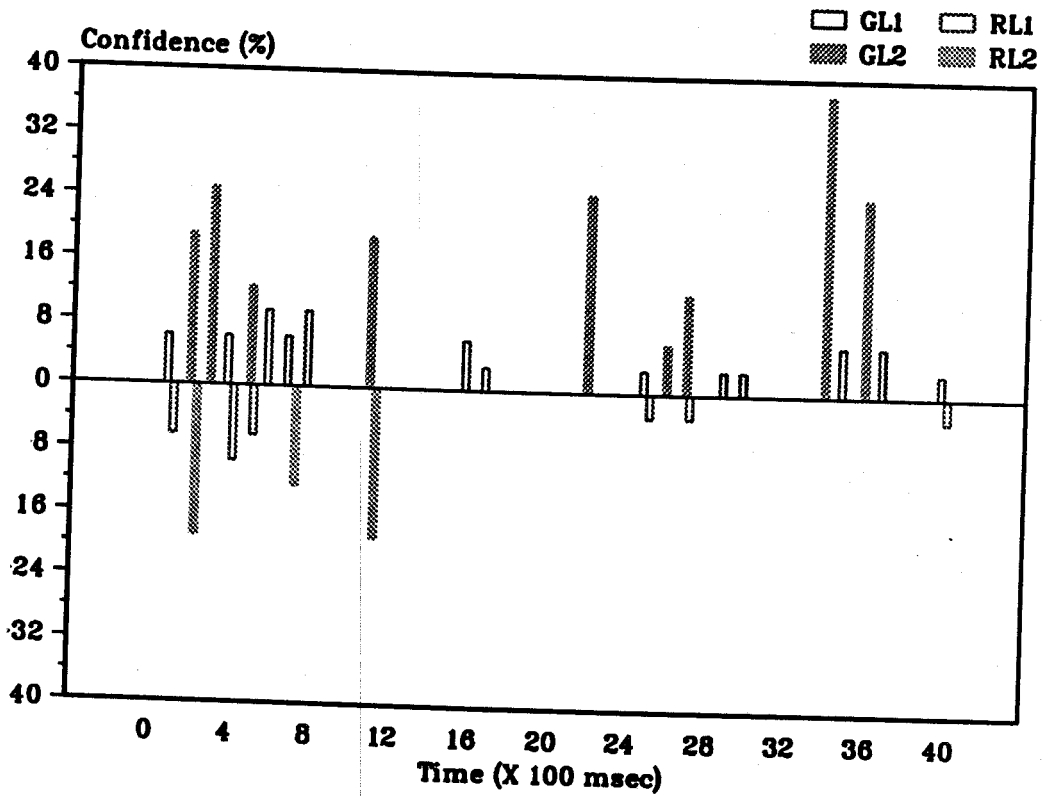


Figure F.1: Raw force data measured by the tactile sensors during the independent grasping and releasing operations performed on sample 1, trial 1 .

(a) Force decision parameters - repeatability test 1: grasping .



(b) Force decision parameters - repeatability test 1: releasing .

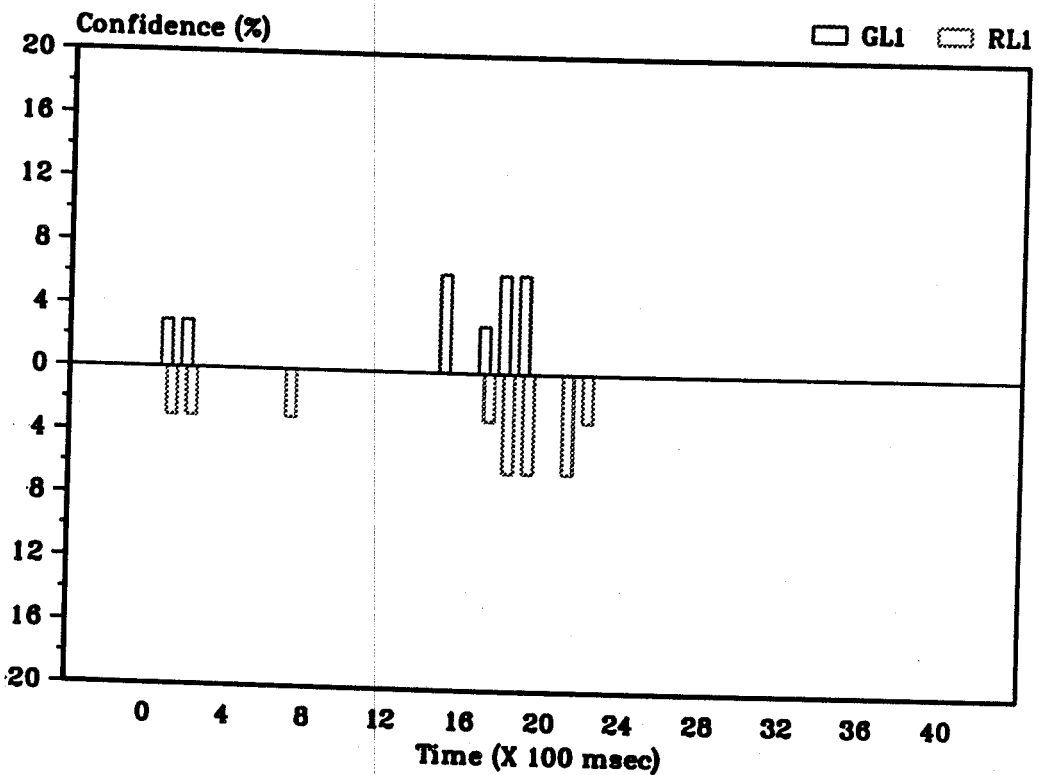


Figure F.2: The force decision parameters of the task status obtained from the TSI expert system using sample 1, trial 1 grasping and releasing data .

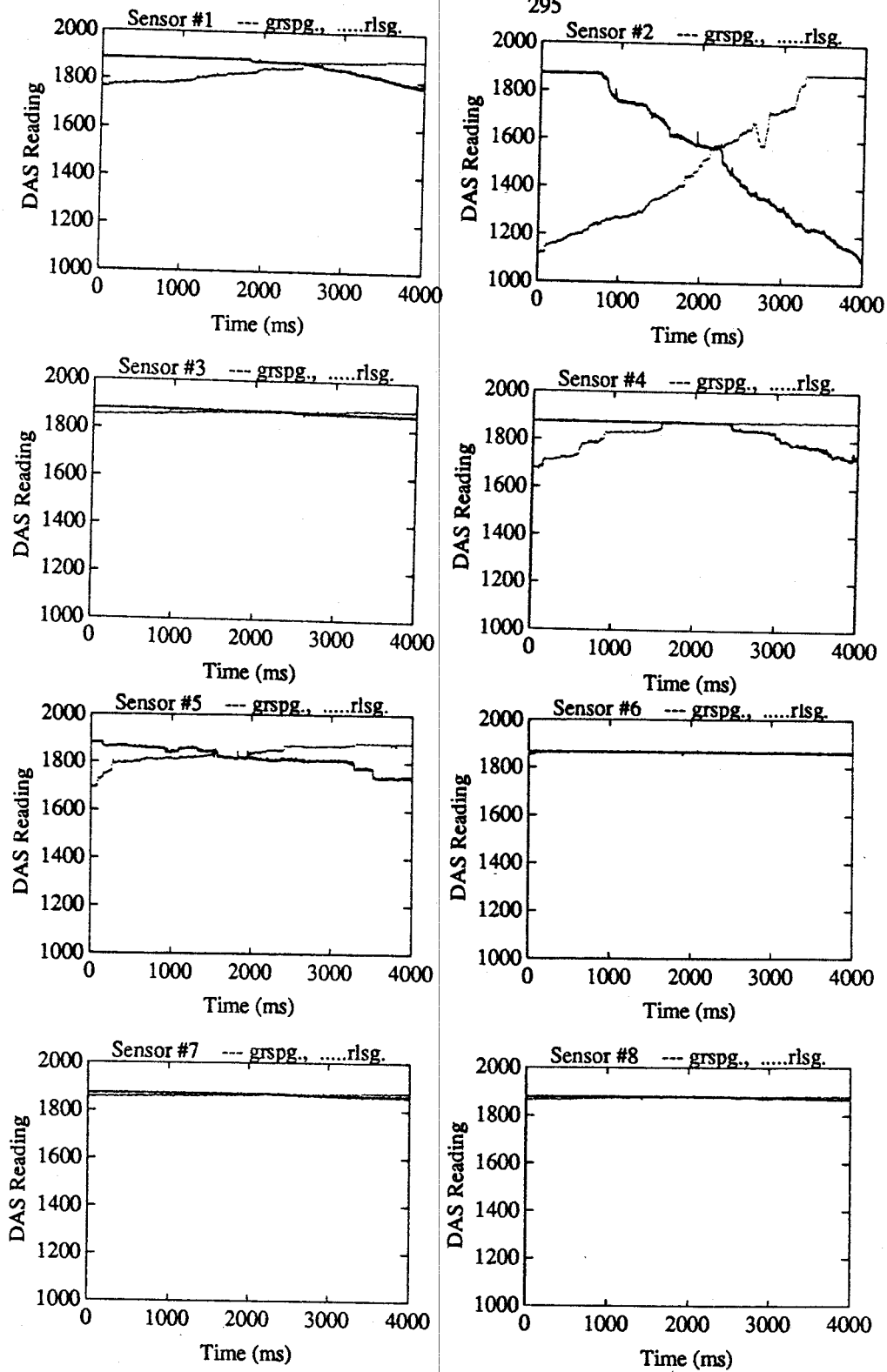
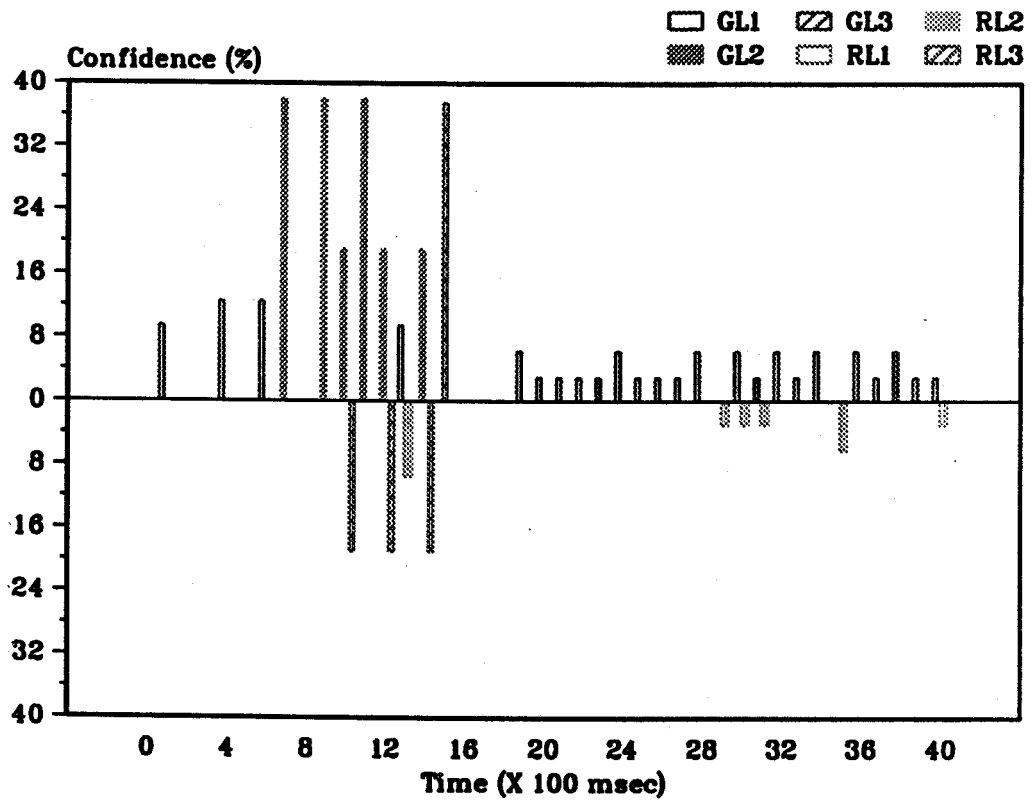


Figure F.3: Raw force data measured by the tactile sensors during the independent grasping and releasing operations performed on sample 1, trial 2 .

(a) Force decision parameters - repeatability test 2: grasping



(b) Force decision parameters - repeatability test 2: releasing

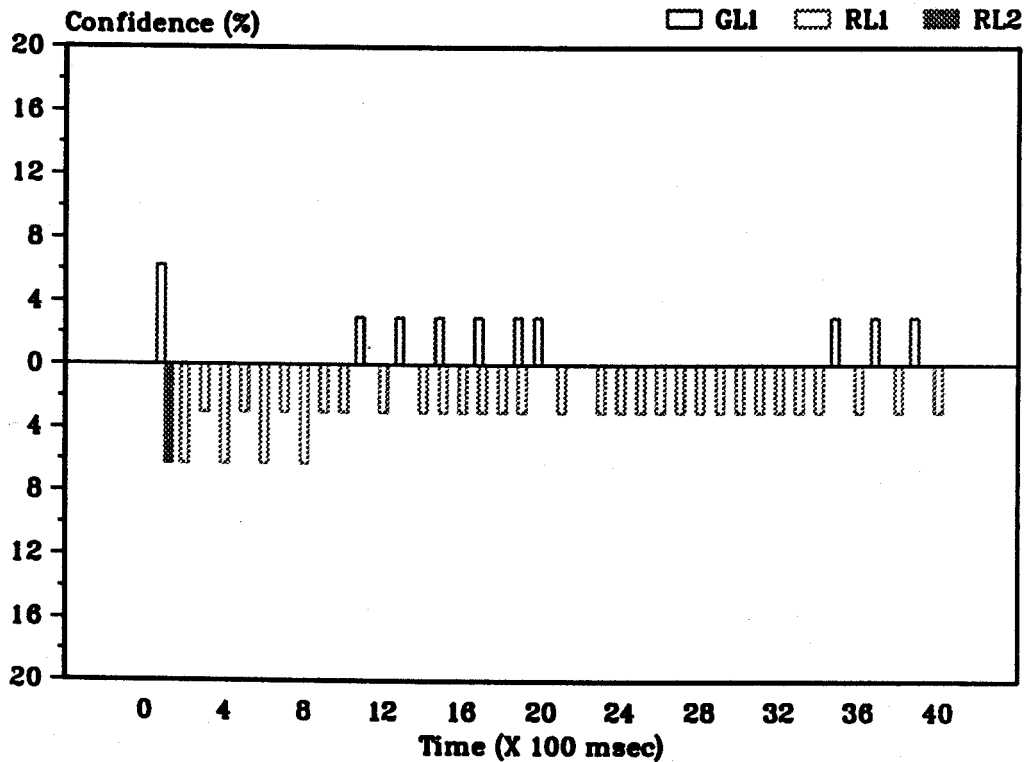


Figure F.4: The force decision parameters of the task status obtained from the TSI expert system using sample 1, trial 2 grasping and releasing data .

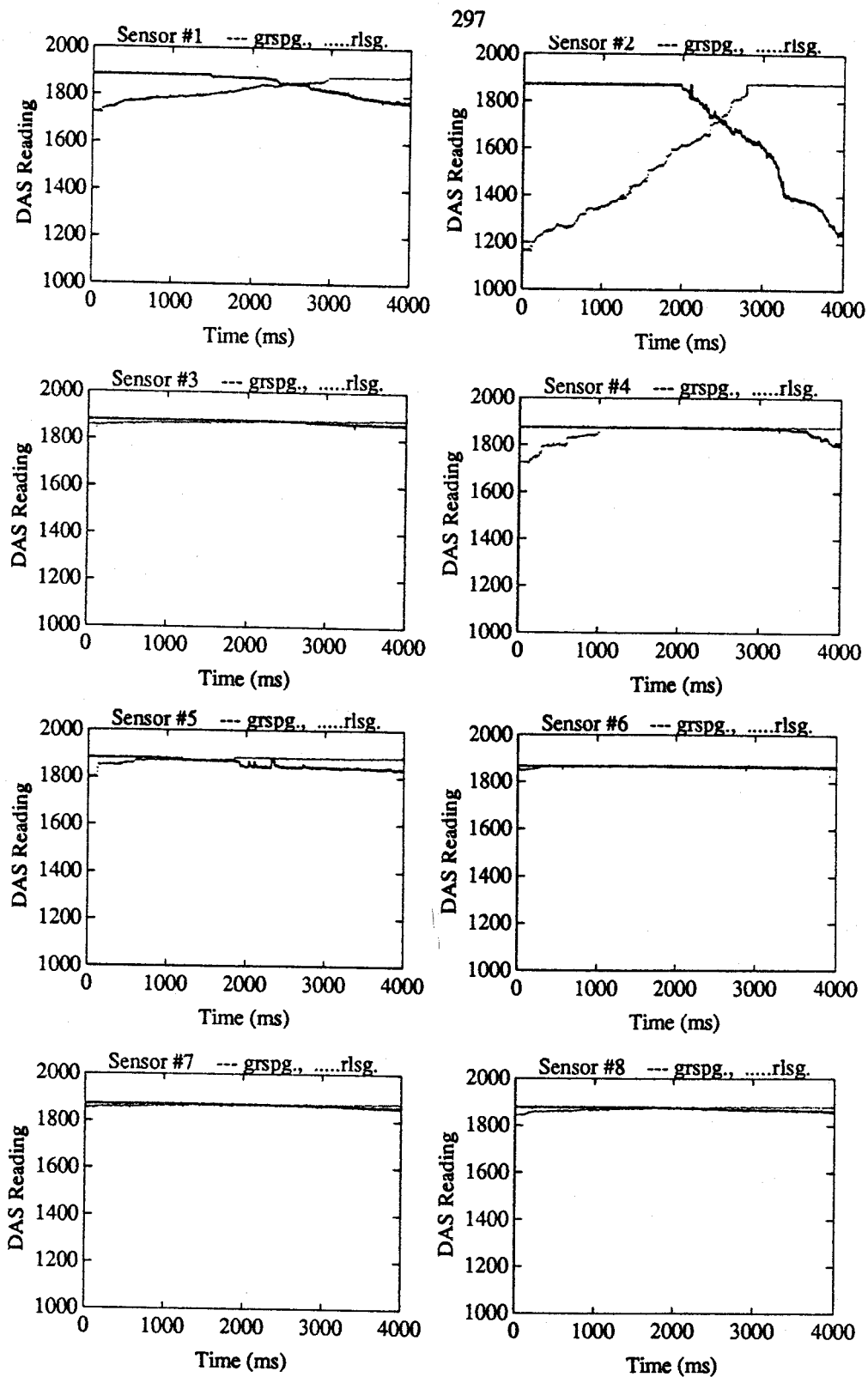
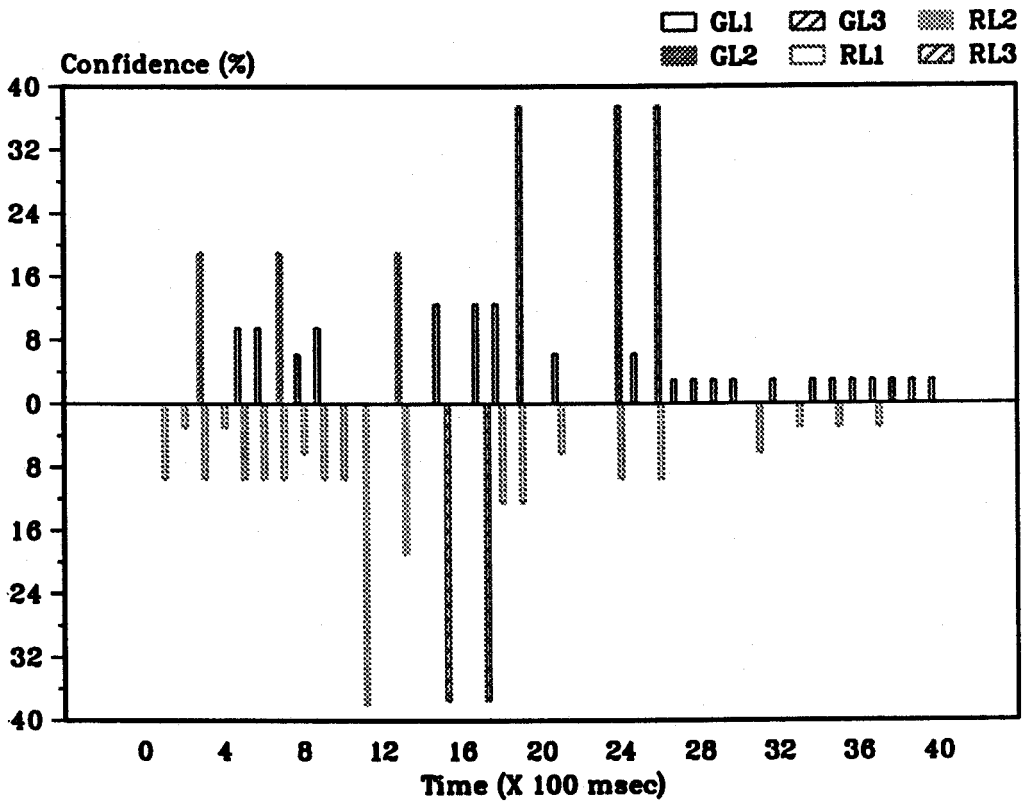


Figure F.5: Raw force data measured by the tactile sensors during the independent grasping and releasing operations performed on sample 1, trial 3 •

(a) Force decision parameters - repeatability test 3: grasping



(b) Force decision parameters - repeatability test 3: releasing

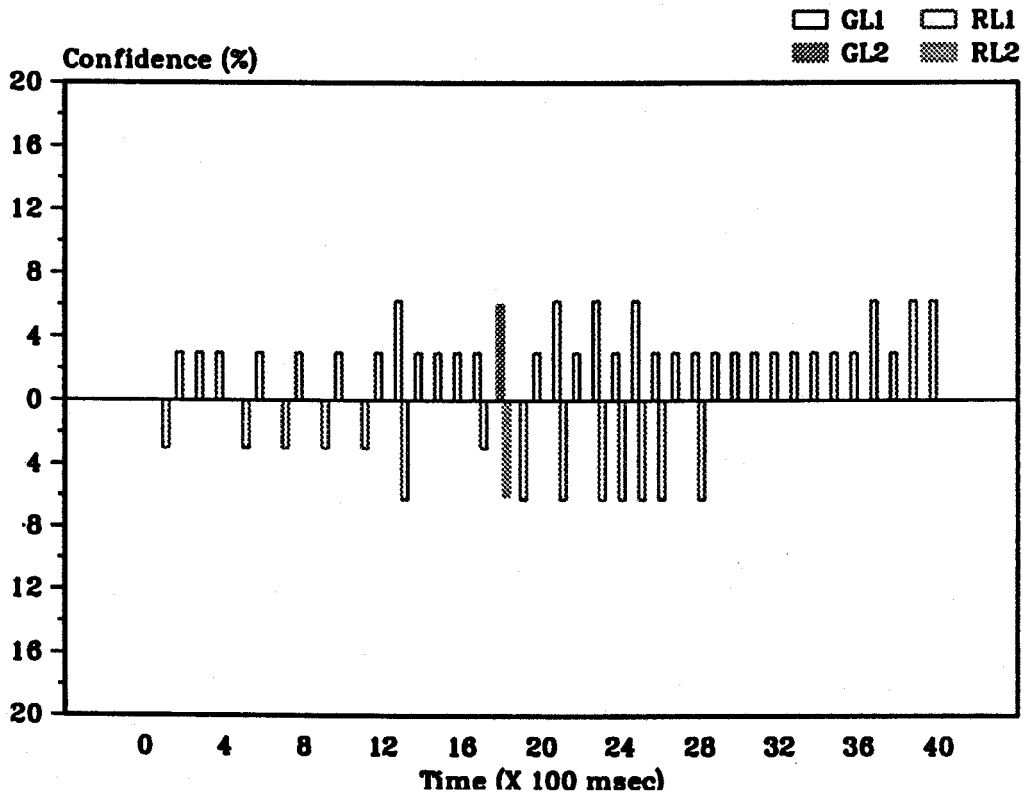


Figure F.6: The force decision parameters of the task status obtained from the TSI expert system using sample 1, trial 3 grasping and releasing data .

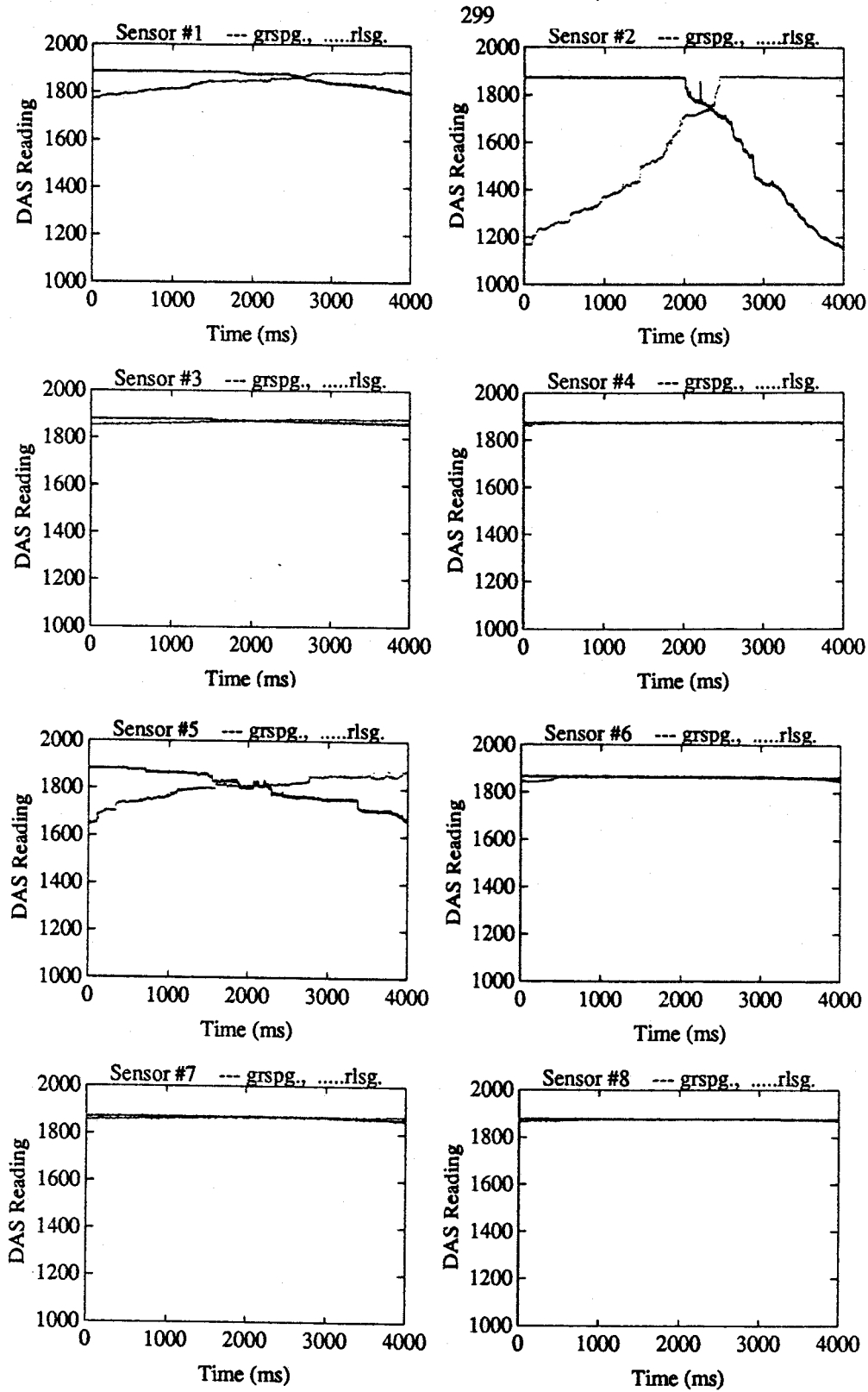
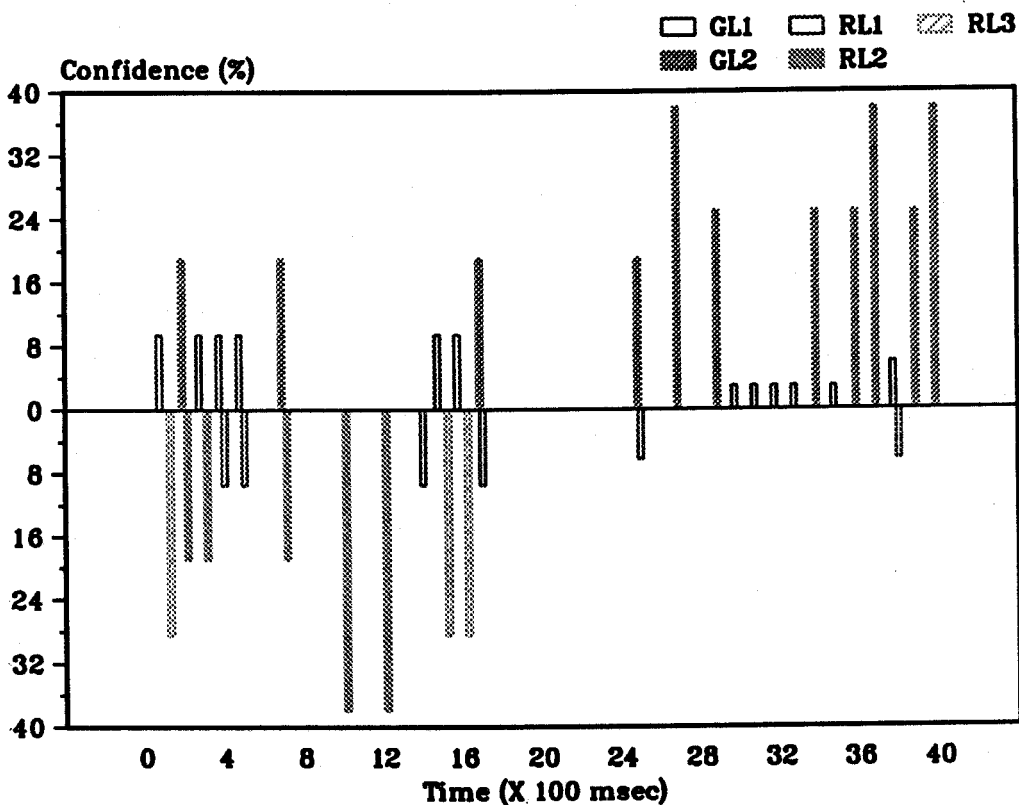


Figure F.7: Raw force data measured by the tactile sensors during the independent grasping and releasing operations performed on sample 1, trial 4.

(a) Force decision parameters - repeatability test 4: grasping .



(b) Force decision parameters - repeatability test 4: releasing .

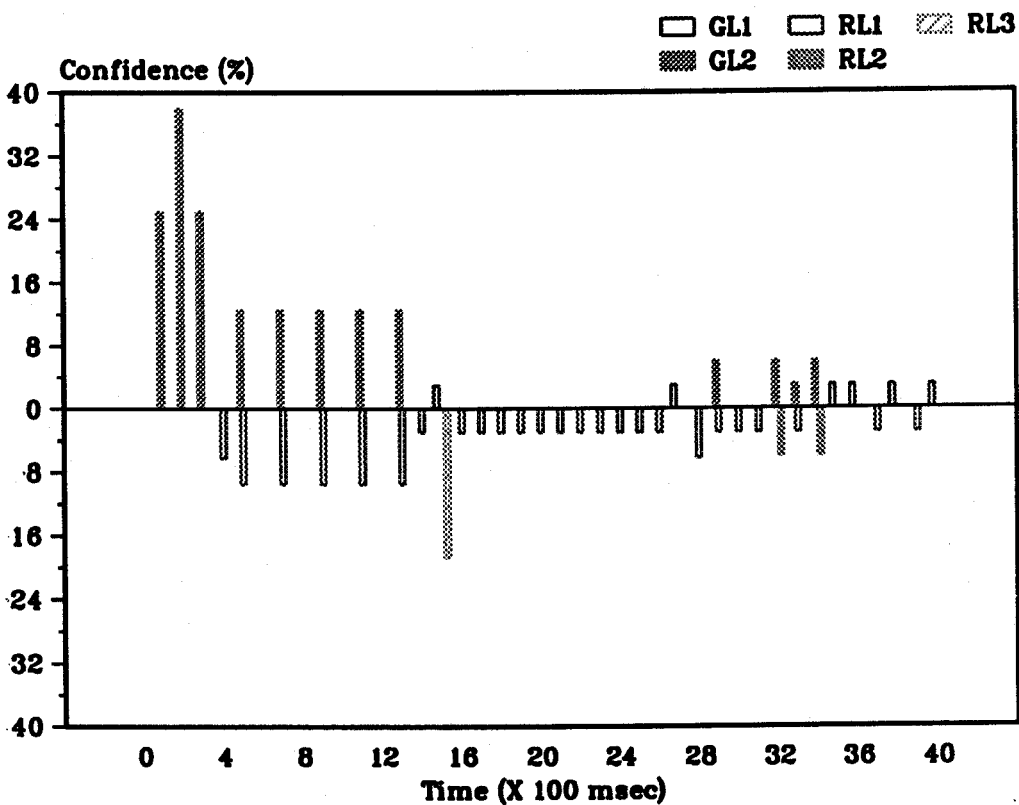


Figure F.8: The force decision parameters of the task status obtained from the TSI expert system using sample 1, trial 4 grasping and releasing data .

F.2. Performance tables obtained using Sample 1 repeatability test data

Table F.1: A summary of the task status parameters obtained from the TSI expert system using sample 1, trial 1 grasping data .

Block no.	Unchanged state	Grasping level	Releasing level	Grasping con. level	Releasing con. level	Dynamic displacement	Static displacement	Decision correct ?
1		1	1	6.25	6.25	Noreast	Souwest	Yes
2		2	2	19	19	No	Soueast	Yes
3		2	0	25	0	No	Nodir	Yes
4		1	1	6.25	9.5	No	Nodir	Yes
5		2	1	12.5	6.25	No	Noreast	Yes
6		1	0	9.5	0	No	Nodir	Yes
7		1	2	6.25	12.5	No	Noreast	Yes
8		1	0	9.5	0	No	Nodir	Yes
9		--	--	--	--	No	Nodir	No
10		--	--	--	--	No	Nodir	No
11		2	2	19	19	Noreast	Noreast	Yes
12		--	--	--	--	No	Nodir	No
13		--	--	--	--	No	Nodir	No
14		--	--	--	--	No	Nodir	No
15		--	--	--	--	No	Nodir	No
16		1	0	6.25	0	No	Nodir	Yes
17		1	0	3	0	No	Nodir	Yes
18	y	0	0	0	0	No	Nodir	Yes
19	y	0	0	0	0	No	Nodir	Yes
20	y	0	0	0	0	No	Nodir	Yes
21	y	0	0	0	0	No	Nodir	Yes
22		2	0	25	0	No	Nodir	Yes
23	y	0	0	0	0	No	Nodir	Yes
24	y	0	0	0	0	No	Nodir	Yes
25		1	1	3	3	No	Nodir	Yes
26		2	0	6.25	0	No	Nodir	Yes
27		2	1	12.5	3	No	Soueast	Yes
28	y	0	0	0	0	No	Nodir	Yes
29		1	0	3	0	No	Nodir	Yes
30		1	0	3	0	No	Nodir	Yes
31	y	0	0	0	0	No	Nodir	Yes
32	y	0	0	0	0	No	Nodir	Yes
33	y	0	0	0	0	No	Nodir	Yes
34		2	0	38	0	South	Nodir	Yes
35		1	0	6.25	0	South	Nodir	Yes
36		2	0	25	0	West	Nodir	Yes
37		1	0	6.25	0	No	Nodir	Yes
38	y	0	0	0	0	No	Nodir	Yes
39	y	0	0	0	0	No	Nodir	Yes
40		1	1	3	3	No	Nodir	Yes

Table F.2: A summary of the task status parameters obtained from the TSI expert system using sample 1, trial 1 releasing data •

Block no.	Unchanged state	Grasping level	Releasing level	Grasping con. level	Releasing con. level	Dynamic displacement	Static displacement	Decision correct ?
1		1	1	3	3	No	Nodir	Yes
2		1	1	3	3	No	Nodir	Yes
3	y	0	0	0	0	No	Nodir	Yes
4	y	0	0	0	0	No	Nodir	Yes
5	y	0	0	0	0	No	Nodir	Yes
6	y	0	0	0	0	No	Nodir	Yes
7		0	1	0	3	No	Nodir	Yes
8	y	0	0	0	0	No	Nodir	Yes
9	y	0	0	0	0	No	Nodir	Yes
10	y	0	0	0	0	No	Nodir	Yes
11	y	0	0	0	0	No	Nodir	Yes
12	y	0	0	0	0	No	Nodir	Yes
13	y	0	0	0	0	No	Nodir	Yes
14	y	0	0	0	0	No	Nodir	Yes
15		1	0	6.25	0	North	Nodir	No
16	y	0	0	0	0	No	Nodir	Yes
17		1	1	3	3	No	Nodir	Yes
18		1	1	6.25	6.25	No	Nodir	Yes
19		1	1	6.25	6.25	East	Nodir	Yes
20	y	0	0	0	0	No	Nodir	Yes
21		0	1	0	6.25	No	Nodir	Yes
22		0	1	0	3	No	Nodir	Yes
23	y	0	0	0	0	No	Nodir	Yes
24	y	0	0	0	0	No	Nodir	Yes
25	y	0	0	0	0	No	Nodir	Yes
26	y	0	0	0	0	No	Nodir	Yes
27	y	0	0	0	0	No	Nodir	Yes
28	y	0	0	0	0	No	Nodir	Yes
29	y	0	0	0	0	No	Nodir	Yes
30	y	0	0	0	0	No	Nodir	Yes
31	y	0	0	0	0	No	Nodir	Yes
32	y	0	0	0	0	No	Nodir	Yes
33	y	0	0	0	0	No	Nodir	Yes
34	y	0	0	0	0	No	Nodir	Yes
35	y	0	0	0	0	No	Nodir	Yes
36	y	0	0	0	0	No	Nodir	Yes
37	y	0	0	0	0	No	Nodir	Yes
38	y	0	0	0	0	No	Nodir	Yes
39	y	0	0	0	0	No	Nodir	Yes
40	y	0	0	0	0	No	Nodir	Yes

Table F.3: A summary of the task status parameters obtained from the TSI expert system using sample 1, trial 2 grasping data .

Block no.	Unchanged state	Grasping level	Releasing level	Grasping con. level	Releasing con. level	Dynamic displacement	Static displacement	Decision correct ?
1		1	0	9.5	0	Northeast	Nodir	Yes
2		--	--	--	--	No	Nodir	No
3		--	--	--	--	No	Nodir	No
4		1	0	12.5	0	South	Nodir	Yes
5		--	--	--	--	No	Nodir	No
6		1	0	12.5	0	South	Nodir	Yes
7		2	0	38	0	Northeast	Nodir	Yes
8		--	--	--	--	No	Nodir	No
9		2	0	38	0	Northeast	Nodir	Yes
10		2	2	19	19	Northeast	Nodir	Yes
11		2	0	38	0	Northeast	Nodir	Yes
12		2	2	19	19	Northeast	Nodir	Yes
13		1	1	9.5	9.5	Northeast	Nodir	Yes
14		2	2	19	19	Northeast	Nodir	Yes
15		3	1	37.5	9.5	South	South	Yes
16		--	--	--	--	No	Nodir	No
17		--	--	--	--	No	Nodir	No
18		--	--	--	--	No	Nodir	No
19		1	0	6.25	0	Northeast	Nodir	Yes
20		1	0	3	0	No	Nodir	Yes
21		1	0	3	0	No	Nodir	Yes
22		1	0	3	0	No	Nodir	Yes
23		1	0	3	0	No	Nodir	Yes
24		1	0	6.25	0	No	Nodir	Yes
25		1	0	3	0	No	Nodir	Yes
26		1	0	3	0	No	Nodir	Yes
27		1	0	3	0	No	Nodir	Yes
28		1	0	6.25	0	No	Nodir	Yes
29		0	1	0	3	No	Nodir	No
30		1	1	6.25	3	No	Nodir	Yes
31		1	1	3	3	No	Nodir	Yes
32		1	0	6.25	0	No	Nodir	Yes
33		1	0	3	0	No	Nodir	Yes
34		1	0	6.25	0	No	Nodir	Yes
35		0	1	0	6.25	No	Nodir	No
36		1	0	6.25	0	Norwest	Nodir	Yes
37		1	0	3	0	No	Nodir	Yes
38		1	0	6.25	0	No	Nodir	Yes
39		1	0	3	0	No	Nodir	Yes
40		1	1	3	3	No	Nodir	Yes

Table F.4: A summary of the task status parameters obtained from the TSI expert system using sample 1, trial 2 releasing data .

Block no.	Unchanged state	Grasping level	Releasing level	Grasping con. level	Releasing con. level	Dynamic displacement	Static displacement	Decision correct ?
1		1	2	6.25	25	East	West	Yes
2		0	1	0	6.25	Northeast	Nodir	Yes
3		0	1	0	3	No	Nodir	Yes
4		0	1	0	6.25	Northeast	Nodir	Yes
5		0	1	0	3	No	Nodir	Yes
6		0	1	0	6.25	Northeast	Nodir	Yes
7		0	1	0	3	No	Nodir	Yes
8		0	1	0	6.25	No	Nodir	Yes
9		0	1	0	3	No	Nodir	Yes
10		0	1	0	3	No	Nodir	Yes
11		1	0	3	0	No	Nodir	No
12		0	1	0	3	No	Nodir	Yes
13		1	0	3	0	No	Nodir	No
14		0	1	0	3	No	Nodir	Yes
15		1	1	3	3	No	Nodir	Yes
16		0	1	0	3	No	Nodir	Yes
17		1	1	3	3	No	Nodir	Yes
18		0	1	0	3	No	Nodir	Yes
19		1	1	3	3	No	Nodir	Yes
20		0	2	0	38	No	Nodir	Yes
21		1	1	3	3	No	Nodir	Yes
22		1	0	3	0	No	Nodir	No
23		0	1	0	3	No	Nodir	Yes
24		0	1	0	3	No	Nodir	Yes
25		0	1	0	3	No	Nodir	Yes
26		0	1	0	3	No	Nodir	Yes
27		0	1	0	3	No	Nodir	Yes
28		0	1	0	3	No	Nodir	Yes
29		0	1	0	3	No	Nodir	Yes
30		0	1	0	3	No	Nodir	Yes
31		0	1	0	3	No	Nodir	Yes
32		0	1	0	3	No	Nodir	Yes
33		0	1	0	3	No	Nodir	Yes
34		0	1	0	3	No	Nodir	Yes
35		1	0	3	0	No	Nodir	No
36		0	1	0	3	No	Nodir	Yes
37		1	0	3	0	No	Nodir	No
38		0	1	0	3	No	Nodir	Yes
39		1	0	3	0	No	Nodir	No
40		0	1	0	3	No	Nodir	Yes

Table F.5: A summary of the task status parameters obtained from the TSI expert system using sample 1, trial 3 grasping data .

Block no.	Unchanged state	Grasping level	Releasing level	Grasping con. level	Releasing con. level	Dynamic displacement	Static displacement	Decision correct ?
1		0	1	0	9.5	Noreast	Nodir	No
2		0	1	0	3	No	Nodir	No
3		2	1	19	9.5	Noreast	Souwest	Yes
4		0	1	0	3	No	Nodir	No
5		1	1	9.5	9.5	Noreast	Nodir	Yes
6		1	1	9.5	9.5	Noreast	Nodir	Yes
7		2	1	19	9.5	Noreast	Souwest	Yes
8		1	1	6.25	6.25	Noreast	Nodir	Yes
9		1	1	9.5	9.5	Noreast	Souwest	Yes
10		0	1	0	9.5	Noreast	Nodir	No
11		0	2	0	38	Noreast	Nodir	No
12		--	--	--	--	No	Nodir	No
13		2	2	19	19	Noreast	Nodir	Yes
14		--	--	--	--	No	Nodir	No
15		1	3	12.5	37.5	Noreast	Noreast	Yes
16		--	--	--	--	No	Nodir	No
17		1	3	12.5	37.5	No	Noreast	Yes
18		1	1	12.5	12.5	North	Nodir	Yes
19		3	1	37.5	12.5	West	South	Yes
20		--	--	--	--	No	Nodir	No
21		1	1	6.25	6.25	Noreast	Nodir	Yes
22		--	--	--	--	No	Nodir	No
23		--	--	--	--	No	Nodir	No
24		3	1	37.5	9.5	South	East	Yes
25		1	0	6.25	0	No	Nodir	Yes
26		3	1	37.5	9.5	South	East	Yes
27		1	0	3	0	No	Nodir	Yes
28		1	0	3	0	No	Nodir	Yes
29		1	0	3	0	No	Nodir	Yes
30		1	0	3	0	No	Nodir	Yes
31		0	1	0	6.25	No	Nodir	No
32		1	0	3	0	No	Nodir	Yes
33		0	1	0	3	No	Nodir	No
34		1	1	3	3	No	Nodir	Yes
35		1	1	3	3	No	Nodir	Yes
36		1	0	3	0	No	Nodir	Yes
37		1	1	3	3	No	Nodir	Yes
38		1	0	3	0	No	Nodir	Yes
39		1	0	3	0	No	Nodir	Yes
40		1	0	3	0	No	Nodir	Yes

Table F.6: A summary of the task status parameters obtained from the TSI expert system using sample 1, trial 3 releasing data .

Block no.	Unchanged state	Grasping level	Releasing level	Grasping con. level	Releasing con. level	Dynamic displacement	Static displacement	Decision correct ?
1		0	1	0	3	No	Nodir	Yes
2		1	0	3	0	No	Nodir	No
3		1	0	3	0	No	Nodir	No
4		1	0	3	0	No	Nodir	No
5		0	1	0	3	No	Nodir	Yes
6		1	0	3	0	No	Nodir	No
7		0	1	0	3	No	Nodir	Yes
8		1	0	3	0	No	Nodir	No
9		0	1	0	3	No	Nodir	Yes
10		1	0	3	0	No	Nodir	No
11		0	1	0	3	No	Nodir	Yes
12		1	0	3	0	No	Nodir	No
13		1	1	6.25	6.25	No	Nodir	Yes
14		1	0	3	0	No	Nodir	No
15		1	0	3	0	No	Nodir	No
16		1	0	3	0	No	Nodir	No
17		1	1	3	3	No	Nodir	Yes
18		2	2	6.25	6.25	No	Nodir	Yes
19		0	1	0	0	No	Nodir	Yes
20		1	0	3	0	No	Nodir	No
21		1	1	6.25	6.25	No	South	Yes
22		1	0	3	0	No	Nodir	No
23		1	1	6.25	6.25	No	South	Yes
24		1	1	3	6.25	No	South	Yes
25		1	1	6.25	6.25	No	South	Yes
26		1	1	3	6.25	No	South	Yes
27		1	0	3	0	No	Nodir	No
28		1	1	3	6.25	No	South	Yes
29		1	0	3	0	No	Nodir	No
30		1	0	3	0	No	Nodir	No
31		1	0	3	0	No	Nodir	No
32		1	0	3	0	No	Nodir	No
33		1	0	3	0	No	Nodir	No
34		1	0	3	0	No	Nodir	No
35		1	0	6.25	0	No	Nodir	No
36		1	0	3	0	No	Nodir	No
37		1	0	6.25	0	No	Nodir	No
38		1	0	3	0	No	Nodir	No
39		1	0	6.25	0	No	Nodir	No
40		1	0	6.25	0	No	Nodir	No

Table F.7: A summary of the task status parameters obtained from the TSI expert system using sample 1, trial 4 grasping data .

Block no.	Unchanged state	Grasping level	Releasing level	Grasping con. level	Releasing con. level	Dynamic displacement	Static displacement	Decision correct ?
1		1	3	9.5	28.5	Northeast	Northeast	Yes
2		2	2	19	19	Northeast	Northeast	Yes
3		1	2	9.5	19	Northeast	Northeast	Yes
4		1	1	9.5	9.5	Northeast	Nodir	Yes
5		1	1	9.5	9.5	Northeast	Nodir	Yes
6		--	--	--	--	No	Nodir	No
7		2	2	19	19	Northeast	Nodir	Yes
8		--	--	--	--	No	Nodir	No
9		--	--	--	--	No	Nodir	No
10		0	2	0	38	Northeast	Nodir	No
11		--	--	--	--	No	Nodir	No
12		0	2	0	38	Northeast	Nodir	No
13		--	--	--	--	No	Nodir	No
14		0	1	0	9.5	Northeast	Nodir	No
15		1	3	9.5	28.5	Northeast	Nodir	Yes
16		1	3	9.5	28.5	Northeast	Nodir	Yes
17		2	1	19	9.5	Northeast	Nodir	Yes
18		--	--	--	--	No	Nodir	No
19		--	--	--	--	No	Nodir	No
20		--	--	--	--	No	Nodir	No
21		--	--	--	--	No	Nodir	No
22		--	--	--	--	No	Nodir	No
23		--	--	--	--	No	Nodir	No
24		--	--	--	--	No	Nodir	No
25		2	1	19	6.25	North	Nodir	Yes
26		--	--	--	--	No	Nodir	No
27		2	0	38	0	East	Nodir	Yes
28		--	--	--	--	No	Nodir	No
29		2	0	25	0	East	Nodir	Yes
30		1	0	3	0	No	Nodir	Yes
31		1	0	3	0	No	Nodir	Yes
32		1	0	3	0	No	Nodir	Yes
33		1	0	3	0	No	Nodir	Yes
34		2	0	25	0	East	Nodir	Yes
35		1	0	3	0	No	Nodir	Yes
36		2	0	25	0	East	Nodir	Yes
37		2	0	38	0	North	Nodir	Yes
38		1	0	6.25	0	Northeast	Nodir	Yes
39		2	0	25	0	East	Nodir	Yes
40		2	0	38	0	Northeast	Nodir	Yes

Table F.8: A summary of the task status parameters obtained from the TSI expert system using sample 1, trial 4 releasing data .

Block no.	Unchanged state	Grasping level	Releasing level	Grasping con. level	Releasing con. level	Dynamic displacement	Static displacement	Decision correct ?
1		2	0	25	0	East	Nodir	No
2		2	0	38	0	Noreast	Nodir	No
3		2	0	25	0	East	Nodir	No
4		0	1	0	6.25	No	Nodir	Yes
5		2	1	12.5	9.5	South	Nodir	Yes
6		--	--	--	--	No	Nodir	No
7		2	1	12.5	9.5	South	Nodir	Yes
8		--	--	--	--	No	Nodir	No
9		2	1	12.5	9.5	South	Nodir	Yes
10		--	--	--	--	No	Nodir	No
11		2	1	12.5	9.5	South	Nodir	Yes
12		--	--	--	--	No	Nodir	No
13		2	1	12.5	9.5	South	Nodir	Yes
14		0	1	0	3	No	Nodir	Yes
15		1	3	3	18.75	North	South	Yes
16		0	1	0	3	No	Nodir	Yes
17		0	1	0	3	No	Nodir	Yes
18		0	1	0	3	No	Nodir	Yes
19		0	1	0	3	No	Nodir	Yes
20		0	1	0	3	No	Nodir	Yes
21		0	1	0	3	No	Nodir	Yes
22		0	1	0	3	No	Nodir	Yes
23		0	1	0	3	No	Nodir	Yes
24		0	1	0	3	No	Nodir	Yes
25		0	1	0	3	No	Nodir	Yes
26		0	1	0	3	No	Nodir	Yes
27		1	0	3	0	No	Nodir	No
28		0	1	0	6.25	No	Nodir	Yes
29		2	1	6	3	No	Nodir	Yes
30		0	1	0	3	No	Nodir	Yes
31		0	1	0	3	No	Nodir	Yes
32		2	2	6	6	No	Nodir	Yes
33		2	1	6	3	No	Nodir	Yes
34		2	2	6	6	No	Nodir	Yes
35		1	0	3	0	No	Nodir	No
36		1	0	3	0	No	Nodir	No
37		0	1	0	3	No	Nodir	Yes
38		1	0	3	0	No	Nodir	No
39		0	1	0	3	No	Nodir	Yes
40		1	0	3	0	No	Nodir	No

G. Performance Evaluation of Interface Program II Using Data from Test Category 4: Simulated Slip Tests

G.1. Validation package obtained using data from artificial slip tests 2, 3 and 4

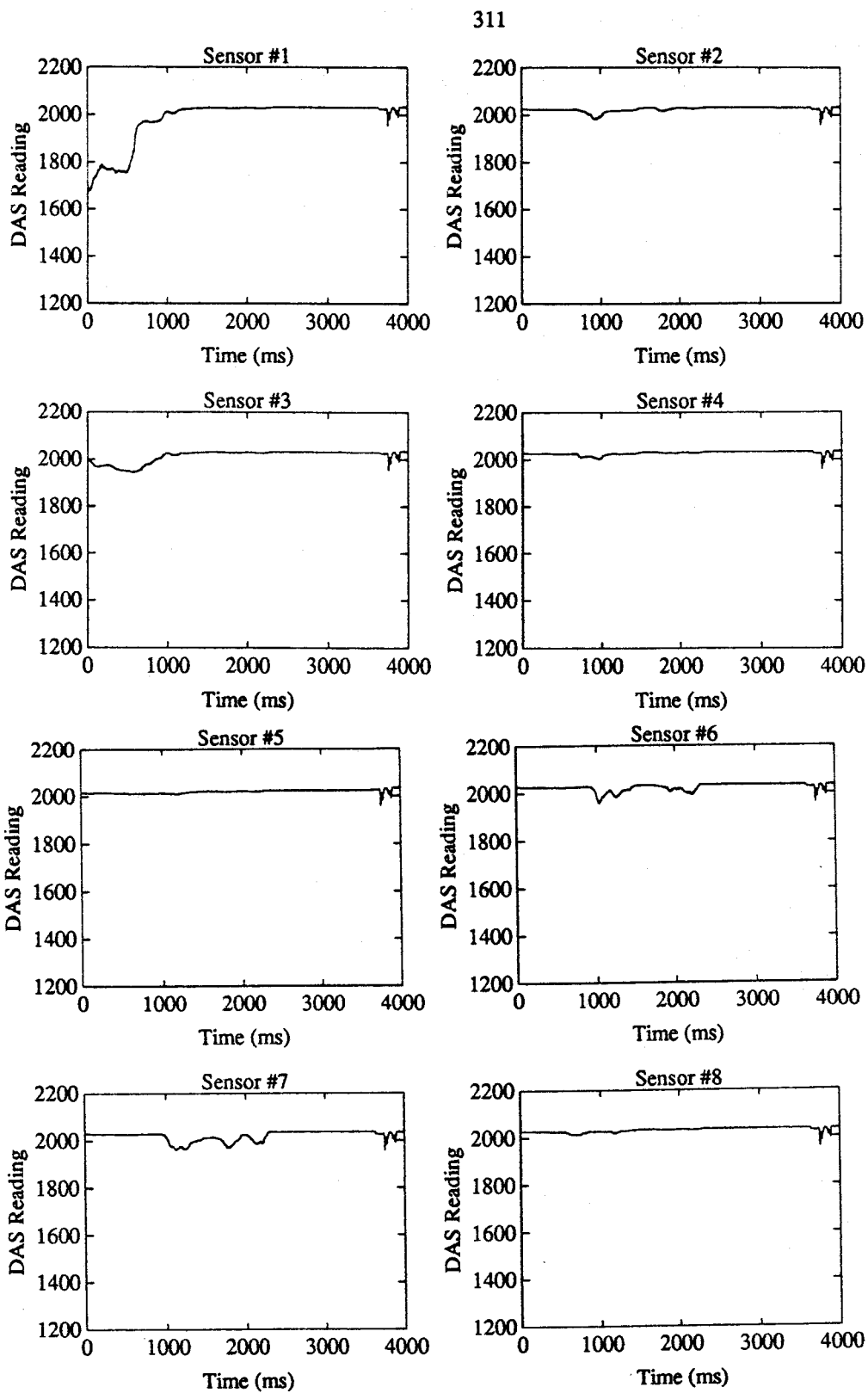
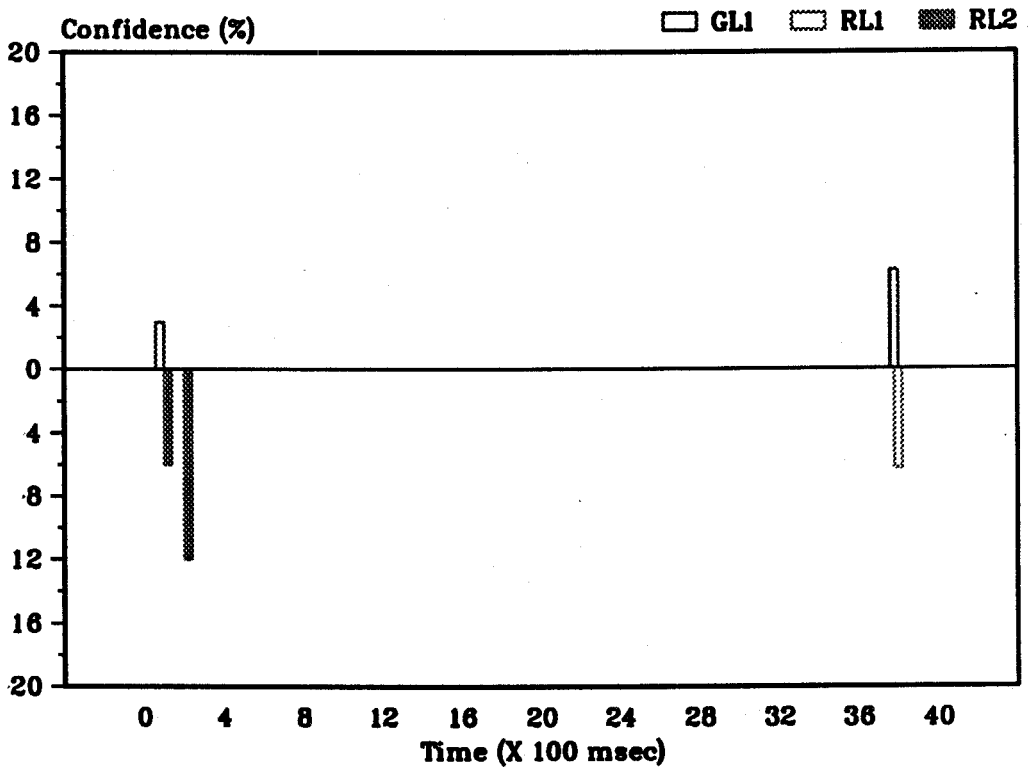


Figure G.1: Raw force data measured by the tactile sensors during the artificial slip test 2 .

(a) Force decision parameters - artificial slip test 2.



(b) Object displacement parameters - artificial slip test 2.

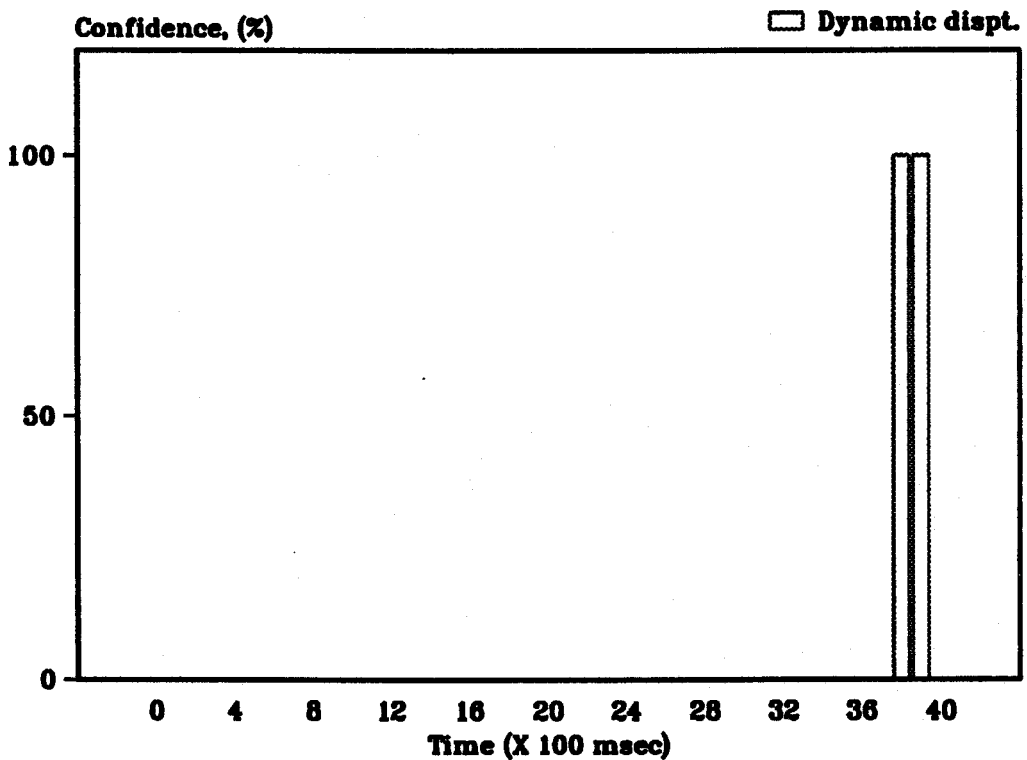


Figure G.2: The force decision and object displacement parameters of the task status obtained from the TSI expert system using artificial slip test 2 data.

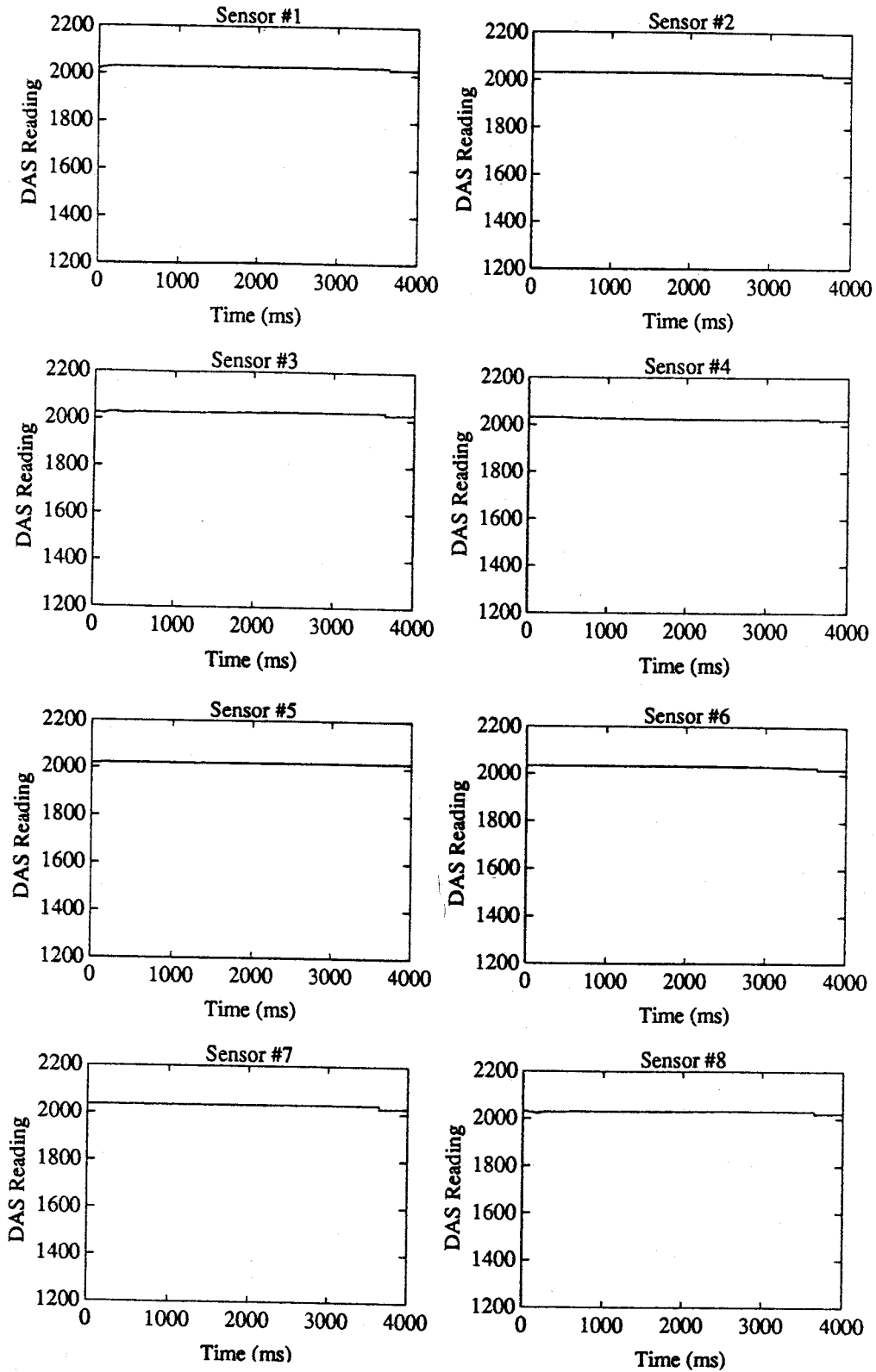
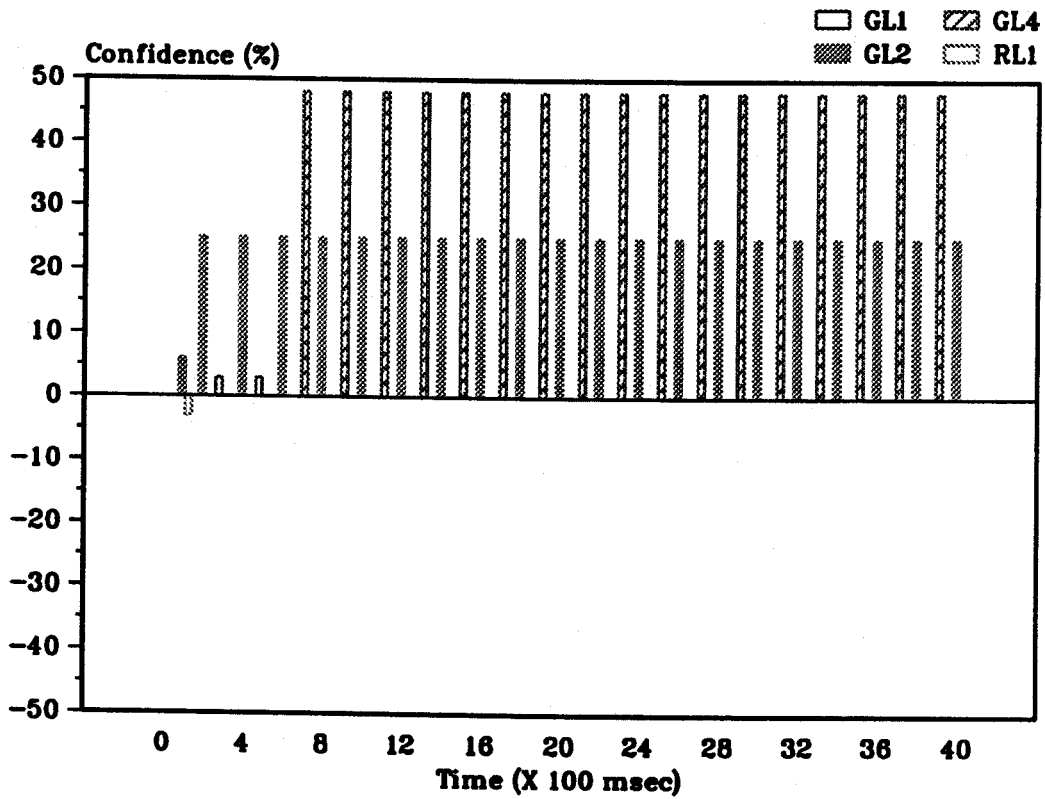


Figure G.3: Raw force data measured by the tactile sensors during the artificial slip test 3.

(a) Force decision parameters - artificial slip test 3.



(b) Object displacement parameters.

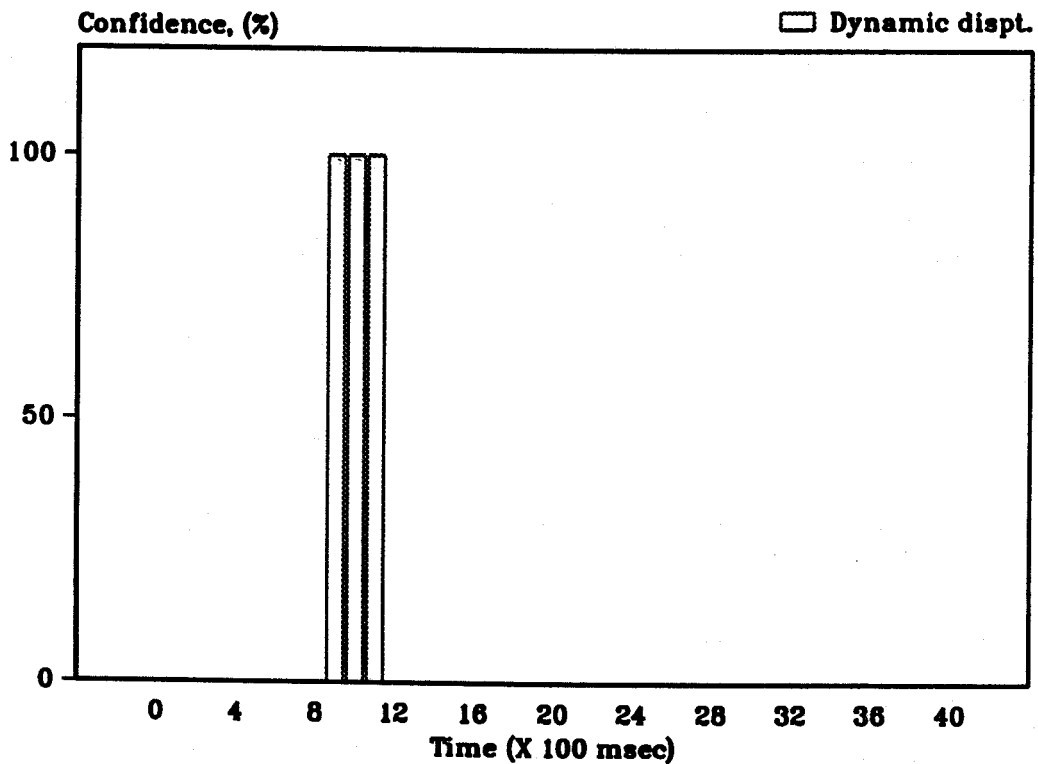


Figure G.4: The force decision and object displacement parameters of the task status obtained from the TSI expert system using artificial slip test 3 data.

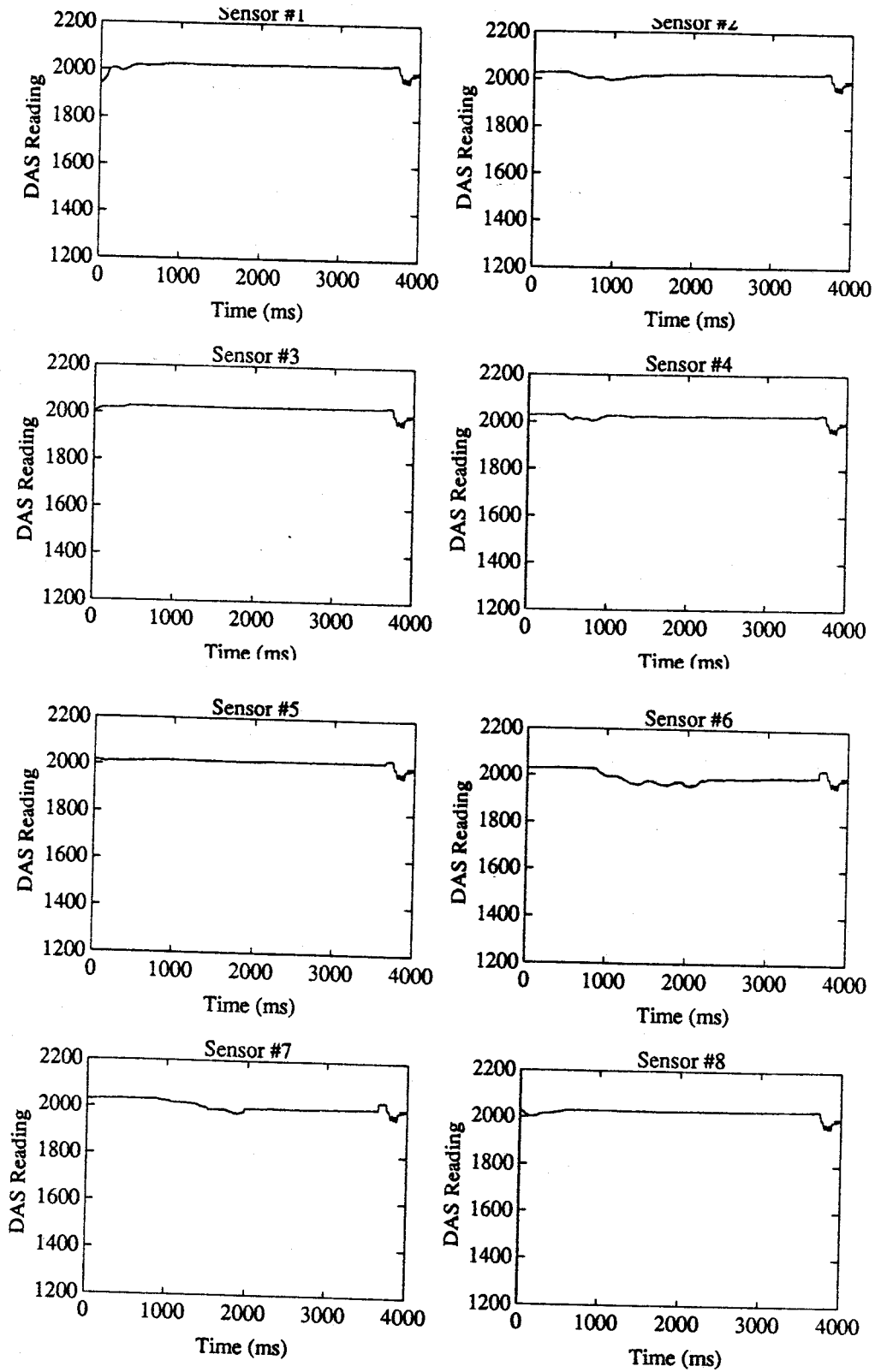
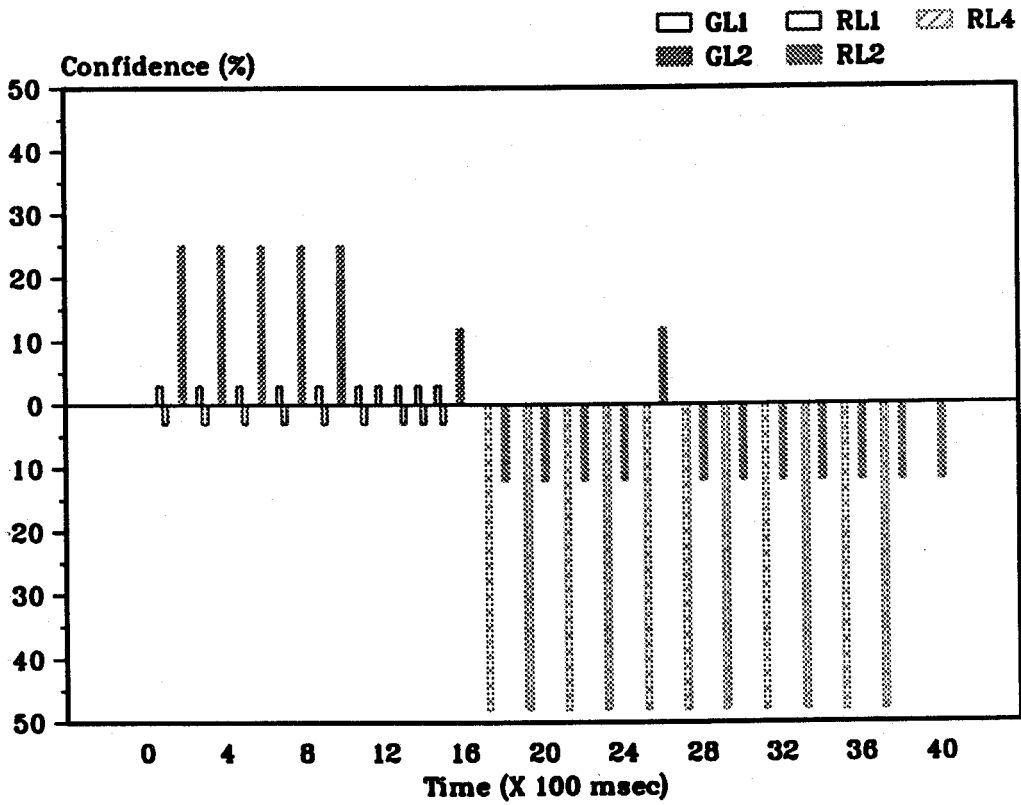


Figure G.5: Raw force data measured by the tactile sensors during the artificial slip test 4.

(a) Force decision parameters - artificial slip test 4 .



Object displacement parameters - artificial slip test 4 .

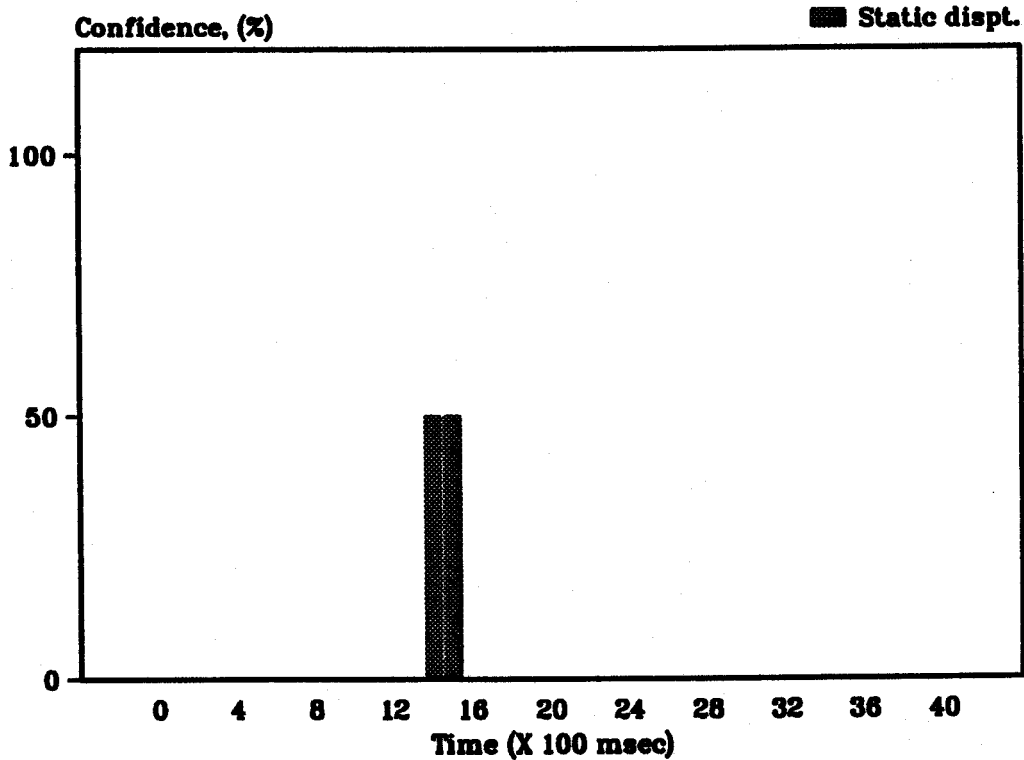


Figure G.6: The force decision and object displacement parameters of the task status obtained from the TSI expert system using artificial slip test 4 data.

G.2. Performance tables obtained using artificial slip test data

Table G.1: A summary of the task status parameters obtained from the TSI expert system using artificial slip test 2 data .

Block no.	Unchanged state	Grasping level	Releasing level	Grasping con. level	Releasing con. level	Dynamic displacement	Static displacement	Decision correct ?
1		1	2	3	6	No	Nodir	Yes
2		0	2	0	12	No	Nodir	Yes
3	y	0	0	0	0	No	Nodir	Yes
4	y	0	0	0	0	No	Nodir	Yes
5	y	0	0	0	0	No	Nodir	Yes
6	y	0	0	0	0	No	Nodir	Yes
7	y	0	0	0	0	No	Nodir	Yes
8	y	0	0	0	0	No	Nodir	Yes
9	y	0	0	0	0	No	Nodir	Yes
10	y	0	0	0	0	No	Nodir	Yes
11	y	0	0	0	0	No	Nodir	Yes
12	Y	0	0	0	0	No	Nodir	Yes
13	y	0	0	0	0	No	Nodir	Yes
14	y	0	0	0	0	No	Nodir	Yes
15	y	0	0	0	0	No	Nodir	Yes
16	y	0	0	0	0	No	Nodir	Yes
17	y	0	0	0	0	No	Nodir	Yes
18	y	0	0	0	0	No	Nodir	Yes
19	y	0	0	0	0	No	Nodir	Yes
20	y	0	0	0	0	No	Nodir	Yes
21	y	0	0	0	0	No	Nodir	Yes
22	y	0	0	0	0	No	Nodir	Yes
23	y	0	0	0	0	No	Nodir	Yes
24	y	0	0	0	0	No	Nodir	Yes
25	y	0	0	0	0	No	Nodir	Yes
26	y	0	0	0	0	No	Nodir	Yes
27	y	0	0	0	0	No	Nodir	Yes
28	y	0	0	0	0	No	Nodir	Yes
29	y	0	0	0	0	No	Nodir	Yes
30	y	0	0	0	0	No	Nodir	Yes
31	y	0	0	0	0	No	Nodir	Yes
32	y	0	0	0	0	No	Nodir	Yes
33	y	0	0	0	0	No	Nodir	Yes
34	y	0	0	0	0	No	Nodir	Yes
35	y	0	0	0	0	No	Nodir	Yes
36	y	0	0	0	0	No	Nodir	Yes
37	y	0	0	0	0	No	Nodir	Yes
38		1	1	6.25	6.25	East	Nodir	Yes
39	y	0	0	0	0	No	Nodir	Yes
40	y	0	0	0	0	No	Nodir	Yes

Table G.2: A summary of the task status parameters obtained from the TSI expert system using artificial slip test 3 data .

Block no.	Unchanged state	Grasping level	Releasing level	Grasping con. level	Releasing con. level	Dynamic displacement	Static displacement	Decision correct ?
1		2	1	6	3	No	Nodir	Yes
2		2	0	25	0	No	Nodir	Yes
3		1	0	3	0	No	Nodir	Yes
4		2	0	25	0	No	Nodir	Yes
5		1	1	3	3	No	Nodir	Yes
6		2	0	25	0	No	Nodir	Yes
7		4	0	48	0	No	Nodir	Yes
8		2	0	25	0	No	Nodir	Yes
9		4	0	48	0	No	Nodir	Yes
10		2	0	25	0	No	Nodir	Yes
11		4	0	48	0	No	Nodir	Yes
12		2	0	25	0	No	Nodir	Yes
13		4	0	48	0	No	Nodir	Yes
14		2	0	25	0	No	Nodir	Yes
15		4	0	48	0	No	Nodir	Yes
16		2	0	25	0	No	Nodir	Yes
17		4	0	48	0	No	Nodir	Yes
18		2	0	25	0	No	Nodir	Yes
19		4	0	48	0	No	Nodir	Yes
20		2	0	25	0	No	Nodir	Yes
21		4	0	48	0	No	Nodir	Yes
22		2	0	25	0	No	Nodir	Yes
23		4	0	48	0	No	Nodir	Yes
24		2	0	25	0	No	Nodir	Yes
25		4	0	48	0	No	Nodir	Yes
26		2	0	25	0	No	Nodir	Yes
27		4	0	48	0	No	Nodir	Yes
28		2	0	25	0	No	Nodir	Yes
29		4	0	48	0	No	Nodir	Yes
30		2	0	25	0	No	Nodir	Yes
31		4	0	48	0	No	Nodir	Yes
32		2	0	25	0	No	Nodir	Yes
33		4	0	48	0	No	Nodir	Yes
34		2	0	25	0	No	Nodir	Yes
35		4	0	48	0	No	Nodir	Yes
36		2	0	25	0	No	Nodir	Yes
37		4	0	48	0	No	Nodir	Yes
38		2	0	25	0	No	Nodir	Yes
39		4	0	48	0	No	Nodir	Yes
40		2	0	25	0	No	Nodir	Yes

Table G.3: A summary of the task status parameters obtained from the TSI expert system using artificial slip test 4 data .

Block no.	Unchanged state	Grasping level	Releasing level	Grasping con. level	Releasing con. level	Dynamic displacement	Static displacement	Decision correct ?
1		1	1	3	3	No	Nodir	Yes
2		2	0	25	0	No	Nodir	Yes
3		1	1	3	3	No	Nodir	Yes
4		2	0	25	0	No	Nodir	Yes
5		1	1	3	3	No	Nodir	Yes
6		2	0	25	0	No	Nodir	Yes
7		1	1	3	3	No	Nodir	Yes
8		2	0	25	0	No	Nodir	Yes
9		1	1	3	3	No	Nodir	Yes
10		2	0	25	0	No	Nodir	Yes
11		1	1	3	3	No	Nodir	Yes
12		1	0	3	0	No	Nodir	Yes
13		1	1	3	3	No	Nodir	Yes
14		1	1	3	3	No	East	Yes
15		1	1	3	3	No	Nodir	Yes
16		2	0	12	0	No	Nodir	Yes
17		0	4	0	48	No	Nodir	Yes
18		0	2	0	12	No	Nodir	Yes
19		0	4	0	48	No	Nodir	Yes
20		0	2	0	12	No	Nodir	Yes
21		0	4	0	48	No	Nodir	Yes
22		0	2	0	12	No	Nodir	Yes
23		0	4	0	48	No	Nodir	Yes
24		0	2	0	12	No	Nodir	Yes
25		0	4	0	48	No	Nodir	Yes
26		0	2	0	12	No	Nodir	Yes
27		0	4	0	48	No	Nodir	Yes
28		0	2	0	12	No	Nodir	Yes
29		0	4	0	48	No	Nodir	Yes
30		0	2	0	12	No	Nodir	Yes
31		0	4	0	48	No	Nodir	Yes
32		0	2	0	12	No	Nodir	Yes
33		0	4	0	48	No	Nodir	Yes
34		0	2	0	12	No	Nodir	Yes
35		0	4	0	48	No	Nodir	Yes
36		0	2	0	12	No	Nodir	Yes
37		0	4	0	48	No	Nodir	Yes
38		0	2	0	12	No	Nodir	Yes
39		--	--	--	--	No	Nodir	No
40		0	2	0	12	No	Nodir	Yes

H. Performance Evaluation of the Control Decision Indicator Expert System

H.1. Control decisions obtained from sample 1 test data

Table H.1: Summary of the results displayed by the CDI expert system - Test Category 1: sample 1 grasping .

Block no.	Time period,ms	Force decision	Confidence, %	Mov.decision	Confidence, %	Remarks
1,2	0 to 200	maintain same	100	do not move	100	--
3,4	201 to 400	maintain same	100	do not move	100	--
5,6	401 to 600	maintain same	100	do not move	100	--
7,8	601 to 800	maintain same	100	do not move	100	--
9,10	801 to 1000	maintain same	100	do not move	100	--
11,12	1001 to 1200	maintain same	75	do not move	100	--
13,14	1201 to 1400	maintain same	100	do not move	100	--
15,16	1401 to 1600	do not increase	43	do not move	100	--
17,18	1601 to 1800	maintain same	100	do not move	100	--
19,20	1801 to 2000	do not increase	83	move North	50	small slip in South direction
21,22	2001 to 2200	do not increase	36	do not move	100	--
23,24	2201 to 2400	do not increase	80	do not move	100	--
25,26	2401 to 2600	increase	54	move North	100	large slip in South direction
27,28	2601 to 2800	do not increase	58	do not move	100	--
29,30	2801 to 3000	do not increase	80	move Northwest	50	small slip in Southeast dir.
31,32	3001 to 3200	do not increase	48	move North	50	small slip in South dir.
33,34	3201 to 3400	do not increase	96	move North	50	small slip in South dir.
35,36	3401 to 3600	do not increase	78	do not move	100	--
37,38	3601 to 3800	maintain same	100	do not move	100	--
39,40	3801 to 4000	maintain same	75	do not move	100	--

Table H.2: Summary of the results displayed by the CDI expert system - Test Category 1: sample 1 releasing .

Block no.	Time period,ms	Force decision	Confidence %	Mov.decision	Confidence %	Remarks
1,2	1 to 200	maintain same	100	do not move	100	--
3,4	201 to 400	do not increase	45	do not move	100	--
5,6	401 to 600	maintain same	100	do not move	100	--
7,8	601 to 800	maintain same	100	do not move	100	--
9,10	801 to 1000	do not increase	38	move West	50	small slip in East direction
11,12	1001 to 1200	maintain same	75	move North	50	small slip in South direction
13,14	1201 to 1400	maintain same	100	do not move	100	--
15,16	1401 to 1600	maintain same	100	do not move	100	--
17,18	1601 to 1800	maintain same	100	do not move	100	--
19,20	1801 to 2000	maintain same	100	do not move	100	--
21,22	2001 to 2200	maintain same	100	do not move	100	--
23,24	2201 to 2400	maintain same	100	do not move	100	--
25,26	2401 to 2600	maintain same	100	do not move	100	--
27,28	2601 to 2800	maintain same	100	do not move	100	--
29,30	2801 to 3000	maintain same	100	do not move	100	--
31,32	3001 to 3200	maintain same	100	do not move	100	--
33,34	3201 to 3400	do not increase	77	do not move	100	--
35,36	3401 to 3600	maintain same	100	do not move	100	--
37,38	3601 to 3800	maintain same	100	do not move	100	--
39,40	3801 to 4000	maintain same	100	do not move	100	--

Table H.3: Summary of the results displayed by the CDI expert system - Test Category 2: sample 1 combined grasping and releasing .

Block no.	Time period,ms	Force decision	Confidence %	Mov.decision	Confidence %	Remarks
1,2	1 to 200	maintain same	100	do not move	100	--
3,4	201 to 400	maintain same	100	do not move	100	--
5,6	401 to 600	increase force	65	move North	100	large slip in South direction
7,8	601 to 800	do not increase	100	move North	100	large slip in South direction
9,10	801 to 1000	maintain same	100	do not move	100	--
11,12	1001 to 1200	maintain same	100	do not move	100	--
13,14	1201 to 1400	do not increase	74	do not move	100	--
15,16	1401 to 1600	maintain same	100	do not move	100	--
17,18	1601 to 1800	maintain same	100	move South	75	slip in North direction
19,20	1801 to 2000	maintain same	100	do not move	100	--
21,22	2001 to 2200	maintain same	100	do not move	100	--
23,24	2201 to 2400	maintain same	100	do not move	100	--
25,26	2401 to 2600	increase force	65	do not move	100	--
27,28	2601 to 2800	do not increase	36	move South	75	slip in North direction
29,30	2801 to 3000	do not increase	36	move Southwest	50	small slip in NE direction
31,32	3001 to 3200	increase force	65	move Southwest	75	slip in NE direction
33,34	3201 to 3400	increase force	72	move Southwest	50	small slip in NE direction
35,36	3401 to 3600	increase force	72	do not move	100	--
37,38	3601 to 3800	increase force	55	move Southwest	50	small slip in NE direction
39,40	3801 to 4000	increase force	72	move Southwest	75	slip in NE direction

H.2. Control decisions obtained from sample 5 test data

Table H.4: Summary of the results displayed by the CDI expert system - Test Category 1: sample 5 grasping .

Block no.	Time period,ms	Force decision	Confidence %	Mov.decision	Confidence %	Remarks
1,2	0 to 200	increase force	76	move Southwest	75	slip in North east direction
3,4	201 to 400	do not increase	43	move Southwest	75	slip in North east direction
5,6	401 to 600	do not increase	36	move South	50	small slip in North direction
7,8	601 to 800	do not increase	36	do not move	100	--
9,10	801 to 1000	maintain same	100	do not move	100	--
11,12	1001 to 1200	do not increase	48	move North	75	slip in South direction
13,14	1201 to 1400	do not increase	85	do not move	100	--
15,16	1401 to 1600	do not increase	91	move East	100	large slip in West direction
17,18	1601 to 1800	do not increase	100	move East	100	large slip in West direction
19,20	1801 to 2000	do not increase	100	move East	100	large slip in West direction
21,22	2001 to 2200	do not increase	100	move East	100	large slip in West direction
23,24	2201 to 2400	maintain same	75	do not move	100	--
25,26	2401 to 2600	maintain same	75	do not move	100	--
27,28	2601 to 2800	maintain same	100	do not move	100	--
29,30	2801 to 3000	do not increase	80	do not move	100	--
31,32	3001 to 3200	maintain same	100	do not move	100	--
33,34	3201 to 3400	maintain same	75	do not move	100	--
35,36	3401 to 3600	maintain same	100	do not move	100	--
37,38	3601 to 3800	do not increase	81	do not move	100	--
39,40	3801 to 4000	maintain same	100	move South	75	slip in North direction

Table H.5: Summary of the results displayed by the CDI expert system - Test Category 1: sample 5 releasing .

Blk.no	Time period,ms	Force decision	Confidence ,%	Mov.decision	Confidence ,%	Remarks
1,2	1 to 200	increase force	84	do not move	100	--
3,4	201 to 400	maintain same	75	do not move	100	--
5,6	401 to 600	maintain same	100	do not move	100	--
7,8	601 to 800	maintain same	100	do not move	100	--
9,10	801 to 1000	increase force	28	do not move	100	--
11,12	1001 to 1200	maintain same	100	do not move	100	--
13,14	1201 to 1400	maintain same	100	do not move	100	--
15,16	1401 to 1600	maintain same	100	do not move	100	--
17,18	1601 to 1800	maintain same	100	do not move	100	--
19,20	1801 to 2000	increase force	84	do not move	100	--
21,22	2001 to 2200	increase force	28	do not move	100	--
23,24	2201 to 2400	increase force	28	do not move	100	--
25,26	2401 to 2600	do not increase	49	do not move	100	--
27,28	2601 to 2800	do not increase	68	move North	100	large slip in South direction
29,30	2801 to 3000	maintain same	100	move North & Southeast	100	large slip in South and NW directions
31,32	3001 to 3200	maintain same	100	do not move	100	--
33,34	3201 to 3400	maintain same	100	do not move	100	--
35,36	3401 to 3600	maintain same	100	do not move	100	--
37,38	3601 to 3800	maintain same	100	do not move	100	--
39,40	3801 to 4000	maintain same	100	do not move	100	--

Table H.6: Summary of the results displayed by the CDI expert system - Test Category 2: sample 5 combined grasping and releasing

Block no.	Time period,ms	Force decision	Confidence, %	Mov.decision	Confidence, %	Remarks
1,2	1 to 200	increase force	58	move Southwest	50	small slip in NE direction
3,4	201 to 400	increase force	85	move Southwest	50	small slip in NE direction
5,6	401 to 600	increase force	85	move Southwest	50	small slip in NE direction
7,8	601 to 800	increase force	85	move East	75	slip in West direction
9,10	801 to 1000	increase force	75	move South	75	slip in North direction
11,12	1001 to 1200	do not increase	90	move East	75	slip in West direction
13,14	1201 to 1400	do not increase	90	move South	100	large slip in North direction
15,16	1401 to 1600	do not increase	90	move North	100	large slip in South direction
17,18	1601 to 1800	do not increase	90	move North	100	large slip in South direction
19,20	1801 to 2000	increase force	85	move North	75	slip in South direction
21,22	2001 to 2200	do not increase	36	do not move	100	--
23,24	2201 to 2400	do not increase	36	do not move	100	--
25,26	2401 to 2600	increase force	84	move Southwest	100	large slip in NE direction
27,28	2601 to 2800	increase force	64	move West	50	small slip in East direction
29,30	2801 to 3000	do not increase	36	do not move	100	--
31,32	3001 to 3200	do not increase	43	move South	100	large slip in North direction
33,34	3201 to 3400	do not increase	36	do not move	100	--
35,36	3401 to 3600	do not increase	43	do not move	100	--
37,38	3601 to 3800	do not increase	90	do not move	100	--
39,40	3801 to 4000	increase force	79	move North	50	slip in South direction

H.3. Control decisions obtained from sample 7 test data

Table H.7: Summary of the results displayed by the CDI expert system - Test Category 1: sample 7 grasping .

Block no.	Time period,ms	Force decision	Confidence, %	Mov.decision	Confidence, %	Remarks
1,2	1 to 200	maintain same	100	move Southwest	75	slip in North-east direction
3,4	201 to 400	do not increase	100	move Southwest	75	slip in North-east direction
5,6	401 to 600	increase force	77	move Northwest	75	slip in South-east direction
7,8	601 to 800	do not increase	48	do not move	100	--
9,10	801 to 1000	do not increase	85	move Northeast	75	slip in South-west direction
11,12	1001 to 1200	maintain same	75	do not move	100	--
13,14	1201 to 1400	do not increase	36	do not move	100	--
15,16	1401 to 1600	do not increase	28	do not move	100	--
17,18	1601 to 1800	do not increase	100	move North	50	small slip in South directn.
19,20	1801 to 2000	do not increase	48	move North	75	slip in South direction
21,22	2001 to 2200	do not increase	48	do not move	100	--
23,24	2201 to 2400	do not increase	85	move North	75	slip in South direction
25,26	2401 to 2600	do not increase	48	move East	75	slip in West direction
27,28	2601 to 2800	do not increase	59	do not move	100	--
29,30	2801 to 3000	do not increase	59	do not move	100	--
31,32	3001 to 3200	maintain same	100	move South	50	small slip in North directn.
33,34	3201 to 3400	do not increase	43	move Northeast	75	slip in South-west directn.
35,36	3401 to 3600	maintain same	100	move South	50	small slip in North direction
37,38	3601 to 3800	increase force	64	move South	62	small slip in North direction
39,40	3801 to 4000	increase force	64	move North	50	small slip in South direction

Table H.8: Summary of the results displayed by the CDI expert system - Test Category 1: sample 7 releasing .

Block no.	Time period,ms	Force decision	Confidence %	Mov.decision	Confidence %	Remarks
1,2	1 to 200	maintain same	100	do not move	100	--
3,4	201 to 400	maintain same	100	do not move	100	--
5,6	401 to 600	maintain same	100	do not move	100	--
7,8	601 to 800	increase force	85	move Southeast	50	small slip in NE direction
9,10	801 to 1000	increase force	28	do not move	100	--
11,12	1001 to 1200	maintain same	100	do not move	100	--
13,14	1201 to 1400	increase force	28	do not move	100	--
15,16	1401 to 1600	increase force	28	do not move	100	--
17,18	1601 to 1800	increase force	28	move South	75	slip in North direction
19,20	1801 to 2000	maintain same	100	move Southwest	75	slip in NE direction
21,22	2001 to 2200	maintain same	75	do not move	100	--
23,24	2201 to 2400	maintain same	100	do not move	100	--
25,26	2401 to 2600	maintain same	100	do not move	100	--
27,28	2601 to 2800	maintain same	100	do not move	100	--
29,30	2801 to 3000	maintain same	100	do not move	100	--
31,32	3001 to 3200	increase force	80	do not move	100	--
33,34	3201 to 3400	maintain same	75	do not move	100	--
35,36	3401 to 3600	maintain same	100	do not move	100	--
37,38	3601 to 3800	maintain same	100	do not move	100	--
39,40	3801 to 4000	maintain same	100	do not move	100	--

Table H.9: Summary of the results displayed by the CDI expert system - Test Category 2: sample 7 combined grasping and releasing .

Block no.	Time period,ms	Force decision	Confidence %	Mov.decision	Confidence %	Remarks
1,2	1 to 200	increase force	16	move Southwest	50	small slip in NE direction
3,4	201 to 400	do not increase	8	move Southwest	50	small slip in NE direction
5,6	401 to 600	do not increase	84	move Southwest	50	small slip in NE direction
7,8	601 to 800	increase force	83	move North	50	small slip in South direction
9,10	801 to 1000	increase force	62	move Northeast	100	large slip in SW direction
11,12	1001 to 1200	do not increase	90	move Northeast	50	small slip in SW direction
13,14	1201 to 1400	increase force	83	move North	75	slip in South direction
15,16	1401 to 1600	do not increase	48	do not move	100	--
17,18	1601 to 1800	do not increase	36	move North	75	slip in South direction
19,20	1801 to 2000	do not increase	36	move North	75	slip in South direction
21,22	2001 to 2200	do not increase	36	move North	75	slip in South direction
23,24	2201 to 2400	do not increase	36	move South	50	small slip in North direction
25,26	2401 to 2600	do not increase	43	do not move	100	--
27,28	2601 to 2800	do not increase	36	move Southwest	50	small slip in NE direction
29,30	2801 to 3000	do not increase	43	move South	50	small slip in North direction
31,32	3001 to 3200	do not increase	36	do not move	100	--
33,34	3201 to 3400	do not increase	36	do not move	100	--
35,36	3401 to 3600	do not increase	43	move Southwest	75	slip in NE direction
37,38	3601 to 3800	do not increase	43	do not move	100	--
39,40	3801 to 4000	do not increase	43	do not move	100	--

I. A Typical User Session with the Task Status Indicator Expert

KES - Copyright (C) 1988, Software Architecture & Engineering, Inc.

Knowledge Engineering System (KES), Release 2.5.
Copyright (C) 1988, Software Architecture & Engineering, Inc.
Loading the knowledge base 'vkb24.pkb'.

Welcome to the Online Status Indicator Expert designed by Vaidy.

This expert will determine the status of the task from the dynamic forces
acquired by a tactile sensing system.

It will display a confidence factor for the decisions.

If you make a mistake while answering, type 's' to terminate the session.

If you want to restart, type 'n' in the direct question mode.

The object was dynamically displaced South

Grasped to level 1

Released to level 1

Confidence in grasping 6.25

No. of releases 1

Confidence in releasing 3

Grasping by sensor 2 at 77 msec

Releasing by sensor 7 at 48 msec

Old data written in 'filetrans3'

Welcome to the Online Status Indicator Expert designed by Vaidy.

This expert will determine the status of the task from the dynamic forces
acquired by a tactile sensing system.

It will display a confidence factor for the decisions.

The object was dynamically displaced South

Grasped to level 2

Released to level 1

Confidence in grasping 12.5

No. of Releases 1

Confidence in Releasing 3

Grasping by sensor 2 at 3 msec

Grasping by sensor 7 at 56 msec

Releasing by sensor 7 at 20 msec

New data successfully written in filetrans4

Do you wish to continue the task ?

- 1. yes
- 2. no

=? 2

Type 's' to stop

Ready for command: s